

# Measurements of Forced and Unforced Aerodynamic Disturbances in a Turbojet Engine

by

Jabin Todd Bell

S.B., Massachusetts Institute of Technology (1991)

Submitted to the Department of Aeronautics and Astronautics in Partial Fulfillment of the  
Requirements for the Degree of

Master of Science in Aeronautics and Astronautics

at the

Massachusetts Institute of Technology  
May 1993

© Massachusetts Institute of Technology, 1993, All Rights Reserved

Signature of Author \_\_\_\_\_  
Department of Aeronautics and Astronautics  
May 20, 1993

Certified by \_\_\_\_\_  
Professor A. H. Epstein  
Professor of Aeronautics and Astronautics

Approved by \_\_\_\_\_  
Professor Harold Y. Wachman  
Chairman, Department Graduate Committee

MASSACHUSETTS INSTITUTE  
OF TECHNOLOGY

JUN 08 1993

LIBRARIES

Measurement of Forced and Unforced Aerodynamics  
Disturbances in a Turbojet Engine

by

Jabin Todd Bell

Submitted to the Department of Aeronautics and Astronautics  
on May 20, 1993 in partial fulfillment of the  
requirements for the Degree of Master of Science in  
Aeronautics and Astronautics

Abstract

A small turbojet engine test stand has been setup to explore the use of active compressor stabilization to suppress surge, a one dimensional compression system instability. The engine is equipped with a variable area nozzle that allows the operating line of the engine to be controlled. The nozzle area and throttle settings are controlled through a computer. This arrangement allows the operating point of the engine to be moved around the operating map. Complete details of the test stand including the data acquisition system are given.

The engine is found to have operating point fluctuations, at constant nozzle and throttle settings, caused by variations in the engine inlet temperature. The engine speed is also found to change as the nozzle area is reduced, at constant throttle setting, while tracing a speed line. An attempt to adjust the data to a constant speed line is made. Curves are fitted to the data for several different engine runs and used to estimate the speed lines. Based on the estimated speed lines the slope of the characteristic is calculated for several engine surge cases.

The natural disturbance levels in the engine are measured at a stable operating point. Surge inception is examined. No evidence of a rotating disturbance prior to surge is found. A characteristic surge cycle of the engine is described.

External forcing is applied to the engine by modulating the massflow through the customer bleed. The forcing is described in terms of the variations in the massflow through the customer bleed. Acoustic behavior of the pressure at the customer bleed is observed and described. The response of the engine to the external forcing is described. The ability to produce the transfer functions between locations in the engine based on the external forcing is demonstrated.

Thesis Supervisor: Dr. Alan H. Epstein  
Title: Professor of Aeronautics and Astronautics

## Acknowledgements

The work in this thesis has involved the cooperation, support and participation of many people. I would like to thank them.

I would first like to thank by advisor, Prof. Epstein. Without his advice and guidance the engine would never have run. I am extremely grateful for the many components of the rig that he designed. His patience while completing and editing this thesis has been appreciated.

I would like to thank the staff of the Gas Turbine Laboratory. Jim Nash and Jim Letendre did most of the assembling, welding, and wiring involved in building the test stand. Viktor Dubrowski machined the engine mounts and shaker valve. Bill Ames has helped with the modifications to the rig. I have also received much assistance from Holley Rathbun, who helped process the many equipment and software orders and Dr. Gerald Guenette, who provided much advice on computers and useful programs. I also thank Diana Park for the last minute alterations to the wiring schematics.

Thanks are also due to Dan Pelletier and the other engineers from Lycoming who came up to help us debug the engine.

I also thank Jed Dennis and Duncan Reijnen for allowing me to "steal" their computer to process the data.

I am particularly grateful for the support and prayers of my parents. Special thanks go to Susan Waldo (soon to be Bell) for not distracting me while I was trying to finish up.

I am also grateful to Liz Zotos for the extended deadlines that enabled me to complete this and graduate.

Funding for this research has been provided by the Office of Naval Research and Textron Lycoming. This support is gratefully acknowledged.

# Table of Contents

	Page
Abstract .....	2
Acknowledgements .....	3
Table of Contents .....	4
Table of Figures .....	8
Table of Tables .....	12
Nomenclature .....	13
1. Introduction .....	16
1.1. Background .....	16
1.2. Modeling .....	17
1.3. Experiments .....	17
1.4. Current Work .....	18
2. Experimental Facility .....	22
2.1. Overview of Facility .....	22
2.2. Engine and Test Stand .....	22
2.2.1. Engine .....	23
2.2.2. Variable Area Nozzle .....	24
2.2.3. Inlet Ducting and Engine Shroud .....	26
2.2.4. Exhaust System .....	27
2.2.5. Actuator/Positioners .....	28
2.2.5.1. Throttle Actuator .....	28
2.2.5.2. Nozzle Positioner .....	29
2.2.6. Fuel System .....	30
2.2.7. Oil System .....	30
2.2.8. Electrical System .....	31



2.2.9. Vacuum .....	31
2.2.10. Cooling Water .....	31
2.2.11. Shaker .....	32
2.2.12. Instrumentation .....	34
2.2.12.1. Pressure .....	36
2.2.12.2. Vibration .....	39
2.2.12.3. Flow .....	40
2.2.12.4. Engine Thrust .....	40
2.2.12.5. Position Indication .....	40
2.2.12.6. Temperature .....	41
2.2.12.7. Rate Measurements .....	42
2.3. Control Computer .....	43
2.3.1. Hardware .....	43
2.3.1.1. ACPC-16 .....	43
2.3.1.2. ACPC-12 .....	44
2.3.1.3. ACPC-I/O .....	44
2.3.1.4. Serial Ports .....	45
2.3.2. Software .....	45
2.3.2.1. Genesis Overview .....	46
2.3.2.2. Data Inputs .....	47
2.3.2.3. Runtime Data Reduction .....	48
2.3.2.4. Data Recorded .....	50
2.3.2.5. Control Outputs .....	50
2.3.2.6. Alarms .....	53
2.3.2.7. Operating Modes .....	53
2.3.2.7.1. Initialization .....	54
2.3.2.7.2. Menu .....	54

2.3.2.7.3. Calibration .....	54
2.3.2.7.4. Running the Engine .....	56
2.3.3. Typical Run Procedure .....	57
2.4. High Speed Data Acquisition Computer .....	58
2.4.1. Hardware .....	59
2.4.1.1. ADTEK Boards .....	59
2.4.1.2. Filter Board .....	59
2.4.2. Software .....	60
2.4.2.1. ADTDVM .....	60
2.4.2.2. MMADCAP .....	60
2.4.2.3. Data Inputs .....	61
2.4.2.4. Calibration .....	62
2.4.3. Run Procedure .....	64
2.5. Error Analysis .....	65
2.5.1. Steady State .....	65
2.5.2. High Speed .....	69
3. Presentation and Analysis of Data .....	92
3.1. Steady State Data .....	92
3.1.1. Operating Point Fluctuations .....	92
3.1.2. Nozzle Position vs. Nozzle Area .....	93
3.1.3. Speed Lines .....	94
3.1.4. Hotwire Linearization .....	98
3.2. High Speed Data .....	99
3.2.1. Data With No External Forcing .....	100
3.2.1.1. Stable Operating Point .....	100
3.2.1.1.1. Time Traces .....	100
3.2.1.1.2. Power Spectra .....	102

3.2.1.2. Surge Inception .....	103
3.2.1.3. Surge Cycle .....	105
3.2.2. Data With External Forcing .....	106
3.2.2.1. Forcing Function Behavior .....	106
3.2.2.1.1 Bleed Massflow .....	107
3.2.2.1.2. Effect of Frequency .....	109
3.2.2.2. Acoustic Behavior of Pressure at the Customer Bleed .....	109
3.2.2.3. Engine Response .....	111
3.2.2.4. Transfer Functions Within the Engine .....	112
4. Summary and Conclusions .....	177
4.1. Summary .....	177
4.2. Conclusions .....	178
4.3. Suggestions for Future Research .....	179
4.3.1. Additional Examination of Collected Data .....	179
4.3.2. Investigations With the Engine .....	179
Appendix A - Calculation of Nozzle Position vs. Nozzle Area .....	181
Appendix B - Frequency Response of the Pressure Taps .....	184
Appendix C - Wiring Schematics for the Control Computer .....	186
Appendix D - Listing of the Original Code Used to Run the Engine .....	191
Appendix E - Initial Pressure Calibrations and Resulting Formulas .....	206
Appendix F - Pre-Run Checklist .....	209
Appendix G - Filter Board Specifications .....	211
References .....	212

## Table of Figures

	Page
Figure 1.1 : Extension of Operating Range With Surge Control .....	20
Figure 1.2 : Schematic of the Basic Compression System .....	21
Figure 2.1 : Overview of Facility .....	71
Figure 2.2 : Engine Test Stand .....	72
Figure 2.3 : Engine Cross Section with Instrumentation Locations .....	73
Figure 2.4 : LTS-101 Operating Map .....	74
Figure 2.5 : Variable Area Nozzle .....	75
Figure 2.6 : Nozzle Area vs. Nozzle Position .....	76
Figure 2.7 : Nozzle and Diffuser Assembly .....	77
Figure 2.8 : Inlet Air Flow and Heat Sources .....	78
Figure 2.9 : Engine Shroud and Insulation Locations .....	79
Figure 2.10 : Inlet Duct .....	80
Figure 2.11 : Side View of Exhaust Ducting .....	81
Figure 2.12 : Front View of Exhaust Ducting .....	82
Figure 2.13 : Nozzle Positioning System (Side View) .....	83
Figure 2.14 : Fuel System Schematic .....	83
Figure 2.15 : Oil System Schematic .....	84
Figure 2.16 : Electrical System Schematic .....	84
Figure 2.17 : Water Cooling System .....	85
Figure 2.18 : Shaker Valve Assembly .....	86
Figure 2.19 : Bleed Valve Venting Options .....	87
Figure 2.20 : Pressure Plumbing Schematic .....	88
Figure 2.21 : Location of Pressure Taps Upstream and Downstream of the Shaker Valve .....	88
Figure 2.22 : Control Computer Connection Schematic .....	89

Figure 2.23 : Diagram of Genesis Components .....	90
Figure 2.24 : Operating Modes .....	90
Figure 2.25 : High Speed Data Acquisition System Schematic .....	91
Figure 3.1 : Inlet Temp Fluctuations at Constant Nozzle and Throttle Positions .....	116
Figure 3.2 : Corrected Engine Speed at Constant Nozzle and Throttle Positions .....	117
Figure 3.3 : Absolute Engine Speed at Constant Nozzle and Throttle Positions .....	118
Figure 3.4 : Pressure Ratio at Constant Nozzle and Throttle Positions .....	119
Figure 3.5 : Corrected Massflow at Constant Nozzle and Throttle Positions .....	120
Figure 3.6 : Pressure Ratio vs. Corrected Engine Speed Throttle Lines .....	121
Figure 3.7 : Corrected Massflow vs. Corrected Engine Speed Throttle Lines .....	122
Figure 3.8 : Pressure Ratio vs. Corrected Massflow Throttle Lines .....	123
Figure 3.9 : Calculated Nozzle Area vs. Nozzle Position .....	124
Figure 3.10 : Corrected Engine Speed vs. Nozzle Area at Constant Throttle Setting .....	125
Figure 3.11 : Speed Line Data, Run 28 .....	126
Figure 3.12 : Curve Fits to the Speed Line Data, Runs 27 and 28 .....	127
Figure 3.13 : Hotwire Linearization Curve .....	128
Figure 3.14 : Stable Operating Point .....	129
Figure 3.15 : Time Traces of Customer Bleed and Combustor at Stable Operating Point .....	130
Figure 3.16 : Time Traces of Zeroth Mode at Throat and Stator Tap at Stable Operating Point .....	131
Figure 3.17 : Spatial Fourier Decomposition of Throat Taps at Stable Operating Point .....	132
Figure 3.18 : Hotwire Outputs with Engine Off and at Stable Operating Point .....	133
Figure 3.19 : PSD of Customer Bleed at Stable Operating Point .....	134
Figure 3.20 : PSD of Combustor at Stable Operating Point .....	135
Figure 3.21 : PSD of Zeroth Mode at the Throat at Stable Operating Point .....	136

Figure 3.22 : PSD of First Mode at the Throat at Stable Operating Point .....	137
Figure 3.23 : PSD of 0° Throat Tap at Stable Operating Point .....	138
Figure 3.24 : PSD of 120° Throat Tap at Stable Operating Point .....	139
Figure 3.25 : PSD of 240° Throat Tap at Stable Operating Point .....	140
Figure 3.26 : PSD of Stator Tap at Stable Operating Point .....	141
Figure 3.27 : PSD of Hotwire at Stable Operating Point .....	142
Figure 3.28 : PSD of Vibrometer at Stable Operating Point .....	143
Figure 3.29 : Time Trace of Throat Taps at Surge Inception, Run 28 .....	144
Figure 3.30 : First Mode at the Throat at Surge Inception, Run 28 .....	145
Figure 3.31 : PSD of the First Mode at the Throat at Surge Inception, Run 28 .....	146
Figure 3.32 : Standard Deviations of Transducer Signals at Surge Inception, Run 28 .....	147
Figure 3.33 : Standard Deviations of Transducer Signals at Surge Inception, Run 27 .....	148
Figure 3.34 : Pressure Traces for First Surge Cycle, Run 28 .....	149
Figure 3.35 : Pressure and Hotwire Traces for First Surge Cycle, Run 28 .....	150
Figure 3.36 : Massflow for First Surge Cycle, Run 28 .....	151
Figure 3.37 : Pressure vs. Massflow for First Surge Cycle, Run 28 .....	152
Figure 3.38 : Total and Static Pressures Up and Down Stream of the Shaker Valve .....	153
Figure 3.39 : Mach Number Downstream of Shaker and Calculated Massflow .....	154
Figure 3.40 : Amplitude of Customer Bleed Massflow Oscillations vs Excitation Frequency , Run 28 .....	155
Figure 3.41 : Amplitude of Customer Bleed Massflow Oscillations vs Excitation Frequency , Run 27 .....	156
Figure 3.41 : Customer Bleed Pressure Traces at Various Excitation Frequencies .....	157
Figure 3.43 : Spectra of Customer Bleed Pressure at 90 Hz .....	158
Figure 3.44 : Spectra of Customer Bleed Pressure at 242 Hz .....	159

Figure 3.45 : Amplitude of Customer Bleed Pressure Oscillations vs Excitation Frequency , Run 28 .....	160
Figure 3.46 : Amplitude of Customer Bleed Pressure Oscillations vs Excitation Frequency , Run 27 .....	161
Figure 3.47 : Customer Bleed Massflow Traces at Various Excitation Frequencies .....	162
Figure 3.48 : Spectra of Customer Bleed Massflow at 90 Hz .....	163
Figure 3.49 : Spectra of Customer Bleed Massflow at 242 Hz .....	164
Figure 3.50 : Customer Bleed and Combustor Pressure Traces at 90 Hz .....	165
Figure 3.51 : Spectra of Combustor Pressure at 90 Hz .....	166
Figure 3.52 : Spectra of Combustor Pressure at 242 Hz .....	167
Figure 3.53 : Spectra of Zeroth Mode at the Throat at 90 Hz .....	168
Figure 3.54 : Spectra of Zeroth Mode at the Throat at 242 Hz .....	169
Figure 3.55 : Spectra of Stator Tap Pressure at 90 Hz .....	170
Figure 3.56 : Spectra of Stator Tap Pressure at 242 Hz .....	171
Figure 3.57 : Spectra of Hotwire at 90 Hz .....	172
Figure 3.58 : Spectra of Hotwire at 242 Hz .....	173
Figure 3.59 : Transfer Function from Customer Bleed Massflow to Zeroth Mode at the Throat .....	174
Figure 3.60 : Transfer Function from Customer Bleed Massflow to Combustor Pressure .....	175
Figure 3.61 : Transfer Function from Combustor Pressure to Zeroth Mode at the Throat .....	176
Figure A.1 : Diagram of the Nozzle Throat .....	183
Figure B. 1 : Diagram of Static Pressur Probe .....	185
Figure C.1 : Rig Wiring Schematic .....	187
Figure C.2 : Wiring Schematic for T400 Terminal Panel .....	188
Figure C.3 : Wiring Schematic for T41 Terminal Panel .....	189
Figure C.4 : Wiring Schematic for the Junction Box .....	190

## Table of Tables

	Page
Table 2.1 : Instrumentation List, Part I .....	34
Table 2.2 : Instrumentation List, Part II .....	35
Table 2.3 : Data Recorded by Genesis .....	51
Table 2.4 : Alarm Conditions .....	53
Table 2.5 : List of Command Keys for the Run Mode .....	57
Table 2.6 : MMADCAP Scale and Voltage Ranges .....	61
Table 2.7 : Inputs Supplied to High Speed A/D .....	63
Table 2.8 : Listing of Calculated Uncertainty for Steady State Pressures .....	68
Table 2.9 : Listing of Uncertainty for Calculated Values and Ambient Pressure .....	69
Table 2.10 : Calibration and Calculated Standard Deviations of Kulite Pressure Transducers from Run 28 .....	70
Table 3.1 : Fluctuations and Uncertainty at Constant Nozzle and Throttle Settings .....	93
Table 3.2 : Nozzle Position to Area Correlations .....	94
Table 3.3 : Surge Points and Slopes from the various curve fits .....	98
Table 3.4 : Sign of the Slope at Engine Surge Point .....	98
Table 3.5 : Disturbance Levels in Engine at 0 and 95 % Speed .....	100
Table 3.6 : Transfer Functions Presented .....	113
Table E.1 : Calibration of Inlet Pressure Transducer .....	206
Table E.2 : Calibration of Compressor Discharge Pressure Transducer .....	207
Table E.3 : Calibration of Turbine Discharge Pressure Transducer .....	207
Table E.4 : Calibration of Oil Pressure Transducer .....	208



## Nomenclature

AF - intermediate value in the turbine inlet temperature calculation

$A_{\text{duct}}$  - area of the duct

$A_{\text{in}}$  - inlet area

$a_3$  - speed of sound at compressor discharge

BLD - ratio of airflow through the customer bleed to airflow through the engine

$K_A, K_B, K_C$  - constants

k - number of points in the data set

M - Mach number

$M_t$  - rotor tip Mach number

$\dot{m}$  - massflow

N1 - absolute engine speed (% speed)

$N1_{\text{corr}}$  - corrected engine speed (% speed)

P3 - measured compressor discharge pressure (psig)

$P_o$  - measured ambient pressure (psia)

$P_{hi}$  - pressure at high pressure of pressure calibration

$P_{lo}$  - pressure at low pressure of pressure calibration

$P_o$  - measured ambient pressure (inches Hg absolute)

$P_s$  - static pressure

$P_T$  - total pressure

$P_{T0}$  - ambient total pressure (psia)

$P_{T3}$  - compressor discharge total pressure (psia)

PSBM - inlet bellmouth static pressure depression from ambient (inches H<sub>2</sub>O)

PTBM - inlet bellmouth total pressure depression from ambient (inches H<sub>2</sub>O)

R - gas constant

$r_t$  - tip radius of rotor

S - fractional standard deviation of the indicated data set from the expected universe average

s - standard deviation for the indicated data set from the expected universe average

$T_1$  - engine inlet temperature ( $^{\circ}$  C)

$T_{T4.1}$  - calculated turbine inlet temperature ( $^{\circ}$  R)

$T_s$  - static temperature

$T_T$  - total temperature

$T_{T3}$  - compressor discharge total temperature

$T_{T0}$  - ambient total temperature

$U_t$  - rotor tip speed

u - velocity

$V_{lo}$  - measured voltage output of transducer at low pressure of pressure calibration

$V_{hi}$  - measured voltage output of transducer at high pressure of pressure calibration

V - the value of the indicated term at 90 to 100 % engine speed

WF - fuelflow rate (lbs/hr)

W - calculated airflow through the engine (lbs/sec)

#### Greek Symbols -

$\gamma$  - ratio of specific heats

$\delta$  - ambient pressure correction factor

$\eta_{th}$  - thermal efficiency of compressor

$\theta$  - ambient temperature correction factor

$\pi$  - pressure ratio across the compressor

$\rho_o$  - ambient density

$\rho_s$  - static density

$\sigma$  - standard deviation

$\varphi$  - massflow coefficient

$\chi$  - slip factor at rotor time, empirical constant

# **1.Introduction**

## **1.1.Background**

The operating range of many turbomachine compression systems is limited by fluid dynamic instabilities. These instabilities take two forms, surge and rotating stall. Surge is a one dimensional, system wide instability that results in large pressure and massflow perturbations. In many cases surge causes reverse flow through the compressor. Rotating stall is a two or three dimensional flow disturbance. It is characterized by massflow and pressure perturbations that rotate around the compressor annulus. The loss in compressor performance caused by rotating stall may trigger surge.

In aircraft propulsion systems, either instability can cause structural damage or overheating (due to reduced massflow), leading to engine failure. Therefore, aircraft engines must be designed to operate far enough from the "stall line" (the boundary between stable and unstable operation, Figure 1.1) that external disturbances will not move the engine to an unstable operating point. This stall margin often results in a performance penalty, because the highest compressor efficiencies occur near the stall line.

The drive to improve the performance of aircraft engines has motivated many researchers to study surge and/or rotating stall. Models that predict surge and stall behavior have been developed and verified experimentally. These models lead to the suggestion that, the onset of aerodynamic instabilities in a turbomachine could be delayed using active feedback control [4] as shown in Figure 1.1. The use of active feedback control to delay surge or rotating stall has been successfully demonstrated in several rig experiments. The work in this thesis is the next step toward delaying surge in a gas turbine engine. A gas turbine engine is set up on a test stand at the Massachusetts Institute of Technology Gas Turbine Lab (MIT/GTL). Its performance and

surge behavior are characterized and the transfer functions between various locations in the engine are measured.

### 1.2.Modeling

Several, similar, low-order, lumped parameter models for the surge process have been developed [3, 8, 14]. A complete description of one variation of these models is given by Simon [14]. The compression system is modeled as a plenum with an inlet duct and exit throttle. The compressor is an actuator disk in the inlet duct (Figure 1.2). The flow in the inlet duct is assumed to be one-dimensional and incompressible. The fluid in the plenum is an ideal gas at uniform pressure and zero velocity. Heat addition in the plenum is used to model a combustor. The pressure ratio and massflow of the compressor and throttle or turbine, are assumed to follow their steady state performance curves (quasi-steady assumption). Simon also included sensors and actuators for feedback control in his model. The system model is then obtained by performing a momentum balance on the duct and mass balance for the plenum. A polytropic relation between pressure and density in the plenum, is assumed. This results in a non-linear system model, in which all the inertia of the system is in the inlet duct, all the compliance in the plenum, and the energy addition or subtraction in the compressor and throttle. This model can be linearized and used to predict the stability of the system. The linearized model is also used for the design of feedback control systems.

### 1.3.Experiments

These surge models have been verified by several experiments. Most of these have been performed using centrifugal compressors, because axial compressors are more sensitive to rotating stall, and tend to go into rotating stall before surging. Centrifugal compressors are less sensitive to rotating stall and tend to surge before going into rotating stall. [4]

Emmons demonstrated good agreement between the surge point predicted by the linearized model and the measured surge point of a compressor [3]. Fink conducted extensive surge tests on a centrifugal compressor [6]. Grietzer examined surge behavior for a low speed axial compressor [9]. Both Fink and Grietzer found that the non-linear model predicted the behavior of the compressors during surge.

The use of feedback control to delay surge has also been demonstrated by several experiments. Pinsley used active control of a throttle valve on the plenum to delay surge on a centrifugal turbocharger [13]. Ffowcs Williams and Huang delayed surge using a speaker in the plenum wall driven by a feedback signal [5]. Passive or structural delay of surge has also been demonstrated. Gysling used a movable plenum wall connected to a mass-spring-damper [10] and Bodine used a tuned resonator [1].

#### 1.4. Current Work

Based on the successful attempts at delaying surge on low speed, low power compressor rigs, it was decided to attempt to delay surge on a small gas turbine engine. Two goals motivated this decision. First the model was validated for the low speed compressors, but it was unclear what impact compressibility should have on the model for high speed compressors. It was apparent that the equivalent of a gas turbine engine would be required to drive a high speed compressor. Using an entire engine also afforded the opportunity of fulfilling the goal of delaying surge in a gas turbine engine. The move from experimental test rigs is a large step. The engine environment introduces numerous constraints and problems not encountered on most test rigs. Some of the more obvious ones are combustion noise, convoluted and inaccessible geometries, and the turbine-compressor interaction.

As a first step toward delaying surge in an engine, a gas turbine engine was set up on a test stand at the Massachusetts Institute of Technology Gas Turbine Lab (MIT/GTL). The engine

was instrumented for the acquisition of steady state and high speed (4000 Hz) data at various locations in the flow path. The behavior and performance of the engine was evaluated and verified by comparison with data from the manufacturer (Textron-Lycoming). The engine was surged on several occasions to acquire data on its behavior prior to and during surge. The dynamic response of the flow in the engine was examined by modulating the customer bleed massflow. This allowed transfer functions between several points in the engine to be calculated.

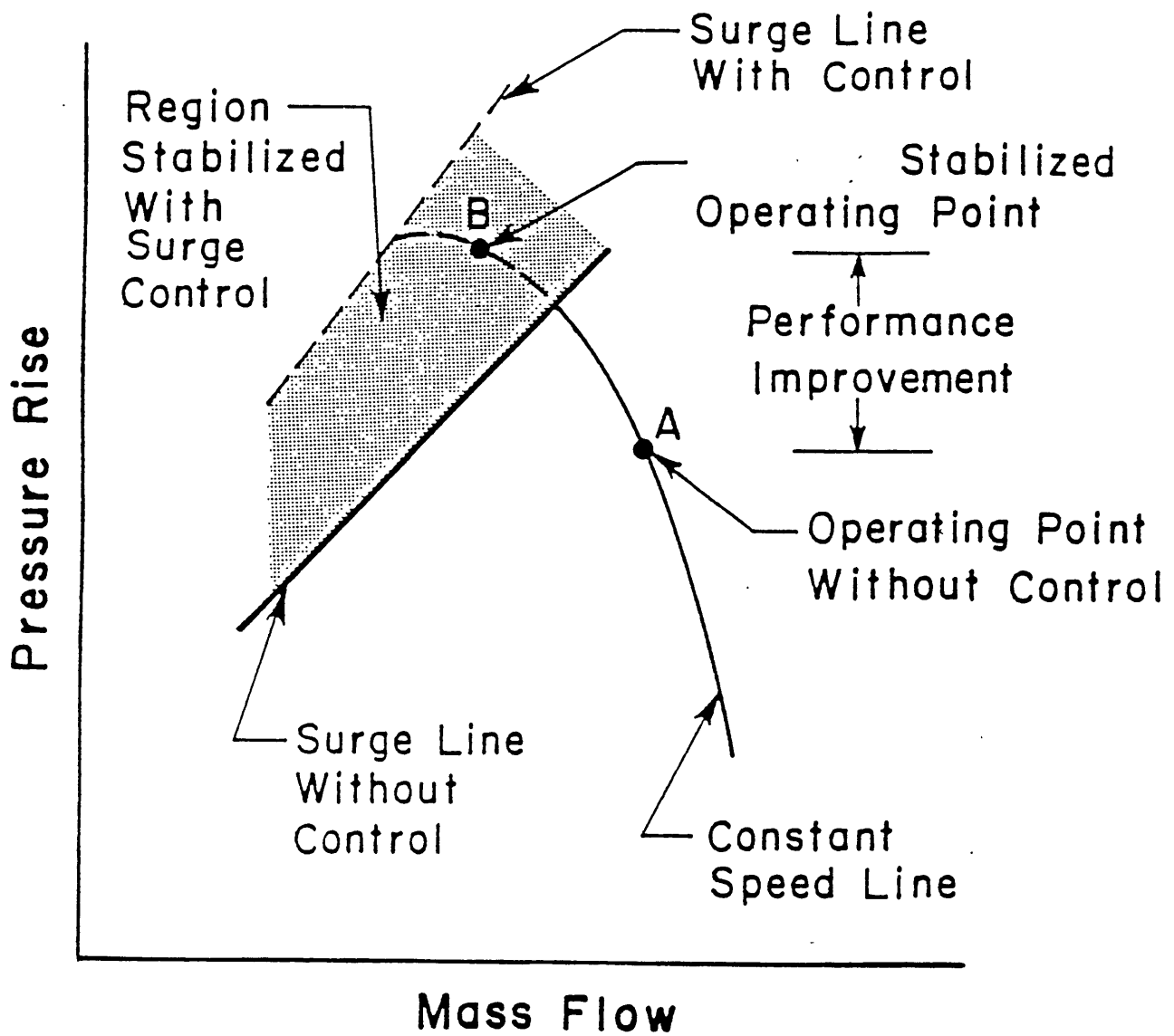


Figure 1.1: Extension of Operating Range with Dynamic Surge Control



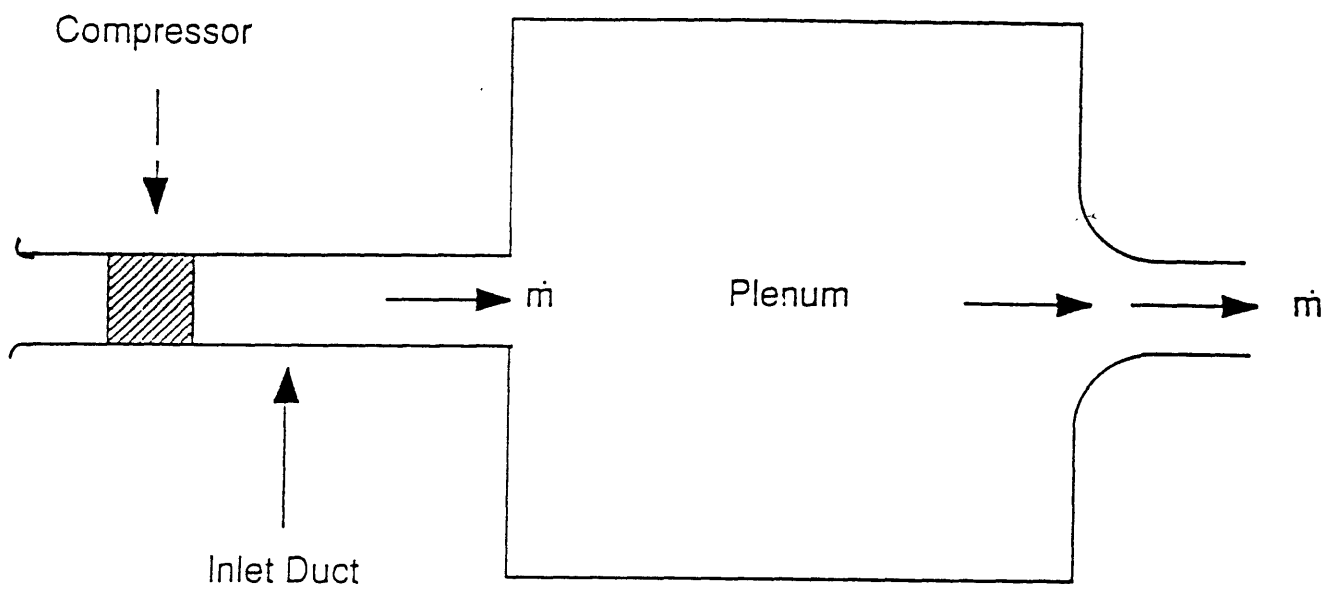


Figure 1.2 : Schematic of Basic Compression System

## **2.Experimental Facility**

### **2.1.Overview of Facility**

The experimental facility described here was built with funding from Textron Lycoming and the Office of Naval Research. The engine is on loan from Textron Lycoming. The facility will be described in detail later, but a general overview is provided here and shown in figure 2.1. This facility has gone through several (minor) modifications and improvements since the engine was first run. Unless otherwise noted the most current rig setup at the time of writing is described.

The engine is in a 20 by 60 foot test cell with a 17 foot ceiling and 18" thick reinforced concrete walls. Inlet air to the engine is provided by ducting that runs from a hole in the roof to the engine inlet. The jet exhaust from the engine is vented through an acoustically insulated duct that passes through another hole in the roof. Power, oil, and fuel are provided to the engine by the test stand. Instrumentation from the engine and exhaust duct is fed into two computers. The control computer monitors and controls the "steady state" performance of the engine. The other computer is the high speed data acquisition computer and is used to collect high speed data for short times while the engine is running.

The engine is operated from the control center in the hall outside the test cell. Access to both computers is provided by putting their keyboards and monitors outside, using extension cables. There are also two closed circuit monitors with cameras in the test cell, and a control panel at the control center. The fuel supply and pump are also both out in the hall, to provide greater safety.

### **2.2.Engine and Test Stand**

This section describes the hardware portion of the rig. Specifically the engine and the various systems and instrumentation attached to it. Most of these are supported by the test stand

structure. The main structure of the test stand is constructed from 3 X 5" steel box beams. Unistrut is used to provide extra support for the inlet bellmouth and to support cabling running to the engine. The entire stand is bolted to the floor for stability. (Figure 2.2)

### 2.2.1. Engine

The engine needs to meet several criteria. It must be small enough and consume a small enough amount of fuel that it is affordable to run in a university setting. It also needs to be very durable structurally so that it can withstand repeated surge cycles. The engine needs to be configured in a way that allows it to be surged in steady state operation. It also should surge before going into rotating stall. As massflow is decreased the turbine inlet temperature increases, so the engine also needs to have an acceptable turbine temperature margin at surge, to allow for reductions in massflow enabled by controlling surge.

The engine that was selected is a modified LTS-101 turboshaft engine (Figure 2.3). It has a combination single stage axial compressor and a single stage centrifugal compressor driven by a single stage gas producer turbine. The compressor configuration provides a strong structure and good surge durability. The diffuser has been modified (the throat opened) to ensure that the centrifugal compressor controls surge at high speed. The combustor is a reverse flow annular combustor with ten fuel nozzles. It consumes approximately 0.6 gallons of fuel per minute at full power, not an unreasonable operating expense. The flow is reversed again before passing through the gas producer turbine. The nozzles on the gas producer turbine have been retrofit to a smaller area. This rematches the compressor and turbine, to provide a turbine inlet temperature safety margin at surge. In its normal configuration an LTS-101 has a single stage power turbine that produces about 650 shp. The power turbine has been removed from this engine, leaving it a gas generator. The turbine is replaced by a variable area nozzle, which will be described later. The variable area nozzle allows the massflow through the engine to be controlled. When

combined with the throttle the variable area nozzle makes it possible to move to any point on the operating map (Figure 2.4).

The useful region for experimentation is limited by the behavior of the flow fence. The flow fence is located upstream of the axial compressor (Figure 2.3). It is a circumferential ring that moves into the flow at low engine speeds. The flow fence creates an impeller tip stall on the axial compressor to stabilize the engine during startup and idle. The flow fence does not fully retract until the engine approaches 95 % speed. When the flow fence is in the flow it changes the operating map of the compressor. The flow fence retraction sets the lower boundary on the region used for experimentation. This results in an experimental region between 95 and 100 % speed.

### 2.2.2. Variable Area Nozzle

The variable area nozzle was designed to set the engine operating point by controlling the massflow through the engine. The massflow through the engine varies as the throat area of the nozzle changes. The nozzle throat design is based on two concentric cones (Figure 2.5). As these two cones are moved closer to each other the gap between them decreases, thus reducing the area of the throat. The center body cone has an opening angle of  $30^\circ$  for most of its length. Near the fully closed position the angle of the inner cone curves to zero. This results in an approximately linear relationship between nozzle area and position for most nozzle positions, it is only near the extreme closed position that it becomes non-linear. The relationship between nozzle position and area can be calculated based on the geometry (See appendix A). The results of that calculation are shown in Figure 2.6. The zero position, on the plot, corresponds to having the throat right at the tip of the centerbody.

Moving the two sections of the nozzle relative to each other required some innovative design. Moving the centerbody section relative to the diffuser and exhaust system, would have required

placing a cooled actuator in the centerbody of the diffuser or turning the exhaust so that an actuator could be placed behind the exhaust. Neither of these seemed promising. Placing an cooled actuator in the centerbody would have been expensive and provided very limited access to the actuator if it needed adjustments. Turning the exhaust system would have increased the noise level and made it more difficult to run the ducting through the available hole in the ceiling. The upstream section of the nozzle throat is mounted on the engine, so it was decided to move the entire engine axially. There was also concern that hot exhaust gases would leak through the gap between the nozzle sections. To prevent leakage a flexible seal was included in the original design. It was to be mounted on two flanges, one on each side of the gap. (One of those flanges was later removed when the gap was found to suck in air, instead of blowing it out. The other was put to another use as described in the next section.)

A diffuser was installed after the nozzle throat and connected to the exhaust system. The diffuser serves two purposes. By expanding the flow to the size of the exhaust ducting it prevents the formation of a free jet and its associated noise. The diffuser also reduces the pressure drop in the exhaust system. The maximum allowable temperature for the 304 stainless steel exhaust ducting is 1000° F. Since the flow temperature would exceed this limit at high power, 8 water cooling sprays were added to the diffuser. Equally spaced about the circumference and sized to handle a total flow rate of 8 gpm, these sprays are supplied by filtered city water.

To insure concentricity, the entire nozzle and diffuser is supported and aligned by three rods, each of which is free to slide radially as the nozzle heats up and expands (Figure 2.7). The throat section of the nozzle was machined from Hastalloy-X™ to insure that it would withstand the temperatures without requiring cooling. The rest of the nozzle and diffuser was made from 316 stainless steel.

### 2.2.3. Inlet ducting and Engine Shroud

When the engine was first run at MIT its map did not match the operating map measured at the plant prior to shipment. It eventually became apparent that this was due to an inlet temperature distortion. The air inlet for the test cell is located almost directly above the exhaust ducting about 25 feet downstream of the engine (Figure 2.8). Hot air from the exhaust ducting and the hot section of the engine would rise and partially mix with the relatively cool air flowing from the inlet in the roof to the engine. Temperature gradients of up to 40° F over a few inches were measured at the engine inlet bellmouth.

Two steps were taken to remove or lessen the temperature distortions. A cooled shroud was added over the hot section of the engine, and insulation was placed over the shroud and the exposed section of the nozzle. Insulated inlet ducting was also installed from the hole in the roof to the engine inlet.

Most of the hot air causing the distortion seemed to be rising off the combustor of the engine and the section of the nozzle before it mates with the exhaust duct (Figure 2.9). It was discovered that the nozzle was sucking air through the mating gap between its two sections and therefore the seal included in the initial design, did not need to be installed. Since the seal was not needed one of the seal flanges was removed. A two piece, stainless steel, telescoping shroud was made and attached to the remaining flange. This shroud extended over the back of the combustor. When the shroud was found to receive significant heating through the flange, copper tubing for water cooling was added near the flange. Two insulation blankets were also added. One covered the shroud the other was placed over the gap between the shroud and the beginning of the exhaust duct. To monitor the shroud temperature a thermocouple was attached to the upper side of the shroud beneath the insulating blanket.

The inlet ducting supplies air from outside directly to the engine inlet, without allowing the heated air from near the exhaust duct to mix with it (Figure 2.10). It is light gauge 36" diameter ducting with insulation. The inlet ducting runs from the inlet box in the ceiling to immediately above the engine inlet. The ducting can be extended to cover the inlet, if required.

#### 2.2.4.Exhaust System

When the engine was being test run at Lycoming's facility in Connecticut the noise level produced by the engine was measured and found to be very high. A sound power level meter with a max level of 140 dB measured 139 dB when placed 3 feet from the engine in the plane of the exhaust. Since the MIT test cell is near several classrooms it was necessary to quiet the engine.

The major noise source appeared to be the exhaust jet produced by the engine. Acoustically insulated exhaust ducting was used to silence the exhaust. The ducting had to go through an existing hole in the ceiling, off center from the engine exhaust. Since the silencing increases with the length of the ducting, it continues as an exhaust stack that rises about forty feet above the roof. Existing structures were used to support the stack. Another branch of the ducting was also needed, in the test cell so that other rigs could use the same exhaust system. The resulting exhaust duct has many elbows and joints (Figures 2.11 and 2.12).

The ducting was constructed by United McGill Corp. It has an outer diameter of 26 inches and an inner diameter of 20 inches. The duct is made of 304 stainless steel. It has a perforated inner wall and 3 inches of acoustic insulation. Immediately downstream of the nozzle diffuser is a muffler with a perforated center body filled with acoustic insulation. The muffler provides additional damping of the higher frequencies. The ducting is an effective sound damper. The engine sound power level has been measured as 105 dB, 10 feet from the engine in the MIT test

cell. When running under normal conditions the engine exhaust can't be heard above the ambient noise level outside the building (the inlet compressor whine is apparent).

To verify that temperatures in the exhaust remain within acceptable limits (less than 1000° F) several thermocouples are installed. A set of six thermocouples is spaced around the circumference of the duct at the diffuser exit to measure the flow temperatures there. Three thermocouples are installed after the first elbow in the ducting to measure the flow temperature. One is in the flow just above the roof line and one measures the metal temperature of the flange attachment on the roof. There is also a pressure tap with the first set of thermocouples to monitor the pressure in the duct.

#### 2.2.5. Actuator/Positioners

Two electro-mechanical actuators are used as positioning systems on the engine rig. A stepper motor is used to control the throttle setting and a linear actuator is used to set the nozzle position/area.

##### 2.2.5.1. Throttle Actuator

The throttle actuator is a Compumotor SX6 microstepping motor driver / indexer, driving a Compumotor S83-93 motor with an incremental encoder and a home switch.

The SX6 can be programmed and controlled using an RS-232C interface. It operates on 90-132 VAC 50/60 Hz supplied power. To control the motor it outputs a 170 VDC signal chopped at 21 kHz. This output caused considerable noise in the instrumentation at 21 kHz, but it was removed with low pass filters. The resolution of the controller is programmable from 200-50800 steps/rev. The default setting of 25000 steps/rev was used.

The motor has a rated stalling torque of 290 in. oz. Its accuracy is  $\pm 5$  arcminutes (unloaded), repeatability  $\pm 5$  arcminutes (unloaded), and hysteresis less than 2 arcminutes unloaded. The



encoder has a resolution of 4000 counts/rev, providing an accuracy of  $\pm 0.09$  degrees ( $\pm 5.4$  arcminutes). Far better than needed to control the throttle.

#### 2.2.5.2. Nozzle Positioner

The section of the stand which supports the engine is mounted on a pair of linear bearings. This allows the engine to be moved, changing the nozzle area. The linear bearings allow the engine to be moved up to 10 inches in the axial direction (Figure 2.13). During normal operation the range of motion is limited to 2 inches by mechanical stops that are bolted to the stand. The stops prevent the actuator from moving the engine too far in either direction and damaging the rig. The additional range of motion allows the engine to be moved away from the exhaust system so that the nozzle can be installed and removed.

The nozzle actuator is a Industrial Devices Corporation H3851 Electric Linear Motion Control System. The H3851 controls a H358A linear actuator with a home switch, end of travel limit switches and a linear potentiometer. It is mounted between the base of the movable section of the stand and the rest of the test stand, as shown in Figure 2.13. The H3581 is programmable over an RS-232C interface. The programs are then executed based on digital inputs to the H3581. It has a 6 inch range of motion and stated accuracy of 0.001 inches. Its unloaded maximum velocity is 2.1 inches/sec, and maximum rated load is 800 lbf in either direction. Load cell measurements indicate that the actual stalling load is 650 to 700 lbf in either direction.

As the nozzle is closed the engine thrust increases, increasing the loading on the actuator. The engine produces 1200 lbf of thrust at surge. This is well above the stalling load of the actuator, so it is necessary to preload the actuator. The preload is supplied by a pulley system with a four to one mechanical advantage (Figure 2.13). The standard weight placed on the pulley system, of 170 lbs is the highest preload that doesn't overload the actuator. To ensure smooth preload as the actuator moved it was necessary to use pulleys with ball bearings.

The actual engine or nozzle position is measured using the linear pot attached to the actuator. The zero position of the linear pot measurement originally matched the commanded zero position of the actuator. Hardware adjustments and software changes have changed the zero commanded position. It was decided to use the measured position as a consistent reference, whose zero position would not change from run to run. Therefore the measured and commanded zero positions no longer coincide.

#### 2.2.6. Fuel System

Fuel for the engine is stored in fifty-five gallon drums. It can be pumped directly from the drum, or transferred to a twelve gallon tank and drawn from that tank (Figure 2.14). A fill pump is used to pump the fuel from the drum either to the 12-gallon tank or directly to the fuel panel. If the 12-gallon tank is used the fuel is drawn from the tank by a Holley fuel pump mounted behind the fuel panel, with a power switch on the front. There are three manual valves mounted on the fuel panel, which are used to select the fuel source (Figure 2.14). The fuel filter is mounted behind the fuel panel. Also on the fuel panel are a pressure gauge and a flow sight gauge. These allow the operator to verify that fuel is being supplied to the engine. The fuel line is run under the floor to the engine in the test cell. There is a manual drain valve at the lowest point in the line, in the room below, and a manual vent valve on the stand. A turbine flow meter is located downstream of the vent valve. It produces a TTL pulse chain, with a frequency proportional to the flow rate. A normally closed solenoid valve is located between the flow meter and the engine. Power must be supplied to this valve or fuel will not reach the engine. Cutting the power to the solenoid is an emergency measure used to shut the engine down.

#### 2.2.7. Oil System

The oil system is a closed recirculating system (Figure 2.15). The oil is stored in a 3 gallon reservoir tank. The oil pump on the engine draws the oil from the tank and pressurizes it. The

oil filter and oil pressure transducer are mounted on the engine after the pump. The oil flows through the engine and gearbox. It is returned through the oil drains, past the chip detects and then passes through a forced air oil cooler. The oil then returns to the reservoir tank. Both the reservoir tank and the gearbox are vented to atmosphere through an oil demister located in the room below the test cell.

#### 2.2.8. Electrical System

The engine requires electrical power for the starter and ignitor. Two 12 volt automotive batteries are connected in series to supply 24 volts. (In normal aircraft applications they would be supplied with 28 volts.) The ignitor is controlled directly by the control computer using a optical isolation module (described in section 2.3.1.3.). The starter draws more current than the optical isolation modules are rated for. So the starter is controlled using a 12 volt solenoid relay that is rated for the higher current (up to 500 amps). The computer then controls the solenoid relay using an optical isolation module (Figure 2.16). The batteries are kept recharged by a battery charger that charges the batteries continuously.

#### 2.2.9. Vacuum

The transducer reference vacuum is provided by a Groschopp pump. The vacuum pump is connected to the pressure transducer rack and a manifold that connects to the back pressures of the Kulite pressure transducers. Quarter inch tubing is used for the connection to the pressure rack and eighth inch tubing is used for the connections to the Kulites.

#### 2.2.10. Cooling water

Cooling water is taken from the city water supply (Figure 2.17). It is filtered using a 5 $\mu$ m filter. The flow rate is measured using a paddle wheel flow meter that produces a sine wave with frequency and voltage proportional to the flow rate. The water is piped under the floor to the test stand. At the test stand the water flow goes to three branches. Each branch has a separate

control valve. The first branch provides cooling water for the pressure transducers and the shaker valve motor, it has a manual shutoff valve. That branch is made up of eighth inch tubing that mates with the sixteenth inch copper tubing used to cool the Kulites. The second branch provides cooling for the shroud, it also has a manual shutoff valve and is made with quarter inch copper tubing.

The third branch supplies the exhaust cooling water. This water is injected into the exhaust flow in the diffuser, to keep the air temperatures in the exhaust below 1000° F. The flow rate to the injectors is controlled by an electro-mechanical valve. The valve is positioned by a 120 VAC motor. The control computer controls the position of this motor, by toggling the power supplied to it. The valve position is indicated by an attached potentiometer. The line from the valve attaches to a manifold with eight branches that feed the eight spray nozzles on the diffuser section of the nozzle. The maximum design water flow is 8 gpm. The water spray effectively cools the exhaust.

Cooling the exhaust too well can lead to another problem. If the acoustic insulation gets wet it loses much of its acoustic damping capabilities, so it is necessary to make sure that the injected water quickly becomes steam. To assure that the water vaporizes the exhaust temps must be kept above 150° C while water is being inject. The control computer monitors the temperature in the exhaust and adjusts the cooling valve accordingly.

#### 2.2.11. Shaker

Given the engine geometry the simplest and most direct way to introduce forcing to the system without modifying the engine is to use the customer bleed air port. The customer bleed is rated to deliver up to 5 % of the massflow through the engine. Time varying the amount of the bleed to create open loop forcing was determined to be relatively simple. The "shaker" valve was attached to modulate the bleed flow through the customer bleed.

The shaker valve was designed to meet several criteria. First, to avoid decoupling the forcing from the engine it has to fit in the space near the customer bleed port. There is less than two and a half inches between the customer bleed port and the inlet scroll. There are also several pressure lines from the engine in that area that must be avoided. The second criteria is that the shaker valve must be able to withstand temperatures that may be in excess of 300° C. The third criteria for the shaker valve is that it be capable of producing variable frequency forcing.

The shaker valve consists of a cylinder valve that is spun by a motor. (Figure 2.18) The cylinder has two holes drilled through it. This produces a small steady state bleed (due to leakage around the cylinder) with 4 large pulses per cylinder revolution. By varying the DC voltage applied to the motor the frequency of the excitation can be varied from 25 to 1000 Hz. To keep the motor from over heating it is cooled by blowing oil free air through it and has a water cooling coil on its outer surface.

In the original design there was twelve foot three inches of 5/8 inches inner diameter (ID) tubing through which the bleed air was vented to atmosphere (Figure 2.19). In that line was another valve that could be opened or closed by a switch out in the control center. When this valve was closed there was no bleed flow from the engine.

That arrangement was modified due to concerns that the acoustic resonance of the tubing was interfering with the forcing of the engine. The 5/8" ID tubing was shortened to 14 inches long. It then vented into a 7 inch diameter flexible copper duct that was approximately twenty three feet long and vented to atmosphere. This arrangement did not include the shutoff valve. Without the shutoff valve there was some flow through the customer bleed port whenever the engine was running. To assure that the shaker valve did not seize up it was run at low frequency whenever the engine was operating. This venting arrangement produced a great deal of noise, but did not appear affect the forcing function (see section 3.2.2.2. for more details).

### 2.2.12. Instrumentation

The instruments attached to the rig are listed in Tables 2.1 thru 2.2 and described in the sections that follow.

Measurement	Transducer Type	Name of Transducer	Connections to the Computers and other Devices
Ambient Pressure	Setra 370	$P_o$	serial connection to control computer
Inlet Bellmouth Depression	Setra 239	P1	voltage output to control computer
Static Pressure at Axial Stator tap	Kulite XCQ-062-250 G (with Pacific Amplifier)	ku10,(ku11, ku16)	output from amp to high speed data computer
Static Pressure at Diffuser Throat	Kulite XCQ-062-250 G (with Pacific Amplifier)	ku12, ku14, ku15	output from amp to high speed data compute
Static Pressure at Customer Bleed	Kulite XCQ-062-250 G (with Pacific Amplifier)	ku17	output from amp to high speed data compute
Static Pressure downstream of Shaker	Kulite XCQ-062-250 G (with Pacific Amplifier)	ku16 (or ku11)	output from amp to high speed data compute
Total Pressure downstream of Shaker	Kulite XCQ-062-250 G (with Pacific Amplifier)	ku11 (or ku14)	output from amp to high speed data compute
Combustor Static Pressure	Setra 204D	P3	voltage output to control computer
Turbine Exit Static Pressure	Setra 204D	P5	voltage output to control computer
Nozzle Static Pressure	panel gauge		none
Exhaust Static Pressure at nozzle diffuser exit	panel gauge		none
Oil Pressure	Omega PX-176	Poil	voltage output to control computer
Inlet Temps (4)	K-type thermocouples	$T_o, T_1$	to control computer
Compressor Discharge Temp	K-type thermocouple	$T_{T3}$	to control computer
Exit Gas Temp	8 K-type thermocouples combined	EGT	to control computer

Table 2.1: Instrumentation List, Part I

Measurement	Transducer	Name	Connections to the Computers and other devices
Exit Gas Temp	a double K-type thermocouple	EGT	to temperature meter on the control panel
Exhaust System Temps (11)	K-type thermocouples	exhaust1	one is connected to the control computer
Nozzle Metal Temp	K-type thermocouple		to control computer
Shroud Metal Temp	K-type thermocouple		to control computer
Shaker Motor Casing Temp	K-type thermocouple		to control computer
Oil Temp	K-type thermocouple	T <sub>oil</sub>	to control computer
Engine Speed	Tachometer to a ratemeter	N1	RS-485 bus from meter to control computer
Fuel Flow Rate	Flow meter to a ratemeter		RS-485 bus from meter to control computer
Cooling Water Flow Rate	Flow meter to a ratemeter		displayed on control panel
Forcing Frequency Applied by Shaker Valve	Tachometer to a ratemeter		displayed on control panel
Velocity in the Bellmouth	Hotwire and Anemometer	htwr	voltage output of anemometer connected to both computers
Vibration of Engine	Vibrometer and Vibration Monitor	vibr	voltage output of monitor to control computer, scope out to high speed computer
Engine Thrust	loadcell with amplifier		amplifier output to control computer
Position of the Flow Fence	linear potentiometer		voltage drop across pot to control computer
Position of the Cooling Water Control Valve	linear potentiometer		voltage drop across pot to control computer
Position of the Nozzle Acuator	linear potentiometer		voltage drop across pot to control computer
Chip in oil line	chip detectors (2)		discrete signals to control computer
Fuel Filter Bypass	bypass indicator		discrete signal to control computer

Table 2.2: Instrumentation List, Part II

### 2.2.12.1. Pressure

There are thirteen pressure transducers attached to the rig that supply pressure readings to the computers, there are also two static wall taps in the exhaust that are monitored by dial gauges. The flow path through the engine and the exhaust is traced as these pressures are described below.

The ambient pressure of the test cell is measured using a Setra model 370 digital pressure gauge. It is located on the control panel in the hall and connected to the pressure rack in the test cell (Figure 2.20) by a quarter inch tube. The Setra 370 is certified per National Bureau of Standard traceable primary standards. It has a range of 600 to 1100  $\pm$  0.01 mbar. The Setra 370 is also used as a reference when calibrating the other transducers. (The calibration procedures are described in detail in the sections dealing with the respective computers.) The Setra 370 is connected to the control computer via a RS-232 serial port.

There are four static wall taps at the throat of the calibrated inlet bellmouth. The depression at these taps is used to calculate the massflow through the engine. Each tap is connected to a solenoid valve on the pressure transducer rack (Figure 2.20) by eighth inch tubing. These solenoid valves are manifolded together and connected to the inlet pressure transducer (P1). The inlet pressure transducer is a Setra 239 pressure transducer with a range of  $\pm$  15 in H<sub>2</sub>O. The output range is  $\pm$  5 VDC and it requires a 15 VDC power supply. It is rated at  $\pm$  0.1 % FS nonlinearity. The inlet pressure transducer can also be connected to the Setra 370 and a vacuum reference. The voltage output from the inlet pressure transducer is connected to the control computer.

Lycoming installed twelve static wall taps in the engine for this project. The first six of these taps are located at midchord between the axial stage stators upstream of the centrifugal compressor (Figure 2.3). They are spaced around the circumference. Uniform spacing was not



possible due to the engine geometry. Each tap has a static pressure probe attached to it. The probe consists of a 14 inch long 30 mil ID tube that is connected to a 50 mil ID sensing plenum. The plenum is 0.25 inches long. The pressures in the sensing plenum are measured by Kulite pressure transducers. Only eight Kulite pressure transducers were available, this limited the number of taps at which pressures could be monitored at any one time. Therefore, the number of stator taps that were monitored by Kulites varied from one to three depending on the run.

The other six static wall taps are located at the diffuser throat (Figure 2.3). They are uniformly spaced about the circumference of the engine. Each tap has a static pressure probe with a 5.5 inch long 40 mil ID tube connecting it to the sensing plenum. These plenums are 0.25 inches long and have an inner diameter of 50 mils. For most runs Kulites were connected to three taps ( located at 0, 120 and 240 degrees) at the throat.

One of the purposes of the pressure taps at the stator and throat locations is to check for rotating disturbances as the engine nears the stall point. Rotating stall typically moves at about half the rotor frequency. At 100% speed the rotor frequency is about 800Hz. So allowing for some variations the pressure taps need to have a response time that allows for the measuring of 500 Hz disturbances. The pressure taps and transducers act as helmholz resonators, where the helmholz frequency can be considered to be the limiting frequency on the response of the taps (see Appendix B). As shown in Appendix B the resulting max frequency responses are 713 Hz for the taps between the stators and 1734 Hz for the taps at the throat.

There are 3 pressure taps on the shaker customer bleed valve assembly (Figure 2.21). Upstream of the shaker is a static pressure tap. When forcing is being applied this tap measures the pressure forcing applied at the customer bleed. When the engine is run without forcing, this tap measures the static pressure at the upstream end of the combustor. Downstream of the shaker valve are total and static pressure taps. These two taps are used to calculate the forcing in terms of bleed massflow. All three of these taps are connected to Kulite pressure transducers.

Two bolts in the combustor were replaced with pressure tapped bolts (Figure 2.3). These taps allow the static pressure in the combustor to be measured. One of these taps is connected directly to a Kulite pressure transducer. The other is connected, by an eighth inch tube, to a solenoid valve on the pressure transducer rack (Figure 2.20). The line from that valve leads to the combustor pressure transducer. It is a Setra 204D pressure transducer with a range of 0 to 250 psid. Its output is 0 to 5 VDC and requires a 15 VDC power supply. It has  $\pm 0.1\%$  FS nonlinearity. The values from this transducer are used to determine the pressure rise through the compressor.

The static tap at the turbine discharge is connected to the pressure transducer rack via eighth inch tubing. On the rack it connects to the turbine discharge pressure transducer (Figure 2.20). This transducer is a Setra model 204D pressure transducer. It has a range of -10 to 50 psid, with an output of -1 to 5 VDC and requires a 15 VDC power supply. It has  $\pm 0.1\%$  FS nonlinearity. This transducer is used to monitor the behavior of the turbine as the nozzle is closed.

Static wall taps at the entrance to the nozzle diffuser and in the exhaust duct at the exit of the diffuser are used to monitor the pressure drop in the exhaust system. These taps are connected to panel gauges via eighth inch tubing. The gauges are located near a window where they can be read from outside the test cell.

The final pressure measured on the rig is the oil pressure. The oil pressure transducer is physically mounted on the engine. It is located on the oil supply line, after the pump and filter (Figure 2.15). This transducer is an Omega PX-176 with a 0-200 psi range. It has a nominal output range of 1 to 6 VDC and is supplied by a 15 VDC power supply. The power supply and voltage output are wired through the pressure transducer rack. The oil pressure transducer was calibrated before installation. Since it is sensitive to temperature variations and the offset is expected to drift with time the pressure produced has an uncertainty of  $\pm 4$  psi. This is

acceptable since its purpose is merely to assure that the oil is being pressurized to an acceptable pressure (at least 80 psia at full power).

The inlet, combustor, and turbine discharge pressure transducers are all mounted on the pressure transducer rack (Figure 2.20). The backpressures on all three transducers are connected together. The backpressure can be vented to atmosphere, connected to the Setra 370 and/or connected to the vacuum. The vacuum and Setra 370 connections are used during the transducer calibrations. The solenoid valves on the pressure transducer rack are controlled by the computer and used to control which pressures are measured.

All the Kulite pressure transducers on the rig are Kulite XCQ-062-250 G pressure transducers. These transducers have a rated pressure of 250 psig and maximum pressure of 500 psig. They have compensated temperature ranges from 60° to 350° F. The sensitivities of the Kulites range from .32 to .59 mV/psi output, with a 10- volt power supply. These transducers are connected to Pacific Amplifiers. The output from the amplifiers is connected to the high speed data acquisition computer. The amps supply the Kulites with 10 volt excitation. They can be set to amplify the Kulites' output signals by factors of 1, 2, 5, 10, 20, 50, 100, 200, 500 or 1000. Each amplifier also contains a lowpass filter that can be set at cutoff frequencies of 10 kHz, 1 kHz, 100 Hz, 10 Hz or taken off line. The input and output offsets are also adjustable. Each Kulite-amplifier pair is calibrated with a reference pressure, before and after every run. When in use the backpressure of the Kulites is evacuated.

#### 2.2.12.2. Vibration

Attached to the engine is a IMO industries velocity vibration transducer type 4-128-0001, with an output of 60.5 mV/ in/sec. The signal from the transducer is fed to a model VM-110 vibration monitor provided by Lycoming. The monitor produces a 0 to 50 mV output that corresponds to 0 to 1.5 in/sec of vibration, this signal is fed to the control computer. It also has a

0 to 5 volt scope output that also corresponds to 0 to 1.5 in/sec and is connected to the high speed data acquisition computer.

#### 2.2.12.3.Flow

The steady state massflow through the engine is calculated from the depression of the static wall taps at the throat of the calibrated bellmouth. A hotwire placed in the bellmouth is used to provide a measure of the massflow with a high frequency response. Holes for three hotwires were drilled three inches from the base of the bellmouth. A TSI model 1210-T1.5 hotwire is inserted through the center hole. It is connected to a TSI model 1050 constant temperature anemometer. The output from the anemometer is fed to both computers. The data from the control computer is used to establish the correlation between the hotwire output voltage and the massflow through the engine. That correlation is used to convert the high speed data into an "instantaneous" massflow through the engine.

#### 2.2.12.4.Engine Thrust

The thrust produced by the engine is measured by a loadcell connected between the nozzle actuator and the engine "cart" (Figure 2.13). A Sensotec 571 loadcell and amplifier are used. It has a range of  $\pm 1000$  lbs force with an output of  $\pm 5$  VDC and an error of  $\pm 5$  lbs. The requires power is supplied by a 15 VDC power source. The loadcell is used as a diagnostic tool and to provide a warning as the thrust of the engine is approaches the level that will cause the nozzle actuator to stall.

#### 2.2.12.5.Position Indication

There are three devices on the rig whose positions are measured using linear potentiometer. The first device is the flow fence. The flow fence actuator is connected to a potentiometer. As the flow fence retracts the position of the potentiometer varies. Full retraction is indicated when the voltage drop across the potentiometer does not change as the engine speed is increased.

There are also linear pots on the nozzle actuator and the valve that controls the flow to the water injectors in the exhaust system diffuser. The potentiometer are supplied by a 15 VDC power supply and the voltage drop across them is measured by the control computer. The information for the nozzle actuator is converted to position (in inches) the other two are left as voltages.

#### 2.2.12.6. Temperature

Temperature measurements are taken at many locations on the rig. There are four thermocouples at the bellmouth inlet. One is inserted into the flow downstream of the compressor to provide compressor discharge temperature ( $T_{T3}$ ). A ring of eight thermocouple located around the circumference of the engine exit are combined in the engine electrical harness to produce a single engine exit temperature (EGT) reading. An additional double thermocouple was inserted into the engine exit to provide an independent measure of the EGT. Six thermocouples are inserted into the flow at the exhaust system diffuser exit. Three more are located after the first elbow in the exhaust duct. A thermocouple measures the temperature of the flange that secures the exhaust duct to the roof. An additional thermocouple is inserted into the exhaust flow above the roof line. Thermocouples are also used to monitor the nozzle metal temperature, the temperature of the shroud that covers the combustor and the temperature of the shaker valve motor casing. A thermocouple inserted into the oil reservoir measures the oil temp.

All the thermocouples used on the rig are K-type thermocouples. One of the EGT thermocouples is attached to an Omega DP41-TC temperature meter. The control computer needs one exhaust thermocouple to control the water injection, the other exhaust thermocouple are not currently connected. The remaining thermocouples are all connected to the control computer, via terminal panels with cold plate junctions.

The Omega temperature meter, has a built in cold plate junction. It is mounted on the control panel in the hall and serves as an independent safety. The power supply to the fuel

solenoid valve passes through a relay board installed in the meter. If the EGT rises above 843° C the meter will open the relay, cutting the power to the solenoid and the fuel to the engine.

#### 2.2.12.7. Rate Measurements

There are four Newport Infinity 7 ratemeters connected to the rig. All four are mounted on the control panel in the hall. Each meter has an RS-485 serial comm port and can be connected to the RS-485 bus mounted inside the control panel. The RS-485 bus is connected to one of the RS-232 serial ports on the control computer, through a RS-232 to RS-485 converter.

The N1 (engine speed) meter measures the frequency of the sine wave output by the engine tachometer. It divides the frequency by 43.17 to produce engine speed in % speed. This value is displayed on the meter and downloaded to the control computer via the serial port. The N1 meter has a relay board installed. The power to the fuel solenoid is wired through this board. If the engine speed goes above 105.6 % speed, the power to the fuel solenoid and thus the fuel supply to the engine, is cut.

The fuel flow ratemeter accepts a TTL signal from the fuel flow meter as its input. The frequency of this signal is measured and divided by 65.8529 to produce flow rate in gallons/minute (gpm). The fuel flow rate is displayed on the meter and downloaded to the control computer via the serial comm port.

The water flow ratemeter receives a sine wave input from the flow meter in the cooling water line. The frequency of that signal is multiplied by 0.13080 to produce flow rate in gpm. The flow rate is displayed on the meter, but not downloaded to the control computer.

The fourth ratemeter is connected to a tachometer on the shaker valve and is used to provide real-time readout of the excitation frequency being produced by the shaker. This value is not downloaded to the control computer.

### 2.3. Control Computer

The control computer is a Dell 433DE, a 486 based PC running at 33 MHz. This computer controls the engine and monitors and records its performance. A process control package called Genesis, produced by Iconics is used. This software package sets the nozzle and throttle positions through two actuators controlled via serial ports, monitors engine speed and fuel flow using the ratemeters connected to another serial port, ambient pressure through the fourth serial port and other pressures, temperatures and voltage signals using 2 A/D boards. It also controls several on/off switches through a digital I/O board and accepts operator commands. The software cycles at 1 Hz scanning all the A/D channels, but it takes about 2 seconds to cycle through the serial port data acquisition routine.

#### 2.3.1. Hardware

There are four boards installed in the control computer that are used to control the engine (Figure 2.22). The first board in the computer is an ACPC-16-16, the second an ACPC-12-16, and the third an ACPC-I/O board. These three boards are all made by Strawberry Tree Inc. The fourth board is a Digiboard comm port board. The serial comm ports built into the computer are also used. Wiring schematics for the connections to this computer are included in Appendix C.

##### 2.3.1.1. ACPC-16

The ACPC-16-16 is a 16 bit analog to digital conversion board with 16 differential inputs. The maximum data acquisition speed of the board is 2.5 KHz (per channel). It has six programmable voltage ranges;  $\pm 25\text{mV}$ ,  $\pm 250\text{mV}$ ,  $\pm 5\text{V}$ ,  $0-50\text{mV}$ ,  $0-500\text{mV}$ ,  $0-10\text{ V}$ , that can be individually selected for each channel. It also has 16 digital input or output channels.

This board has two terminal panels, each panel is connected to the board in the computer by two ribbon cables and functions as a break out panel for the signals. The first panel is a T41

panel. This panel handles the first 8 analog inputs and the first 8 digital I/O channels. Optical isolation modules can be installed on the digital I/O channels on this terminal panel.

The second terminal panel is a T11 panel. This panel has the second eight analog inputs and digital I/O channels. This board has a built in cold plate junction for use with thermocouples, but can also accept simple voltage inputs. This board does not have space for the optical isolation modules.

#### 2.3.1.2.ACPC-12

The ACPC-12-16 is a 12 bit analog to digital conversion board with 16 differential inputs. The maximum data acquisition speed of the board is 10 KHz (per channel). It has six programmable voltage ranges;  $\pm 25\text{mV}$ ,  $\pm 250\text{mV}$ ,  $\pm 5\text{V}$ ,  $0-50\text{mV}$ ,  $0-500\text{mV}$ ,  $0-10\text{ V}$ , that can be individually selected for each channel. It also has 16 digital input or output channels. The ACPC-12-16 also has two terminal panels. Both of these panels are the T11 panels described above.

#### 2.3.1.3.ACPC-I/O

The ACPC-I/O board has the capability to handle 160 digital input or output channels. Connected to this board is one T400 terminal panel. The T400 panel had spaces for 40 high power optical isolation modules or 20 low cost (2 channel) optical isolation modules.

The optical isolation modules are optically isolated solid state relays that allow the I/O board to sense or control discrete signals with voltages above 5 volts. They also protect the board from voltage spikes. Different isolation modules are used for different voltage levels. One type of opto-isolation module is used to switch 12, 15 and 28 VDC signals. Other types are used to control 120 VAC signals and TTL (5 VDC) signals.



#### 2.3.1.4. Serial Ports

The Digiboard comm port board provides four additional RS-232 comm ports for the computer. The two serial comm ports built into the computer (ports 1 and 2) and two of the ports on the Digiboard (ports 3 and 4) were used. Comm port 1 is set at 9600 baud, 8 bits, 1 stop bit, and no parity. It is connected to the Setra 370 pressure transducer. Comm port 2 is set to 9600 baud, 7 bits, 2 stop bits, and odd parity. It is connected to the Newport ratemeters via the RS-232 to RS-485 converter and the RS-485 bus. Comm port 3 is set to the same parameters as comm port 1. It is connected to the H3851 linear actuator controller (the nozzle actuator). Comm port 4 is also set to the same parameters as comm port 1. It is connected to the Compumotor SX6 (throttle controller).

#### 2.3.2. Software

Two sets of control software have been used to run the engine. It was first run using a program written in C (a listing is in Appendix D). This program was used until the Genesis software package was available to run the engine (there were some software to hardware interface problems). Both programs acquire data from the analog and digital inputs and via the serial ports. The programs calculate several values based on the data, display the data on the screen and record it. The programs provide operator control of the nozzle and throttle settings and the digital outputs (to the starter, ignitor and fuel valve). Both also provide a warning if alarm conditions occur, while running the engine.

The Genesis configuration has the following advantages. It includes a calibration routine for the steady state pressure transducers, and it also provides a display of the operating map with the current operating point indicated by a dot on the map. Genesis also has a color display, which is used to indicate alarms and it has programmed responses to some of the alarm conditions. It also controls the position of the valve on the supply line to the water injectors on the exhaust diffuser,

to keep the exhaust temperatures within acceptable limits. In addition the Genesis configuration records more data signals and has a faster cycle speed, providing tighter control of the engine.

#### 2.3.2.1. Genesis Overview

There are four distinct parts of the Genesis system, they are the configuration builder, the display builder, the usertask and the runtime system. The interaction of these systems is described below and diagrammed in Figure 2.23.

The configuration builder allows the operator to develop and construct complex process control configurations using a graphical, flow chart type system. Each device, input or output signal has a box. Signals are then routed to other boxes where they are acted upon converted from volts to psi, delayed, counted, etc. The configuration builder produces a configuration database that all the other parts of Genesis interact with.

The display builder is called from within the configuration builder. It allows the operator to build complex graphical displays. These displays can include any value in the configuration database, objects that change size, location, or color based on the magnitude or state of any value in the configuration. They can also include several options for user input. The first of these is a data entry block, which allows the operator to enter a value and have it inserted into the configuration database. The second is a definable keymacro. A key on the keyboard is specified to trigger a particular action, ie. changing the state of a digital value, switching to another display, etc. or several of these things at once. The display is stored in a display file.

The usertask is a routine written in C, that runs in the background in runtime. It acts as an interface between the configuration database and the serial ports. The usertask takes specified values from the configuration database, inserts them into command strings and sends the commands over the serial ports to the actuators. It also polls the Setra 370 and Newport ratemeters over the serial ports. The reply from the meters is converted to the database format

and then inserted into the database. The usertask also contains an initialization routine, which is run as part of the runtime startup.

The runtime system is used to run the engine. It interacts with the database changing and updating the values in it based on the inputs, calculations, commands, etc. Runtime also controls the display. It splits the screen into two sections. Runtime reads the selected display file and places it in the upper portion of the runtime display. It handles any operator commands and send the current values from the database to the screen. Runtime also coordinates the interaction between the database and the usertask. The second section of the screen is a small portion at the bottom of the display that allows more direct access to the configuration database and the runtime system. The lower section is particularly useful for debugging because it provides the ability to override normal configuration behavior.

#### 2.3.2.2.Data Inputs

As listed in Tables 2.1 and 2.2 the following signals are connected to the control computer and read by Genesis. The inlet, combustor, turbine discharge and oil pressure signals are all read on the  $\pm 5$  V scale and then converted to pressures. The voltage drops across the linear pots are measured on the 0-10 V scale. The vibration monitor output is read on the  $\pm 50$  mV scale. The hotwire anemometer and the loadcell signals are both read on the  $\pm 5$  V scale. The remaining signals are all K-type thermocouples whose outputs are converted to  $^{\circ}$  C by the device driver for the Strawberry Tree boards. The following temps are monitored by Genesis; four inlet temps, the compressor discharge temp, the engine exit temp, the oil temp, the temp of the hot section of the nozzle, the air temp in the exhaust duct (at the exhaust diffuser exit), the shroud metal temp, and the temp of the shaker motor casing. Other temperatures are available (and connected to the computer), but currently not monitored.

The following discrete input signals are also monitored; the two chip detects and the fuel filter impending bypass indicator (from the engine). Connected but not currently monitored are throttle and nozzle actuator move complete signals, the exhaust cooling valve full open and full closed indicators, and the state of the fuel solenoid valve.

There are also three data values that are read via the serial ports. The engine % speed (N1) and fuel flow rate are both read from the frequency ratemeters using comm port 2. The ambient pressure is read from the Setra 370 via comm port 1.

### 2.3.2.3.Runtime Data Reduction

The first calculations performed by Genesis are the volts to engineering units conversions. The pressures, the loadcell, the vibrometer and the nozzle actuator linear pot signals are all converted. The pressures are converted using,

$$pressure(psi) = (volts \times scale) + offset, \quad (2.1)$$

where the scale and offset are provided by the calibration routine. The loadcell conversion is,

$$lbf = volts \times 200. \quad (2.2)$$

The vibrometer signal is preprocessed and amplified by the vibration monitor, so the required conversion is,

$$in/sec = volts \times 30. \quad (2.3)$$

The conversion for the nozzle actuator linear pot is,

$$inches = (volts - 5.3681) \times \frac{6.3682}{10} + 1.331 \quad (2.4)$$

Other calculated values are the pressure ratio, corrected massflow, corrected speed (of the engine), and turbine inlet temp. The formula for the pressure ratio is as follows,

$$\frac{P_{T3}}{P_{T0}} = \pi = \frac{P3+P0}{P0} \times 1.01 \quad (2.5)$$

The factor of 1.01 is added to convert combustor pressure from the measured static pressure to total pressure. This conversion was specified by Lycoming.

The formula for the corrected engine speed is as follows,

$$N1_{corr} = \frac{N1}{\sqrt{\theta}} \quad (2.6)$$

where,

$$\theta = \frac{T_1(^{\circ}F)+459.7}{518.7} \quad (2.7)$$

$T_1$  is the inlet temp provided by one of the thermocouples on the inlet bellmouth. Genesis converts from °C to °F when placing the values in the formula.

The corrected massflow and turbine inlet temperature are calculated using formulas provided by Lycoming. For these formulas the following definitions apply;

$$AF = \frac{W\sqrt{\theta}}{\delta} \times \frac{\delta}{\sqrt{\theta}} \times \frac{(0.9688-BLD)(3600)}{\left(\frac{WF \times LHV}{18500}\right)} \quad (2.8)$$

where WF is the fuel flow rate,

$$WF(lbs/hr) = fuelflow(gpm) \times 60 \times 6.74 \quad (2.9)$$

LHV is the fuel lower heating value (18550 BTU/lbm) and BLD is the ratio of the massflow through the customer bleed to massflow through the engine.  $\theta$  is defined as above and  $\delta$  is the standard correction factor of,

$$\delta = \frac{P_o}{29.92} \quad (2.10)$$

$P_o$  is in inches Hg absolute for these formulas. PSBM is the bellmouth static depression from ambient in inches  $H_2O$ . PTBM is the bellmouth total pressure depression from ambient and is assumed to be zero.  $T_{T3}$  is in °F for these formulas. Genesis performs the units conversions when applying the formulas.

The corrected massflow formula is,

$$\frac{W\sqrt{\theta}}{\delta} = 43.32 \left[ 0.192335 \left( \frac{PSBM-PTBM}{P_o} \right)^{0.5} - 0.007874 \left( \frac{PSBM-PTBM}{P_o} \right)^{1.5} + 0.000046 \right] \quad (2.11)$$

and the turbine inlet temperature formula is,

$$T_{T4.1} = \frac{72675}{AF} - \frac{302264}{AF^2} + 0.9576 \times T_{T3} - 6.679 \times \frac{T_{T3}}{AF} + 43.6 \quad (2.12)$$

#### 2.3.2.4.Data Recorded

The configuration uses Genesis historian blocks to save data to the disk. Each historian block can record up to 20 items of data. There are three historian blocks in the configuration, one records data during the calibration for later use in determining the reliability of the calibration. The other two blocks record data while in the run mode, unless they have been disabled by an operator command. The data recorded by each block is listed in Table 2.3.

#### 2.3.2.5.Control Outputs

Genesis produces three types of control signals. The first two are sent over the serial ports, using the usertask. One goes to the throttle actuator the other to the nozzle actuator. The third type is the discrete output signals that control various off/on systems.

Genesis sends a series of initializing commands to the throttle actuator (SX6) via comm port 4. These commands put the actuator in the absolute position mode, based on encoder counts. In this mode the controller moves the motor to and maintains it at a position, commanded as

Block	Calibration Historian	Run Historian #1	Run Historian #2
Records	when in the calibration mode	when in the engine run mode unless disabled	
Data Recorded	calculated inlet pressure (psi) calculated combustor pressure (psi) calculated turbine discharge pressure (psi) offset of inlet pressure offset of combustor pressure offset of turbine discharge pressure scale of inlet pressure scale of combustor pressure scale of turbine discharge pressure voltage output of inlet pressure transducer voltage output of combustor pressure transducer voltage output of turbine discharge pressure transducer the state of the following solenoid valves from the pressure rack 5, 6, 7&9, 8, 11,12	ambient pressure (psi) P1 (psi) P3 (psi) P5 (psi) oil pressure (psi) inlet temp #1 (° C) inlet temp #2 (° C) inlet temp #3 (° C) inlet temp #4 (° C) combustor discharge temperature (° C) calculated turbine inlet temp (° F) EGT (° C) shroud metal temp (° C) nozzle metal temp (° C) voltage drop across cooling water valve voltage drop across the flow fence pot shaker motor casing temp (° C) fuel flow (gpm) N1 (% speed)	N1corr(% speed) pressure ratio corrected massflow (lbs/sec) loadcell reading (lbsf) vibrometer output (in/sec) fuel solenoid state starter state ignitor state commanded throttle position (degrees) hotwire output (volts) nozzle position from potentiometer (inches) state of chip detects state of fuel filter bypass state of nozzle activation marks count inlet pressure tap being scanned trigger state oil temp (° C)

Table 2.3: Data Recorded by Genesis

encoder counts from the zero position. (If forced away from that position the actuator will attempt to return.) The speed (.1 rev/sec) and the starting and stopping accelerations (5 rev/sec<sup>2</sup>)

are both set as well. The actuator is commanded to find the home switch. The home switch is positioned to match the throttle off position. That location is defined as the zero position by setting the encoder counts to zero.

To command the throttle to a new position, the computer sends the new position in encoder counts followed by the move command. The throttle on the engine moves through a 98° arc between the off and maximum power positions. Therefore Genesis is programmed to only command positions between 0 and 98 degrees. The throttle position can be commanded in 0.1 degree increments or moved in 1 degree increments.

The nozzle controller (H3581) is programmed over comm port 3. The initialization sets the controller's response to several digital input signals, ie. jog, run program #, etc. The number of the program to be executed after a reset is also specified and that program is downloaded. The reset program contains the commands needed to find the home switch and set that as the zero position for this actuator. Then a reset command is given.

To position the actuator a positioning program is downloaded from the computer to the actuator. This program contains the new position and the move velocity and starting and stopping accelerations. The positioning program is triggered by the digital inputs to the H3581.

Genesis also controls several discrete outputs using the opto-isolators. The outputs are at several different voltage levels. Sixteen 120 VAC signals are controlled. Thirteen of these signals operate solenoid valves on the pressure rack (Figure 2.20). The other three are the fuel shutoff solenoid valve control and the open and close commands for the valve on the exhaust cooling water supply. There are also five TTL (5 VDC) signals. One is used to trigger the high speed data acquisition. The other four are used to trigger programs on the nozzle actuator. (One of those four is an override that turns the other three off.) The starter and ignitor are also controlled using discrete outs. The starter is a 12 VDC signal and the ignitor a 24 VDC signal.



### 2.3.2.6. Alarms

Genesis checks for the alarm conditions listed in Table 2.4. If a warning alarm is triggered the alarmed value is displayed in yellow type on the screen. If an absolute alarm is triggered the value is shown in red. When not in an alarm state the values are displayed in green. Absolute alarms require immediate action which may include shutting down the engine. If an absolute alarm on N1 or EGT occurs, Genesis moves the throttle to the idle position. N1 and EGT are also monitored by independent meters on the control panel. As explained earlier, these meters can cut the fuel to the engine if N1 or EGT are too high.

Alarm State	Alarm Level	Programmed Response
oil temp high, warning	99° C	value displayed in yellow
oil temp high, absolute	110° C	value displayed in red
oil pressure high, warning	100 psig	value displayed in yellow
oil pressure high, absolute	120 psig	value displayed in red
oil pressure low, warning	80 psig	value displayed in yellow
oil pressure low, absolute	20 psig	value displayed in red
chip detect absolute	chip detected	"chip detect" is listed on display
N1 high, warning	102 % speed	value displayed in yellow
N1 high, absolute	103 % speed	value displayed in red and the throttle is moved to idle
EGT high, warning	732° C	value displayed in yellow
EGT high, absolute	843° C	value displayed in red and the throttle is moved to idle

Table 2.4: Alarm Conditions

### 2.3.2.7. Operating Modes

The Genesis configuration used to run the engine has four displays each of which corresponds to an operating mode. These displays are the initialization screen, a menu screen, the pressure transducer calibration display and the engine run display. The operator can move between these screens as indicated by the arrows in Figure 2.24.

#### 2.3.2.7.1. Initialization

When runtime is started the discrete output signals may default to the on condition, causing the starter and ignitor to turn on. The starter and the ignitor will not turn on if the racks in the test cell are not turn on. So the runtime software is started before the racks are turned on. The configuration starts in the initialization mode, which turns off the discrete outputs that control the starter and ignitor. The operator is then instructed to turn on the racks in the test cell. Once the racks are turned on the operator may move to the menu by pressing the space bar.

#### 2.3.2.7.2. Menu

The menu display contains the software credits and a menu with three selections. The available selections are calibrating the pressure transducers, running the engine, or exiting the software. Each option is selected by hitting a key on the keyboard. "x" exits the software, "c" calibrates the transducers and "a" moves to the engine run screen.

#### 2.3.2.7.3. Calibration

All the steady state pressure transducers (oil, inlet, combustor and turbine discharge) were calibrated before they were installed. The initial calibration and resulting formulas are in Appendix E. When the switch was made to using Genesis this calibration procedure was added.

Since the oil pressure transducer is mounted on the engine and the pressure only needs to be known to  $\pm 5$  psig, Poil is not calibrated by this procedure. It is just calculated using this formula,

$$press = (volts - 1.0273) \times 39.9 \quad (2.13)$$

The inlet, combustor and turbine discharge pressure transducers are all calibrated using the same method, but different pressures. The inlet pressure transducers is calibrated first and then compressor and turbine discharge pressure transducers are calibrated together. The calibration

starts by taking 100 data points at 0 psid. These points are averaged together and used to calculate the offset. A known pressure is then applied to the transducer and another 100 data points taken. These points are also averaged together and then used, along with the 0 psid data to calculate the scale. Note, this assumes that the pressure to voltage relationship is linear. The resulting equations for the offset and scale are;

$$offset = \bar{V}_{lo}, \quad (2.14)$$

and

$$scale = \frac{\bar{P}_{hi} - \bar{P}_{lo}}{\bar{V}_{hi} - \bar{V}_{lo}} \quad (2.15)$$

For these formulas, Vs are voltages and Ps are pressures. The subscript lo denotes values from the zero psid point, while the subscript hi denotes values from the reference pressure readings.

The calibration pressure applied to the inlet pressure transducer is about -.35 psid. Several steps are needed to produce this pressure. The ambient pressure is measured using the Setra 370 and stored. Then the back pressure is closed off from the atmosphere and the Setra 370 is connected to the front of the inlet pressure transducer. The front pressure of the inlet pressure transducer is opened to the vacuum pump until the pressure has dropped at least .30 psi, as indicated by the Setra 370. It is then closed off from the vacuum and 100 data points are taken.

To apply a pressure to the combustor and turbine discharge transducers, the backpressures are evacuated using the vacuum pump. With the back pressures at vacuum there is a one atmosphere pressure differential across the transducers. This is used as the calibration pressure.

The calibration display shows the status of the calibration and several values related to it. The pressure being read by the Setra 370 is shown. The current offsets and scales for all three transducers are displayed, and the number of data points taken at the current pressure are

indicated. The display also shows the state of each solenoid valve on the pressure rack (open or closed).

The operator may exit the calibration mode at any time by pressing the space bar. If interrupted the calibration is invalidated. It should be restarted and completed before the engine is run.

#### 2.3.2.7.4. Running the Engine

The engine run mode display contains a great deal of information. It lists the following values; Ambient pressure, inlet pressure, combustor pressure, turbine discharge pressure, oil pressure, the four inlet temps, the compressor discharge temp, the calculated turbine inlet temp, the EGT, the shroud, nozzle, exhaust, shaker motor casing, and oil temps. It also lists the fuel flow rate, engine speed both absolute and corrected, the corrected massflow through the engine, the calculated pressure ratio, the loadcell and vibration levels, the volts across the flow fence and cooling valve pots, and the nozzle position from the pot on the actuator. The commanded throttle position is also displayed. The display also lists the state of the chip detects, fuel filter bypass, data logging, fuel solenoid, the starter, the ignitor, and the nozzle actuator. It also indicates if the inlet pressure is being read from all four taps simultaneously or if they are being scanned through (read one at a time). The control keys for those states are indicated in the labeling. If any of the values in these listing are out of the acceptable range this is indicated by a change in the color the value is displayed in. Green indicates an acceptable value, yellow a dangerous one, and red an unacceptable value requiring immediate action. There are also two data entry blocks that allow the user to directly input commanded nozzle and throttle positions. Also on this display is an operating map on which the current pressure ratio and massflow are indicated by a red dot. The range of this map is limited to near 95 % speed, where most of the data was collected.

There are many keystroke commands for this mode. For safety most of them require that two keys be pressed at the same time, like "ALT-S" which toggles the starter off and on. There are two exceptions, the panic buttons, "" and "-", and the "Esc"ape key. The panic buttons are located on the upper outside corners of each side of the keyboard. They return the engine to idle. The escape key exits the run mode and sets the throttle position to zero, if its not already there. All of the commands are listed in Table 2.5.

<u>Keys</u>	<u>Action</u>
data entry	set nozzle axial position to 0.001 in.
data entry	set throttle position to 0.1°
ALT-q	bump throttle - 5°
ALT-w	bump throttle -1°
ALT-e	bump throttle +1°
ALT-r	bump throttle +5°
ALT-a	toggle nozzle actuator active
ALT-s	toggle starter
ALT-i	toggle ignitor
ALT-f	toggle fuel solenoid
ALT-l	toggle data logging
ALT-n	toggle inlet pressure tap scanning
ALT-b	trigger high speed data
ALT-m	make a mark on data record
`	"panic", return to idle
-	"panic", return to idle
Escape	set throttle to zero and exit run mode

Table 2.5: List of Command Keys for the Run Mode

### 2.3.3. Typical Run Procedure

A typical run follows the this procedure. After going through the pre-run checklist (Appendix F), Genesis is started on the computer. The racks in the test cell are turned on when the program indicates that the computer is properly initialized. Then the pressure transducers are

calibrated using the calibration routine. Once the transducers are calibrated Genesis is switched to run mode. The starter and ignitor are turned on. When 10 % engine speed is indicated the throttle is moved to 25°. After light off the throttle setting is gradually increased. The starter and ignitor are turned off at about 30 % speed and the throttle setting is increased until the engine reaches idle, 50 % speed. The engine is given a few minutes to warm up. Then the engine speed is increased to 95 % or until the flow fence is fully retracted, whichever occurs later. From 95 % speed the engine speed may be increased to map a throttle line, but the most common situation is to activate the nozzle actuator and begin to trace a speed line, by closing the nozzle. Genesis turns on the exhaust cooling water automatically when the exhaust temp exceeds 375° C. It then controls the water flow rate to keep the exhaust temp between 150 and 375 degrees C. High speed data is taken at several points as the nozzle is closed. As the engine is brought closer to surge the high speed A/D system is triggered before each nozzle movement. If the engine surges the panic button is hit returning the engine to idle. The nozzle is opened again, and the engine returned to idle (if not already there). The engine is run at idle for 2 minutes to allow it to cool off and then shutdown. The pressure calibration is run again to check the drift during the run. Genesis is shut down and the data analyzed.

#### 2.4. High Speed Data Acquisition Computer

The high speed data acquisition computer is a Dell 425E. It is a 486 based PC running at 25MHz with an EISA bus and 16 Mbytes of memory. The computer has three high speed A/D boards and a programmable filter board installed, with a breakout panel for each board on the back of the computer cart (Figure 2.25). MMADCAP, the data acquisition software supplied with the A/D boards, is used for the high speed data acquisition. The data is backed up using the tape drive installed in the computer.

### 2.4.1. Hardware

#### 2.4.1.1. ADTEK Boards

The first three slots in the computer contain ADTEK AD-380 A/D boards. These boards have 8 12-bit differential data channels a piece. They can sample at up to 333 kHz per channel. Each channel has its own programmable gain amplifier, sample and hold, and A/D converter so the noise and crosstalk problems of a multiplexer are removed. The channels can be set to the following ranges  $\pm 10$  V,  $\pm 5$  V,  $\pm 2.5$  V or  $\pm 1.75$  V. The boards can run using internal or external clocking. For internal clocking the first board supplies the clocking signal for any other boards in use. The data acquisition can also be set to be triggered by the software or an external signal supplied to the first board.

#### 2.4.1.2. Filter Board

The programmable filter board is a Techfilter board made by Onsite Instruments. It is provided with software that allows the user to set the filter parameters. It is a lowpass filter (specifications are listed in Appendix G). The cutoff frequency can be set in 1 Hz increments from 1 to 250 Hz, in 10 Hz increments from 250-2500 Hz and in 100 Hz increments from 2500 to 25 kHz. All the channels are filtered at the same cutoff frequency, unless they are independently set to bypass the filter. Each channel can be set for single ended or differential signals and for AC or DC coupling of the signals. An additional gain of 1, 10, 100 or 1000 is applied to the output of each channel. The breakout panel for this board has sixteen input and sixteen output BNC connectors.

### 2.4.2. Software

Two programs are used to collect data on this computer. ADTDVM allows the computer to function as a multi-channel digital voltmeter. MADCAP and MMADCAP are the high speed data acquisition programs that were supplied with the ADTEK boards.

#### 2.4.2.1. ADTDVM

ADTDVM allows the computer to function as a multi-channel digital voltmeter. It displays in real time the voltage applied to each channel. ADTDVM will also record the voltages, as counts of the A/D converters, in GTL format files. The voltages can be stored once a second for a specified number of seconds. Once it has finished recording ADTDVM saves the data from each channel in a separate file. Before ADTDVM is run, a companion program, setlog, must be run. Setlog produces a configuration file for ADTDVM. The configuration file specifies the number of boards in use, the gain, name and file name to be used for each channel.

#### 2.4.2.2. MMADCAP

Two high speed data acquisition programs were supplied with the ADTEK boards. MADCAP will take high speed data using one ADTEK board. Multi-MADCAP (MMADCAP) will take high speed data using up to four ADTEK boards. MADCAP contains several extra utilities that not included in MMADCAP. Since ten to eighteen channels of data were collected for most runs, MMADCAP was used to collect data from the engine.

Before it can be used to take data MMADCAP must be configured. The configuration options include; the number of boards to be used, the gain of each channel, triggering source, clocking source, clock rate, the name of the data file and the number and size of data buffers to be used. The gain settings in MMADCAP correspond to input voltage ranges as listed in Table 2.6. Two or three boards were used for most of the engine runs when high speed data was taken. The gain settings of each channel varied with the input, but a gain of 2 was most common. The



triggering source was set to external, so that the control computer could start the data acquisition. The first ADTEK board provided the clocking signal. The clock rate was set to produce a sampling rate of 4000 Hz per channel. The data was always saved in a file named "adtek.dat". The data buffers were set so that when completely full they used most of the computer's memory (15.6 Mbytes). The configuration is saved in a separate file that can be loaded into MMADCAP.

Once data acquisition has been started MMADCAP takes the 12-bit count from the A/D converter for each channel and places it in a buffer in memory. MMADCAP continues to fill buffers until all the specified buffers are full or the escape key is hit. After MMADCAP stop taking data the contents of the memory are downloaded to the hard drive into the specified data file. Any data in that file is replaced every time MMADCAP is run. Therefore after each set of data is taken the operator must exit MMADCAP and rename the data file. If more data is desired MMADCAP must be restarted. To simplify this process two batch files were written. The first batch file is "hide.bat". It takes the new name for the data file as an input. If that name has not already been used it renames the data file. If the name has been used it returns an error message. The second batch file "run.bat", calls MMADCAP with the proper configuration file already loaded.

Scale	Range
1	±10 V
2	±5 V
4	±2.5 V
8	±1.75 V

Table 2.6: MMADCAP Scale and Voltage Ranges

#### 2.4.2.3.Data Inputs

There are ten primary signals that are normally supplied to the high speed A/D. Eight of the primary signals come from the Kulite pressure transducers. Three of these are at the diffuser

throat, one is at the combustor and one is at the customer bleed (Figure 2.3). There is also one that is located at the stator pressure tap on the engine. The remaining two transducers have been moved. They were originally at the stator pressure tap. When the shaker valve was added they were moved to the total and static pressure taps downstream of it (Figure 2.21). The hotwire anemometer and the vibration monitor are the other two primary signals. Table 2.7 lists all the signals that have been connected to the high speed A/D. It includes both the primary signals and other signals that were only connected for a few runs. The inlet and combustor pressure transducers were connected to measure their response time as the solenoid valves were switched. Two methods of measuring the engine speed were tried. A frequency to voltage converter was connected to the tachometer signal from the engine and its output fed to the high speed A/D. The second method was to connect the analog voltage output board in the N1 ratemeter to the high speed A/D. Both methods produced signals with high noise levels that masked any variations in N1.

In an attempt to improve the sensitivity to the disturbances created by the forcing, the AC coupled versions of the signals from the stator and throat taps were connected to the high speed A/D. These signals were produced using the AC coupling feature of the filter board, which removes the DC component of the signals. The resulting signals were then amplified and read by the high speed A/D. This did not appear to improve the sensitivity noticeably when compared with the DC signals recorded at the same time, so it was discontinued.

#### 2.4.2.4. Calibration

To calibrate the Kulites the following procedure is carried out before every run. ADTDVM is set to record data for four minutes. Two minutes after data recording is started the vacuum pump is turned on and the vent valve closed, thus evacuating the backpressure of the Kulites. After the run the procedure is repeated except that the pump is turned off and the vent opened at

Transducer	Measurement	Amplifier Setting	Filter Board Setting gain / coupling	Gain Setting on ADTEK board
Kulite 10	* Stator pressure tap	1000	1 / DC	2
	Stator pressure tap	1000	10 / AC	4
Kulite 11	Stator pressure tap	1000	1 / DC	2
	Stator pressure tap	1000	10 / AC	4
	Static pressure downstream of shaker	200	1 / DC	2
	* Total pressure downstream of shaker	200	1 / DC	2
Kulite 12	* Throat pressure tap	200	1 / DC	2
	Throat pressure tap	200	10 / AC	4
Kulite 13	* Combustor pressure tap	100	1 / DC	2
Kulite 14	* Throat pressure tap	200	1 / DC	2
	Throat pressure tap	200	10 / AC	4
Kulite 15	* Throat pressure tap	200	1 / DC	2
	Throat pressure tap	200	10 / AC	4
Kulite 16	Stator pressure tap	1000	1 / DC	2
	Stator pressure tap	1000	10 / AC	4
	Throat pressure tap	200	1 / DC	2
	* Static pressure downstream of shaker	200	1 / DC	2
Kulite 17	* Static pressure at the customer bleed port	100	1 / DC	2
Hotwire	* Velocity in the bellmouth	-1 volt offset	1 / DC	2
Vibrometer	* Engine Vibration		1 / DC	2
P1	Bellmouth tap depression		usually not filtered	2
P3	Combustor Pressure		usually not filtered	2
N1	Engine Speed (from ratemeter analog output)		1 / DC	2
N1	Engine Speed (from frequency to voltage converter)		1 / DC	2

\* indicate the primary signals

Table 2.7: Inputs Supplied to High Speed A/D

the two minute mark. This provides two pressures from which to calculate the scale and offset of each transducer amplifier pair, zero psid and the ambient atmospheric pressure.

ADTDVM stores the calibration data in GTL format files. After the run these files are converted to a MATLAB compatible format. A MATLAB routine loads the calibration files and asks the user to select the high and low pressure data points. The user is also asked to enter the ambient pressure at the time of each calibration and the sampling frequency of the high speed data. MATLAB then averages the ambient pressures from the two calibrations. It also averages the zero pressure points for each transducer and the reference pressure points for each transducer, from before and after the run. These values and the sampling frequency are then saved in a file called "run<run #>.cal".

Every time the high speed data is loaded into MATLAB it is converted from 12-bit counts to engineering units (psi or volts) using the run<run #>.cal file. The kulite signals are converted to psia using the following formula,

$$pressure = (counts - zero\ counts) \times \frac{P_o}{ref\ counts - zero\ counts} \quad (2.16)$$

The other signals are converted to voltages using,

$$volt = (count - 2048) \times \frac{10}{2048 \times scale} \quad (2.17)$$

where scale is the scale value set in MADCAP.

### 2.4.3.Run Procedure

Each run has a separate directory on the hard disk. That directory contains the configuration files for MMADCAP and AD and any high speed data collected during the run (including the calibration data).

The procedure for a typical run follows. The Kulites are calibrated before the engine is started, using AD. When the engine is running MMADCAP is started using "run.bat". The operator commands MMADCAP to begin acquiring data. MMADCAP waits for the trigger signal from the control computer. Once the trigger signal is received it begins acquiring data.

After the data collection is complete the operator exits MMADCAP and uses "hide.bat" to rename the data file. MMADCAP is then restarted. This cycle is repeated as often as desired. After the engine has been shutdown the Kulites are calibrated again.

The data files are renamed using the following convention. r<run>v<record>.dat is the name of the data file. Run is the engine run number and record is the number of the record from that run. For example, "r28v1.dat" is the name of the first set of high speed data taken for run 28.

### 2.5.Error Analysis

The uncertainty of the instrumentation can be calculated from the recorded calibration data, for both the steady state and high speed data. The uncertainties are computed in terms of standard deviations ( $\sigma$ ) and calculated as described in reference [1]. That means there is a 68 % probability that the actual value is within  $\pm 1\sigma$  of the value stated, a 95 % probability that it is within  $\pm 2\sigma$  and 99.7 % probability that it is within  $\pm 3\sigma$ . The uncertainties listed in Tables 2.8 thru 2.10 are  $\pm 3\sigma$ . The standard deviations are represented using two different variables, s and S. s is the standard deviation in units. S is the fractional or non-dimensional standard deviation. It is normalized by the value being considered. V is the value (representative of the values produced at 90 to 100 % engine speed) of the data being considered.

#### 2.5.1.Steady State

The uncertainties calculated in this section are representative of uncertainties produced by the steady state the calibration routine used for runs 24, 25, 27 and 28. Less accurate methods of calibrating the steady state data were used prior to run 24 (and a leak in a vacuum line invalidated the calibration for run 26). The data from runs 27 and 28 is used for these calculations since some of the required data is not available from the other runs.

When in calibration mode Genesis records the outputs of the pressure transducers and the reference pressure measured by the Setra 370. From this data it is possible to calculate the

standard deviation of each data point from the expected universe average. It is also possible to find the drift of the transducers by comparing the data from different calibrations.

The formula for the standard deviation from the expected universe average is,

$$S = \sqrt{\frac{\sum_{n=1}^k x_n^2 - k\bar{x}^2}{k-1}}, \quad (2.18)$$

where  $k$  is the number of data points,  $x_n$  is the  $n^{\text{th}}$  data point and  $\bar{x}$  is the mean of the data points. The standard deviation of the data at O psid ( $l_o$ ) and the reference pressure ( $h_i$ ) were calculated with this formula. The standard deviations of the pressure readings from the Setra 370 were also calculated.

The offset and scale factors are calculated using equations 2.14 and 2.15, which are based on the average zero pressure and reference pressure data. These averages are taken over 100 data points this decreases the standard deviation by a factor of ten, because the standard deviation of an average is [1],

$$S_{ave} = \frac{S_{pt}}{\sqrt{\# \text{ of pts averaged}}} \quad (2.19)$$

The resulting standard deviations of the scale and offset are,

$$S_{offset} = \frac{S_{l_o}}{10} \quad (2.20)$$

and

$$S_{scale} = \frac{1}{10} \times \sqrt{\frac{s_{lo}^2 + s_{hi}^2}{V_{(hi-lo)}^2} + \frac{s_{P_{hi}}^2 + s_{P_{lo}}^2}{V_{(P_{hi}-P_{lo})}^2}} \quad (2.21)$$

These equations produce the fractional standard deviations listed in Table 2.8.

An additional source of error is the drift of the transducer output during the run. The drifts are estimated by calculating both the offset and scale for several runs and comparing them. They are listed in Table 2.8 as well. As can be seen the potential error do to drift is significantly larger than the standard deviation for all the scale and offset values. Therefore the drifts (marked by \* on the table), are used instead of the standard deviations for the remainder of the calculations. It is also assumed that the standard deviation of the input voltage is the same as the offset drift, since transducer drift appears to be the main error source.

Based on the formula for the pressure (equation 2.1) the standard deviation of the calculated pressure is,

$$S_{pressure} = \sqrt{\frac{s_{input}^2 + s_{offset}^2}{V_{(input-offset)}^2} + S_{scale}^2} = \frac{S_{pressure}}{V_{pressure}} \quad (2.22)$$

Once the standard deviations of the pressures have been found the standard deviations of the massflow and pressure ratio can also be calculated. The formula for the standard deviation of the corrected massflow (WA) is based on equation 2.11, it is,

$$S_{WA} = \frac{\sqrt{s_{.5}^2 + s_{1.5}^2}}{(V_{.5} + V_{1.5} + .000046)} \quad (2.23)$$

Where,

variable	Inlet	Combustor	Turbine Discharge
$s_{lo}$ (volts)	0.000298	0.000309	0.000811
$V_{lo}$ (volts)	-0.03895	-0.01692	-0.04107
$s_{hi}$ (volts)	0.002138	0.000239	0.000456
$V_{hi}$ (volts)	-4.92053	0.26706	1.35871
$S_{P_{lo}}$ (%)	0.005	0	0
$S_{P_{hi}}$ (%)	0.006	0.003	0.003
$s_{offset}$ (volts)	2.68e-5	3.09e-4	8.11e-5
offset drift (volts)	0.013 *	0.013 *	0.0013 *
$S_{scale}$ (%)	0.0049	0.0138	0.0066
scale drift (%)	0.275 *	0.059 *	0.195 *
$S_{pressure}$ (%)	0.5	0.91	0.26
Uncertainty (%)	1.50	2.73	0.78

Table 2.8 : Listing of the Calculated Uncertainty for Steady State Pressures

$$s_{.5} = V_{.5} \times \sqrt{(.5)^2 S_{PSBM}^2 + (.5)^2 S_{P_o}^2} \quad (2.24)$$

and

$$s_{1.5} = V_{1.5} \times \sqrt{(1.5)^2 S_{PSBM}^2 + (1.5)^2 S_{P_o}^2} \quad (2.25)$$

Where  $S_{PSBM} = S_{P_1}$  and  $V_{.5} = 0.11087$  and  $V_{1.5} = 0.0015082$ . The values of  $V_x$  were selected to match the region of interest.

The formula for the standard deviation of the pressure ratio ( $\pi$ ) is based on equation 2.5.

$$S_{\pi} = \sqrt{\frac{s_{P_3}^2 + s_{P_o}^2}{V_{(P_3+P_o)}^2} + S_{P_o}^2} \quad (2.26)$$



The resulting fractional standard deviations are listed in Table 2.9, along with the uncertainties they result in

C alculated Value	S (%)	Uncertainty (%)
P <sub>o</sub>	0.00335	0.0100
WA	0.24	0.72
π	0.799	2.397
N1 <sub>corr</sub>	0.19	0.57

Table 2.9: Listing of Uncertainty for calculated values, and the ambient pressure.

The other calculated value of interest is N1<sub>corr</sub>, corrected engine speed. The equation used to find S<sub>N1corr</sub> is based on equation 2.6. In this equation S<sub>N1</sub>=0.001 and S<sub>inletemp</sub>=0.0033.

$$S_{N1corr} = \sqrt{S_{N1}^2 + (.5)^2 S_{inletemp}^2} \tag{2.27}$$

2.5.2.High Speed

The uncertainties calculated in this section are based on the data from run 28. These values are representative the high speed data from any run, since the same calibration routine was used for all the high speed data acquisition.

Since the calibrations from before and after the run are both averaged together to calculate the pressures, the standard deviation of the population of all those points will be used to calculate the standard deviations of the resulting pressures. This accounts for any drift in the transducer outputs that occurs during the run. Assuming that the fractional standard deviation of any measurement is the same as the fractional standard deviation of the reference pressure

measurements the following formula, based on equation 2.16, results. (Note: the averaged values are based on approximately 230 data points.)

$$S_{ku} = \sqrt{\frac{\left(\frac{s_{hi}}{V_{hi}} \times V_{run}\right)^2 + \frac{s_{lo}^2}{230}}{\left(V_{run} - V_{lo}\right)^2} + S_{P_{hi}}^2 + \frac{s_{hi}^2 + s_{lo}^2}{230 \times \left(V_{hi} - V_{lo}\right)^2}} = \frac{S_{ku}}{V_{ku}} \quad (2.28)$$

The calibration values, standard deviations of the calibration values, the calculated fractional standard deviation and uncertainty of the pressure measurement are listed in Table 2.10, for the primary pressure signals (these signals are marked on Table 2.7).

	$V_{lo}$ (cnts)	$s_{lo}$ (cnts)	$V_{hi}$ (cnts)	$s_{hi}$ (cnts)	$S_{ku}$ (%)	Uncertainty (%)
ku10	440.84	30.31	2419.40	28.39	1.45	4.35
ku11	425.39	12.20	759.19	8.71	1.59	4.77
ku12	425.38	8.52	916.87	8.03	1.13	3.39
ku13	400.46	6.64	620.85	4.88	1.00	3.00
ku14	387.94	11.51	887.56	10.38	1.47	4.41
ku15	424.37	2.72	1028.90	3.51	0.42	1.26
ku16	412.75	30.14	815.84	2.98	0.77	2.31
ku17	430.17	6.70	638.27	8.80	1.77	5.31

Table 2.10: Calibration and Calculated Standard Deviations of Kulite Pressure Transducers From Run 28

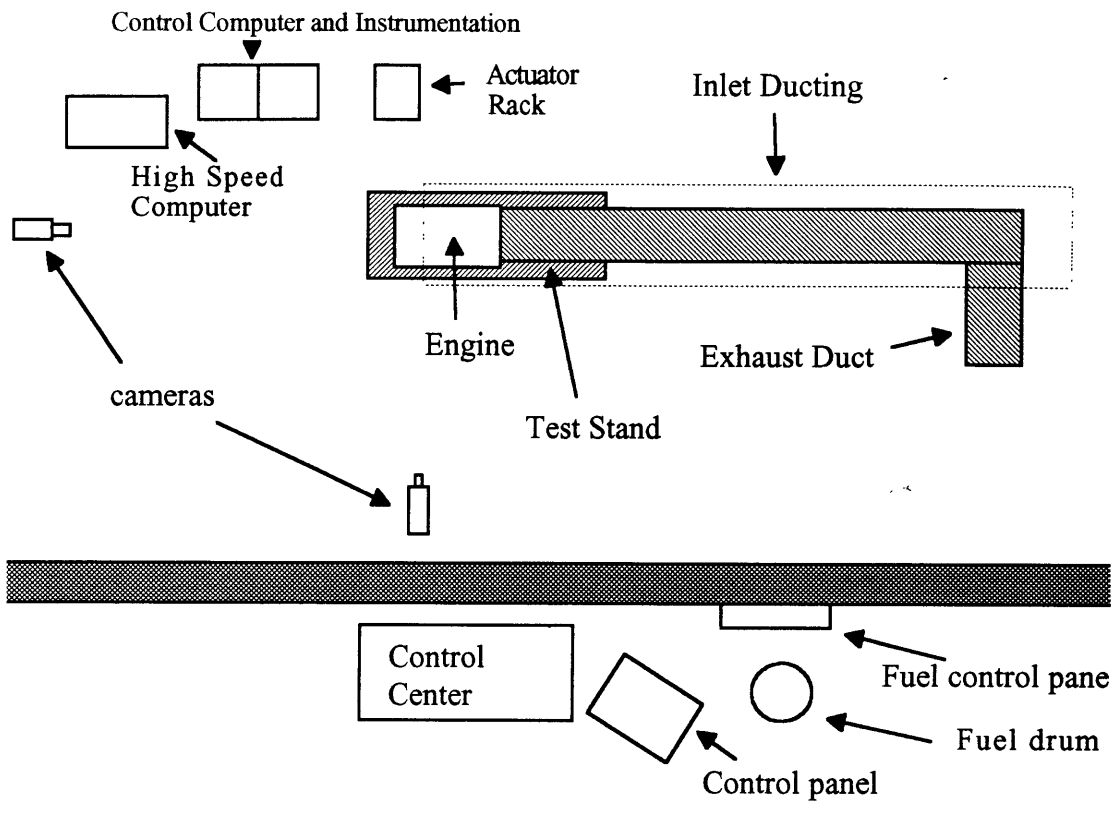


Figure 2.1: Overview of Facility

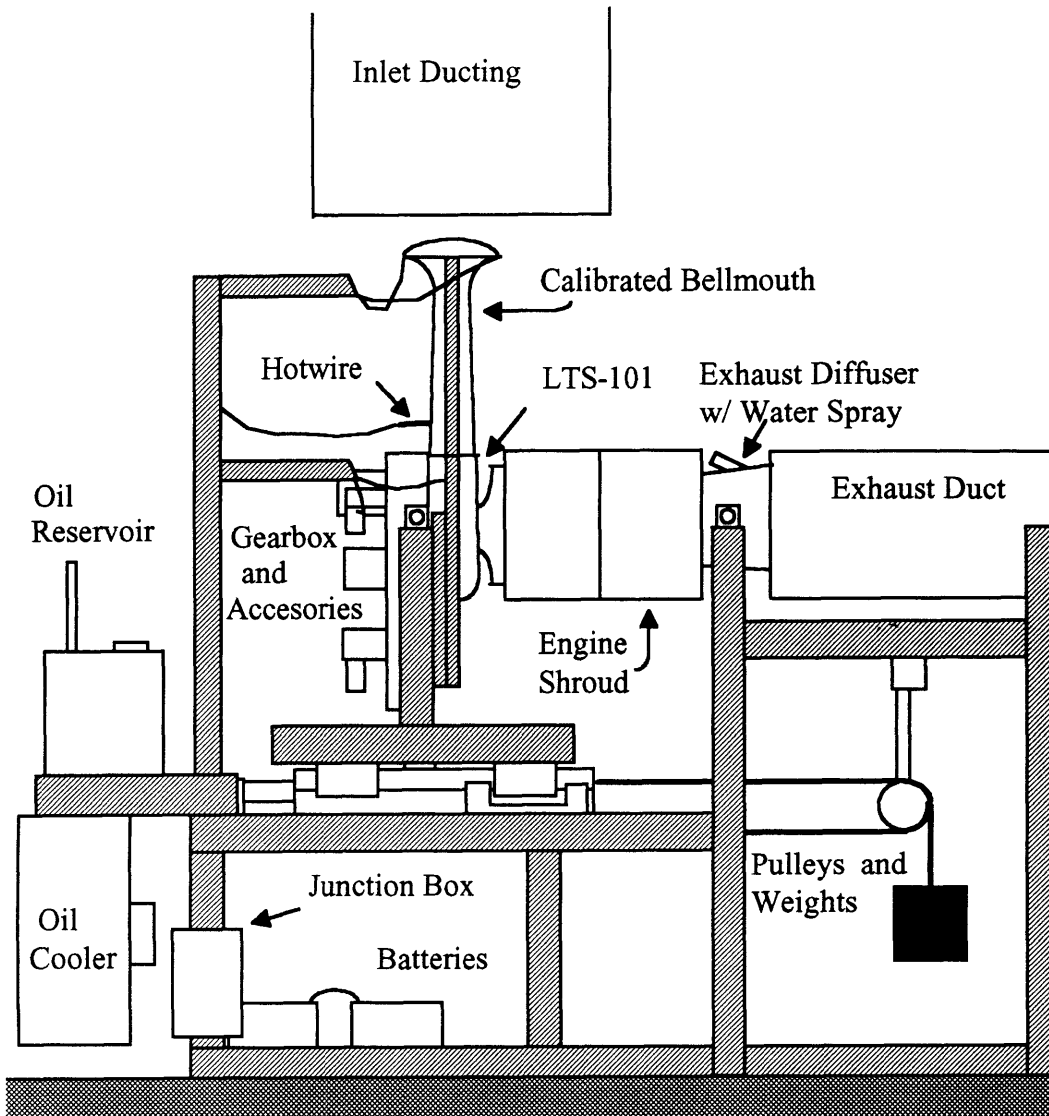


Figure 2.2: Engine Test Stand



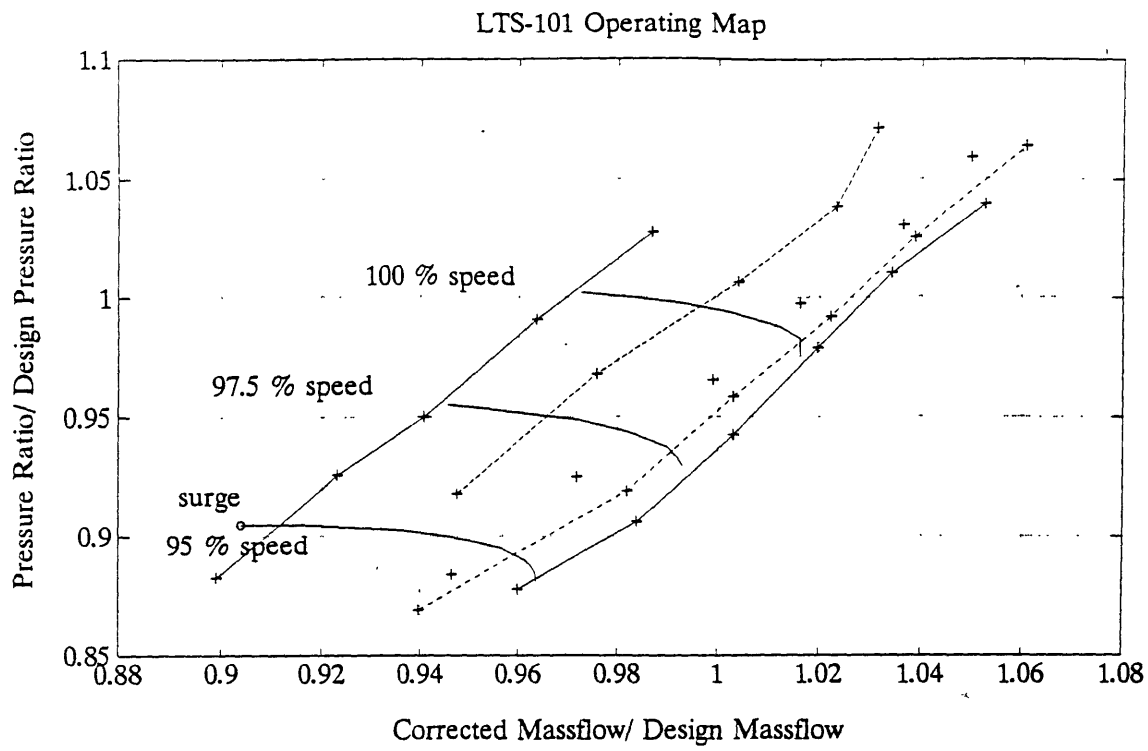


Figure 2.4 : LTS-101 Operating Map

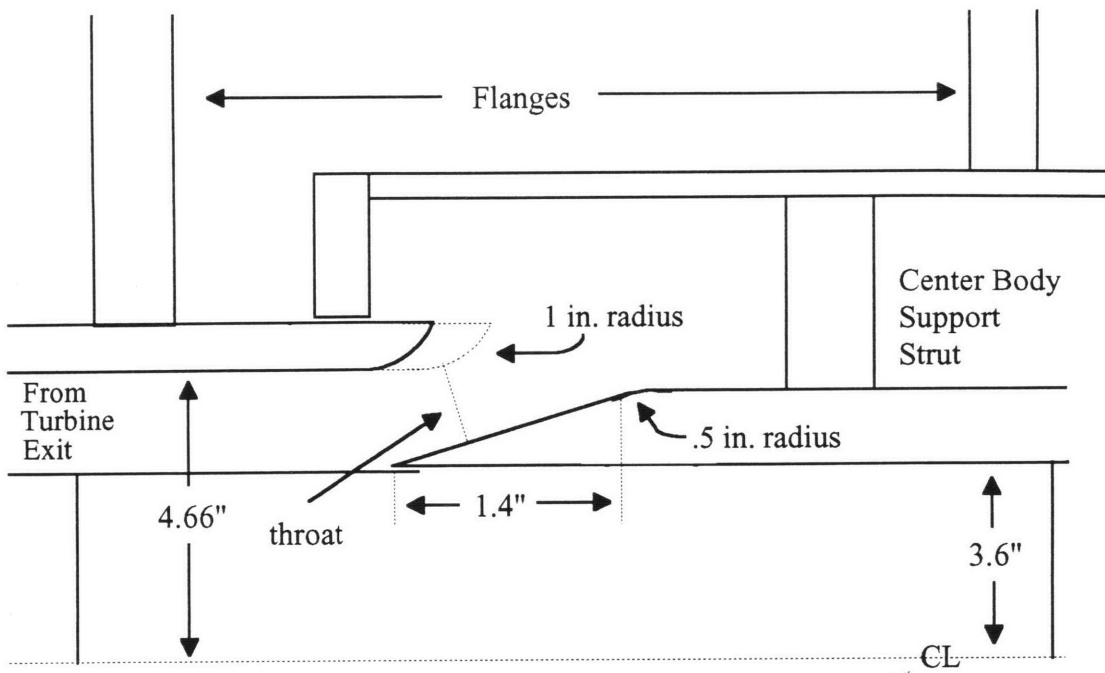


Figure 2.5: Variable Area Nozzle

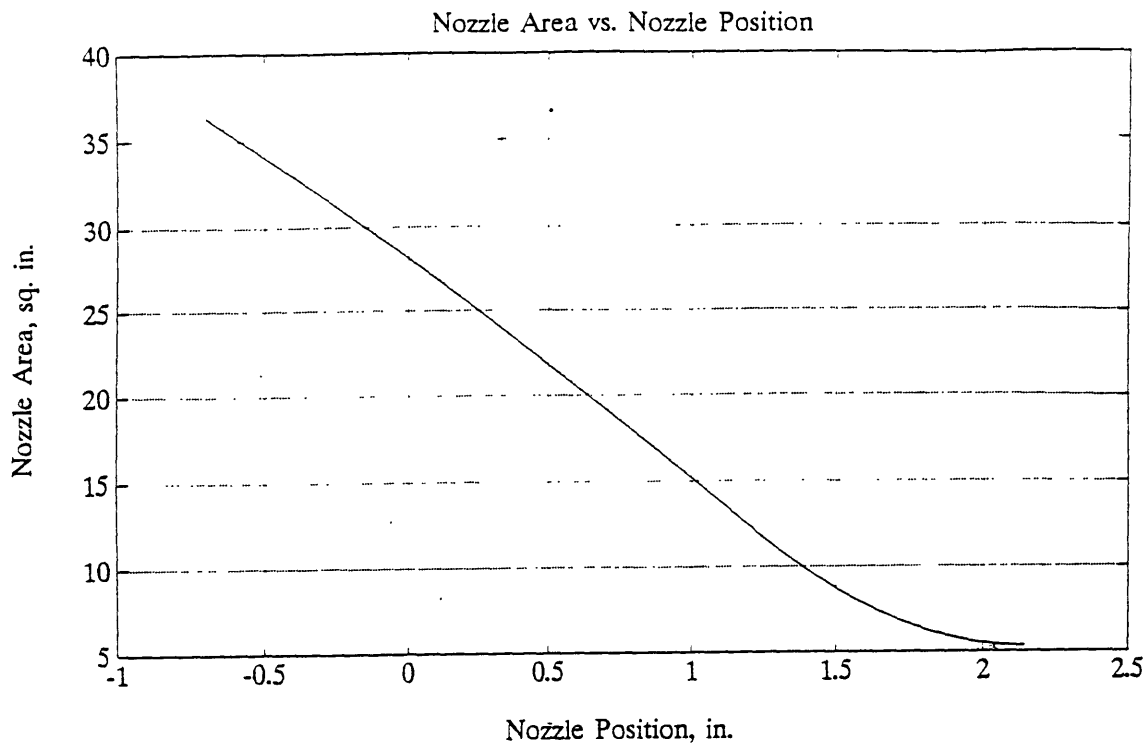


Figure 2.6 : Nozzle Area vs. Nozzle Position



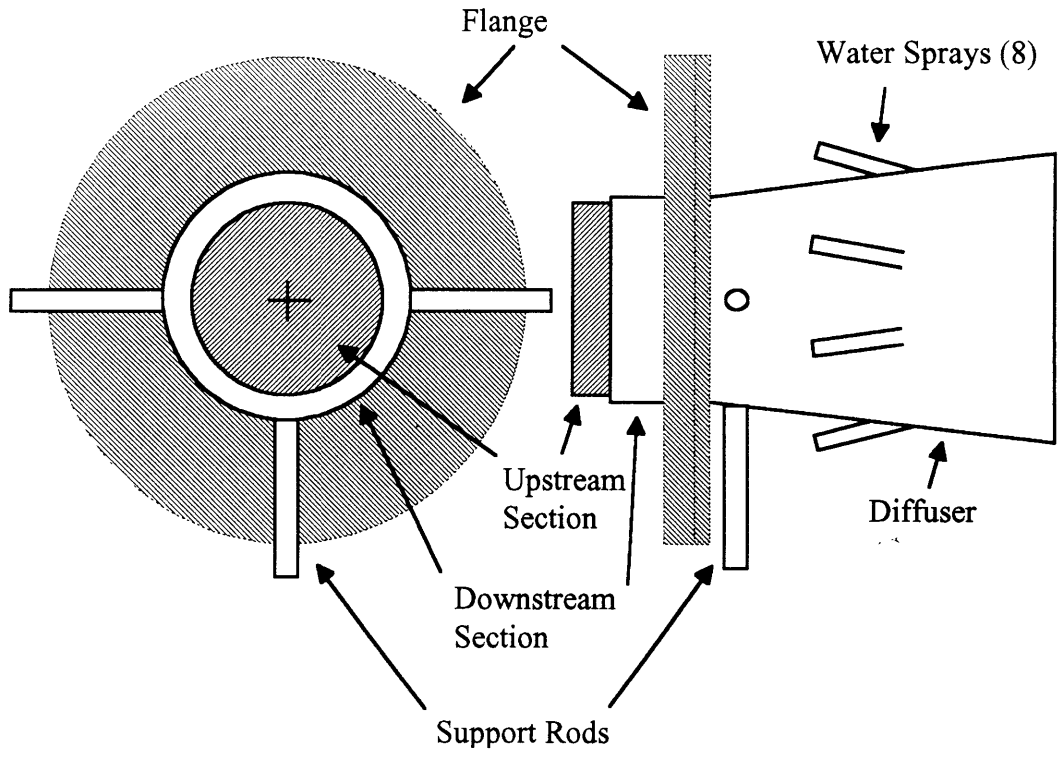


Figure 2.7: Nozzle and Diffuser Assembly

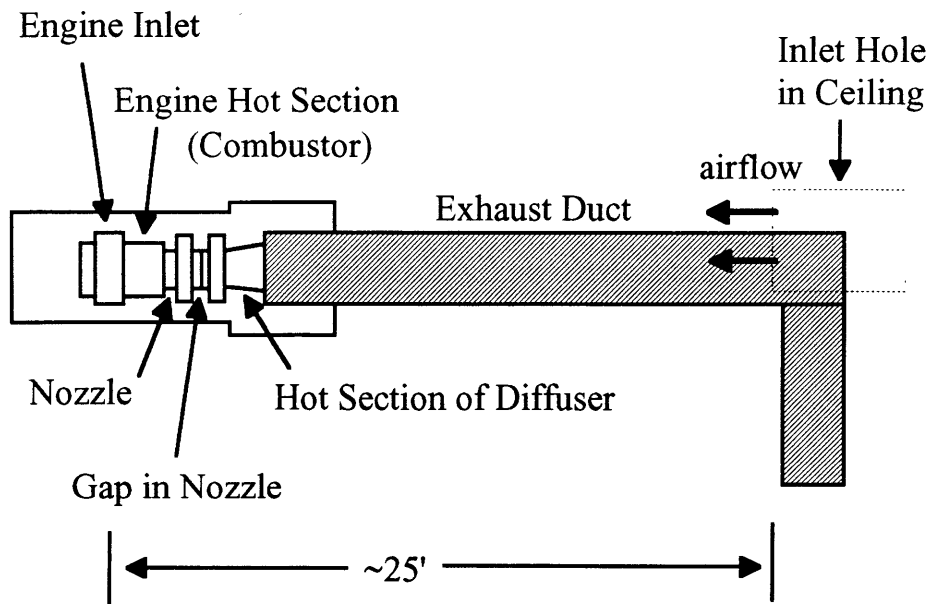


Figure 2.8: Inlet Air Flow and Hear Sources

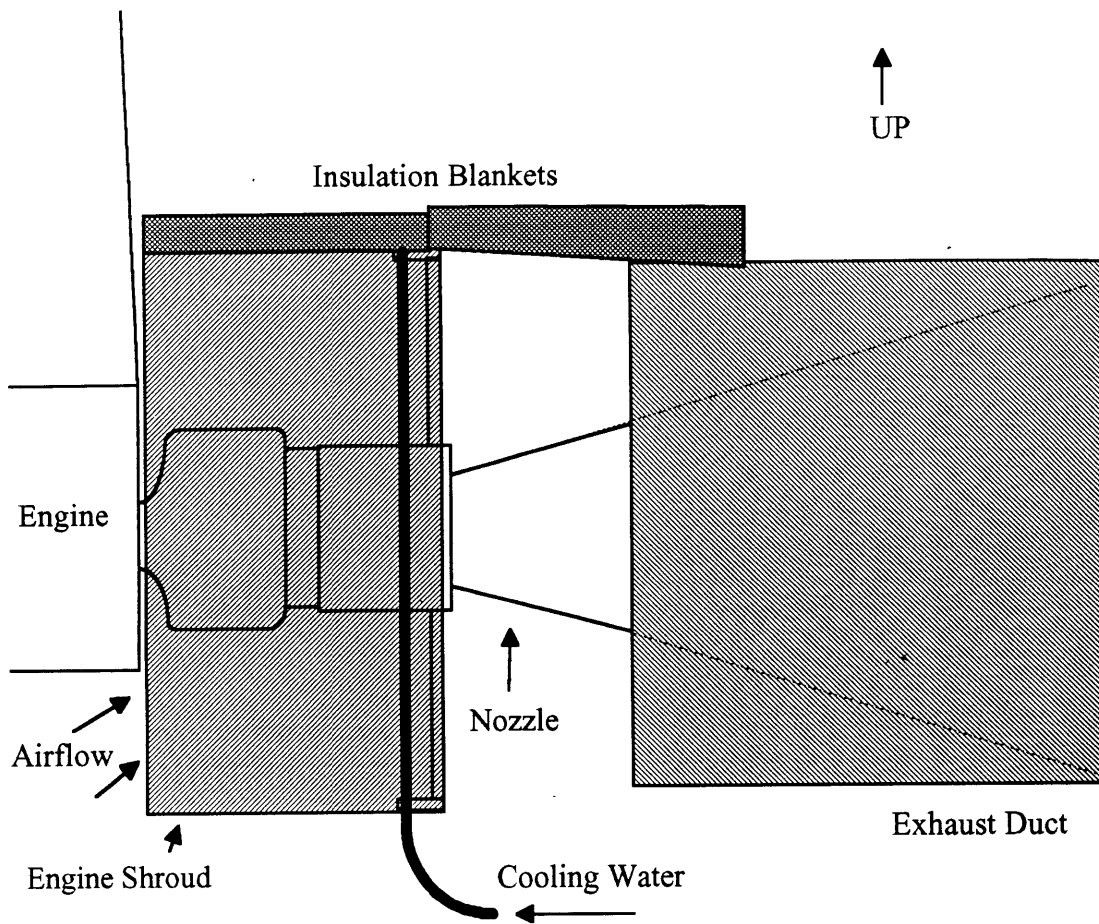


Figure 2.9: Engine Shroud and Insulation Locations

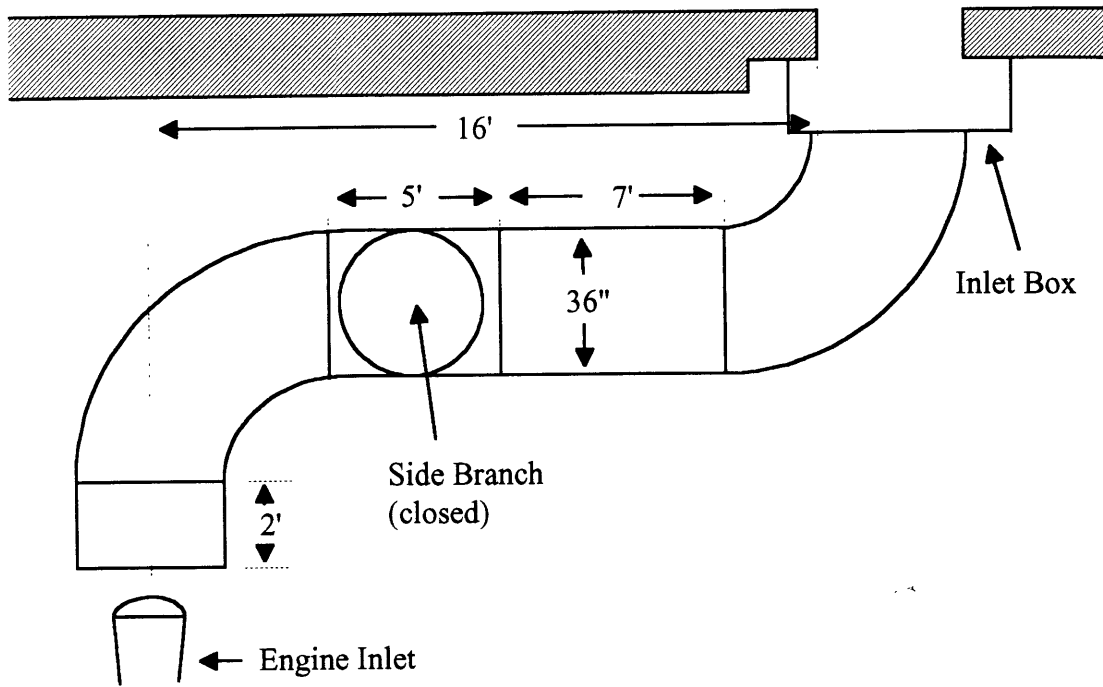


Figure 2.10: Side View of Inlet Duct

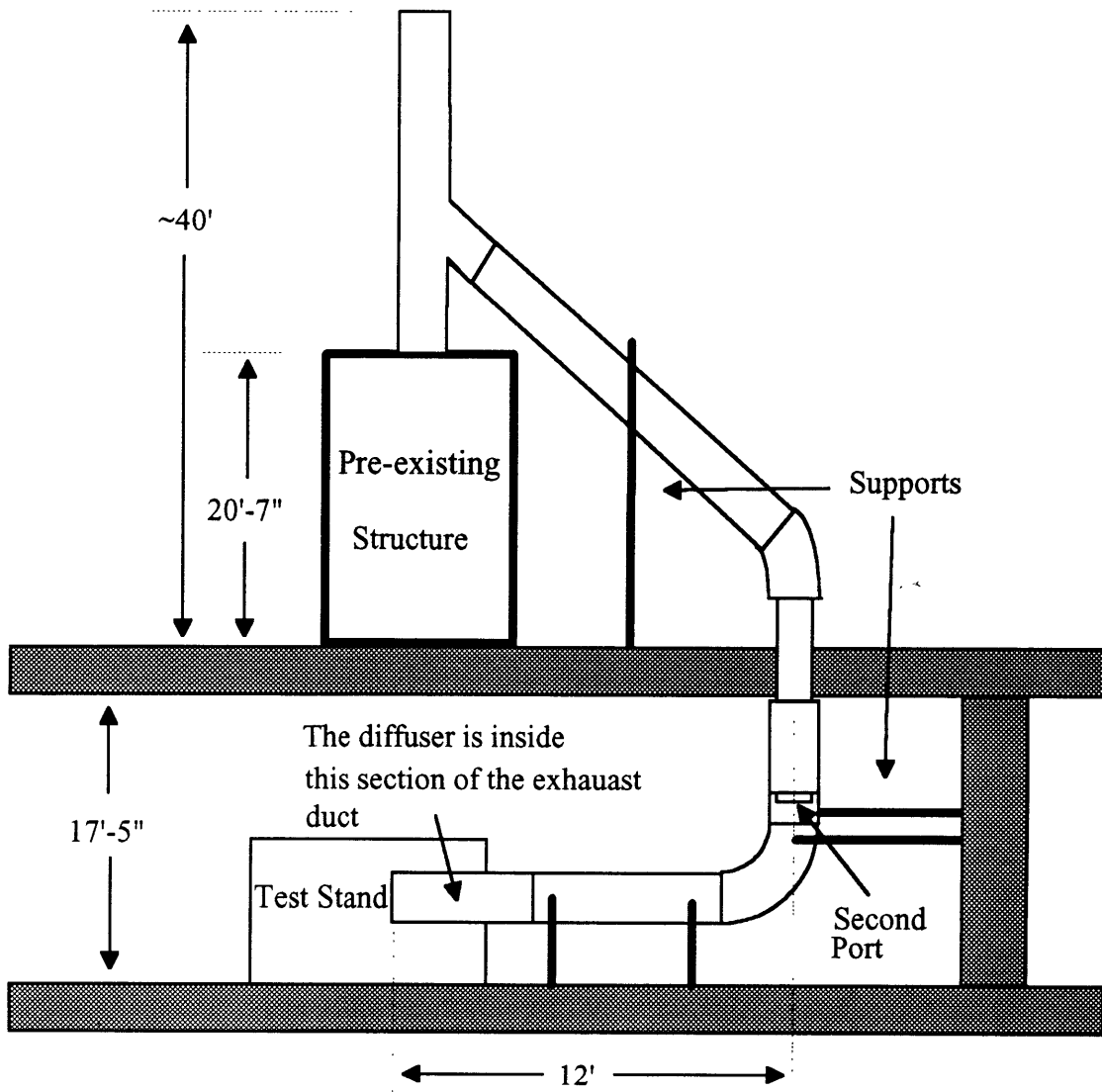


Figure 2.11: Side View of Exhaust Ducting

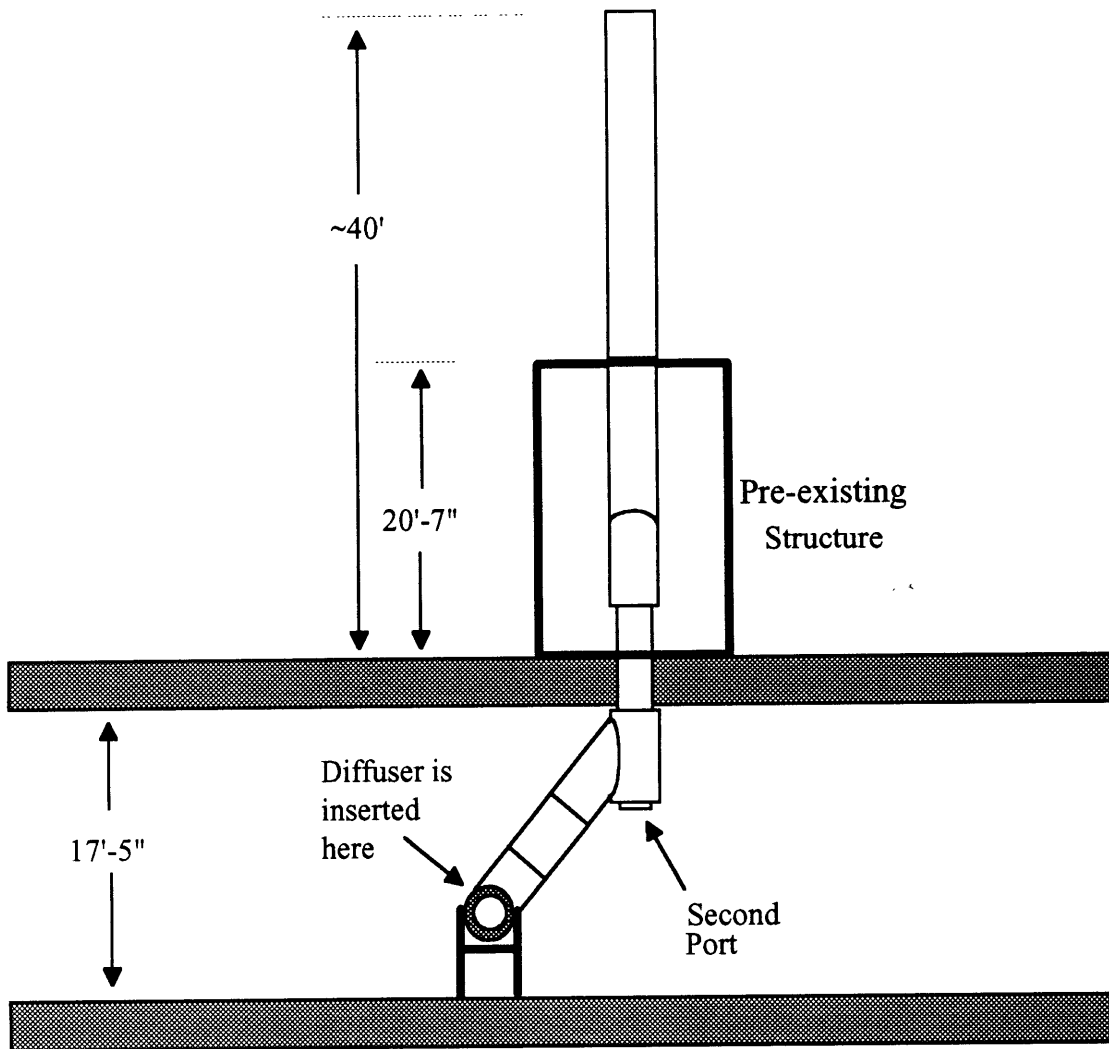


Figure 2.12: Front View of Exhaust Ducting

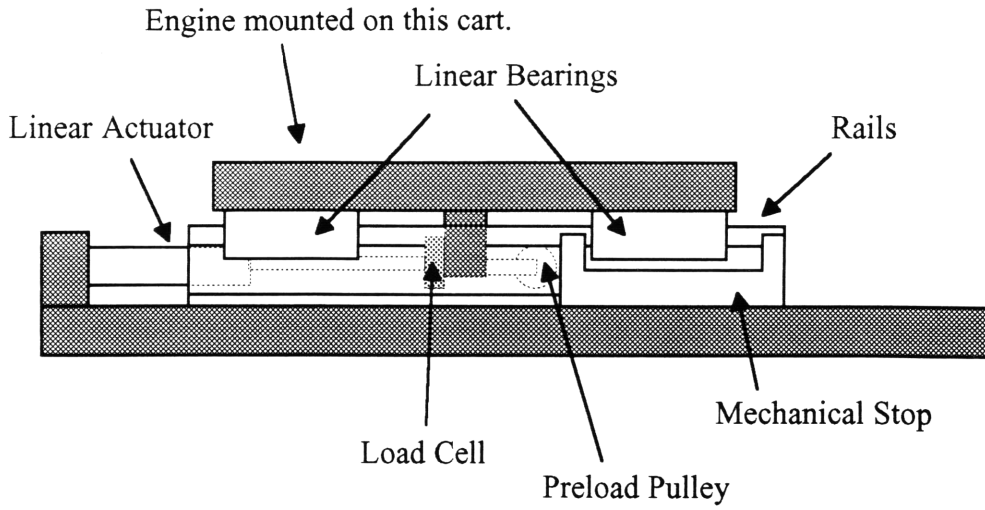


Figure 2.13: Nozzle Positioning System (Side View)

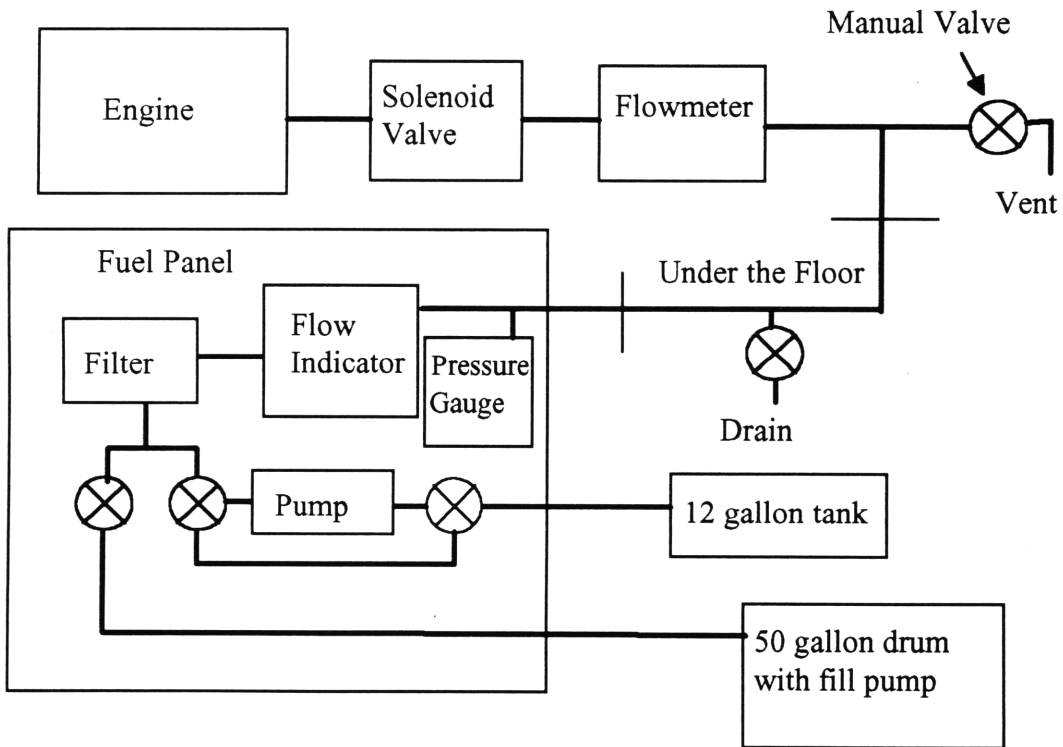


Figure 2.14: Fuel System Schematic

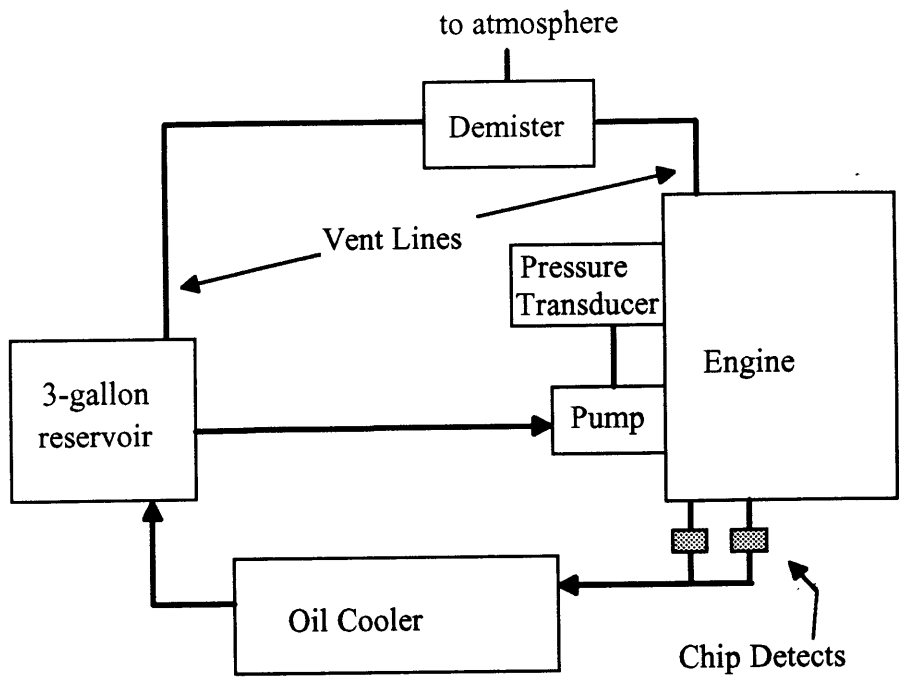


Figure 2.15: Oil System Schematic

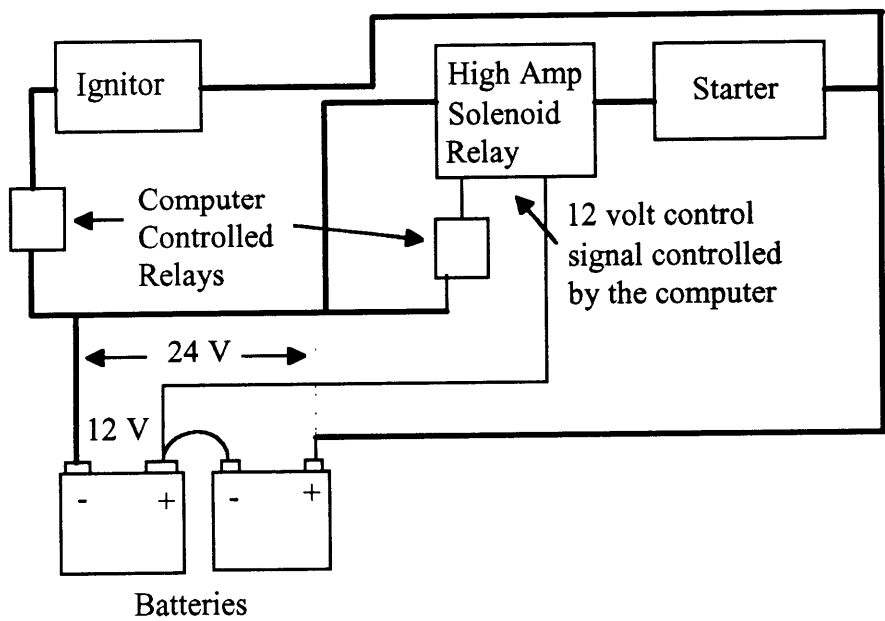


Figure 2.16: Electrical System Schematic



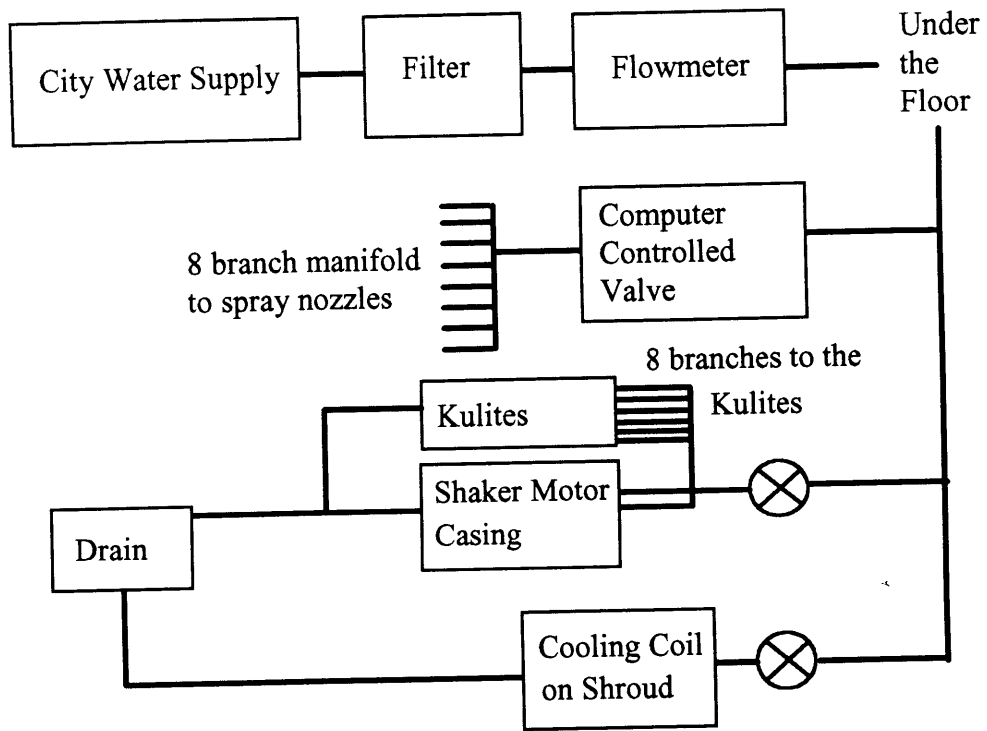


Figure 2.17: Water Cooling System Schematic

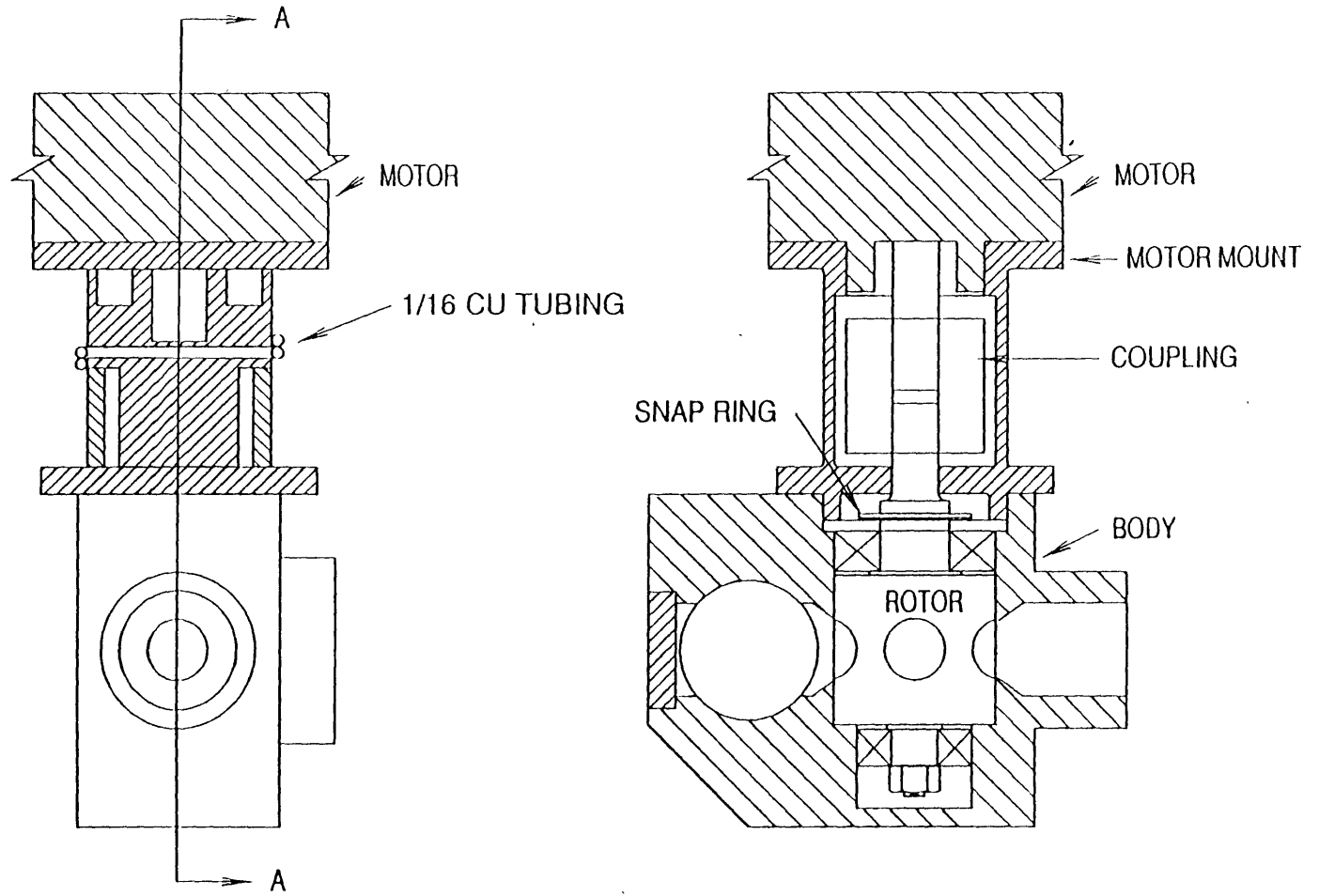


Figure 2.18 : Shaker Valve Assembly

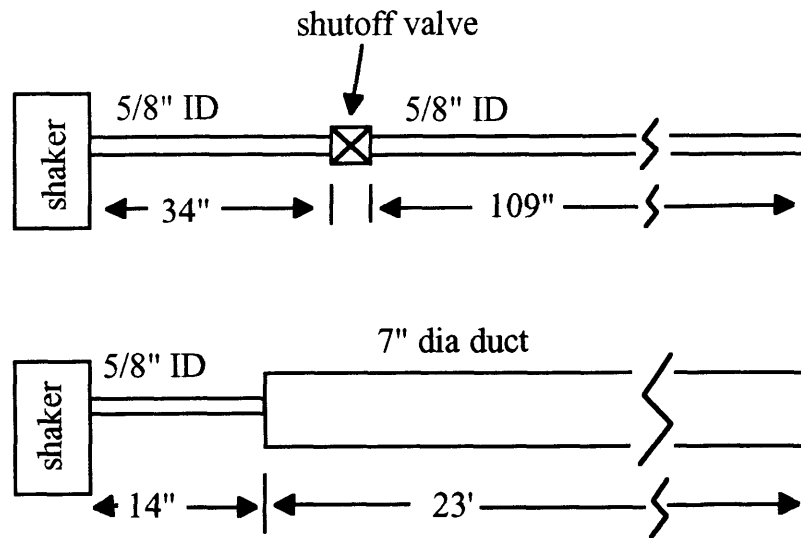


Figure 2.19: Customer Bleed Valve Venting Options

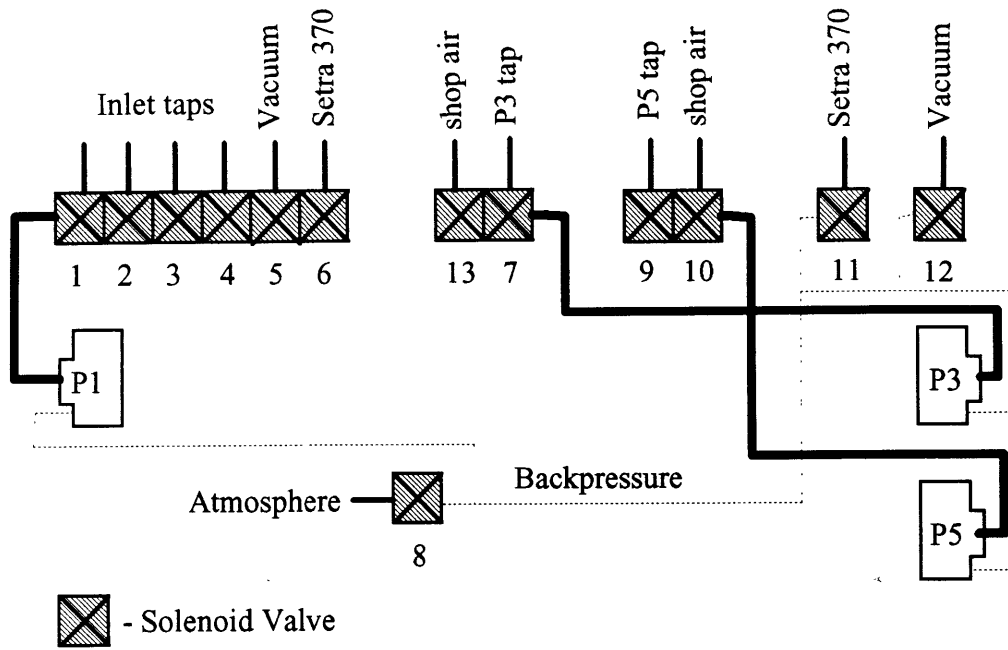


Figure 2.20: Pressure Plumbing Schematic

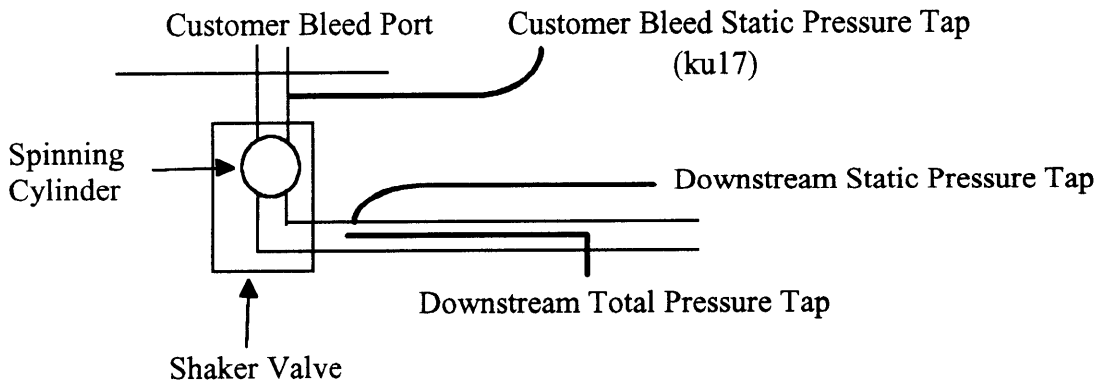


Figure 2.21: Location of Pressure Taps Upstream and Downstream of the Shaker Valve

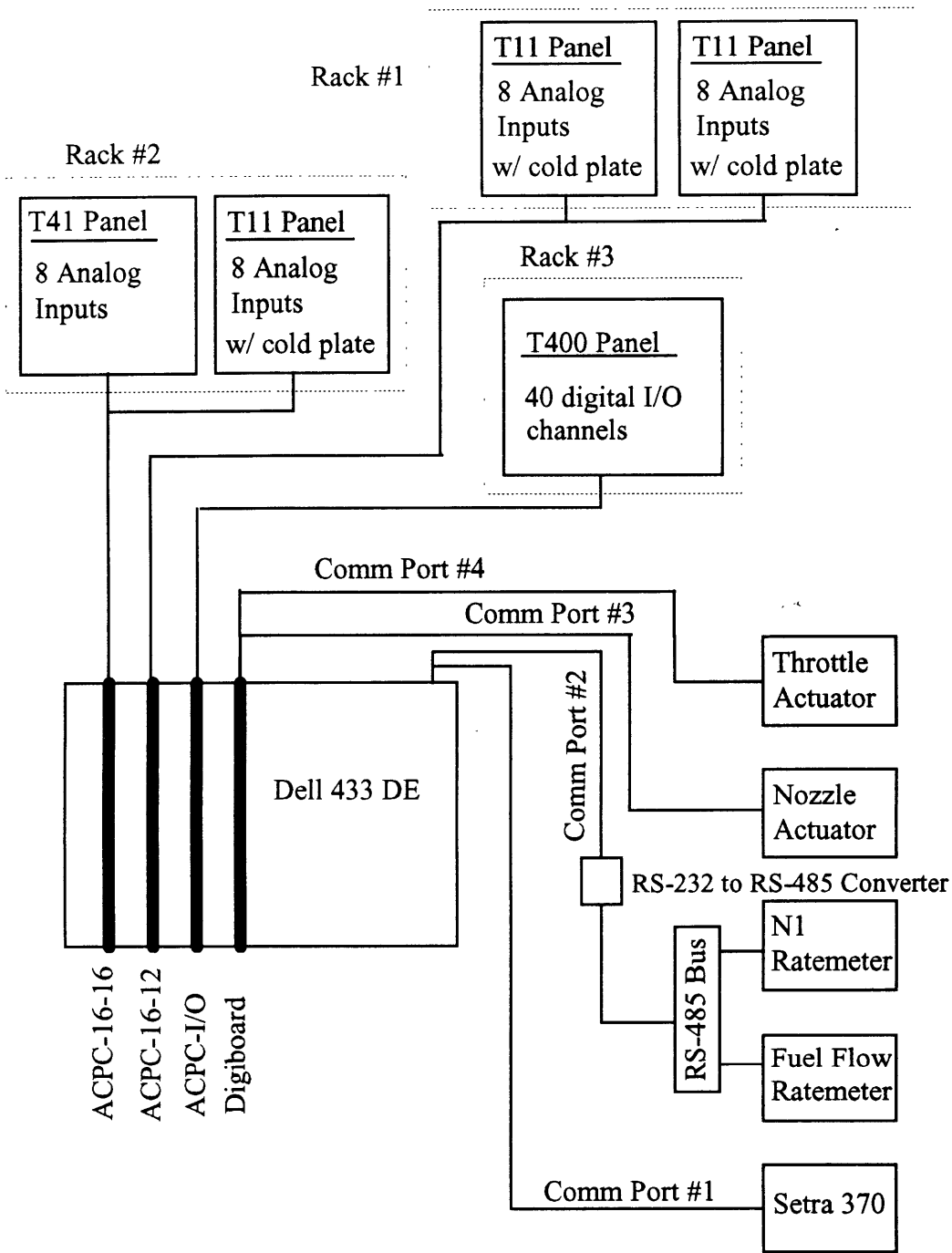


Figure 2.22: Control Computer Connection Schematic

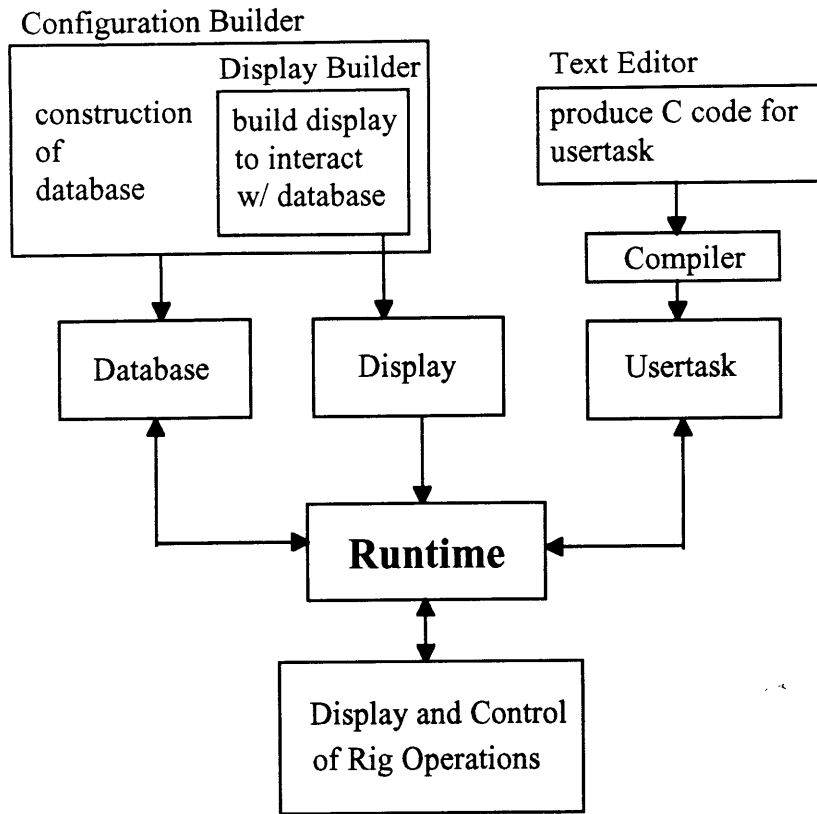


Figure 2.23: Diagram of Genesis Components

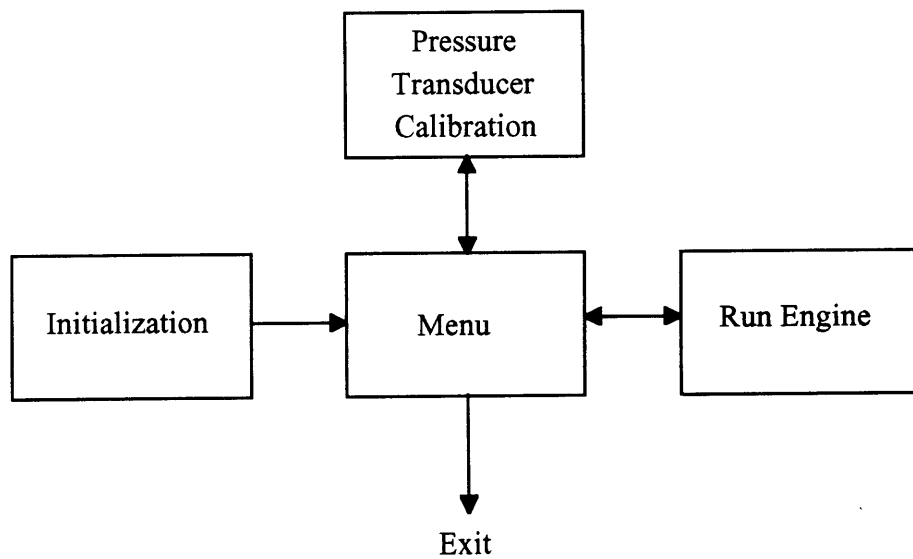


Figure 2.24: Operating Modes

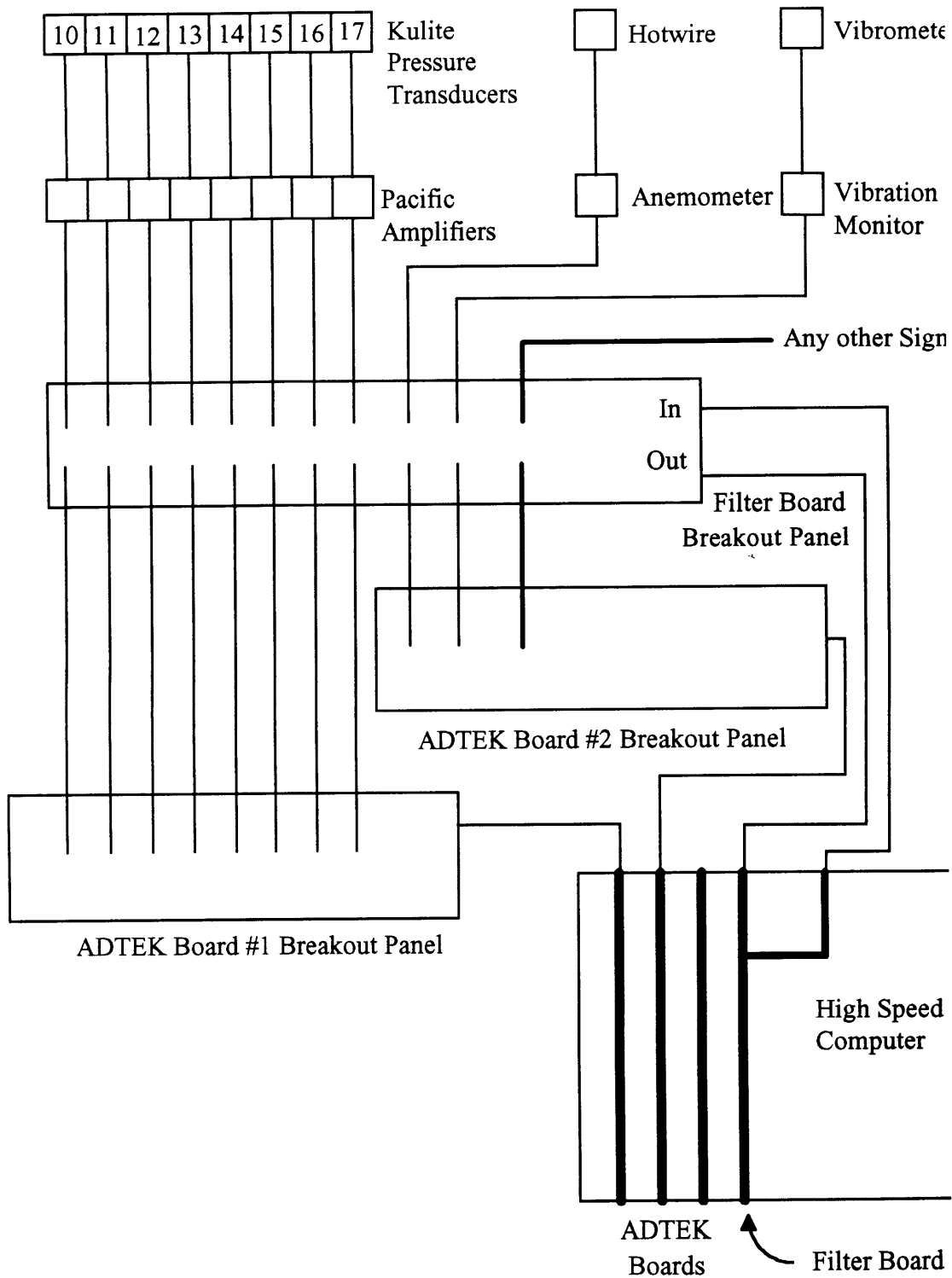


Figure 2.25: High Speed Data Acquisition System Schematic

### **3.Presentation and Analysis of Data**

There are two classes of data that are generated from each engine run. The steady state data is produced by the Genesis process control software. This data is sampled at 1 Hz. The high speed data is produced by the MMADCAP software, which is set at a sampling rate of 4000 Hz.

#### **3.1.Steady State Data**

The steady state data is recorded in ACSII files. These files are modified to produce ASCII flat files, which are loaded into MATLAB [12] for post processing. MATLAB is used to plot the data as time traces and operating maps. These plots are used to check the engine's performance.

All the pressure ratios and massflows presented in this thesis have been divided by design values to non-dimensionalize them. The design values are the expected values for 100 % engine speed with the measured compressor efficiency. They were selected from compressor maps provided by Lycoming.

##### **3.1.1.Operating Point Fluctuations**

At constant nozzle and throttle position there are variations in the engine operating parameters as shown in Figures 3.1 thru 3.5 and listed in Table 3.1. Table 3.1 also contains the uncertainty of the values calculated in section 2.5.1. While the uncertainty and the fluctuations are of approximately the same magnitude, the effects of the uncertainty are not expected to vary significantly during the run and therefore does not account for the fluctuations.

The variations occur on the time scale of minutes and appear to be caused by changing inlet temperature (Figure 3.1). The fluctuations in inlet temperature are on the order of one or two degrees Celsius. The inlet temperature fluctuations correspond to corrected engine speed fluctuations of  $\pm 0.30$  % (Figure 3.2). The fuel controller undercompensates for the fluctuations in corrected engine speed, resulting in absolute engine speed variations of



$\pm 0.15\%$  (Figure 3.3). Comparison of the pressure ratio ( $\pm 0.6\%$ , Figure 3.4) and corrected massflow ( $\pm 0.35\%$ , Figure 3.5) fluctuations with the engine speed fluctuations, indicates that the variations in engine speed cause the variations in pressure ratio and massflow. This is supported by Figures 3.6 and 3.7. In Figure 3.6 pressure ratio is plotted against corrected engine speed. This plot includes five throttle lines measured by Lycoming before the engine was shipped. Each throttle line has a constant exit area. Figure 3.7 contains a similar plot of corrected massflow vs. corrected engine speed. The variations in pressure ratio, corrected massflow, and corrected engine speed produce clusters of data points that approximately follow a throttle line.

Figures 3.4 and 3.5 also show a slight decrease in the pressure ratio and corrected massflow with time. This decrease does not correspond to a decrease in engine speed and may account for some of the scatter away from the throttle lines in Figures 3.6 and 3.7. The long time scale of these variations suggests that they are related to the heating of the engine and nozzle and the resulting changes in the geometry of the nozzle area.

	Inlet Temperature	Corrected Engine Speed	Absolute Engine Speed	Pressure Ratio	Corrected Massflow
Fluctuations	$\pm 1.5^\circ\text{C}$	$\pm 0.30\%$	$\pm 0.15\%$	$\pm 0.60\%$	$\pm 0.35\%$
Uncertainty	$\pm 1.5^\circ\text{C}$	$\pm 0.57\%$	$\pm 0.3\%$	$\pm 2.34\%$	$\pm 0.72\%$

Table 3.1: Fluctuations and Uncertainty at Constant Nozzle and Throttle Settings

### 3.1.2. Nozzle Position vs. Nozzle Area

The predicted relationship between nozzle position and nozzle area was calculated in chapter 2 (Figure 2.6). Those calculations can be checked using data from runs 27 and 28 and the constant exit area, throttle lines measured by Lycoming. As can be seen in Figure 3.8 clusters of points from the data line up with the throttle lines. Determining the axial position of the nozzle for each cluster of points and pairing it with the exit area of a throttle line leads to the

correlations listed in Table 3.2. These points are plotted with the calculated position vs. area curve in Figure 3.9. After the position from the calculation is adjusted to match the zero position of the data the two are found to correspond well. This indicates that the variable area nozzle is performing as intended, and allows the nozzle area to be estimated by matching the measured nozzle position to the calculated area.

Position (in.)	Area (in. <sup>2</sup> )
1.09	14.65
1.18	12.65
1.31	10.65
1.40	9.65

Table 3.2: Nozzle Position to Area Correlation

### 3.1.3. Speed Lines

A standard description of the behavior of a compressor is the pressure ratio vs. massflow curve at constant corrected speed. To create this curve using with the rig, the throttle position is set and the nozzle closed down in steps. As shown in Figure 3.6 this procedure causes the corrected engine speed to droop by 1 to 2 percent. This does not produce a constant speed line. To estimate the constant speed line the data should be adjusted to a constant corrected engine speed. This adjustment should also collapse the scatter in the data caused by the  $\pm 0.3\%$  fluctuations in corrected speed described earlier.

The data was adjusted to a constant speed line using a method similar to the one used by Gysling [10]. The following assumptions are used to adjust the data; the efficiency of the compressor and the massflow coefficient are constant for the range being considered, and the temperature ratio across the compressor is a function of the impeller tip speed (Mach number). The compressor efficiency,  $\eta_{th}$  is found using,

$$\eta_{th} \equiv \frac{\left(\frac{P_{T3}}{P_{T0}}\right)^{\frac{\gamma-1}{\gamma}} - 1}{\frac{T_{T3}}{T_{T0}} - 1} \quad (3.1)$$

$\eta_{th}$  is calculated for all the data points above 90 % speed, where the nozzle is still in the zero position, and averaged. The resulting value is assumed to be the constant value of  $\eta_{th}$ .

The following empirical equation [11] is used to find the relationship between engine speed and the temperature ratio ,

$$\frac{T_{T3}}{T_{T0}} = 1 + \frac{\gamma-1}{2} \chi M_t^2 \quad , \quad (3.2)$$

where  $\chi$  is an empirical constant and  $M_t$  (the rotor tip Mach number) is proportional to engine speed,

$$M_t = \frac{U_t}{a_3} = \frac{2\pi r_t \left(\frac{47867}{60}\right) (N1)}{a_3} = \frac{K_A(N1)}{a_3} \quad (3.3)$$

where  $K_A$  is a constant.  $a_3$  is the speed of sound at the compressor exit and is assumed to be constant for small changes in the corrected engine speed. Several constants are combined to produce,

$$K_B = \frac{\gamma-1}{2} \times \chi \times \frac{K_A^2}{a_3^2} \quad (3.4)$$

Substituting equations 3.3 and 3.4 into 3.2 results in,

$$\frac{T_{T3}}{T_{T0}} = 1 + K_B(N1)^2 \quad (3.5)$$

Rearranging equation 3.5 lead to,

$$K_B = \frac{\frac{T_{T3}}{T_o} - 1}{(N1)^2} \quad (3.6)$$

$K_B$  can be calculated from the available data.  $K_B$  is calculated for each point above 90 % speed, where the nozzle hasn't been moved (same points as were used to find compressor efficiency).

The resulting values are averaged to produce the value of  $K_B$  used for the rest of the calculations.

Substituting equation 3.4 into 3.1 results in,

$$\eta_{th} = \frac{\left(\frac{P_{T3}}{P_0}\right)^{\frac{\gamma-1}{\gamma}} - 1}{K_B(N1)^2} \quad (3.7)$$

which can be rearranged to produce,

$$\frac{P_{T3}}{P_0} = \left[ \eta_{th} K_B (N1)^2 + 1 \right]^{\frac{\gamma}{\gamma-1}} \quad (3.8)$$

For small changes in  $N1$ , equation 3.8 can be linearized to produce,

$$\left(\frac{P_{T3}}{P_0}\right)_{adj} = \left(\frac{P_{T3}}{P_0}\right)_{meas} + \frac{\delta \frac{P_{T3}}{P_0}}{\delta(N1)} \left[ (N1)_{adj} - (N1)_{meas} \right] \quad (3.9)$$

where

$$\frac{\delta \frac{P_{T3}}{P_0}}{\delta(N1)} = \frac{\gamma}{\gamma-1} \left[ \eta_{th} K_2 (N1)^2 + 1 \right]^{\left(\frac{\gamma}{\gamma-1}-1\right)} \left[ 2\eta_{th} K_2 (N1) \right] \quad (3.10)$$

It is also assumed that the massflow coefficient ( $\phi$ ) is constant, so

$$\phi = \frac{\dot{m}}{\rho_0 A_{in} U_t} = \frac{\dot{m}}{K_C(N1)} = const \quad (3.11)$$

which leads to

$$\dot{m}_{adj} = \dot{m}_{meas} \times \frac{(N1)_{adj}}{(N1)_{meas}} \quad (3.12)$$

Figure 3.11 shows the raw data from attempting to trace a speed line and the same data adjusted to 95 % speed. Adjusting the data results in a marginal reduction of the scatter in the data. The adjustment appears to have little to no affect on the scatter caused by the fluctuations at constant nozzle and throttle settings. It appears to adjust the mean values at each nozzle and throttle setting somewhat better more effectively. This is demonstrated by the four "clouds" of data labeled 1, 2, 1', and 2' on Figure 3.11. Cloud 1 is at  $96.4 \pm 0.2$  % corrected speed, as the nozzle starts to close. Cloud 2 is at  $95.5 \pm 0.1$  % corrected speed, with the nozzle fully open. Clouds 1' and 2' are the same data points after adjusting to 95 % corrected speed. Although clouds 1' and 2' did not collapse into a single point, they are considerably closer to each other than clouds 1 and 2.

To estimate the zero slope point on the characteristic and the slope at the surge point, second order curves were fit to both the raw and adjusted data. Table 3.2 contains the resulting data for surges from runs 25, 27 and 28. It was not reasonable to calculate similar data for other surge points, because the steady state pressures were not well calibrated. The fractional standard deviation of the measured data from the curve fit is also included as an indication of the quality of the curve fit. For slopes near zero the uncertainty of the slope is  $\pm 0.2316$ .

As shown in Figure 3.12 the curve fits to the adjusted data from runs 27 and 28 are within 0.1 % of one another. Near the surge points (massflow ratio = 0.91 to 0.93) these curves also match the constant speed line provided by the manufacturer. This indicates that the adjusted data is a better representation of the speed line than the unadjusted data, particularly near surge.

The airflow through the customer bleed was being modulated when the engine surged during runs 25 and 27. This may explain the apparently negative slope at surge. As a brief check of this the surge points from runs 22 and 23 were examined. Although the quantitative data is not

available, because of the calibration technique in use at the time, the qualitative data indicates that the engine surged at a positive slope. There was no airflow through the bleed at the surge point for either run. The qualitative analysis, summarized in Table 3.4, indicates that modulating the bleed massflow can destabilize the engine.

		Surge Point		Slope @	Zero Slope Location		Fractional
		$\pi/\pi_{des}$	Massflow/ design	Surge	$\pi/\pi_{des}$	Massflow/ design	Standard Dev of data (%)
Run 25	raw data	0.917	0.931	0.3794	0.9206	0.9323	0.55
	adjusted	0.909	0.925	-0.6688	0.9217	0.9217	0.57
Run 27	raw data	0.915	0.921	11.8801	0.9074	0.9161	0.294
	adjusted	0.906	0.916	-0.0760	0.9067	0.9138	0.360
Run 28	raw data	0.906	0.913	-1.6394	0.9005	0.9189	0.369
	adjusted	0.906	0.913	0.0224	0.9037	0.9136	0.420

\* indicates the preferred curve fit

Table 3.3: Surge Points and Slopes from the various curve fits.

Run	Sign of the Slope	Forcing at Customer Bleed
run 22	positive	no forcing
run23	positive	no forcing
run 25	negative	forcing
run 27	negative	forcing
run 28	positive	no forcing

Table 3.4: Sign of the Slope at Engine Surge Point

### 3.1.4. Hotwire Linearization

The steady state data can also be used to linearize the hotwire output signal. The hotwire senses the velocity in the inlet bellmouth. This velocity is proportional to the massflow through the engine. So the hotwire is linearized to match the corrected massflow through the engine, as measured by the calibrated bellmouth. The data shown in Figure 3.13 is of the expected shape for a hotwire calibration curve, reinforcing the validity of this linearization. A second order

curve was fit to the data. There are large fluctuations ( $\pm .2$  volts) in the hotwire output near the primary region of interest (near non-dimensional massflows of 1) so the curve was fit over the entire range of the signal. This curve can be used to linearized the hotwire output for the high speed data.

### 3.2.High Speed Data

MMADCAP records the high speed data at 4000 Hz and stores it in ADCAP format. The high speed data files can be very large, up to 15.6 Mbytes. The data is converted into a MATLAB compatible format and split into 2 Mbyte chunks for processing. Each original ADCAP file is a single record. They are sequentially numbered starting at 1 for each run. The pieces are also numbered sequentially for each record. All the data from a piece can be loaded into MATLAB at one time. If a trace over the whole record is desired the pieces of that record must each be loaded, one at a time, the desired data stored and the rest cleared.

The pressures in this thesis have been divided by a mean or reference pressure ( $\bar{P}$ ) to non-dimensionalize them. The reference pressures used may vary from run to run, but are not changed for data from the same run. The pressures from inside the engine (at the upstream, throat and combustor locations) were divided by the mean pressure for that location. The pressure taps on the customer bleed both upstream and downstream of the shaker were divided by the mean combustor pressure. Any massflow or pressure ratio data has been non-dimensionalized as described in section 3.1.

High speed data was taken without external forcing to examine the normal operating conditions and noise levels. High speed data was also taken with external forcing. This data was used to determine the response of the disturbances within the engine and to calculate the transfer functions between the sensor locations within the engine.

### 3.2.1. Data With No External Forcing

High speed data with no external forcing is available for three operating regions. They are stable operation far from surge, operation immediately prior to surge (pre-surge), and operation during surge.

#### 3.2.1.1. Stable Operating Point

The data presented in this section is from a sixteen second segment of data from run 28, when the engine was at approximately 95 % corrected speed and not near surge. The closest the engine came to the eventual surge point, during those sixteen seconds is indicated on Figure 3.14.

##### 3.2.1.1.1. Time Traces

Time traces of the pressure signals from within the engine are shown in Figures 3.15 and 3.16. These pressures are measured at the combustor, throat and stator taps shown in Figure 2.3. The customer bleed tap is shown on Figure 2.21. The disturbance levels of these signals range from 0.5 to 1.25 %, this is above the disturbance levels of about 0.3 % that are observed when the engine is off (Table 3.5).

Location	Engine Off	Run 28, @ 95%, away from surge
Stator Tap	± 0.3 %	± 1.25 %
Throat at 0°	± 0.3 %	± 0.75 %
Throat at 120°	± 0.3 %	± 0.75 %
Throat at 240°	± 0.3 %	± 1.0 %
Combustor	± 0.3 %	± 0.5 %
Customer Bleed w/o bleed	± 0.2 %	± 0.5 %
Zeroth Mode at the Throat	± 0.2 %	± 0.5%
Hotwire Output	± 0.01 volts	+0.1 / -0.5 volts

Table 3.5 : Disturbance Levels in Engine at 0 and 95 % speed



With the exception of the throat there is only one pressure tap being monitored at each axial location. There are three taps in use at the diffuser throat, spaced at 120° intervals around the circumference. The pressure measurements from these three taps can be combined to produce a spatial Fourier decomposition around the compressor annulus. A discrete Fourier Transform is used to produce the zeroth and first order modes of the spatial decomposition. The results of this are shown in Figure 3.17. The zeroth mode behaves much like an average of the three taps, while the first mode is a complex value that contains the magnitude and phase of any rotating pressure perturbations. Coherent rotating perturbations will cause the phase to vary linearly with time. For operation near 95 % speed away from the surge point there is no evidence of a rotating disturbance. Working with the zeroth mode at the throat reduces the influence of disturbances that are not uniform around the circumference, without reducing the sensitivity to the one-dimensional disturbances, associated with surge and the response to modulating the customer bleed.

Figure 3.18 shows two time traces of the hotwire output. The first is with the engine off. It shows small perturbations ( $\pm 0.01$  Volts on a 1 Volt signal) which are probably the results of air near the hotwire rising as it is heated by the wire. The second trace shows the hotwire output while at the stable operating point near 95 % engine speed. The disturbance level is now  $+0.1 / -0.5$  Volts for a 2.5 Volt signal. These disturbances may be caused by temperature variations in the inlet air, turbulence, or some other source. In any case these disturbances make it very difficult to extract any useful information from the single hotwire.

The vibrometer signal is taken from the scope out of the vibration monitor and has a DC level of zero. It is primarily used to examine the spectral content of the engine vibration.

### 3.2.1.1.2. Power Spectra

Power spectra are produced using the spectrum function in MATLAB. Spectrum accepts a data time trace and a window size. The time trace is then split up into windows of the specified number of data points (1024 points were used for all the PSDs in this thesis). Each window is Hanning windowed and then a fast Fourier transform (FFT) is performed on it. The absolute value of the resulting FFT is then squared and multiplied by a scale factor to produce the PSD of each window. All the windows in the time trace are then averaged to produce the PSD of the time trace. The scale factor is proportional to the window size. Therefore, keeping the window size constant allows the spectra of a signal at two different times to be compared, even if they were taken over different lengths of time. The PSDs were used to measure spectral content, so the exact scale factor used by MATLAB was never determined, and units are not included on the y axis of the power spectra.

Figures 3.19 thru 3.28 contain the PSDs of the pressure signals, the hotwire output and the vibrometer signal for the sixteen second interval that matches the time traces shown in Figures 3.15 and 3.16. There are several significant features of these PSDs. There are noticeable peaks at one-half, one, and two times the rotor frequency (approximately 750 Hz) on most of the pressure signals these peaks are most apparent at the stator tap (Figure 3.26). There is also a peak at 825 Hz that appears on all the signals. This peak even appears on the hotwire signal (Figure 3.27), which has no other peaks. Another signal although weaker also appears at 1420 Hz on most of the pressures. The fact that these peaks appear on the vibrometer indicates that they are not aerodynamic disturbances, but rather electrical or vibrational in nature. This argument is strengthened by their appearance on the power spectrum of the stator tap. The stator taps are expected to have a maximum frequency response to pressure perturbations of 713 Hz (see section 2.2.12.1).

Also of interest are the broadband peaks near 500 and 600 Hz on the customer bleed (Figure 3.19) and the combustor (Figure 3.20) pressure taps. These peaks appear to be caused by acoustics. The wavelength of a 500 to 600 Hz acoustic disturbance, at the pressures and temperatures present in the combustor, matches the distance around the circumference of the combustor.

Figure 3.21 contains the PSD of the zeroth mode at the throat. Comparison with the PSDs of the throat taps (Figures 3.23 thru 3.25) shows that the zeroth mode contains the spectral information of the taps. The PSD of the first mode at the throat is shown in Figure 3.22. Since the first mode is complex it may have both positive and negative frequencies. These frequencies correspond to disturbances rotating in opposite directions around the annulus. If a rotating disturbance exists it will produce a peak at only the positive or negative value of the rotational frequency. The PSD has no peaks, so there is no evidence of a rotating disturbance.

#### 3.2.1.2. Surge Inception

As the engine approaches surge two changes in the pressure disturbance structure may occur. A rotating pressure disturbance may develop. If this grows it may become rotating stall and trigger surge. The other possible change is that the disturbance levels will increase slightly as the damping in the system decreases.

The check for rotating disturbances involves three steps. First the time traces of the three Kulites at the diffuser throat are plotted together for the time immediately prior to surge. This is done in Figure 3.29, where zero time corresponds to the point at which the engine begins to surge. A rotating disturbance would appear as a peak or trough in the pressure that moves from one trace to another as time progresses. There is no evidence of such a disturbance. Second the spatial Fourier decomposition of the throat taps is taken immediately prior to surge. A rotating disturbance would produce an increase in the magnitude of the first mode (Figure 3.30) and the

phase would vary linearly with time. This does not happen.. The third check for rotating disturbances is to plot the PSD of the first mode. A disturbance rotating in either direction should show up as a peak on the PSD. Figure 3.31 contains the PSD of the first mode at the throat from the last quarter second (1024 data points) before the engine surges. There are no peaks on the PSD. No evidence has been found that would indicate that the surge is preceded or triggered by a rotating disturbance. Similar results are found for other engine surges.

The disturbance level of a signal can be checked by calculating its standard deviation. The larger the noise signal the higher the standard deviation will be. For Figure 3.32 the fractional standard deviations of each signal are calculated for several quarter second intervals (1024 data points). Each interval is shifted by 0.064 seconds (256 data points). The final interval ends when the engine begins to surge. (The time scales on these plots indicate how many seconds before surge each interval ends.) The fractional standard deviations of all the pressures, the hotwire and the vibrometer double between 1 and 0.5 seconds prior to surge. (All the standard deviations increase by an order of magnitude when the engine surges.)

Approximately one second before the engine surged the nozzle was commanded to close slightly. The increase in the disturbance level at that point can then be explained two ways. Closing the nozzle may have moved the engine to an operating point very near surge where the system damping is low, thus resulting in an increase in the disturbance level. It is also possible that the actual motion of the engine as the nozzle is closed is responsible for the increase in the disturbance level. The disturbance levels at the combustor, customer bleed, and the throat decrease slightly between 0.5 seconds prior to surge and surge, but they do not return to their previous levels. This may indicate that a combination of the two possibilities is what actually occurs.

When the same plots (Figure 3.33) are produced for the surge from run 27 they show no evidence of an increase in the disturbance level prior to surge (several of the disturbance levels

are higher in general because the flow through the bleed valve is being modulated). The nozzle was not in motion immediately prior to surge for run 27. This may indicate that the disturbance increase is related to the motion of the nozzle.

### 3.2.1.3. Surge Cycle

The pressure and hotwire traces from the first surge cycle are shown in Figures 3.34 and 3.35. The raw hotwire output and a modified hotwire output are both included in Figure 3.35. The modified hotwire output has been flipped down below 1 Volt to indicate the region of suspected reverse flow. In this region the velocity or massflow indicated by the hotwire is not quantitatively correct. The hot air blowing out the front of the engine changes the calibration curve of the hotwire. The reverse flow region was selected based on the behavior of the hotwire and the pressures. The initial time of reversal is very clear, the return to forward flow is not.

In the first 0.003 seconds after the engine starts to surge, the static pressure at the throat jumps by a factor of 1.5, the hotwire signal drops to near zero velocity and then back up again. The spike in the throat static pressure and the dropout in the hotwire signal indicate that the massflow through the compressor has reversed. (The hotwire only indicates velocity not direction.) The static pressures at the combustor tap and the customer bleed tap both begin to drop, while the pressure at the stator tap starts to increase. After the initial spike the static pressure at the throat begins to decrease. As the blowdown continues the static pressure at the stator rises, apparently due to the higher pressure air coming back through the combustor. The pressures at the combustor and customer bleed decrease together. The static pressure at the stator reaches 1.2 times its pre-surge level 0.008 seconds after the surge began. At 0.018 seconds the pressure at the stator tap has returned to its steady state level, and there is a small peak in the static pressure at the throat. That peak probably corresponds to the recovery of the centrifugal compressor, because the combustor pressures begin to rise. Before they recover the combustor

pressures drop to about 30 percent of their normal levels. The hotwire does not appear to indicate a reversal in the flow until the static pressure at the stator has dropped below ambient pressure, 0.022 seconds after the surge began. After the flow returns to the forward direction the pressures recover to about 95 % of their pre-surge levels, before the engine surges again. This surge cycle repeats at eight to nine times a second.

Figure 3.36 shows the massflow through the engine estimated by linearizing the hotwire signal. The quantitative magnitude of the negative massflows are not correct, because the hotwire signal does not correspond only to velocity when the flow is reversed.

This data can also be used to produce a pressure vs. massflow map of the surge cycle (Figure 3.37). Where instantaneous pressure from the combustor is plotted against the massflow indicated by the hotwire. Once again any massflows indicated as negative may not have the indicated magnitude. This map indicates that the massflow through the compressor reverses as the pressure begins to drop, emptying the combustor. The pressure continues to drop until it has reached a level where the flow reverses again and the compressor begins to refill the combustor. The surge pattern shown here is typical for this engine.

### 3.2.2.Data With External Forcing

#### 3.2.2.1.Forcing Function Behavior

As detailed in chapter 2 the external forcing is applied to the engine by modulating the flow through the customer bleed. The forcing function can be described in terms of the bleed massflow. There are three pressure taps on the customer bleed to measure the forcing function (Figure 2.21). There is a pressure tap upstream of the shaker valve to monitor the pressure perturbations it produces. The massflow through the bleed is calculated using the total and static pressures measured downstream of the bleed valve.

Although the bleed valve area change with time is approximately sinusoidal the resulting mass bleed and pressure perturbations are not, due to duct dynamics, so harmonics of the fundamental forcing frequency are present. The amplitude and behavior of the forcing signal also vary somewhat with the frequency.

### 3.2.2.1.1. Bleed Massflow

The bleed massflow was calculated using total to static pressure ratios to find the Mach number and then the bleed massflow. The total temperature is assumed to remain constant between the compressor discharge and the customer bleed. The bleed massflow can be calculated two ways. The first calculation is based on the total and static pressures from the taps downstream of the shaker (Figure 3.38). The second calculation uses the tap upstream of the shaker in the customer bleed as the static pressure and assumes that the total pressure upstream of the shaker valve is the same as in the combustor. The combustor total pressure is calculated using equation 2.5 (Figure 3.38).

Both calculations follow this procedure. The isentropic Mach number is found using,

$$M = \sqrt{\frac{2}{\gamma-1} \left[ \left( \frac{P_T}{P_S} \right)^{\frac{\gamma-1}{\gamma}} - 1 \right]} \quad (3.13)$$

Above Mach 1 losses in the  $P_T$  reading are caused by shocks before the Pitot tube, but for Mach numbers near one these losses remain small. Since  $M_{\max}=1.05$  shock losses would result in an error of less than 0.025 %, they are neglected for these calculations. Then the massflow is found using,

$$\dot{m} = \rho_s u A_{duct} = \frac{P_s}{RT_s} \times M \sqrt{\gamma RT_s} \times A_{duct} = \frac{P_s M \sqrt{\gamma}}{\sqrt{RT_s}} A_{duct} \quad (3.14)$$

where

$$T_s = \frac{T_T}{\left(1 + \frac{\gamma-1}{2} M^2\right)} \quad (3.15)$$

Equations 3.13 thru 3.15 lead to the following error propagation formulas (the same notation is used here as in section 2.5.). For simplicity errors in the estimation of  $\gamma$  and R are neglected until the final calculation of the standard deviation of the bleed massflow, where they are exaggerated.

$$S_M = .5 \times \sqrt{\left(\frac{\gamma-1}{\gamma}\right)^2 \left(S_{P_T}^2 + S_{P_S}^2\right)} \times \frac{V_{pr}}{V_{pr-1}} \quad (3.16)$$

$$S_{T_S} = \sqrt{S_{T_T}^2 + \left(\frac{\gamma-1}{\gamma}\right)^2 \left(S_{P_T}^2 + S_{P_S}^2\right)} \quad (3.17)$$

$$S_\gamma = .1/1.4 \quad (3.18)$$

$$S_R = S_\gamma \quad (3.19)$$

$$S_{\dot{m}} = \sqrt{S_{P_S}^2 + S_M^2 + \left(.5S_\gamma\right)^2 + \left(.5S_R\right)^2 + \left(.5S_{T_S}\right)^2} \quad (3.20)$$



This results in an uncertainty of 16.0 % of the bleed massflow.

Figure 3.39 shows the results of these calculations with the signals shown in Figure 3.38. The Mach number in the tube downstream of the shaker valve is shown on the left. The right hand plot contains three bleed massflow calculations. The upper trace (2) is calculated using the static pressure from upstream of the shaker and assuming that the total pressure is the same as the total pressure in the combustor. This calculation does not agree with the other two. One of the massflows that match was calculated using the total and static pressure probes downstream of the shaker valve (1). The other matching bleed massflow was calculated using the static pressure measured upstream of the shaker and assuming a 6 % loss in the total pressure between the combustor and the customer bleed (2'). This pressure loss is not unreasonable, with the convoluted flow path from the combustor to the customer bleed and within the bleed valve.

The bleed massflow used to characterize the forcing and to find the transfer functions within the engine is the one calculated based on the total and static pressure taps downstream of the shaker valve.

#### 3.2.2.1.2. Effect of Frequency

The magnitude of bleed massflow varies with the excitation frequency (Figure 3.40). As the excitation changes from 100 to 350 Hz the RMS and peak values of bleedflow vary by about 10 %. The largest amount of bleed flow occurs between 200 and 250 Hz. The behavior of the bleedflow was also apparently unaffected by the modification to the bleed venting (Figure 3.41).

#### 3.2.2.2. Acoustic Behavior of Pressure at the Customer Bleed

There is a range of frequencies (200-250 Hz) at which the pressure signal from the customer bleed port develops a second peak and the second harmonic becomes more powerful than the fundamental. Before the total and static pressure taps were installed downstream of the shaker

valve (to measure massflow through the bleed), this behavior raised concerns that the massflow modulation was also being affected.

Figure 3.41 shows the time traces of the customer bleed (valve inlet static pressure) signal at several different excitation frequencies. At about 90 Hz the pressure oscillations have broad ragged peaks with sharp narrow troughs. The peak narrows as the excitation frequency increases, until shortly before 195 Hz the signal develops a distinct double peak. One peak is at the level of the original peak, while the other grows above it. The high peak continues to grow until about 250 Hz. Then the lower peak starts to move down into the trough. The lower peak eventually settles to the bottom of the trough.

The second peak appears as the second harmonic of the excitation moves over the broadband peak in the spectra of the signal from the customer bleed. As the second harmonic moves up the broadband peak it increases in power until it surpasses the power of the fundamental. Figures 3.43 and 3.44 provide a comparison between the power levels of the second harmonic at excitation frequencies of 90 and 242 Hz. (The excitation frequency is indicated by the dashed line.) 242 Hz is in the region of frequency doubling, 90 Hz is not. In the range of the frequency doubling the second harmonic of the pressure signal is slightly more powerful than the fundamental.

The frequency doubling also increases the amplitude of the pressure oscillations at the customer bleed (Figure 3.44). The peak to peak amplitude of the oscillations almost doubles as the excitation frequency is increased from 100 to 250 Hz. To assure that this behavior was not caused by the acoustic dynamics of the bleed valve venting system, the system was modified (Figure 2.19). This modification had no apparent impact on the behavior of the pressure at the customer bleed. This can be seen by comparing Figures 3.45 and 3.46. Figure 3.45 shows the signal amplitude and RMS from run 28, Figure 3.46 is the same information from run 27. Run

27 had the modified venting system, for run 28 the venting was returned to the original configuration.

When the total and static taps were installed downstream of the shaker, it became apparent that the bleed massflow does not have similar behavior. The oscillations in the massflow are somewhat ragged at the lower excitation frequencies, but there is only one peak at 242 Hz (Figure 2.47). In fact, the second harmonic has lower power at 242 Hz (Figure 3.49) than at 90 Hz (Figure 3.48).

The doubling is not caused by the venting of the bleed, as was demonstrated when it was modified. It is not caused by a doubling in the forcing signal (the massflow through the bleed). It is connected to the location of the broadband peak in the spectra of the customer bleed pressure signal, which is thought to be acoustic in nature. It now appears that the doubling behavior of the pressure oscillations at the customer bleed is caused by acoustic dynamics internal to the engine.

### 3.2.2.3.Engine Response

The response of pressures within the engine to the modulation of customer bleed massflow varies with location and the excitation frequency. The strongest measured response occurs at the combustor pressure tap. That response is difficult to see on a time trace (Figure 3.50), but is clearly evident on a power spectra of the signal at all excitation frequencies between 50 and 800 Hz. The spectra from the combustor pressure tap show that it responds to forcing at the fundamental frequency at 90 Hz (Figure 3.51) and to both the fundamental and second harmonic frequencies in the frequency doubling region (Figure 3.52). The second harmonic is also apparent at higher frequencies, but begins to fade with increasing frequency.

The pressures at the throat respond much more weakly than at the combustor tap. The spectra of the zeroth mode at the throat reveal only slight peaks at the fundamental excitation

frequency and only at excitation frequencies below 175 Hz. A slight peak can be seen at 90 Hz (Figure 3.53) but not at 242 Hz (Figure 3.54).

The response to the forcing at the stator tap location is very weak at all frequencies. Very small peaks appear on the spectra at the excitation frequencies of both 90 and 242 Hz (Figures 3.55 and 3.56), but these peaks could also be caused by the random disturbances in the engine. The spectra of the hotwire signal show even less response to the bleedflow modulation (Figures 3.57 and 3.58).

#### 3.2.2.4. Transfer Functions Within the Engine

Transfer functions within the engine can be found based on the response of the disturbances in the engine to the customer bleed massflow modulation. To produce these transfer functions requires a lot of manipulation of the data, ie. computer time. The data from an entire record during which forcing was applied is loaded into MATLAB. There is not enough memory for all the data from the record, so only the traces of interest are used. The massflow through the customer bleed is calculated for the record. The entire record is divided into windows of 1024 data points (approximately a quarter second). The spectra of the bleed massflow is found for each window. The frequency of the highest peak on the spectra is the excitation frequency. This value is selected and stored. The windows are then combined into groups, where the excitation frequency is the same for every window in the group. The spectra of the input and output signals are then found as described in section 3.2.1.1.2. for each group of windows. The transfer function is the spectra of the output divided by the spectra of the input. The resulting transfer function for each group spans the frequency range from 8 to 2000 Hz. The magnitude and phase of the transfer function at the excitation frequency is recorded for every group. The information from each group is then combined to produce a transfer function that covers the range of excitation frequencies applied at the customer bleed. This methodology was found to be

necessary to reduce the affects of the disturbances present in the engine caused by sources other than the forcing. If the input and output signals do not have a measurable response to the forcing the resulting transfer function is not accurate.

Before finding the transfer functions between two signals, each signal was scaled by its mean value. The magnitude of the resulting transfer function then indicates the percent disturbance produced at the output for a one percent disturbance at the input. If the magnitude is one, a one percent input disturbance produces a one percent disturbance in the output.

The transfer functions between the bleed massflow modulation and the locations within the engine are of interest when determining the effectiveness of a controller, that actuates bleed massflow. They, along with transfer functions between locations within the engine can also be used to compare the engine to the surge stability model (discussed briefly in section 1.2.). As shown above the only locations in the engine that have a measurable response to the bleed massflow are at the customer bleed, the combustor tap and the diffuser throat. The following transfer functions can then be found (Table 3.6); bleed massflow to zeroth mode at the throat, bleed massflow to combustor pressure, and combustor pressure to zeroth mode at the throat. Transfer functions can also be calculated based on the pressure at the customer bleed. None of those transfer functions are presented here because they merely contain the same information as the transfer functions based on the bleed massflow. The transfer functions presented here are from record 6 of run 28, the transfer functions produced from other runs are similar.

Input	Output
Bleed Massflow	Zeroth Mode at the Throat
Bleed Massflow	Combustor Pressure
Combustor Pressure	Zeroth Mode at the Throat

Table 3.6 : Transfer Functions Presented

The magnitude, phase, and coherence of transfer function from the bleed massflow to the zeroth mode at the throat are shown in Figure 3.59. Below 150 Hz there is a detectable signal at the throat caused by the bleedflow modulation. In this region the coherence between the input and output is reasonably high and there is little scatter in the calculated phase. The magnitude is very low. The maximum magnitude of 0.01 means that the  $\pm 100\%$  perturbation of the bleed massflow produces a  $\pm 1\%$  oscillation in the zeroth mode of the throat. As the excitation frequency increases the magnitude of the transfer function decreases to about 0.001 at 200 Hz. As the frequency increases from 100 to 200 Hz there is a distinct decrease in the coherence of the two signals and an increase in the scatter of the phase. In this range the magnitude of the response of the zeroth mode of the throat drops below the level of the disturbances from other sources. Above 200 Hz the transfer function is actually the transfer function between the modulation of the bleed massflow and the noise in the zeroth mode of the throat, not its response to the forcing. In this region the indicated magnitudes are below 0.001, which means the  $\pm 100\%$  oscillation of the bleedflow would produce a  $\pm 0.1\%$  oscillation in the zeroth mode at the throat. That is well below the observed disturbance level of  $\pm 0.5\%$  in the zeroth mode at the throat, with no external forcing.

Figure 3.60 contains the transfer function from the bleed massflow to the combustor pressure. The behavior of this transfer function is similar to that of the bleed massflow to the zeroth mode at the throat. The primary difference is that the magnitude of this transfer function does not drop below 0.001. There is a detectable response to the modulation of the bleed massflow for the entire frequency range shown. There is little scatter in the phase of the transfer function and the coherence remains high for most of the frequency range, except near 250 Hz, where the magnitude is near 0.001.

The transfer function from the combustor pressure to the zeroth mode at the throat is expected to be,

$$\frac{0^{th} @ throat}{combustor} = \frac{\frac{0^{th} @ throat}{\dot{m}_{bleed}}}{\frac{\dot{m}_{bleed}}{combustor}} \quad (3.21)$$

Although it was calculated from the data independently comparison of Figures 3.59 thru 3.61 shows that this is in fact the result. Above 200 Hz there is no measurable response in the zeroth tap of the throat to the excitation, while the response at the combustor is still detectable. This creates an apparent peak at 250 Hz. The actual behavior of the transfer function above 200 Hz is not known.

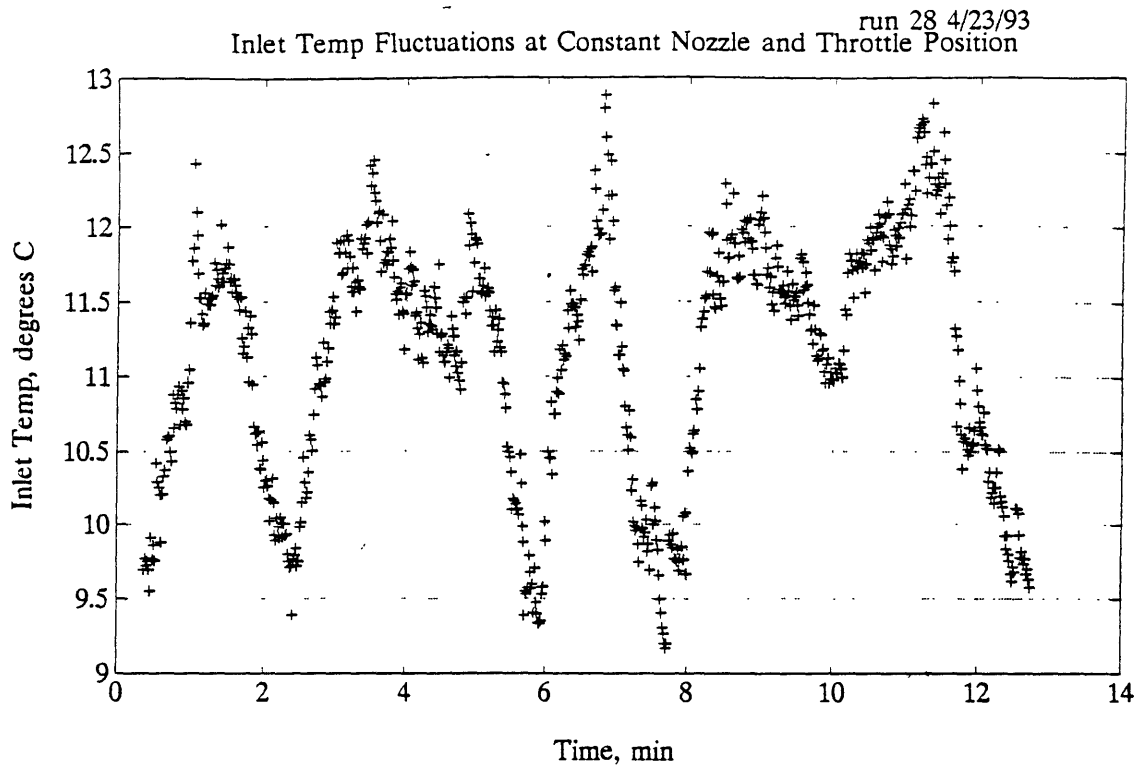


Figure 3.1 : Inlet Temp Fluctuations at Constant Nozzle and Throttle Positions



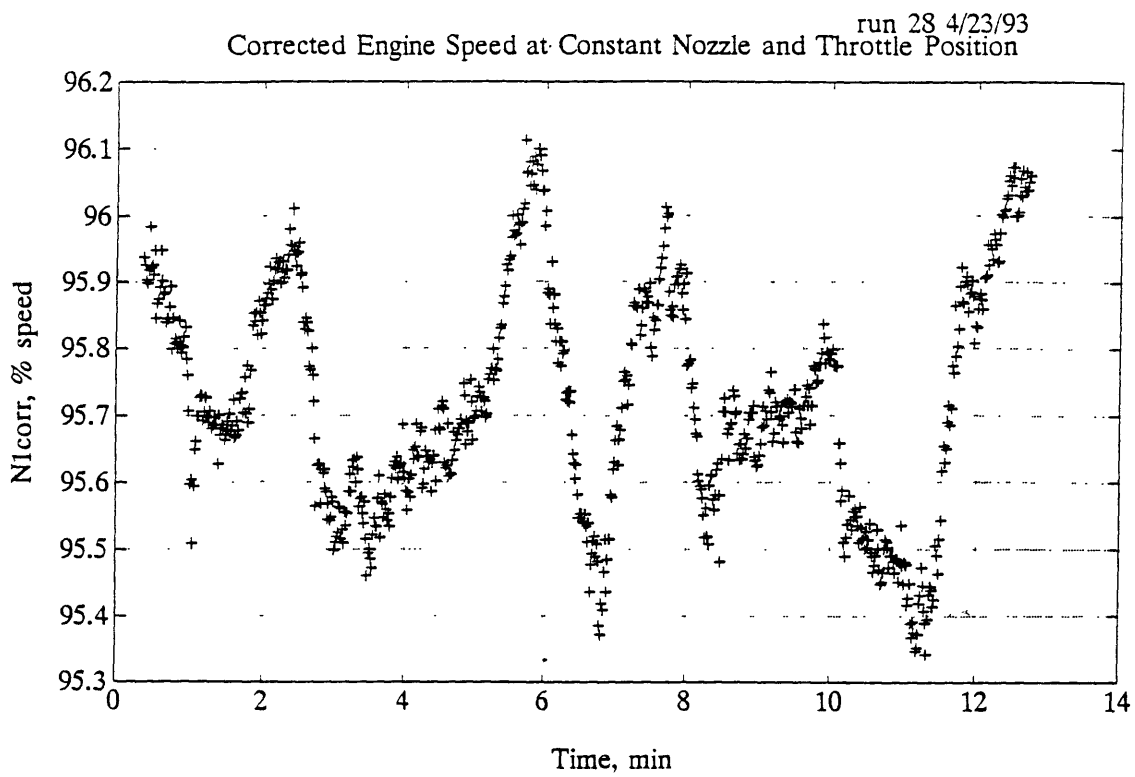


Figure 3.2 : Corrected Engine Speed at Constant Nozzle and Throttle Positions

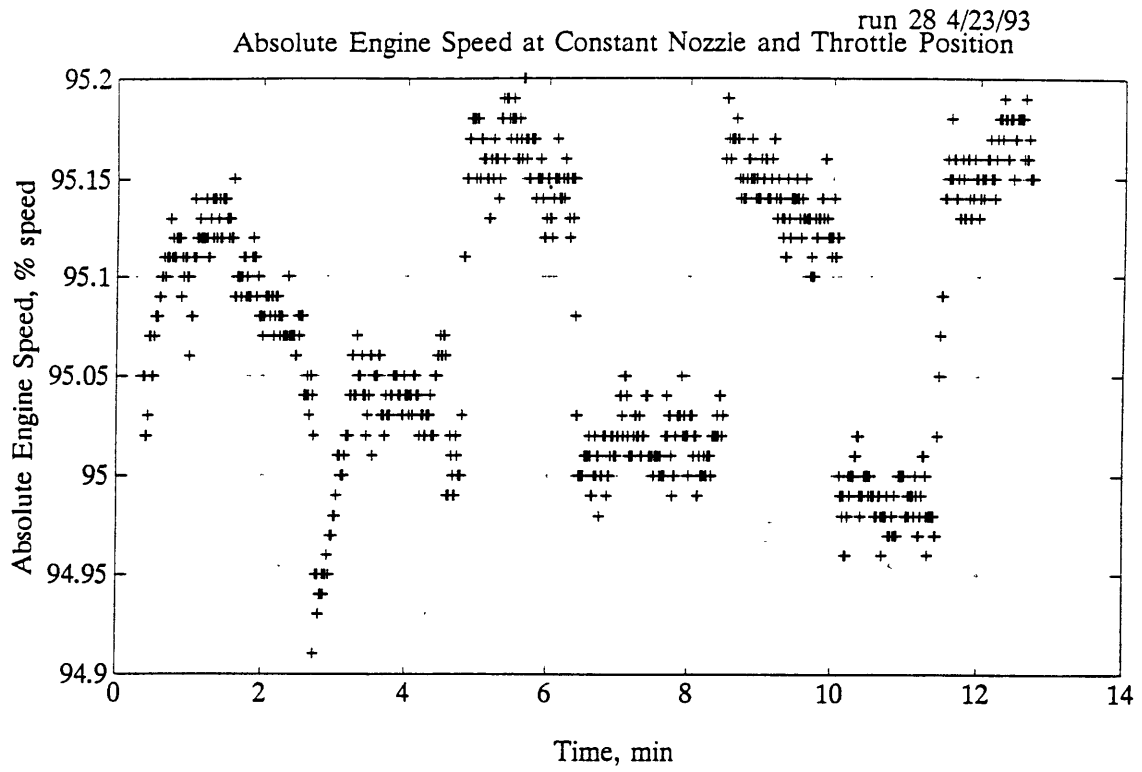


Figure 3.3 : Absolute Engine Speed at Constant Nozzle and Throttle Positions

run 28 4/23/93

Pressure Ratio at Constant Nozzle and Throttle Position

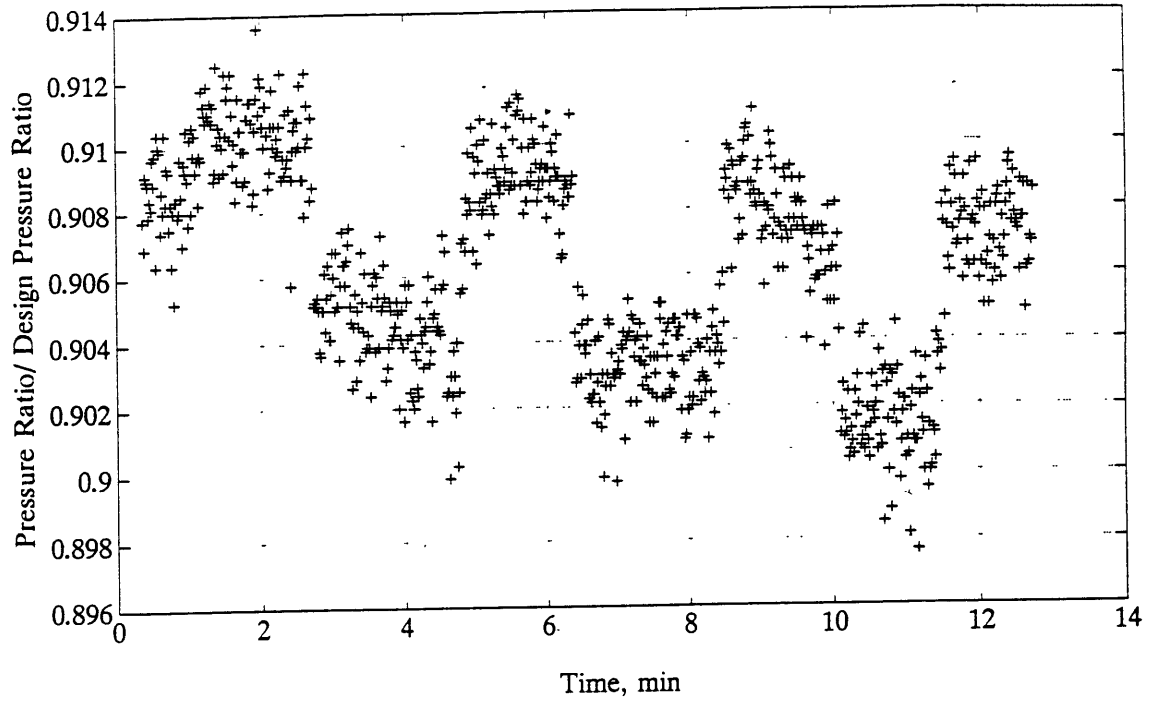


Figure 3.4 : Pressure Ratio at Constant Nozzle and Throttle Positions

run 28 4/23/93

Corrected Massflow at Constant Nozzle and Throttle Position

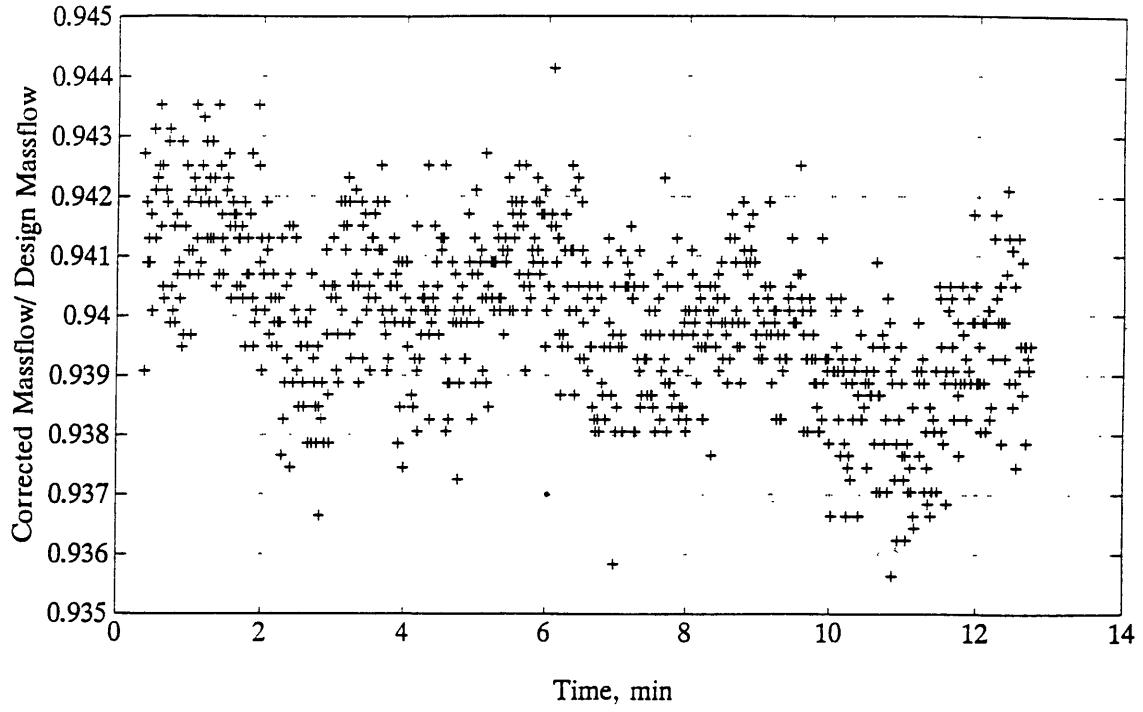


Figure 3.5 : Corrected Massflow at Constant Nozzle and Throttle Positions

run 28 4/23/93  
Constant Nozzle Area Lines from Lycoming and Data Points from Rig

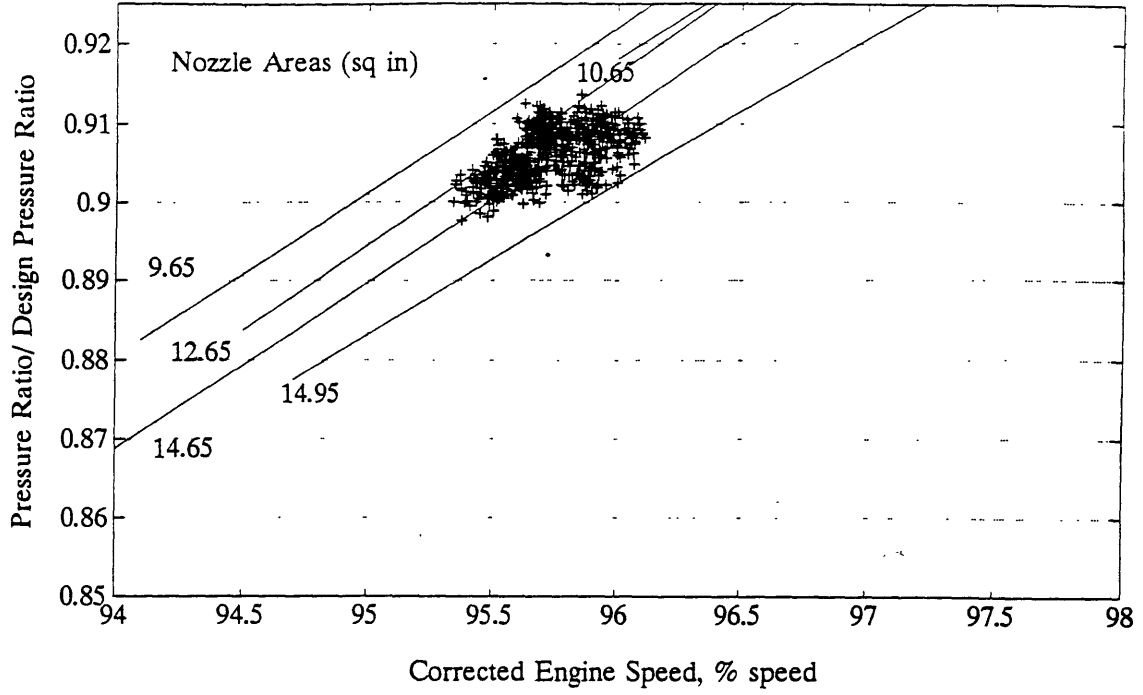


Figure 3.6 : Pressure Ratio vs. Corrected Engine Speed Throttle Lines

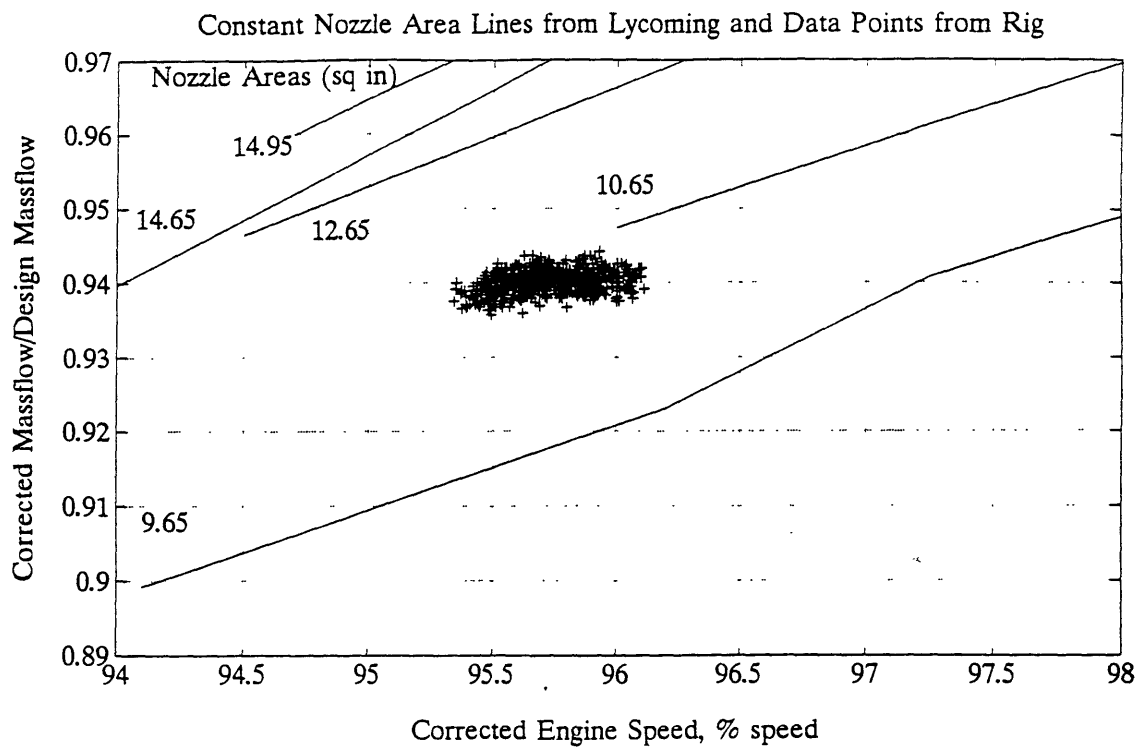


Figure 3.7 : Corrected Massflow vs. Corrected Engine Speed Throttle Lines

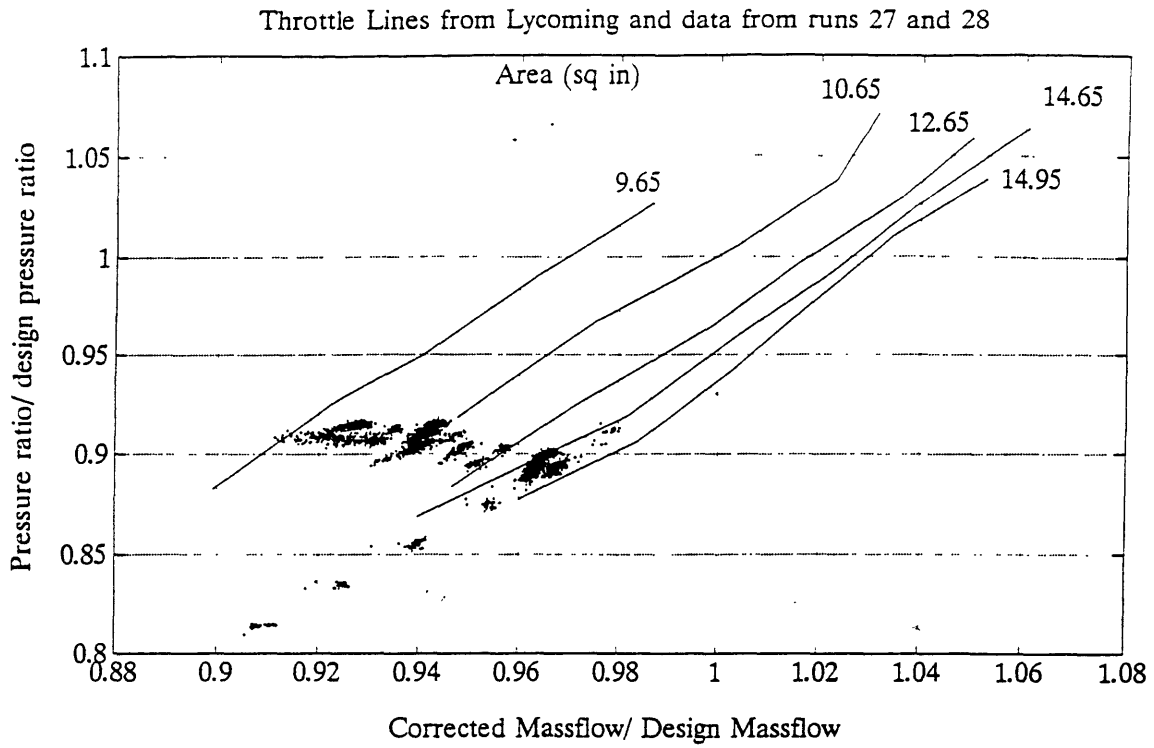


Figure 3.8 : Pressure Ratio vs. Corrected Massflow Throttle Lines

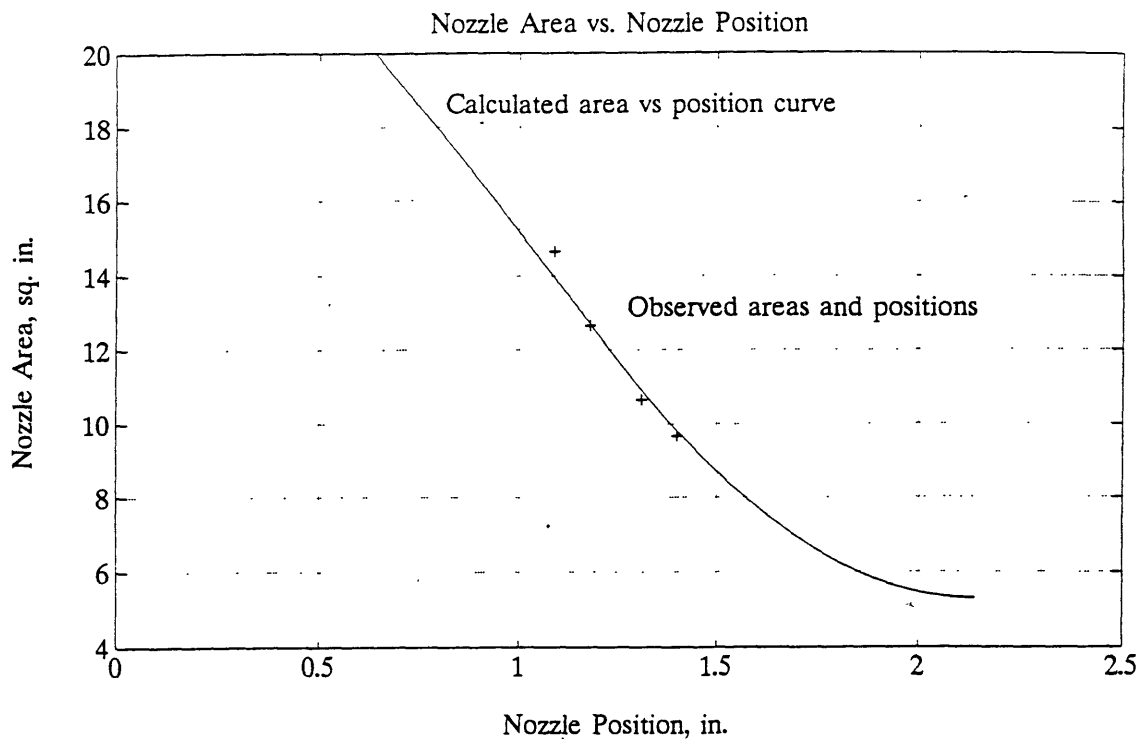


Figure 3.9 : Calculated Nozzle Area vs. Nozzle Position



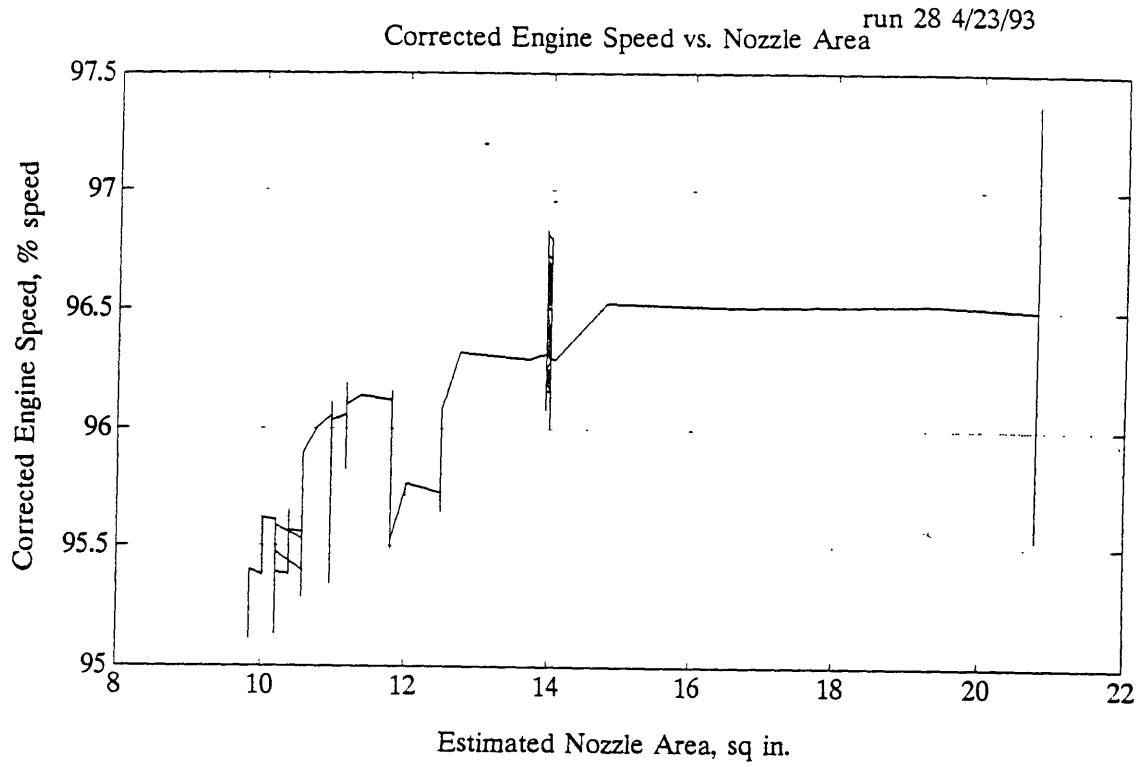


Figure 3.10 : Corrected Engine Speed vs. Nozzle Area at Constant Throttle Setting

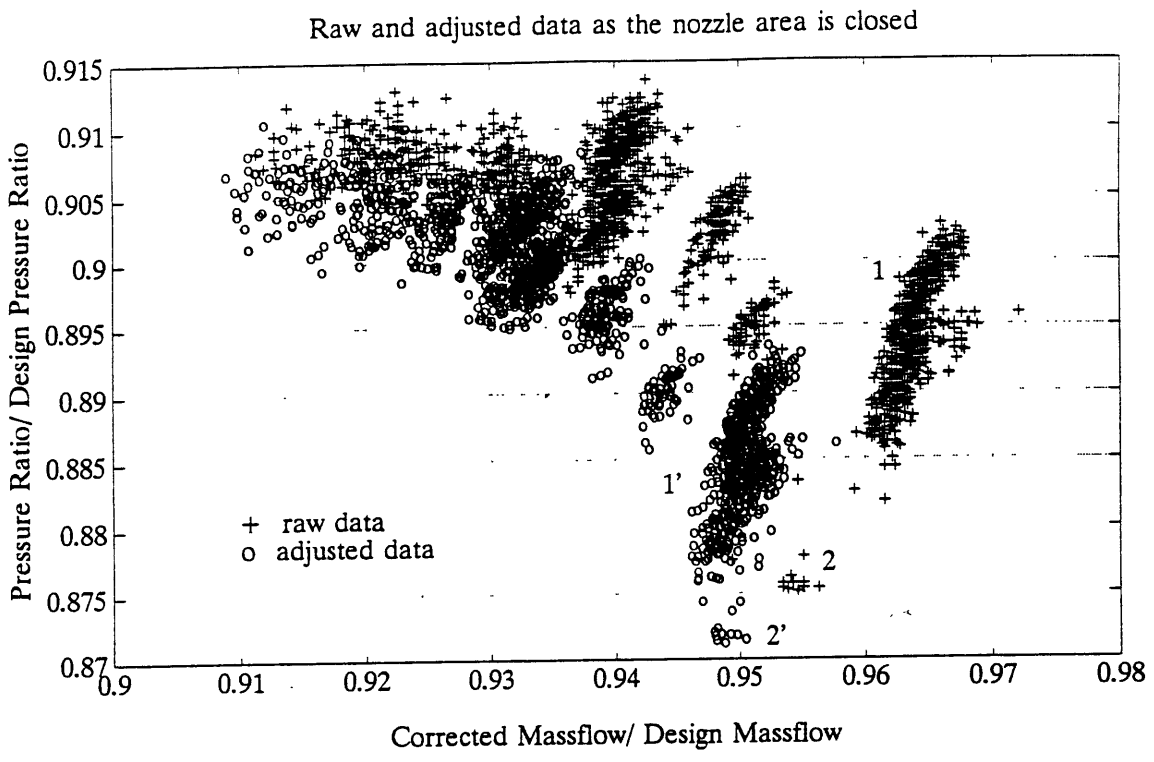


Figure 3.11 : Speed Line Data, Run 28

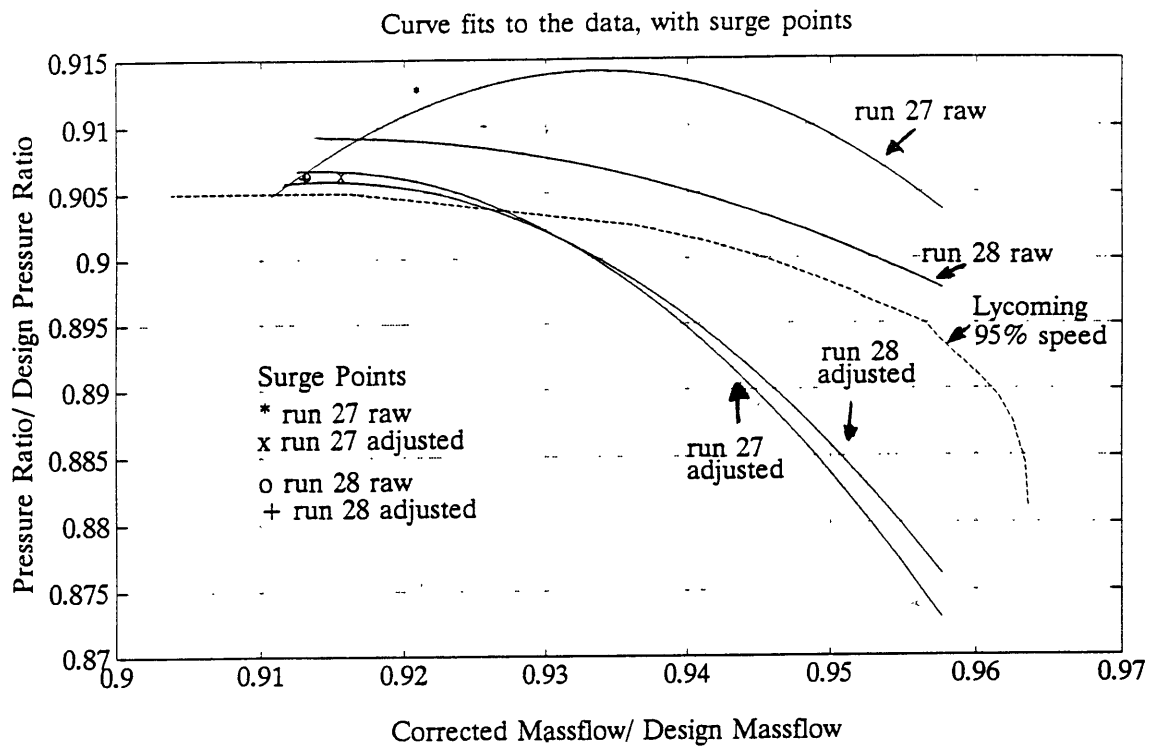


Figure 3.12 : Curve Fits to the Speed Line Data, Runs 27 and 28

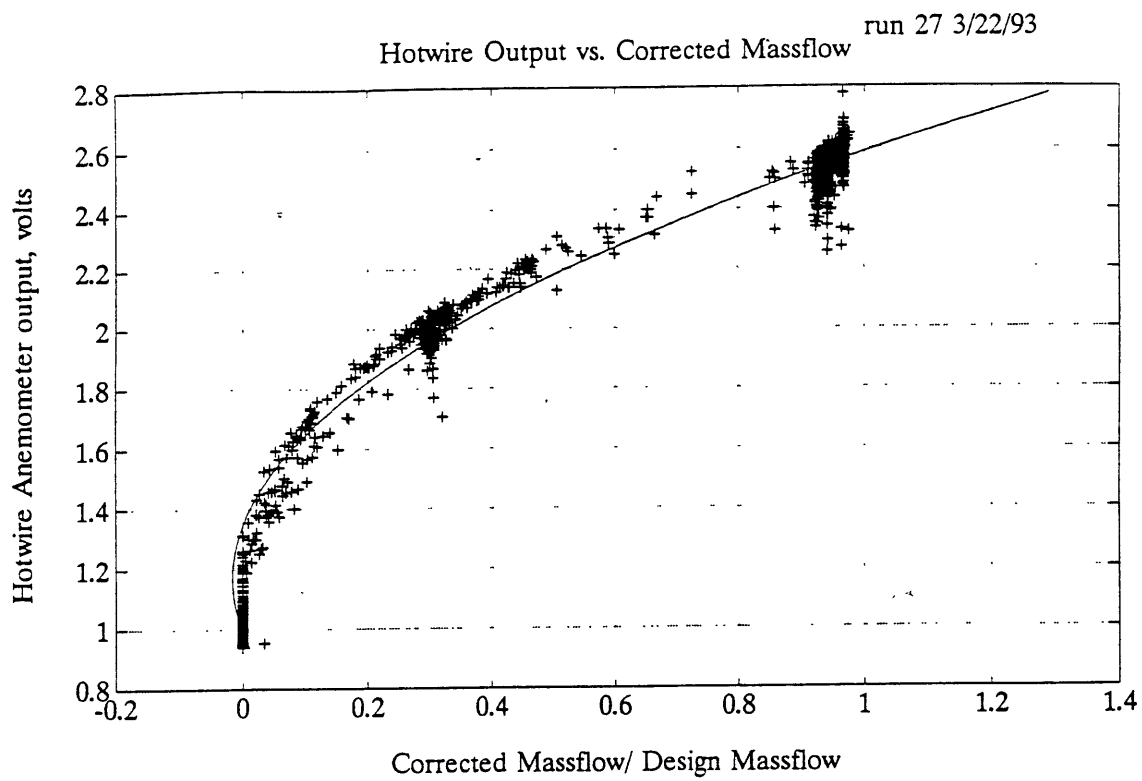


Figure 3.13 : Hotwire Linearization Curve

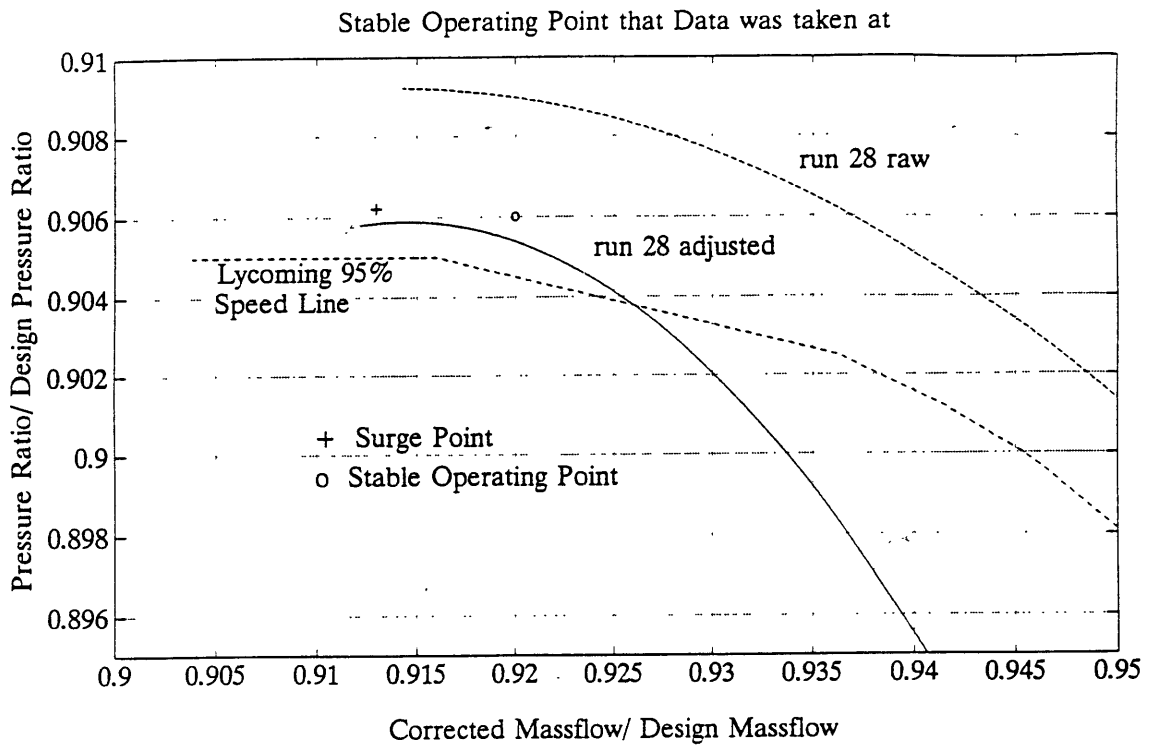


Figure 3.14 : Stable Operating Point

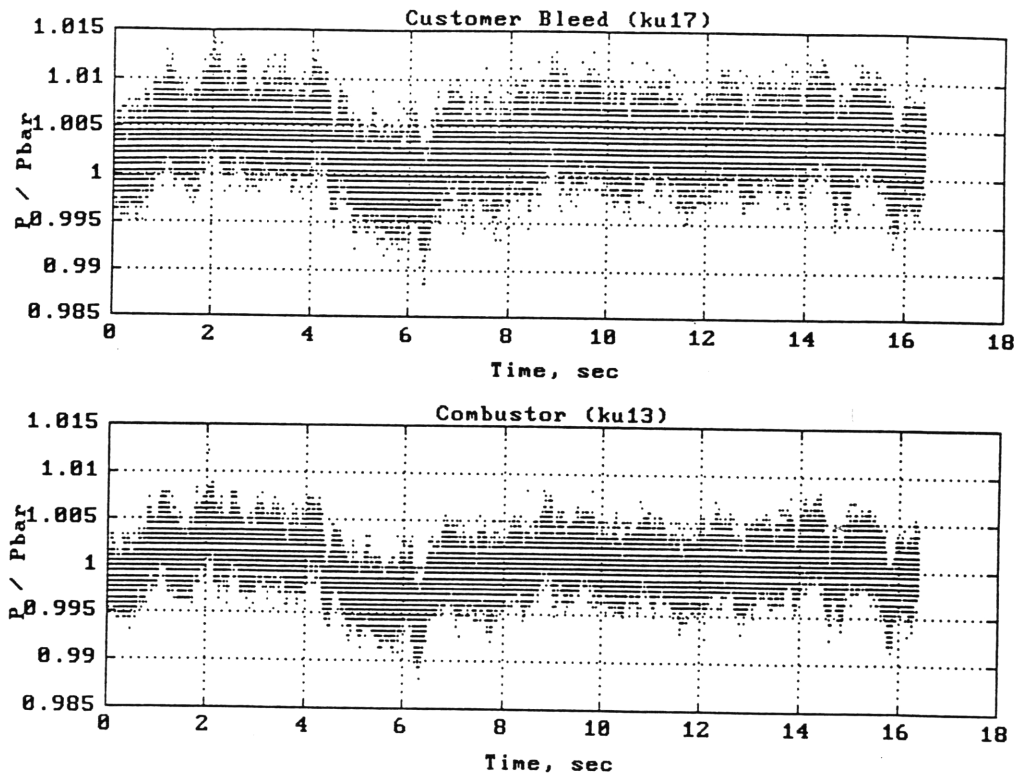


Figure 3.15 : Time Traces of Customer Bleed and Combustor at Stable Operating Point

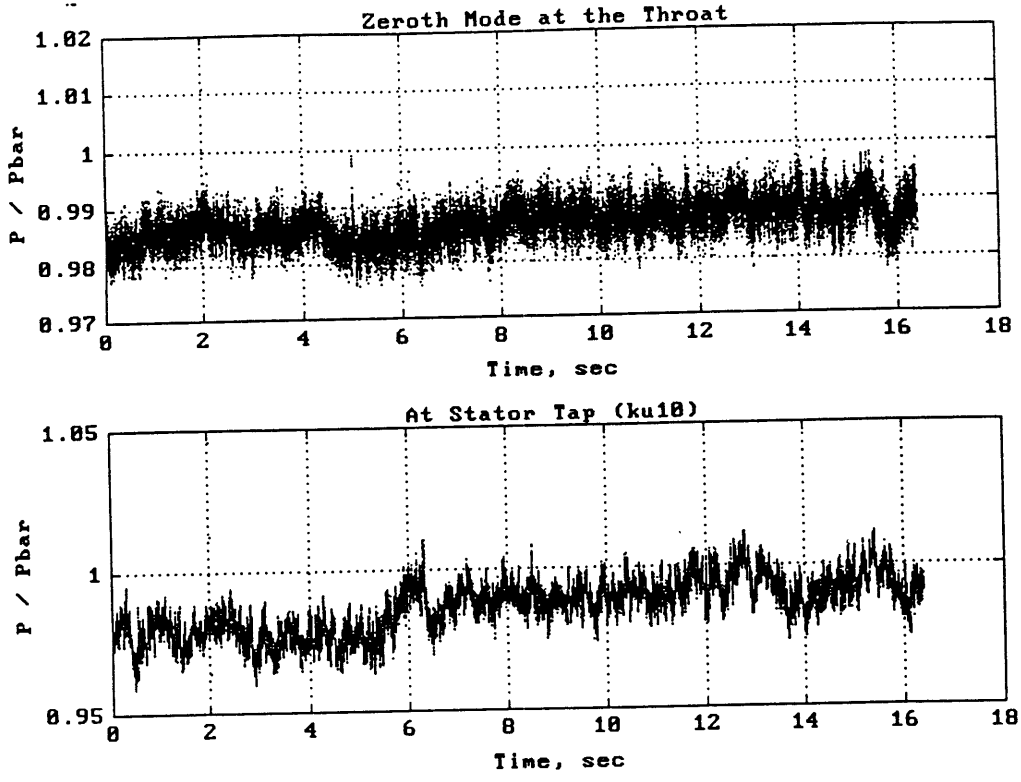


Figure 3.16 : Time Traces of Zeroth Mode at Throat and Stator Tap at Stable Operating Point

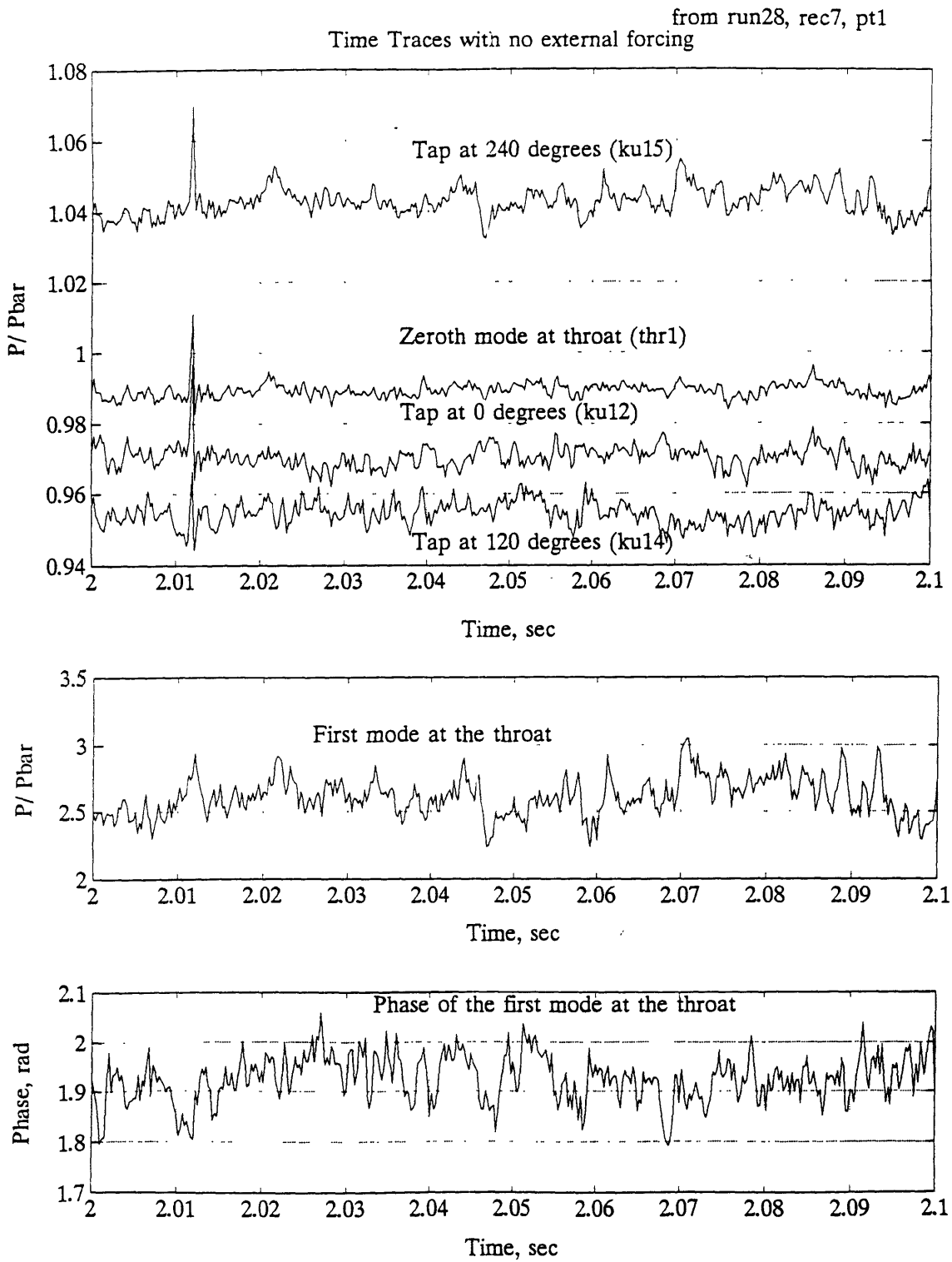


Figure 3.17 : Spatial Fourier Decomposition of Throat Taps at Stable Operating Point



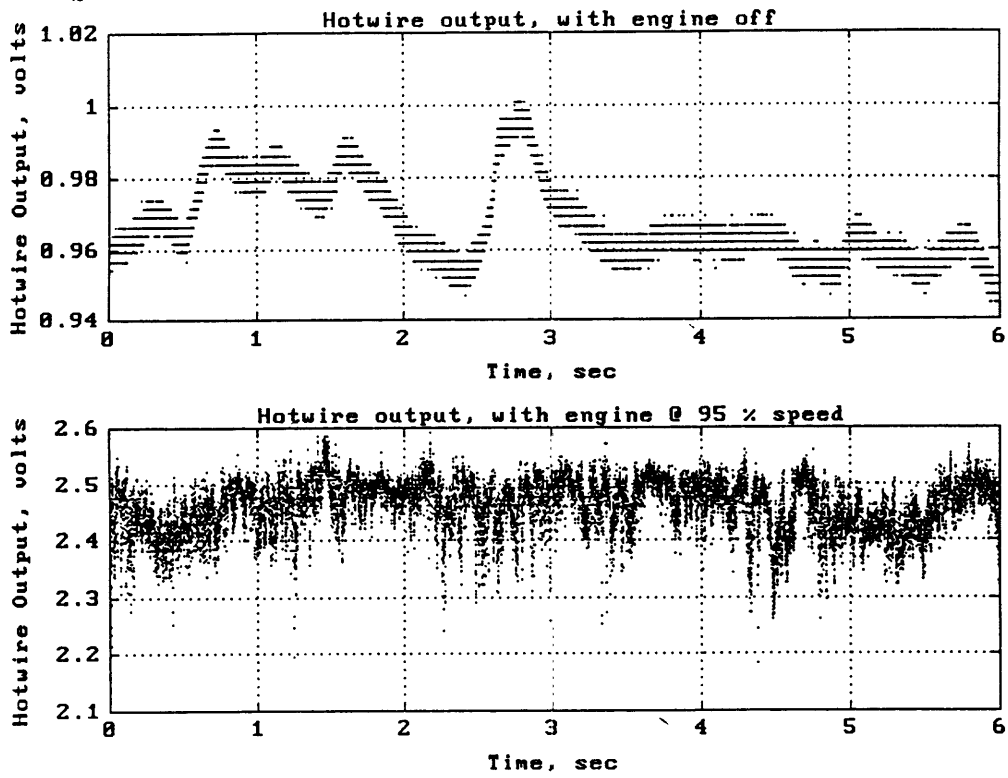


Figure 3.18 : Hotwire Outputs with Engine Off and at Stable Operating Point

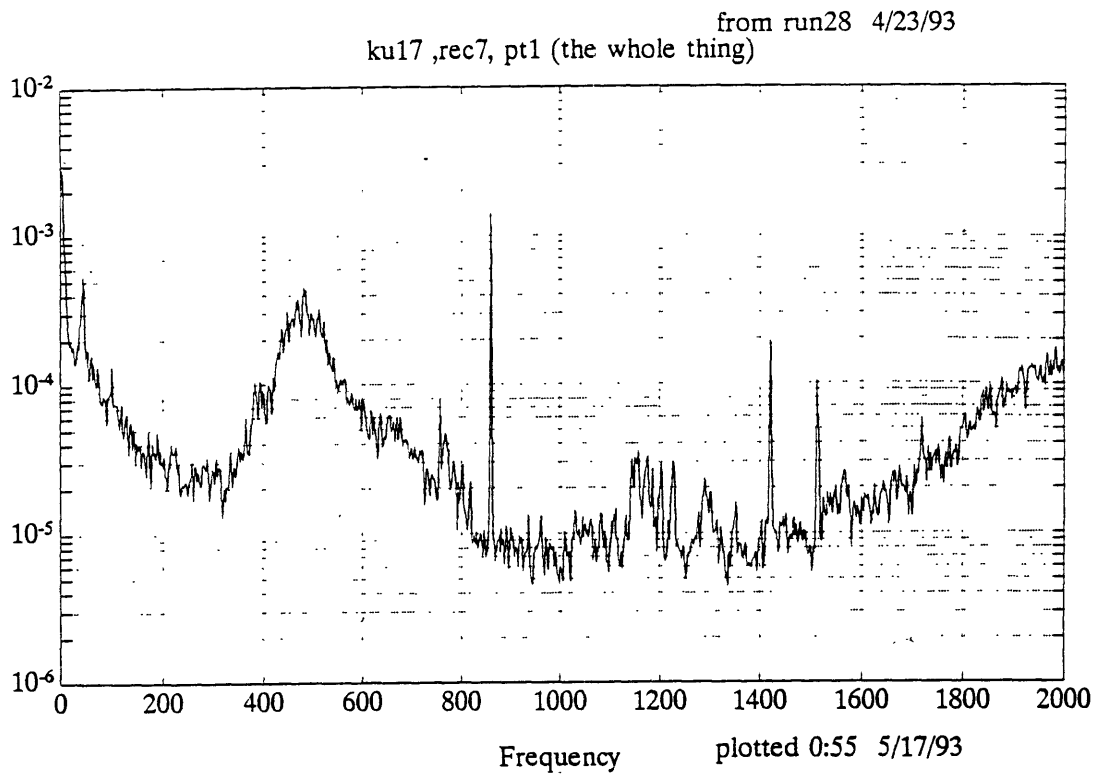


Figure 3.19 : PSD of Customer Bleed at Stable Operating Point

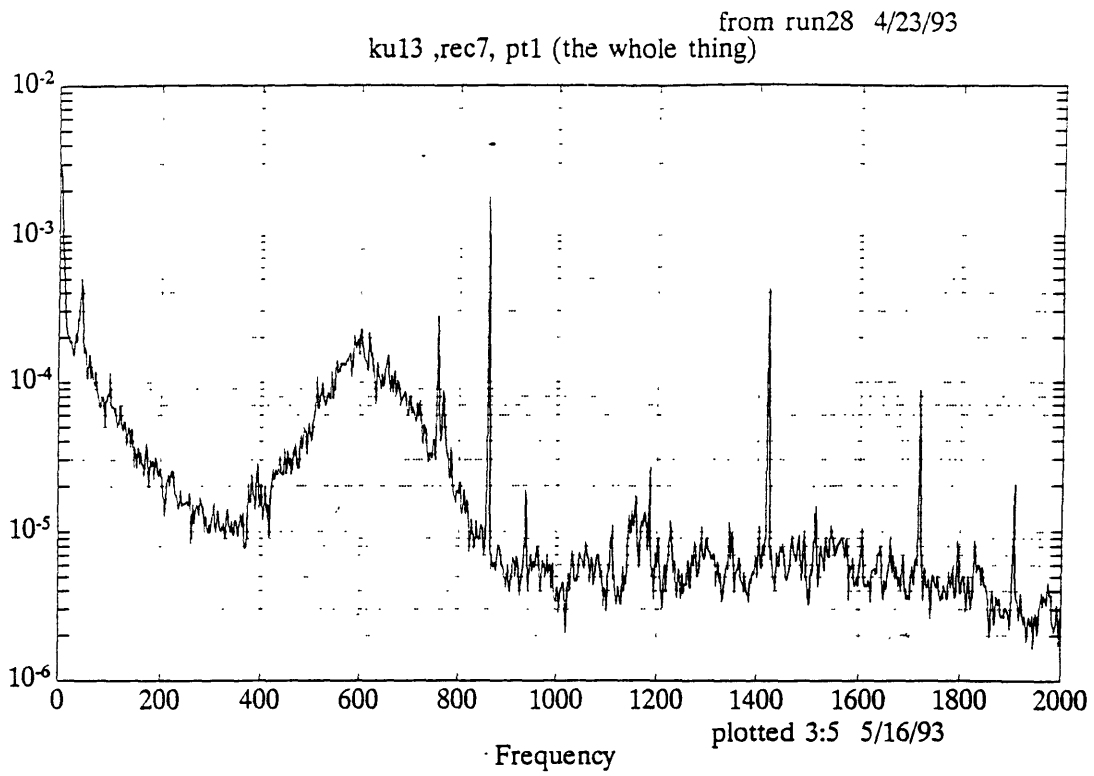


Figure 3.20 : PSD of Combustor at Stable Operating Point

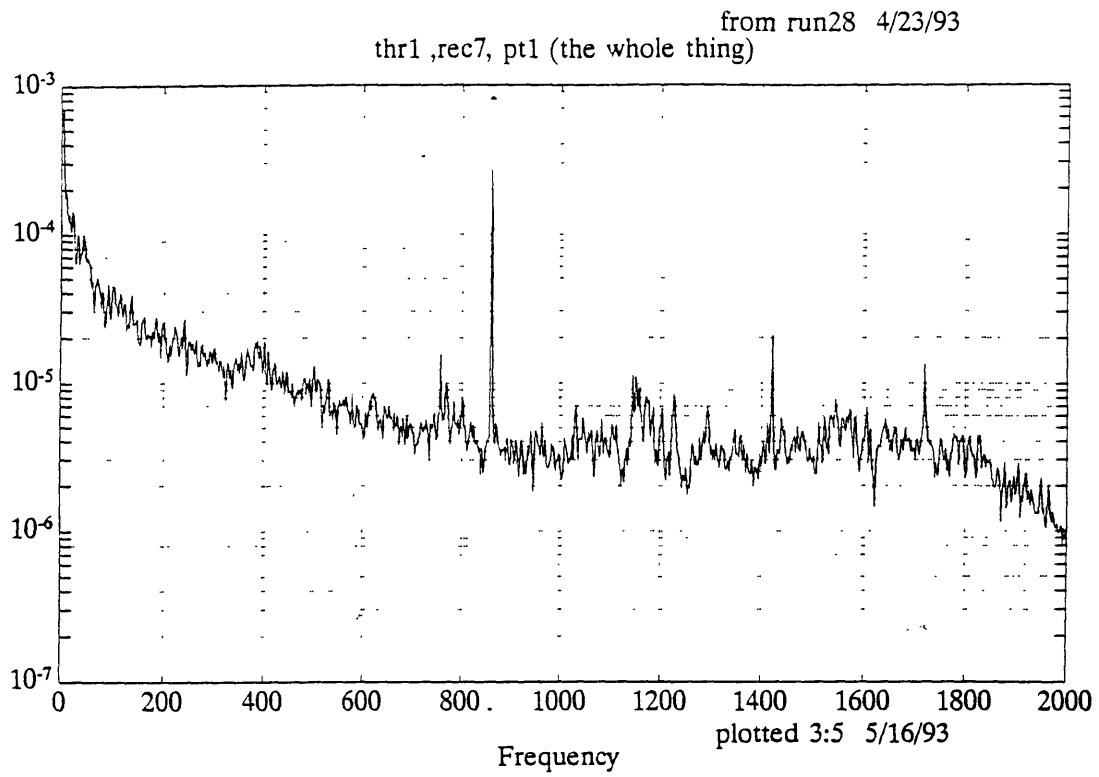


Figure 3.21 : PSD of Zeroth Mode at the Throat at Stable Operating Point

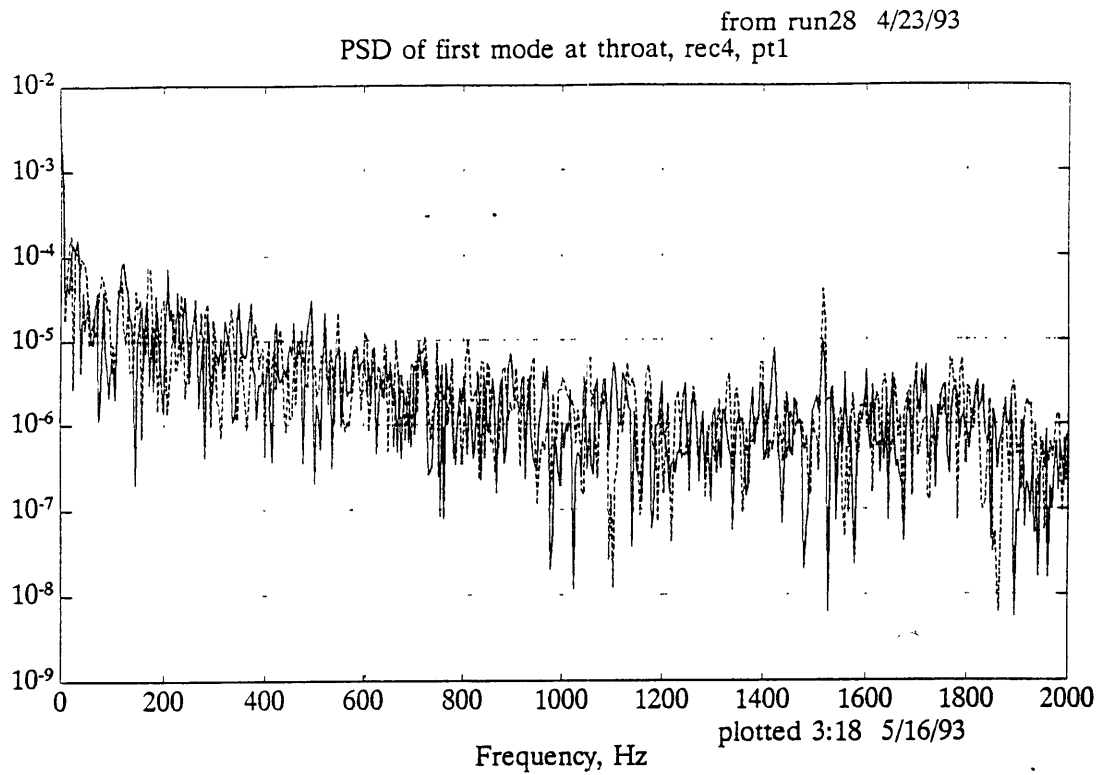


Figure 3.22 : PSD of First Mode at the Throat at Stable Operating Point

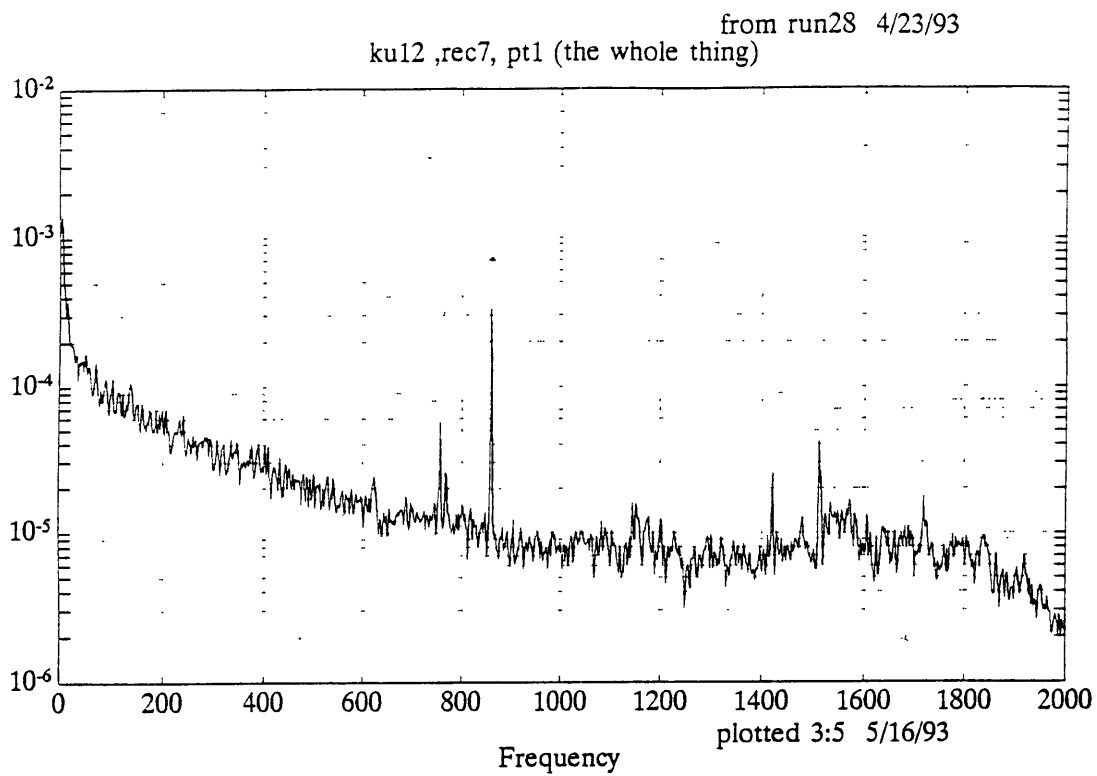


Figure 3.23 : PSD of 0° Throat Tap at Stable Operating Point

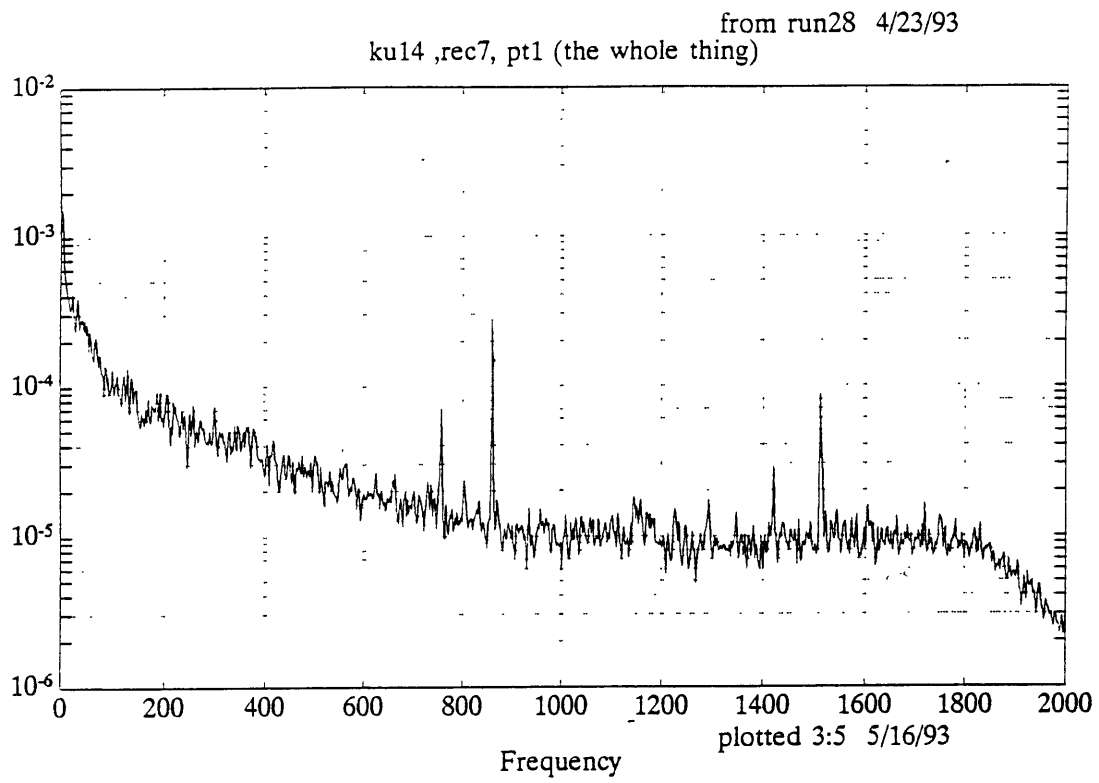


Figure 3.24 : PSD of 120° Throat Tap at Stable Operating Point

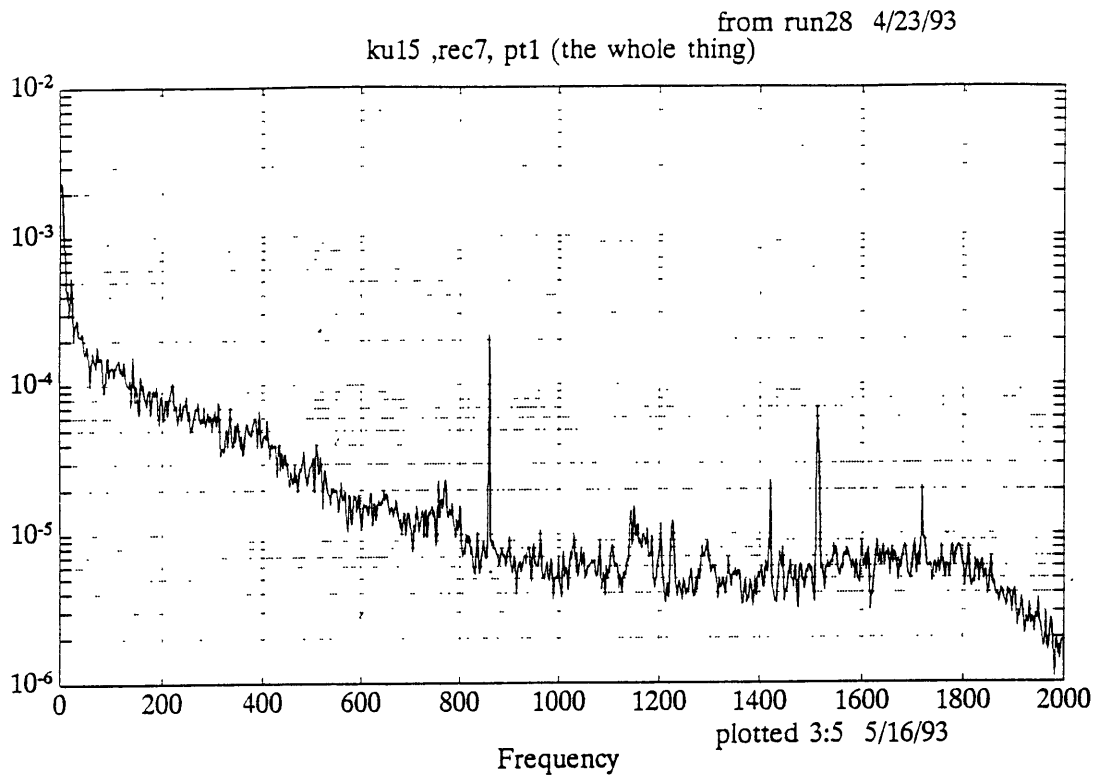


Figure 3.25 : PSD of 240° Throat Tap at Stable Operating Point



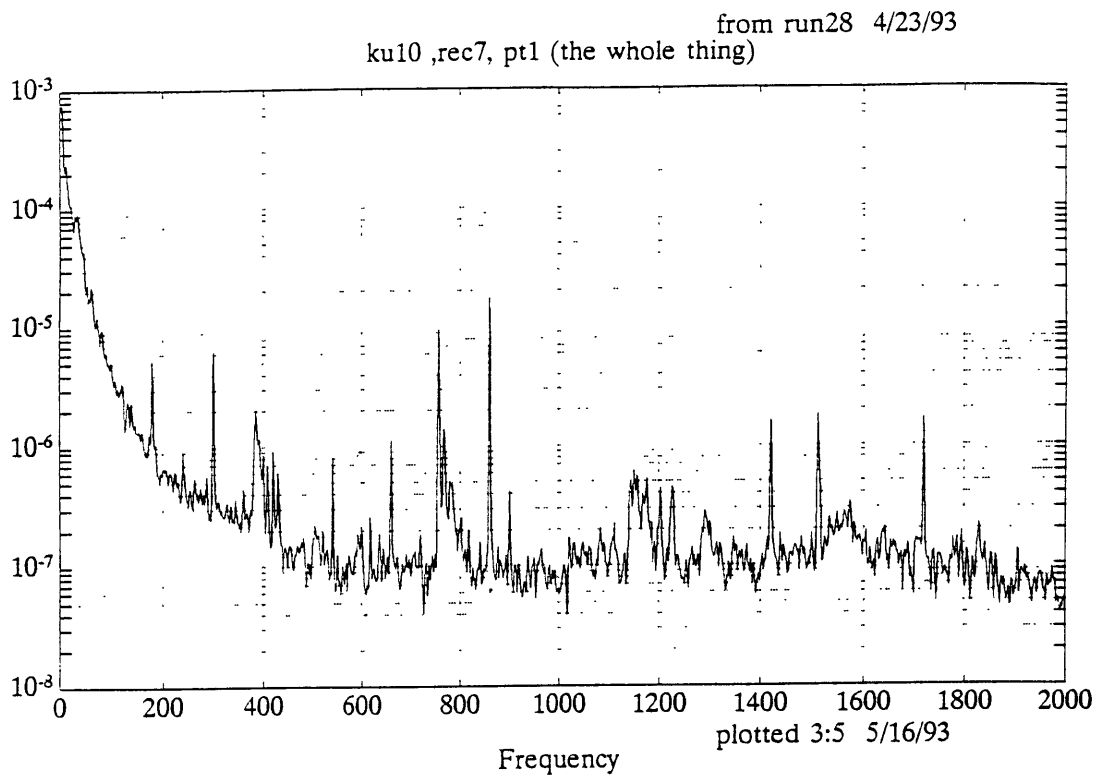


Figure 3.26 : PSD of Stator Tap at Stable Operating Point

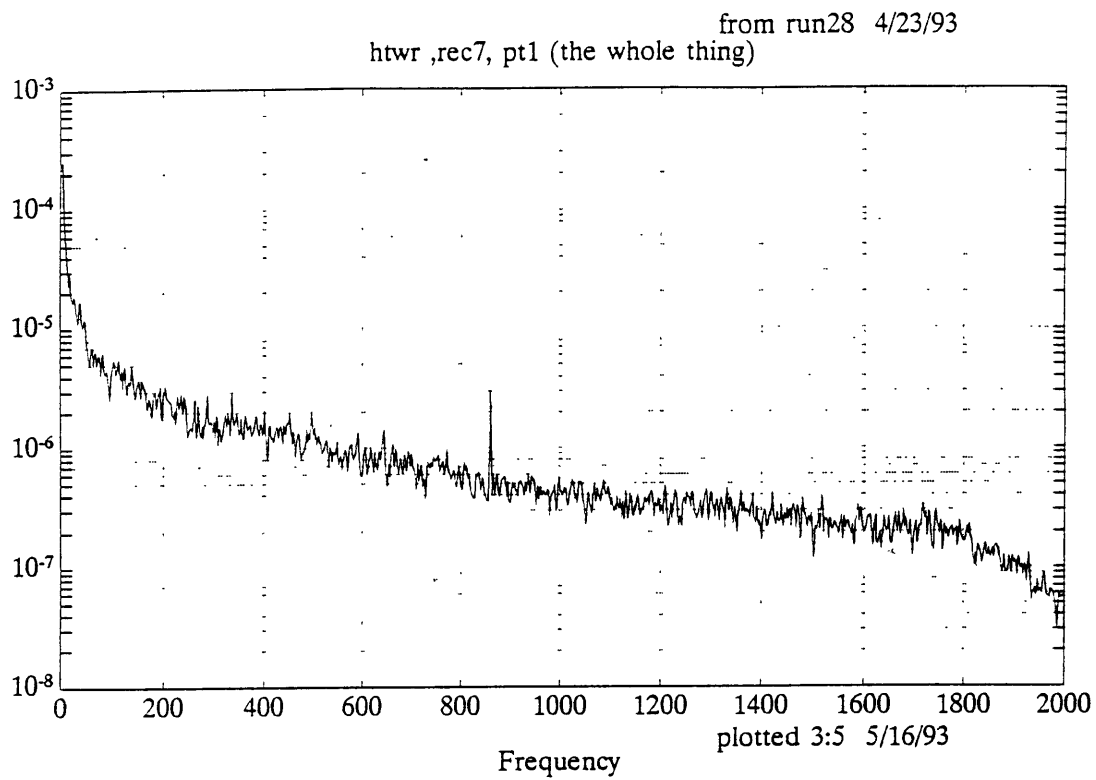


Figure 3.27 : PSD of Hotwire at Stable Operating Point

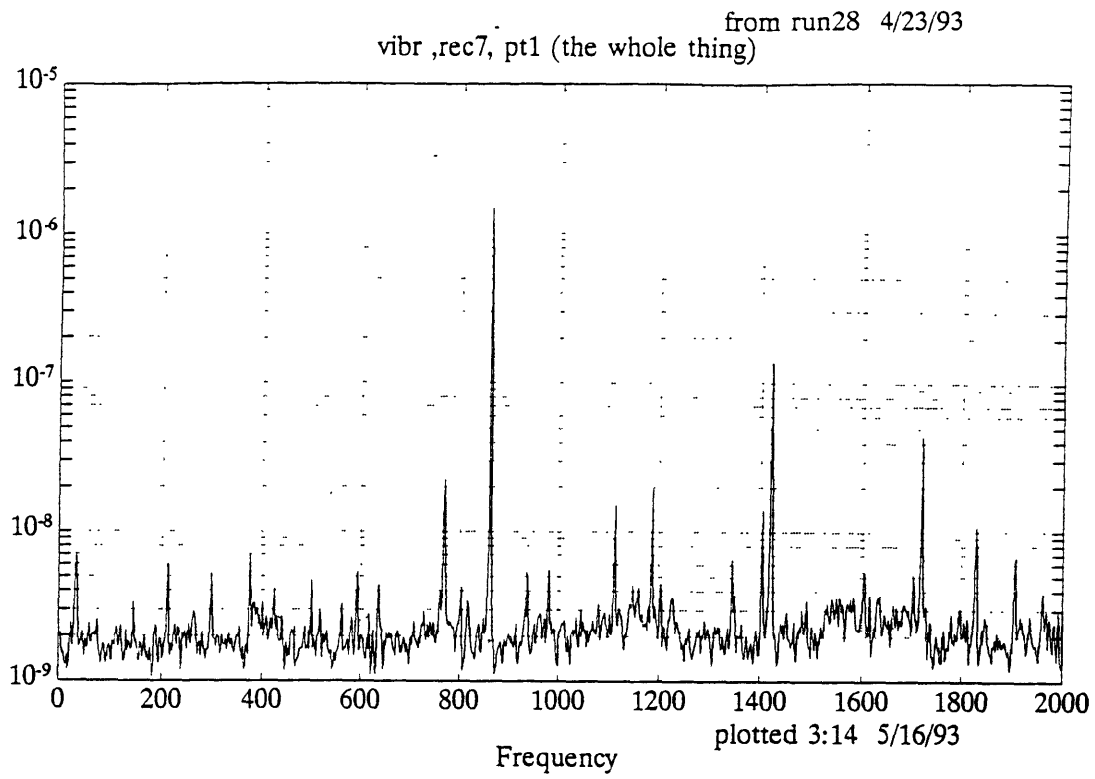


Figure 3.28 : PSD of Vibrometer at Stable Operating Point

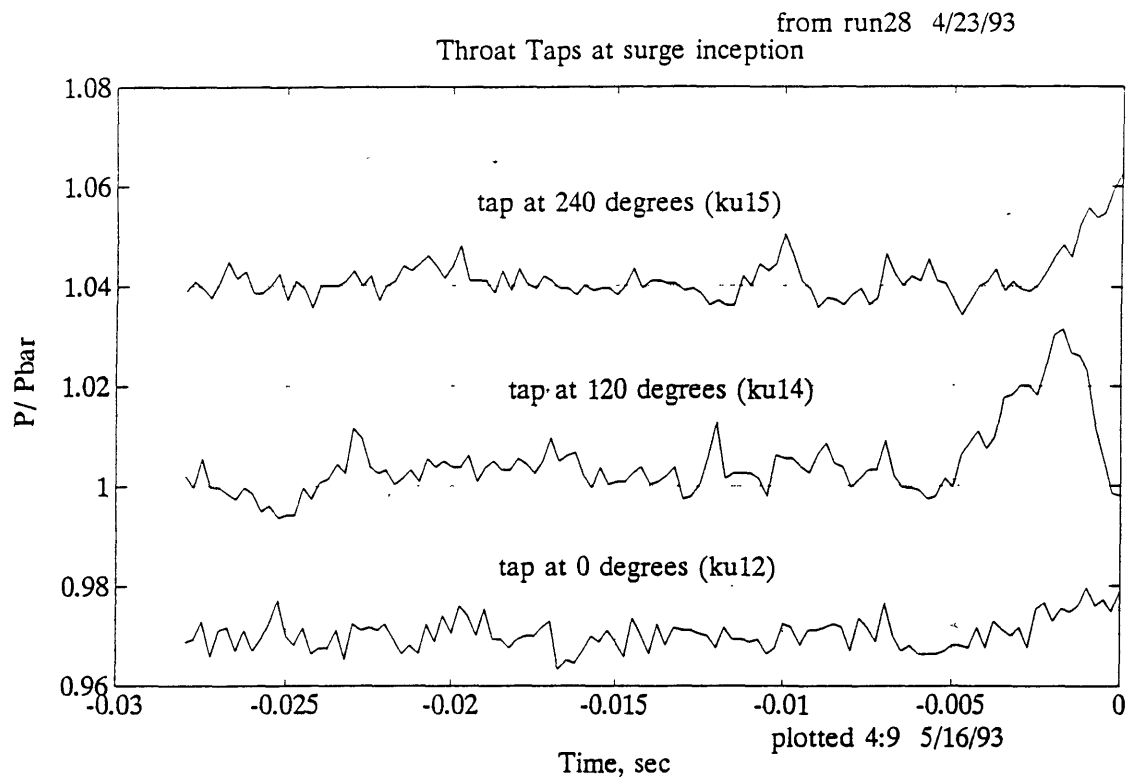


Figure 3.29 : Time Trace of Throat Taps at Surge Inception, Run 28

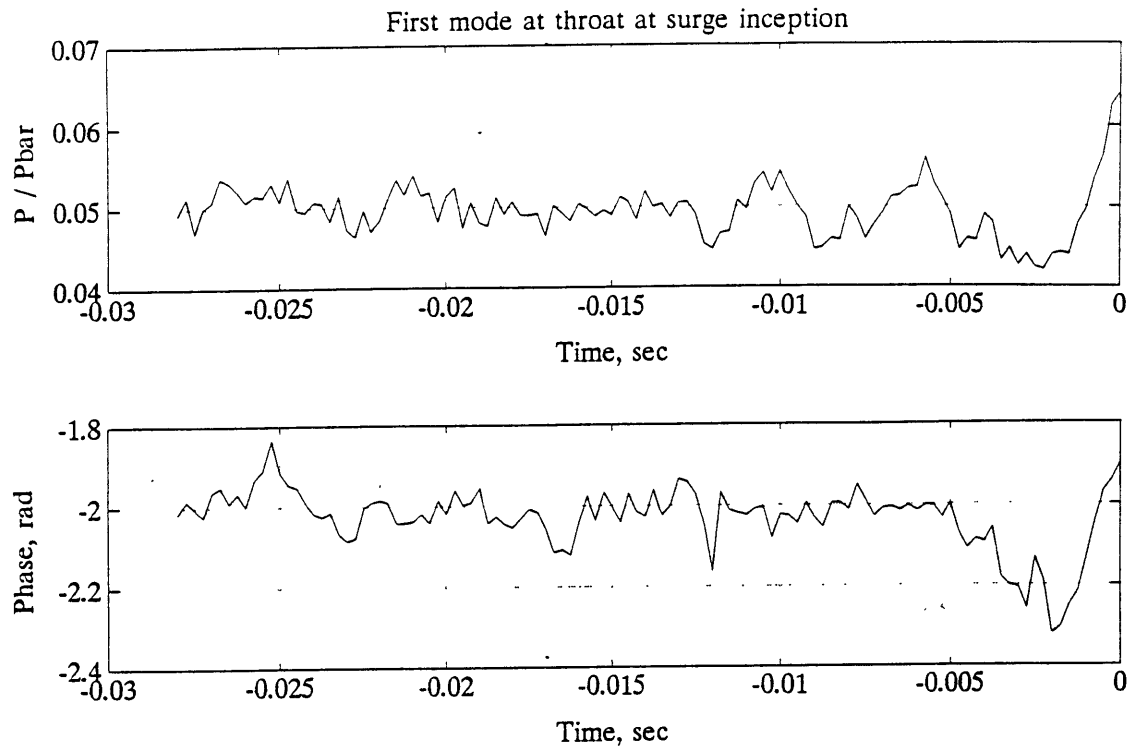


Figure 3.30 : First Mode at the Throat at Surge Inception, Run 28

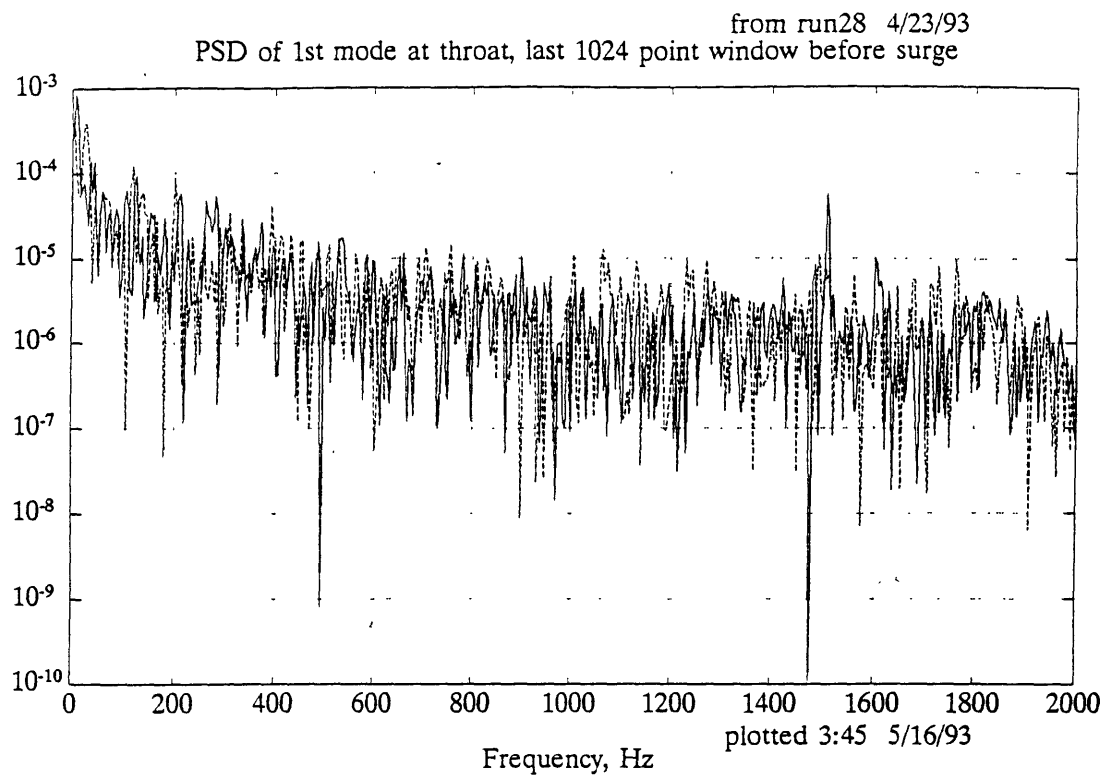


Figure 3.31 : PSD of the First Mode at the Throat at Surge Inception, Run 28

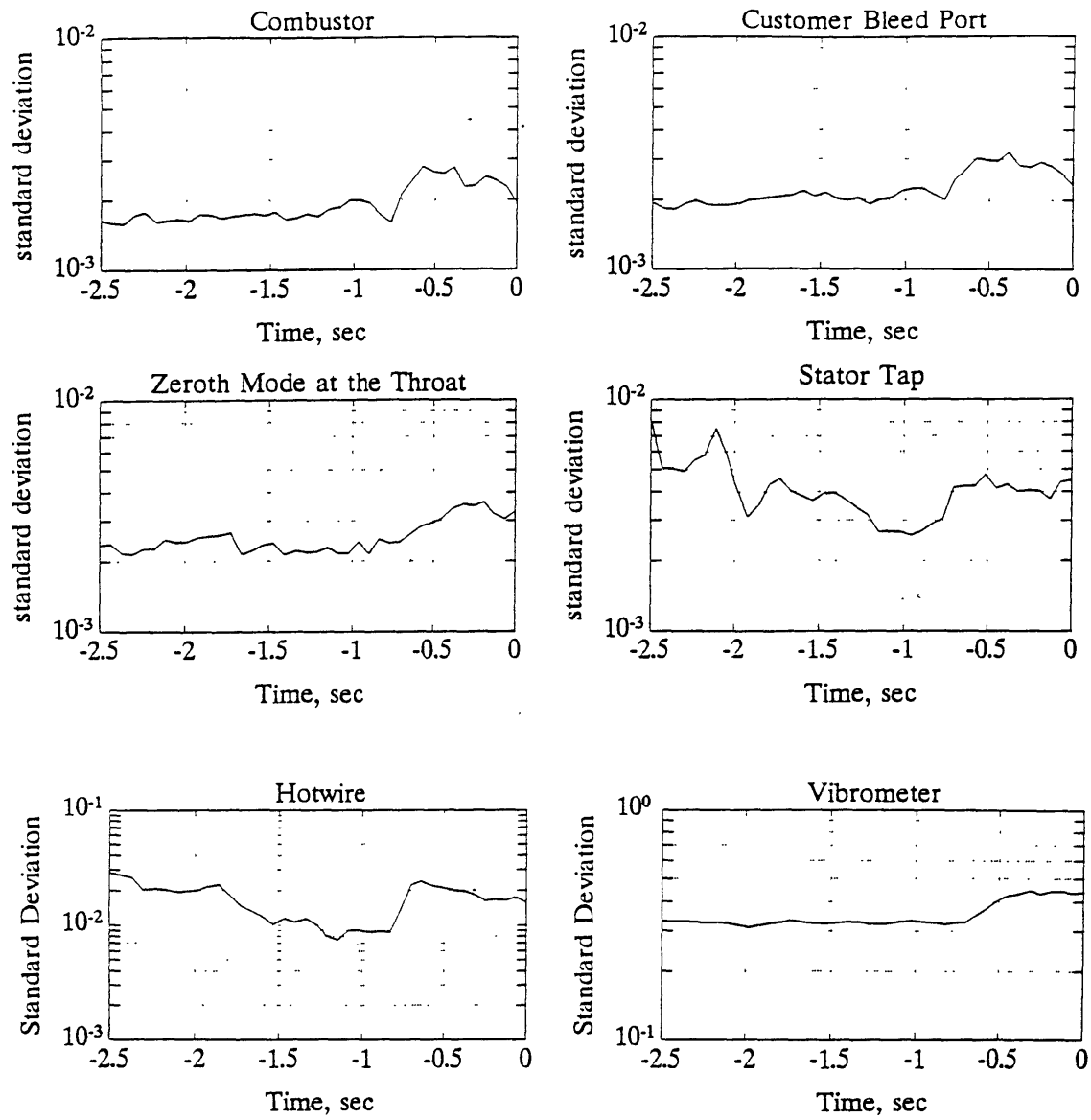


Figure 3.32 : Standard Deviations of Transducer Signals at Surge Inception, Run

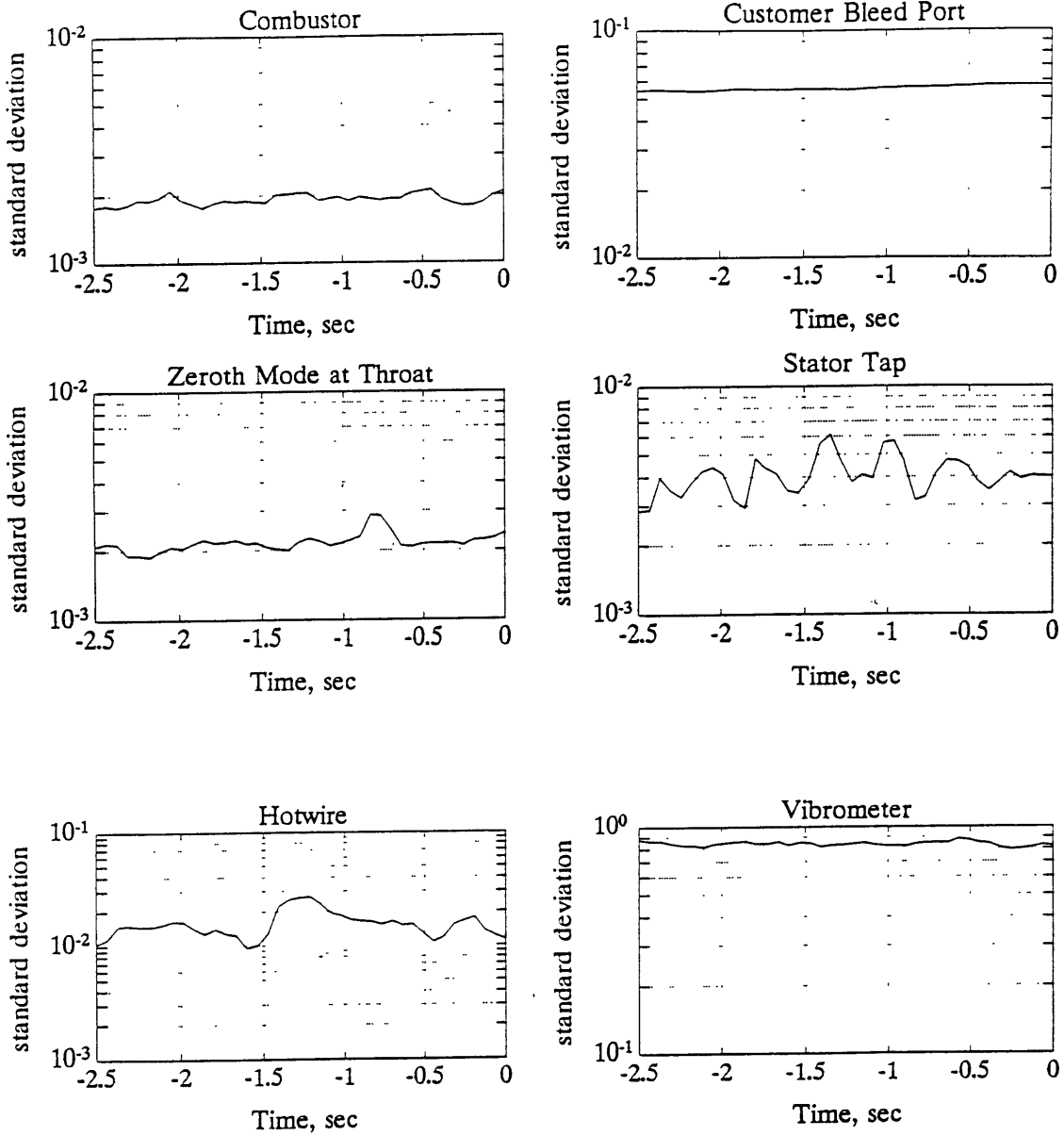


Figure 3.33 : Standard Deviations of Transducer Signals at Surge Inception, Run

27



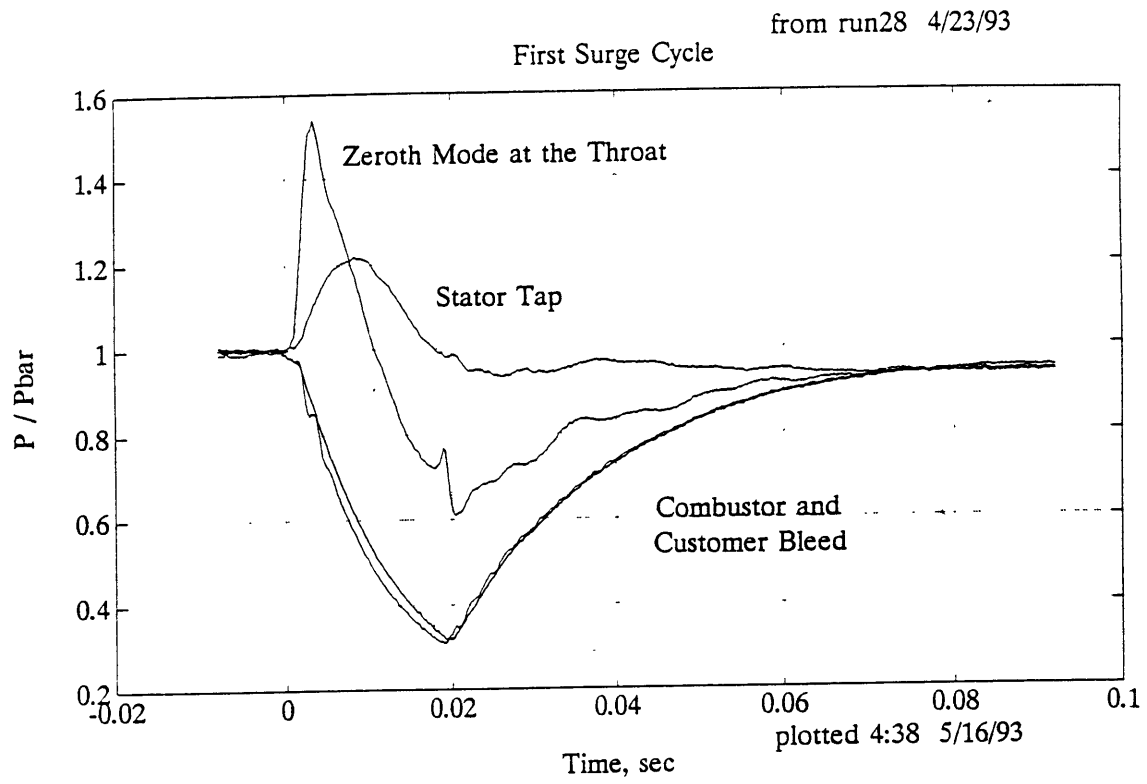


Figure 3.34 : Pressure Traces for First Surge Cycle, Run 28

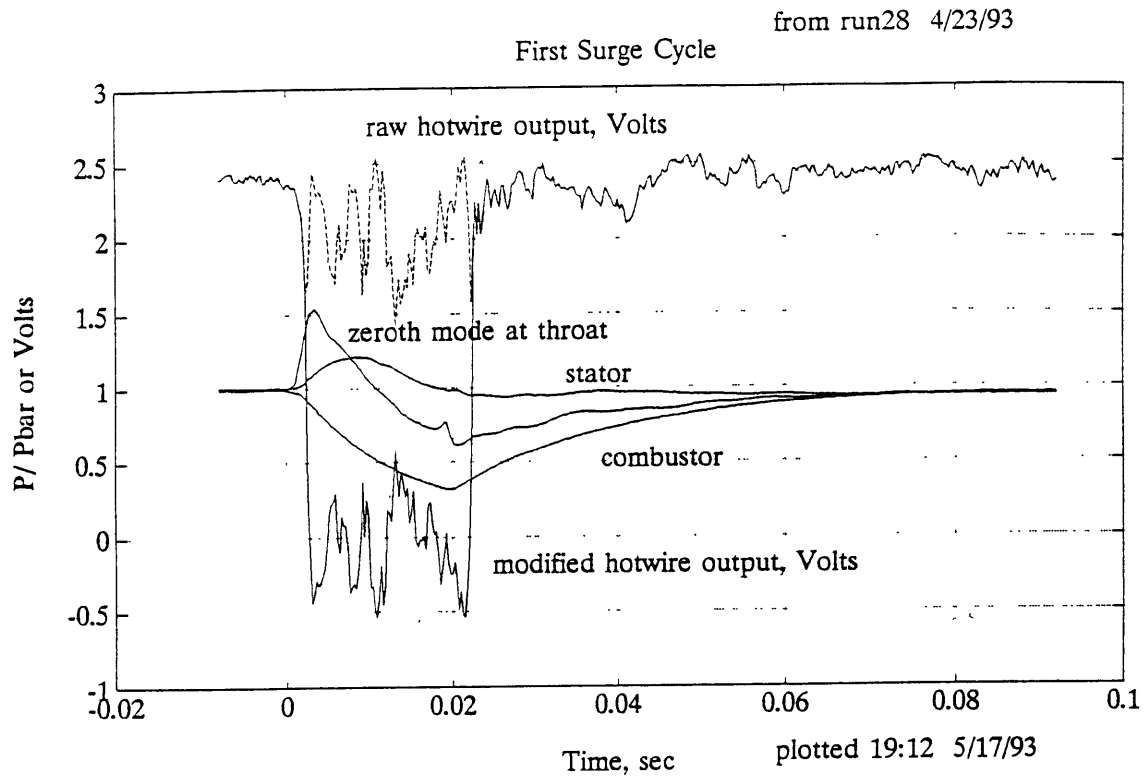


Figure 3.35 : Pressure and Hotwire Traces for First Surge Cycle, Run 28

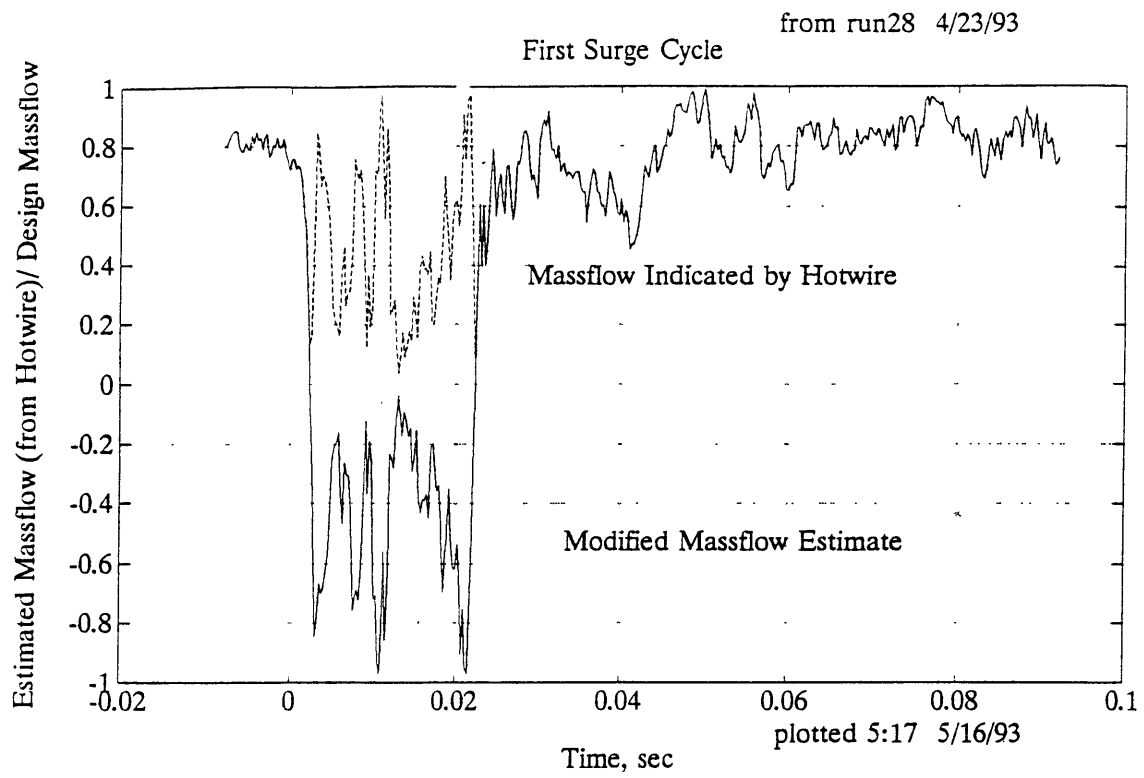


Figure 3.36 : Massflow for First Surge Cycle, Run 28

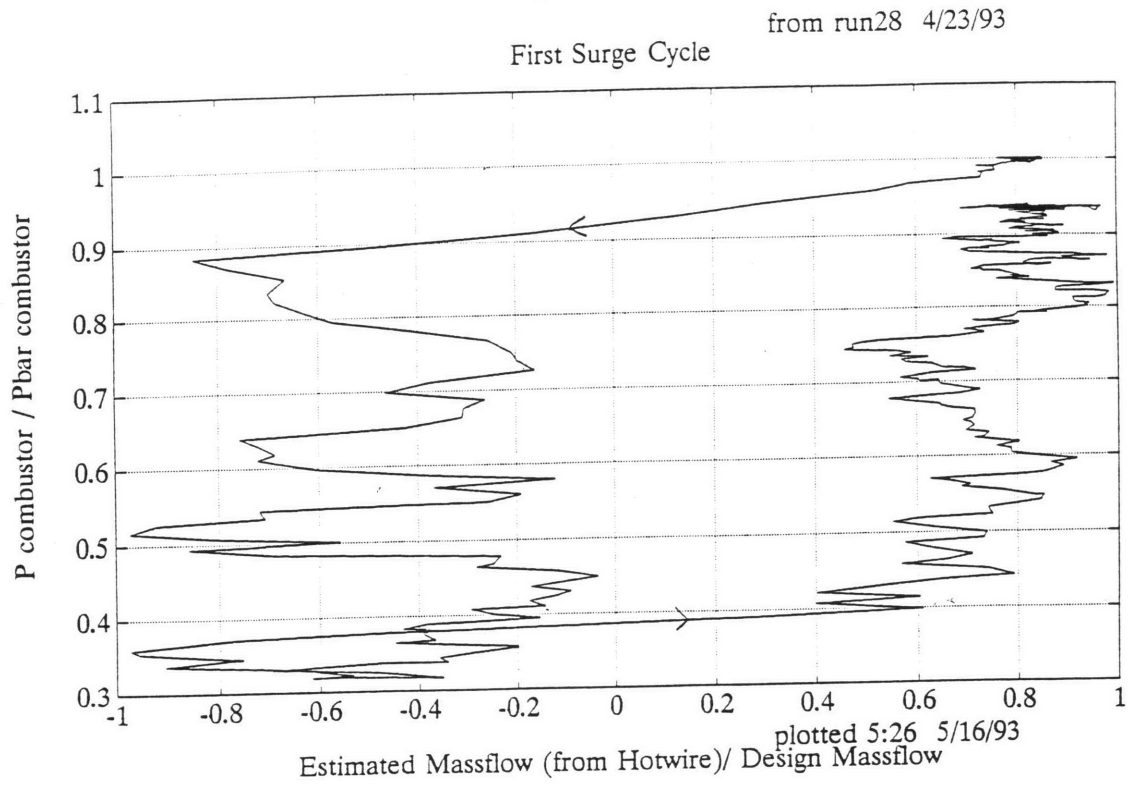


Figure 3.37 : Pressure vs. Massflow for First Surge Cycle, Run 28

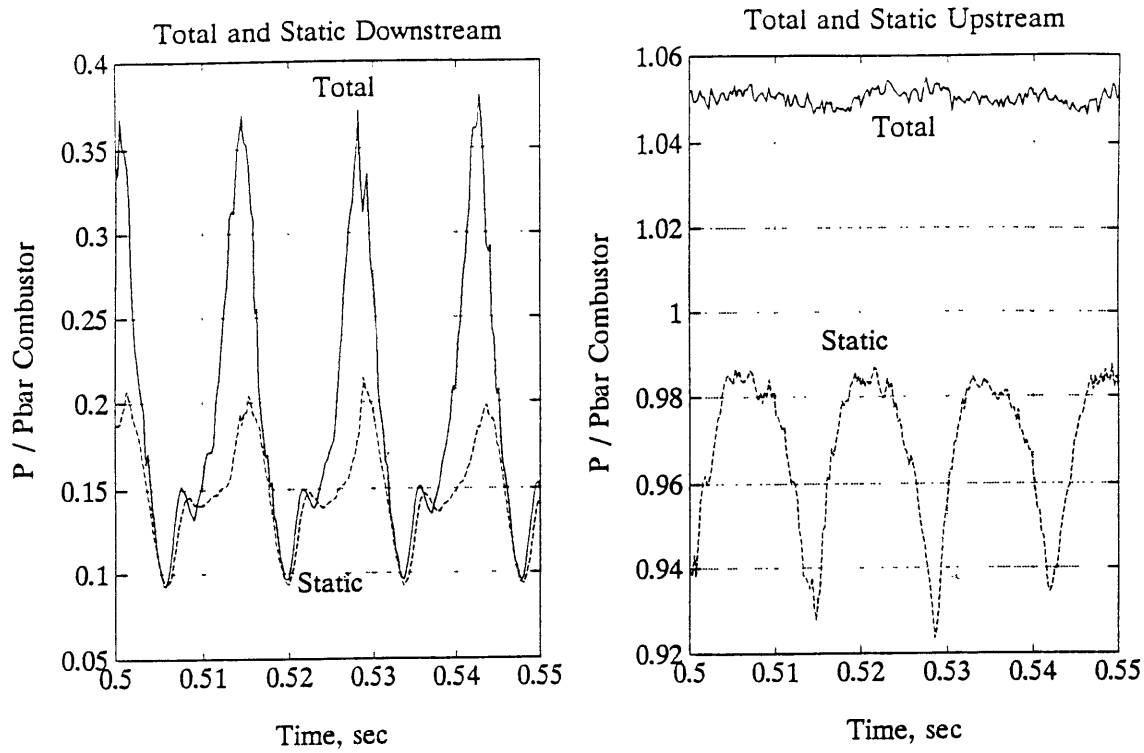


Figure 3.38 : Total and Static Pressures Up and Down Stream of the Shaker Valve

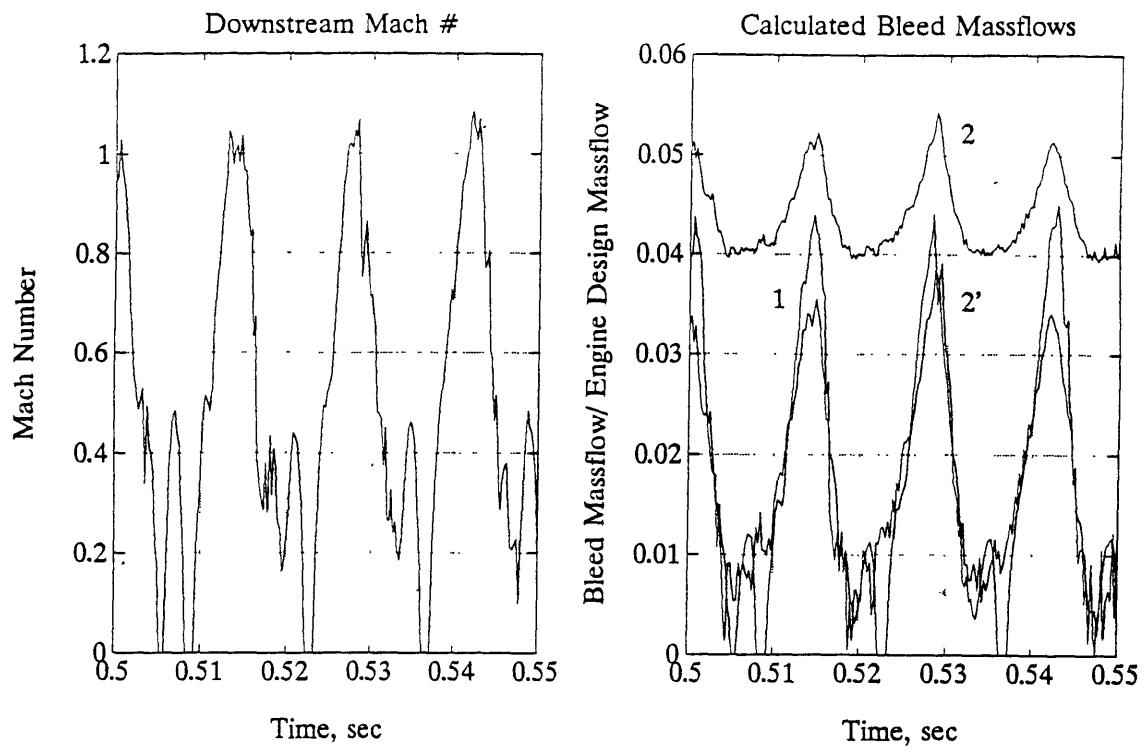


Figure 3.39 : Mach Number Downstream of Shaker and Calculated Massflow

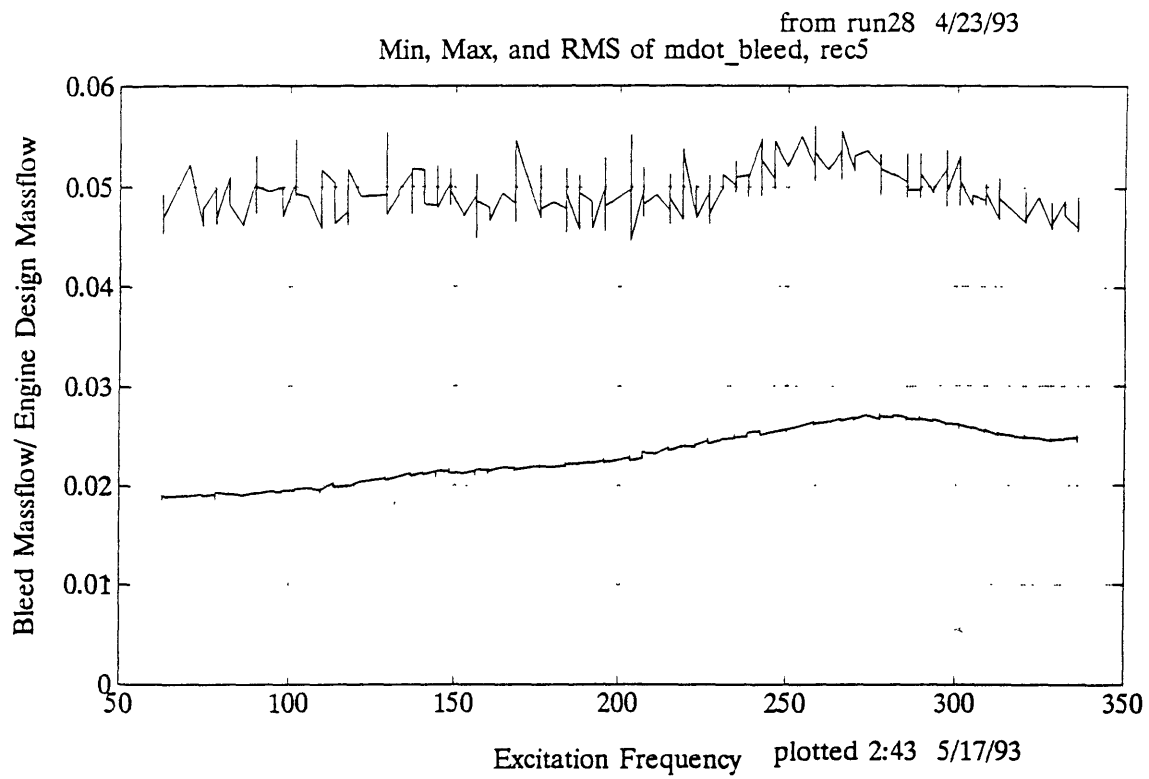


Figure 3.40 : Amplitude of Customer Bleed Massflow Oscillations vs Excitation Frequency , Run 28

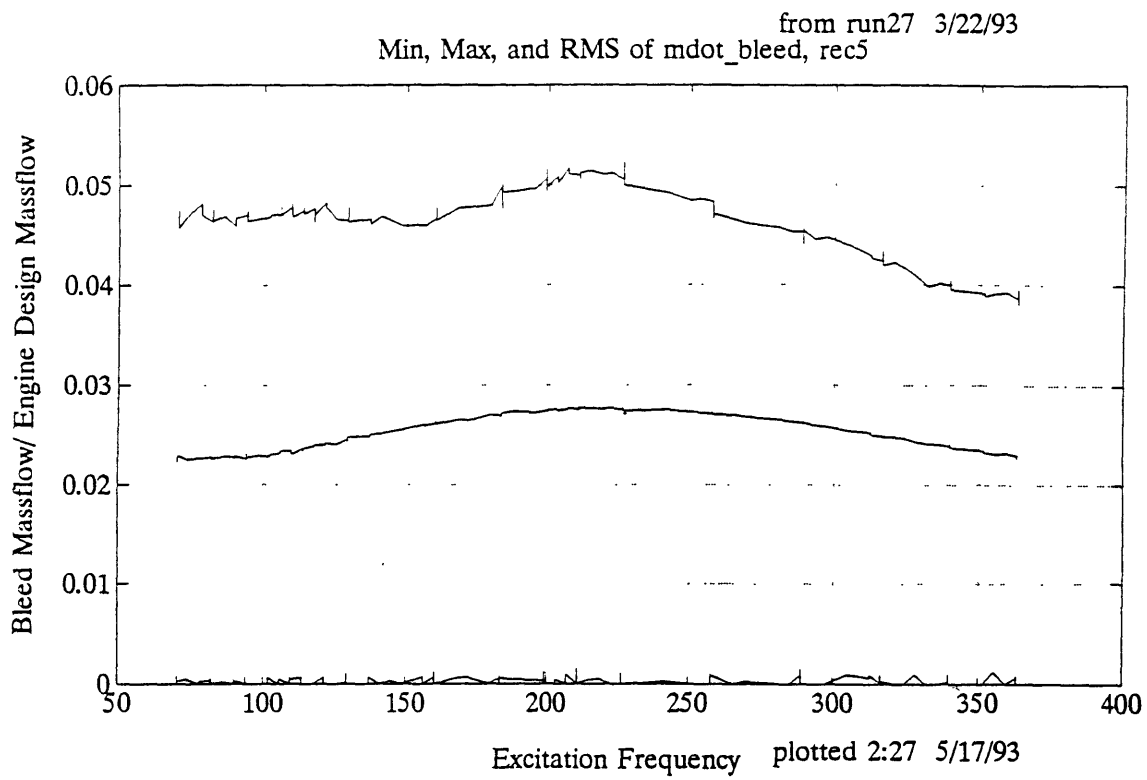


Figure 3.41 : Amplitude of Customer Bleed Massflow Oscillations vs Excitation Frequency , Run 27



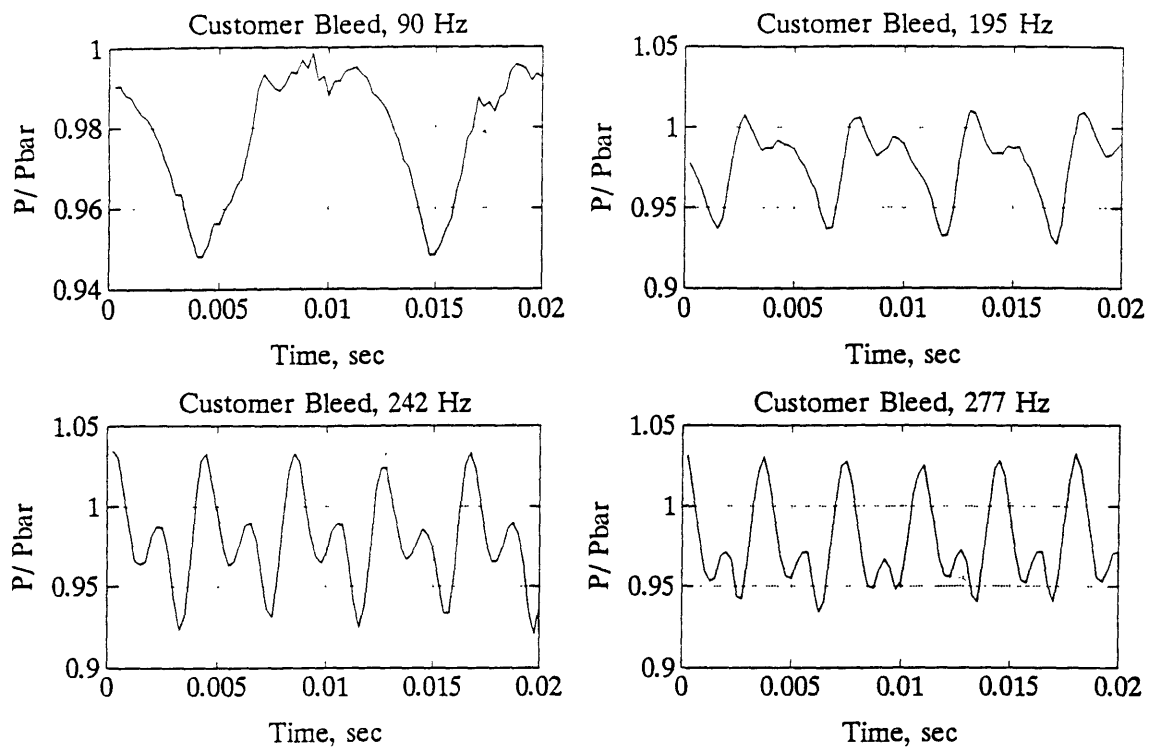


Figure 3.41 : Customer Bleed Pressure Traces at Various Excitation Frequencies

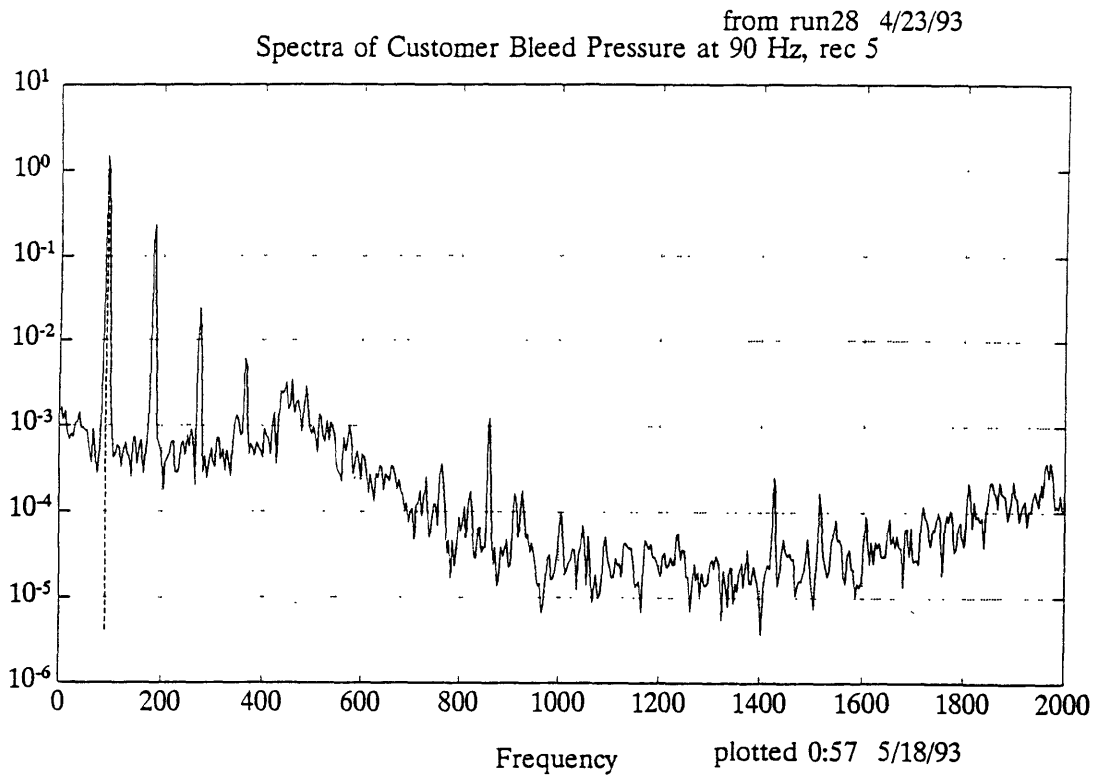


Figure 3.43 : Spectra of Customer Bleed Pressure at 90 Hz

from run28 4/23/93  
Spectra of Customer Bleed Pressure at 242 Hz, rec 5

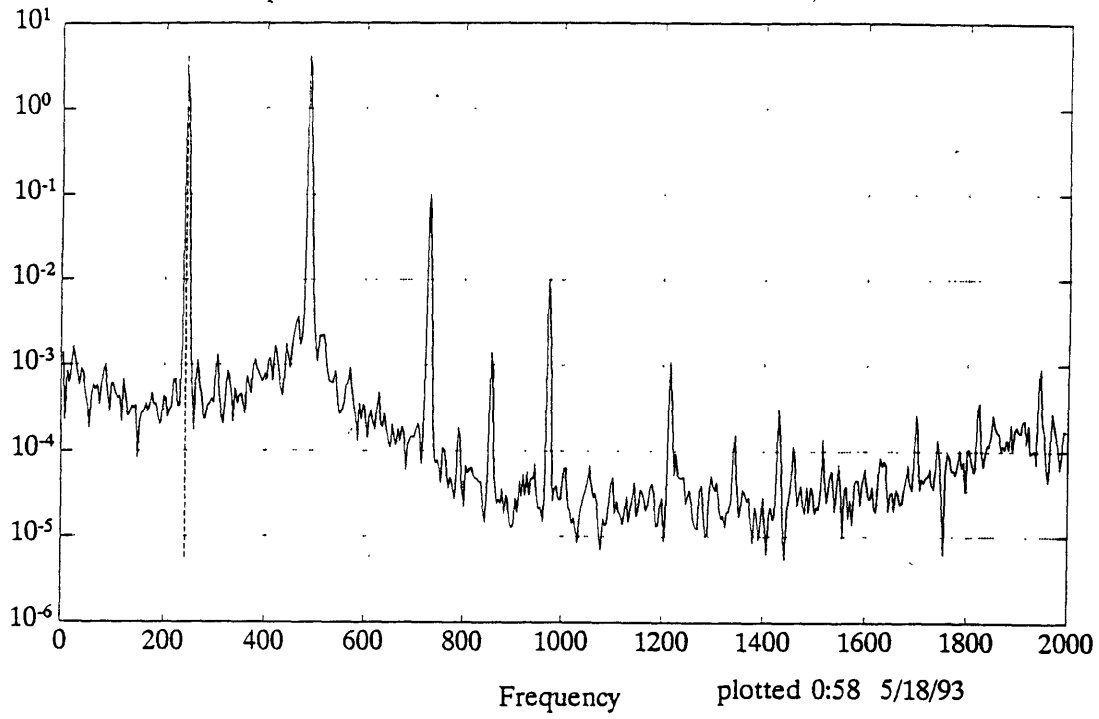


Figure 3.44 : Spectra of Customer Bleed Pressure at 242 Hz

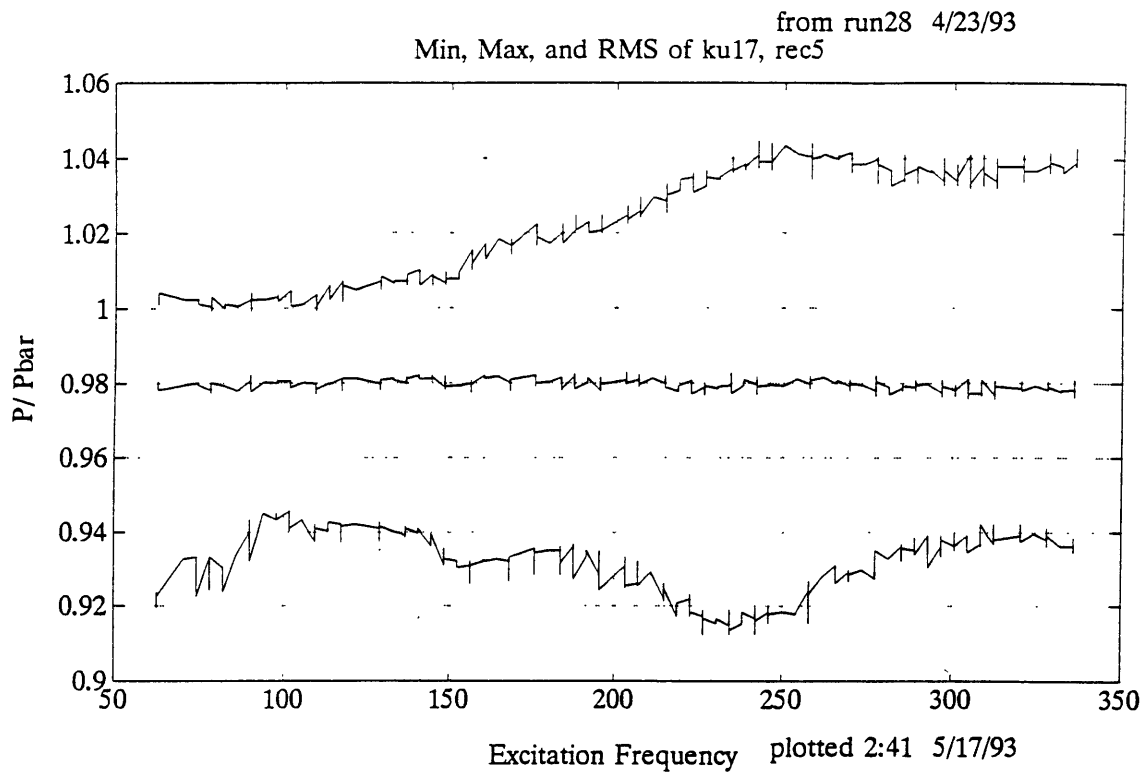


Figure 3.45 : Amplitude of Customer Bleed Pressure Oscillations vs Excitation Frequency , Run 28

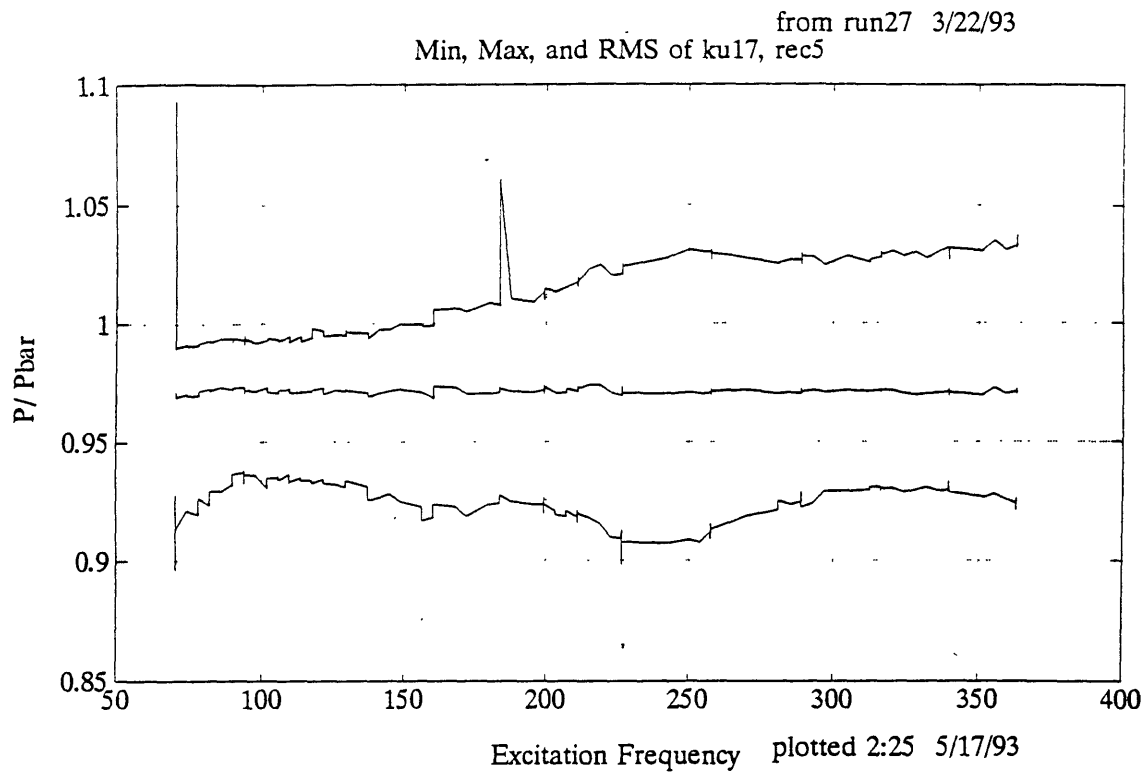


Figure 3.46 : Amplitude of Customer Bleed Pressure Oscillations vs Excitation Frequency , Run 27

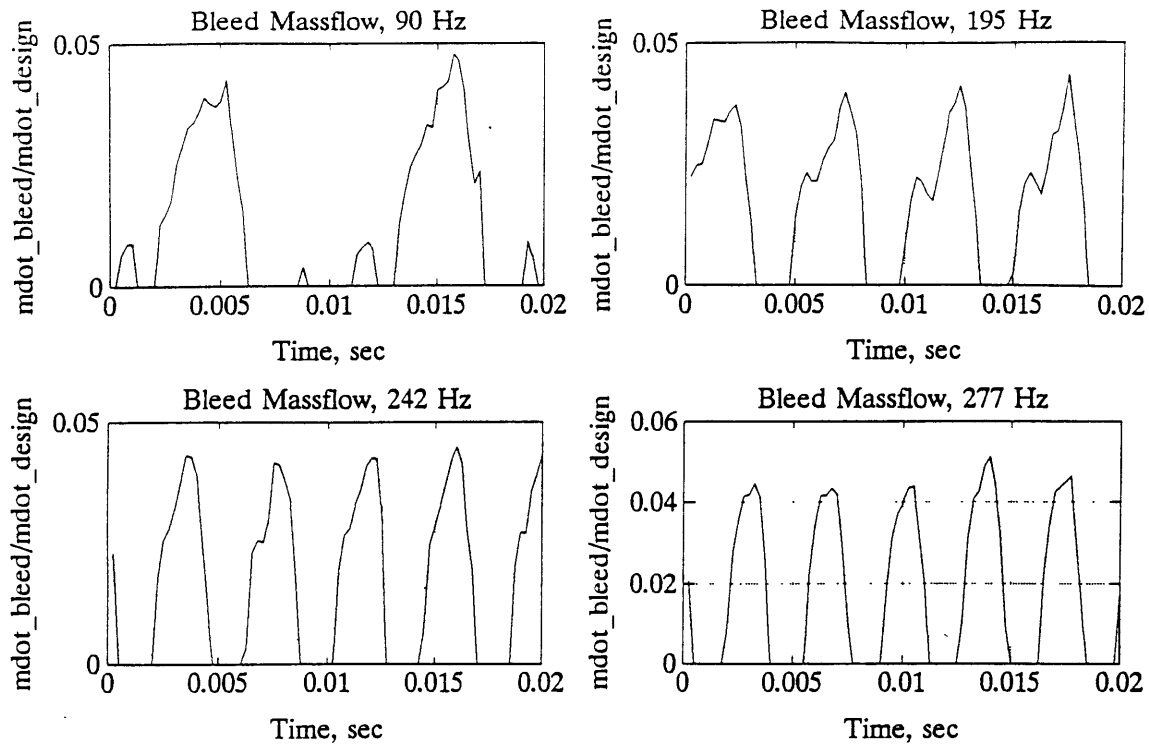


Figure 3.47 : Customer Bleed Massflow Traces at Various Excitation Frequencies

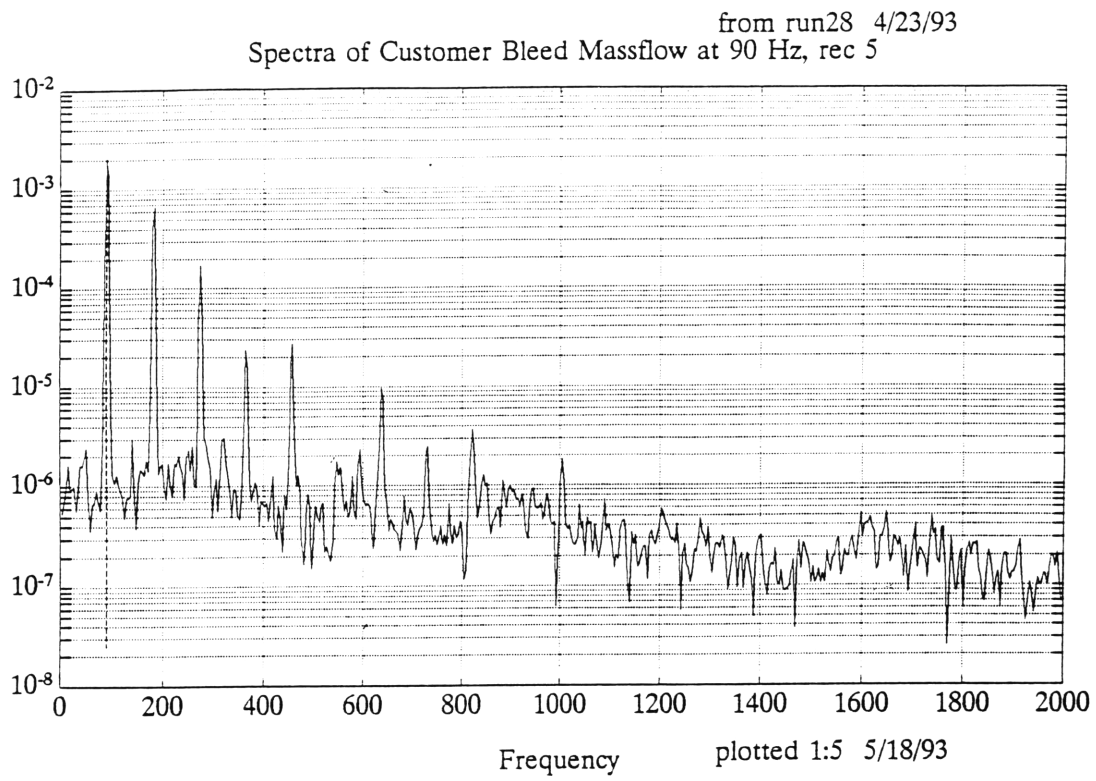


Figure 3.48 : Spectra of Customer Bleed Massflow at 90 Hz

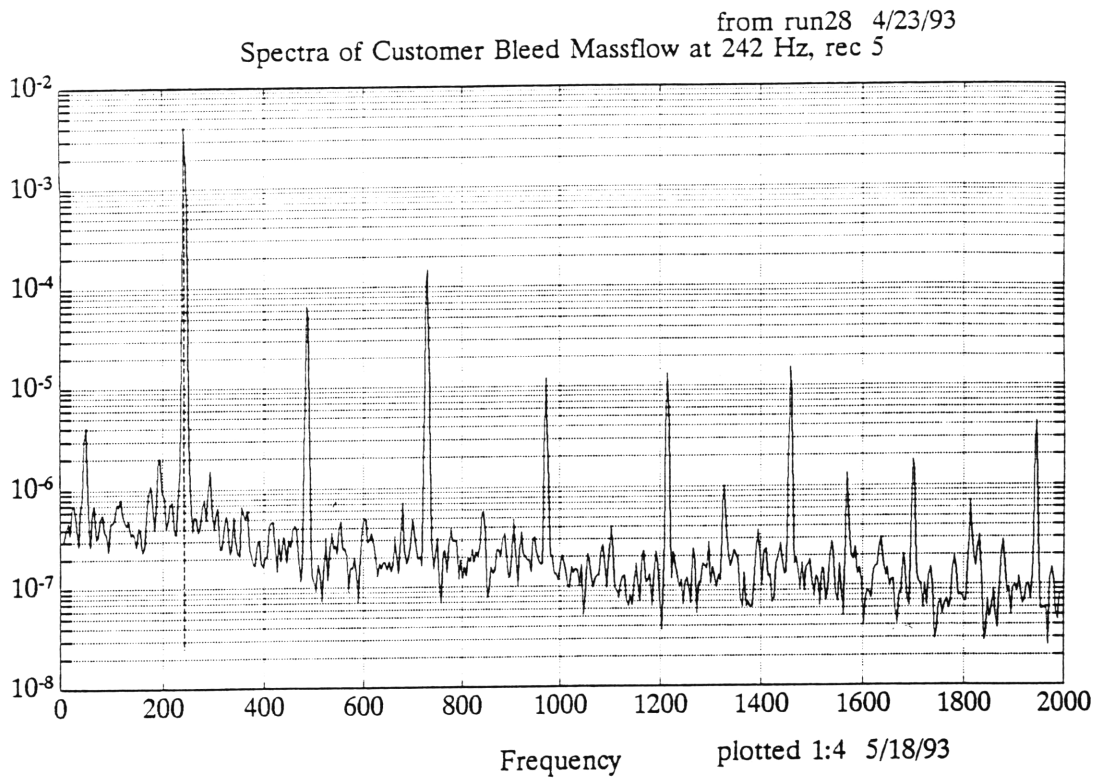


Figure 3.49 : Spectra of Customer Bleed Massflow at 242 Hz



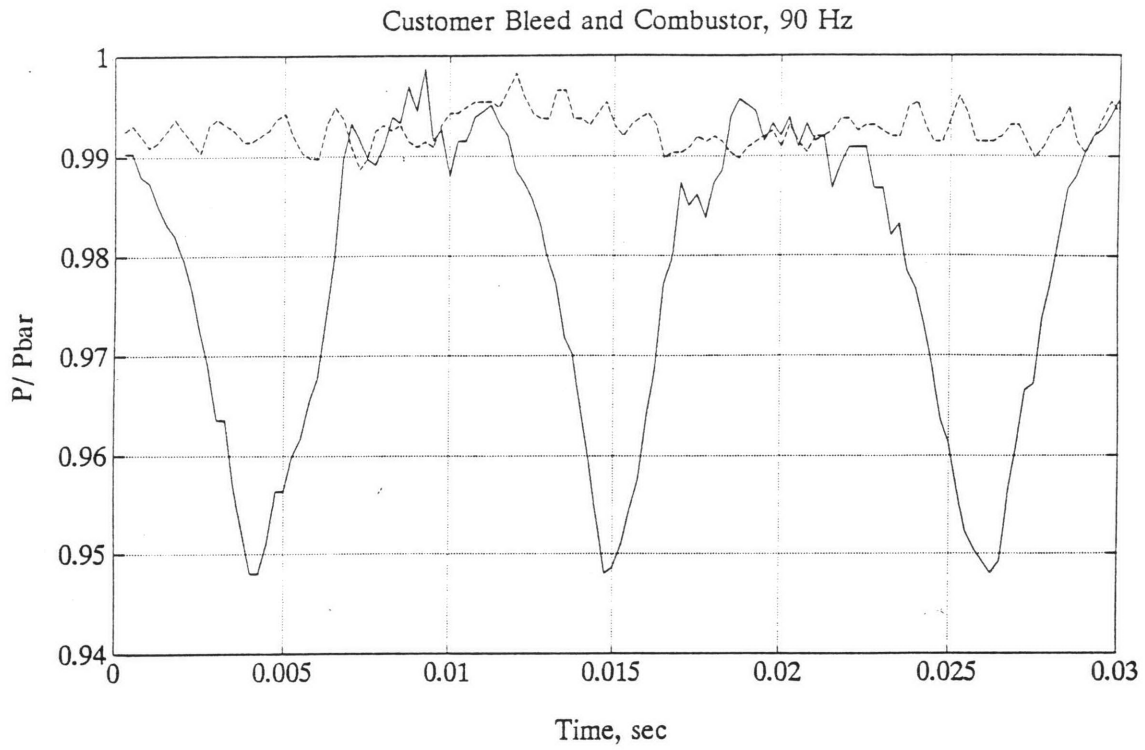


Figure 3.50 : Customer Bleed and Combustor Pressure Traces at 90 Hz

from run28 4/23/93  
Spectra of the Combustor Pressure, 90 Hz

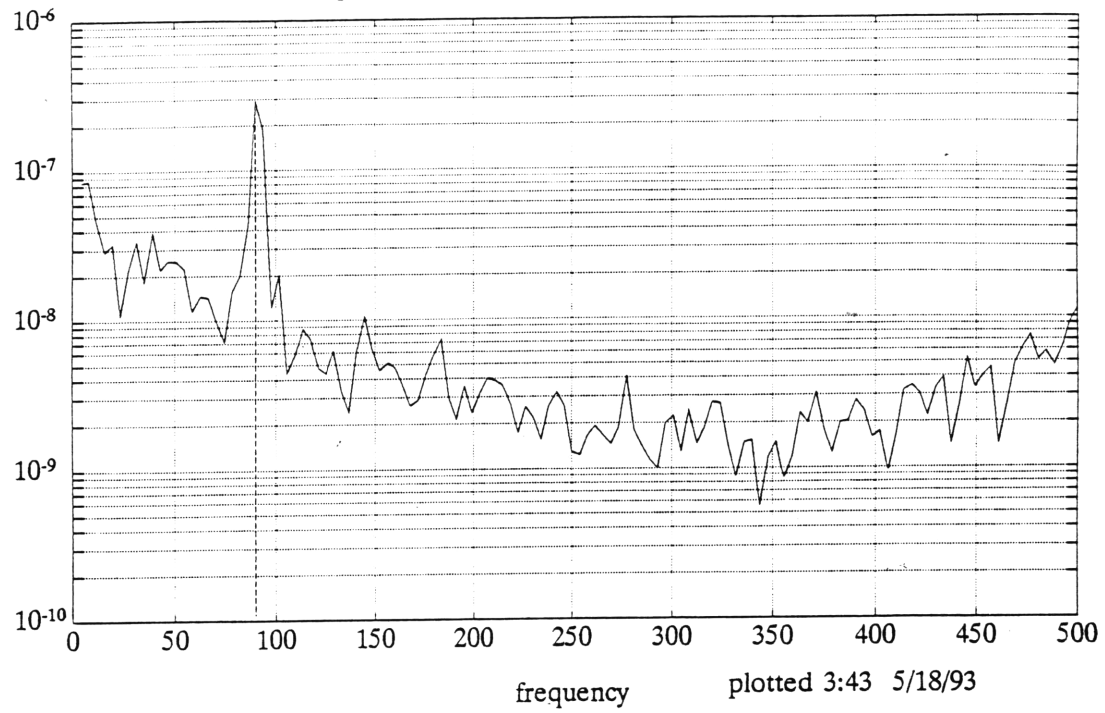


Figure 3.51 : Spectra of Combustor Pressure at 90 Hz

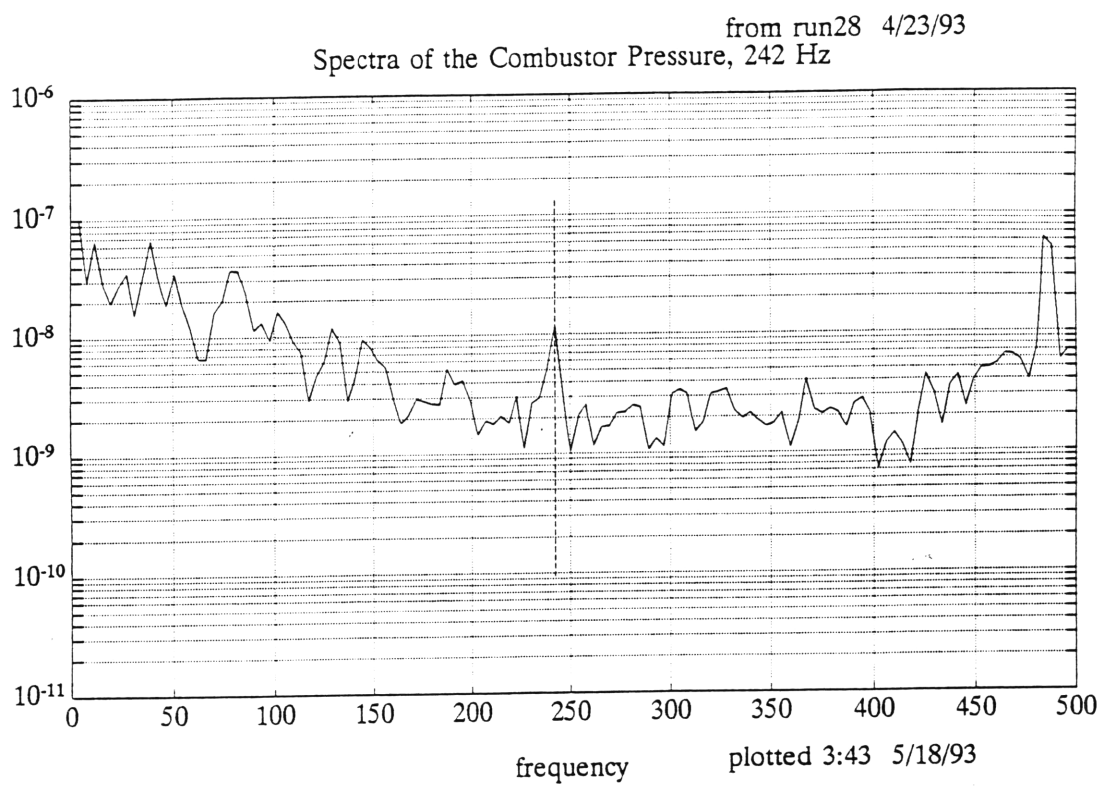


Figure 3.52 : Spectra of Combustor Pressure at 242 Hz

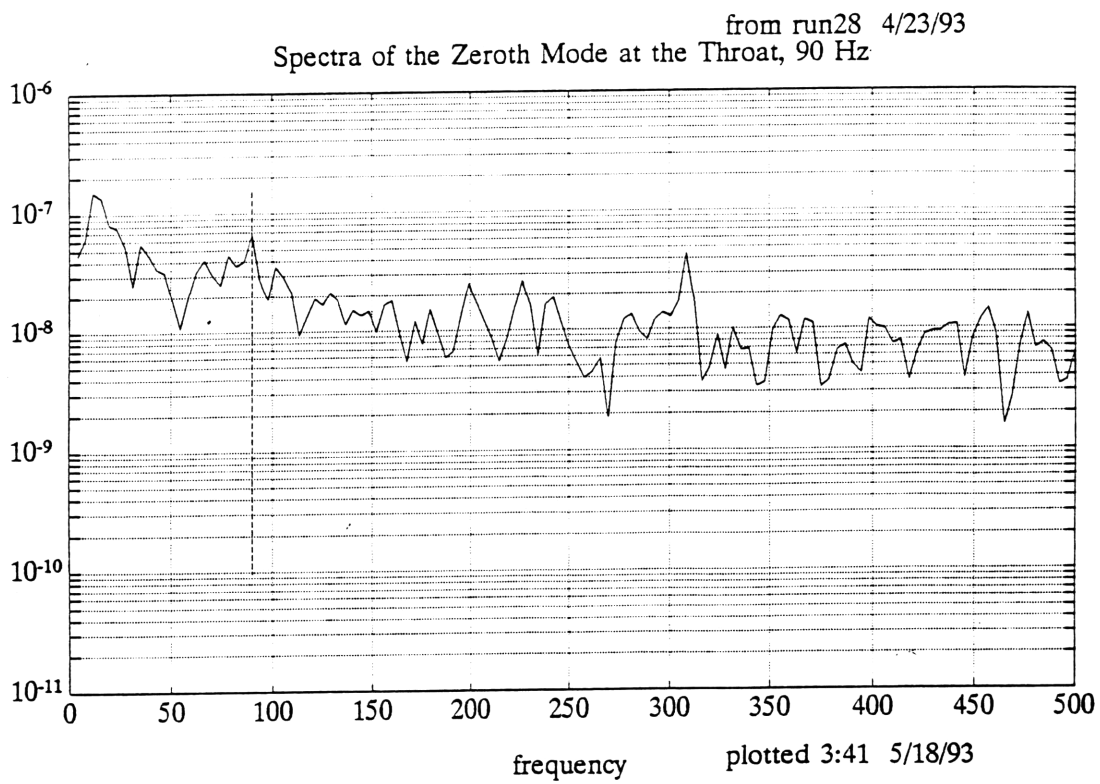


Figure 3.53 : Spectra of Zeroth Mode at the Throat at 90 Hz

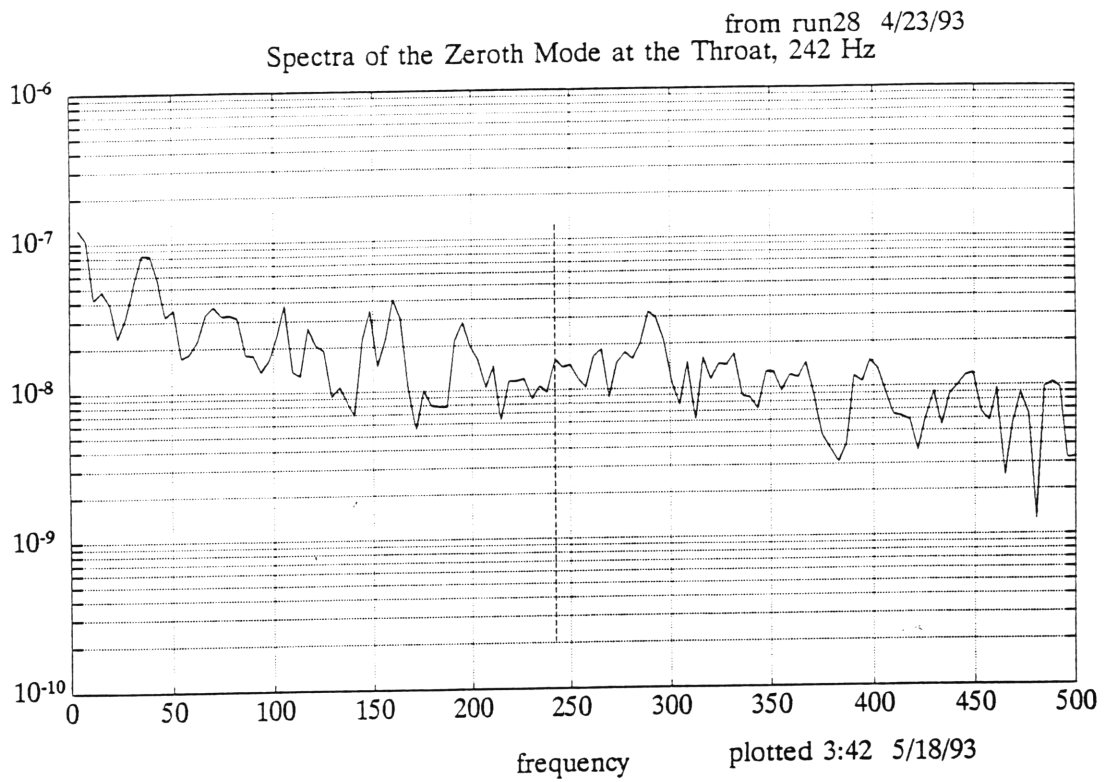


Figure 3.54 : Spectra of Zeroth Mode at the Throat at 242 Hz

from run28 4/23/93  
Spectra of Stator Tap Pressure, 90 Hz

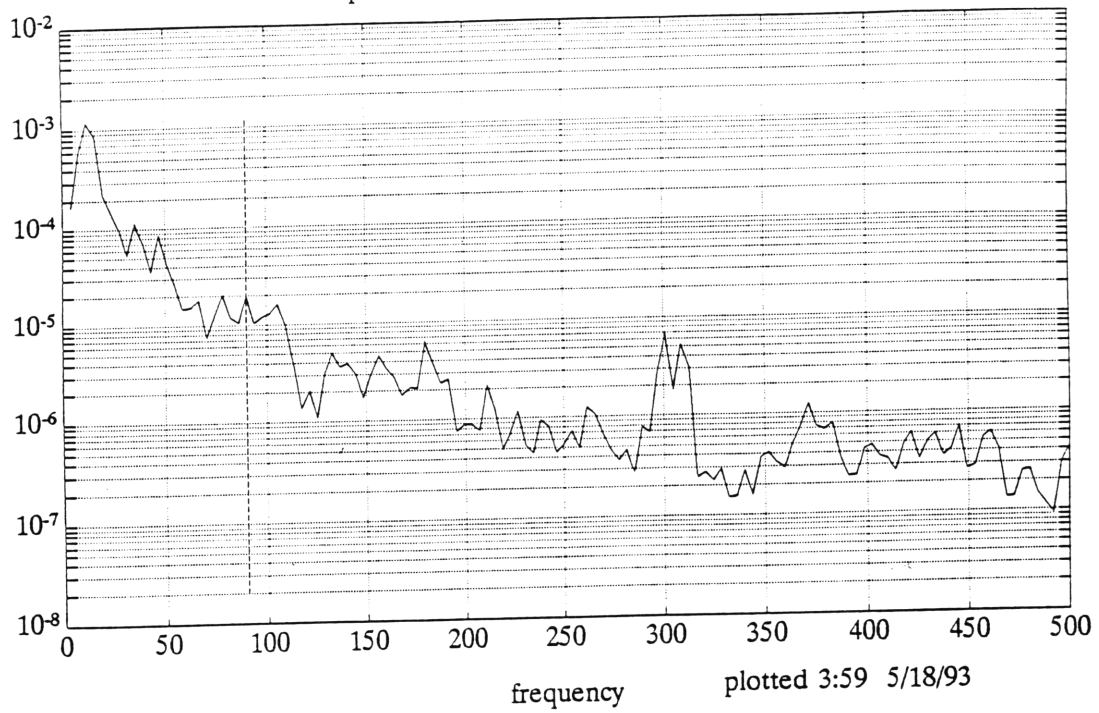


Figure 3.55 : Spectra of Stator Tap Pressure at 90 Hz

from run28 4/23/93  
Spectra of Stator Tap Pressure, 242 Hz

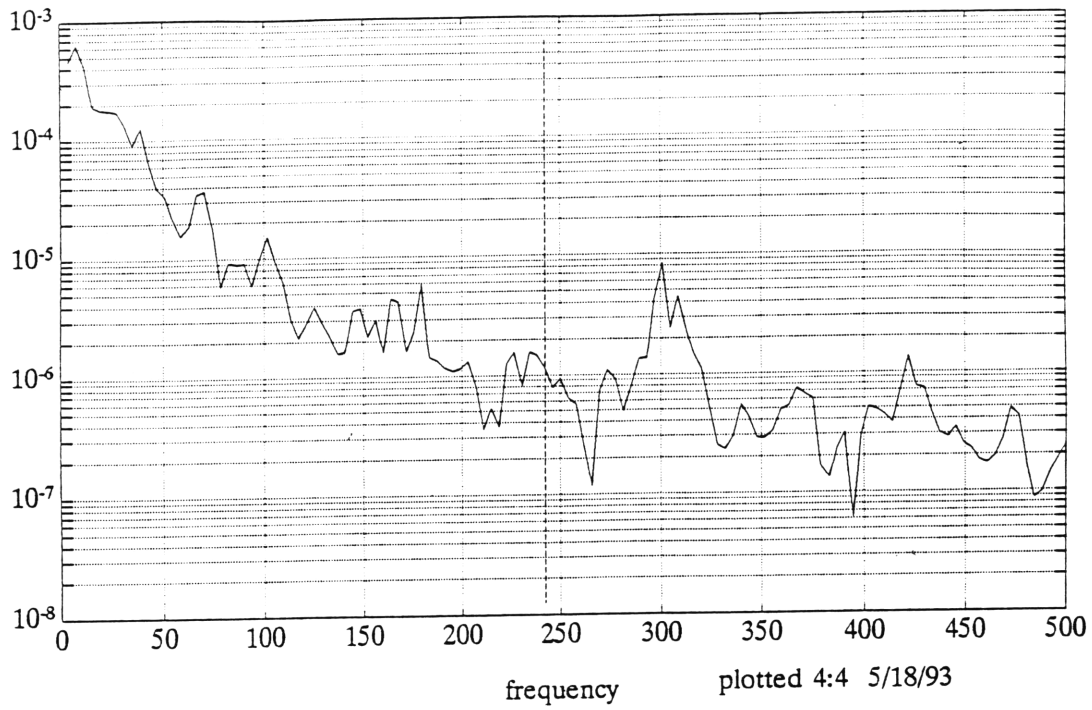


Figure 3.56 : Spectra of Stator Tap Pressure at 242 Hz

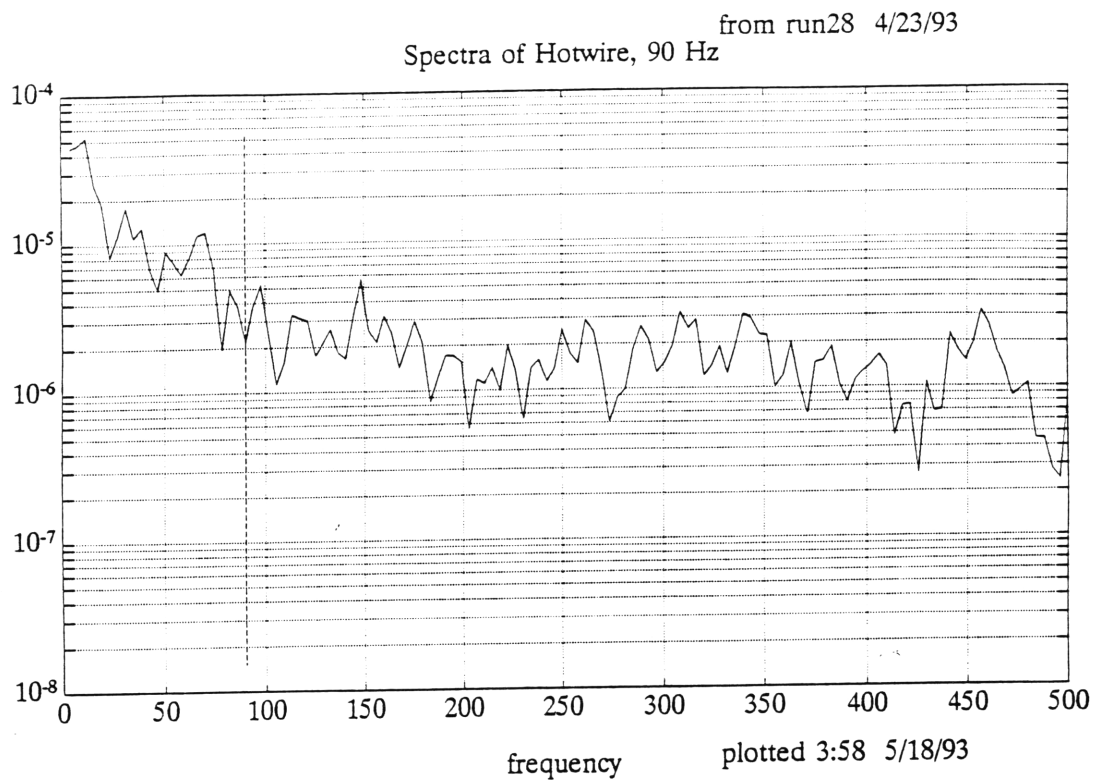


Figure 3.57 : Spectra of Hotwire at 90 Hz



from run28 4/23/93  
Spectra of Hotwire, 242 Hz

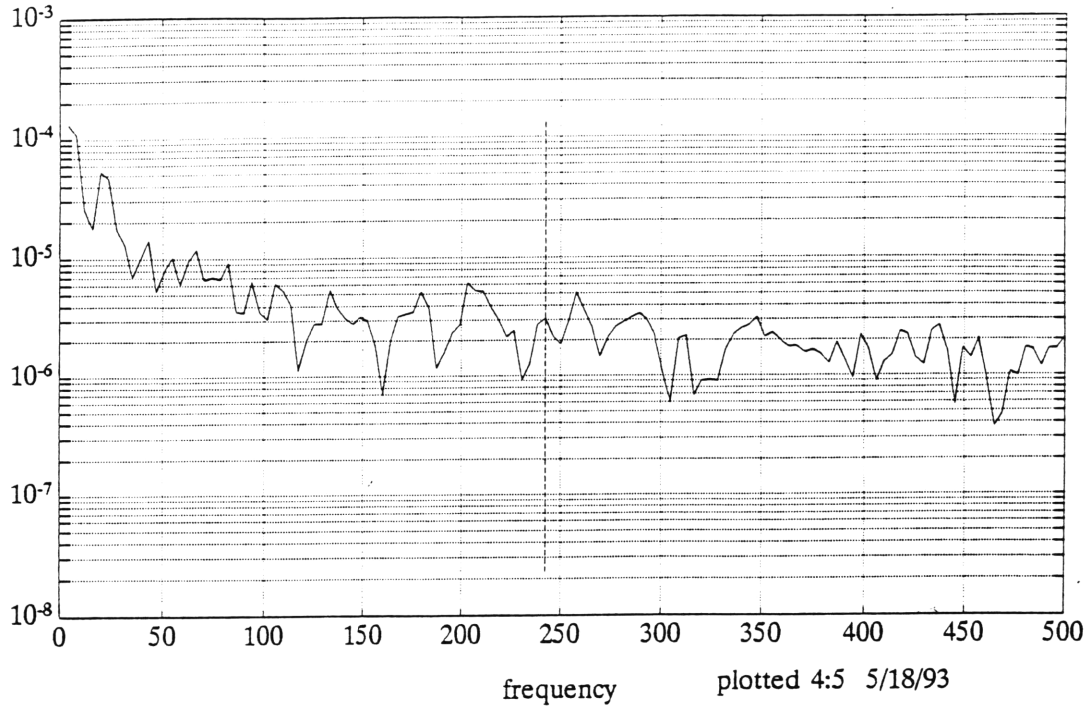


Figure 3.58 : Spectra of Hotwire at 242 Hz

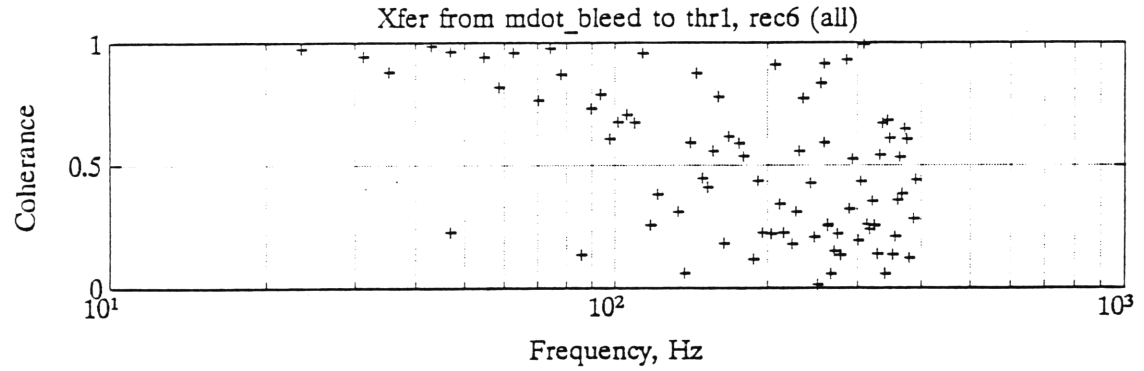
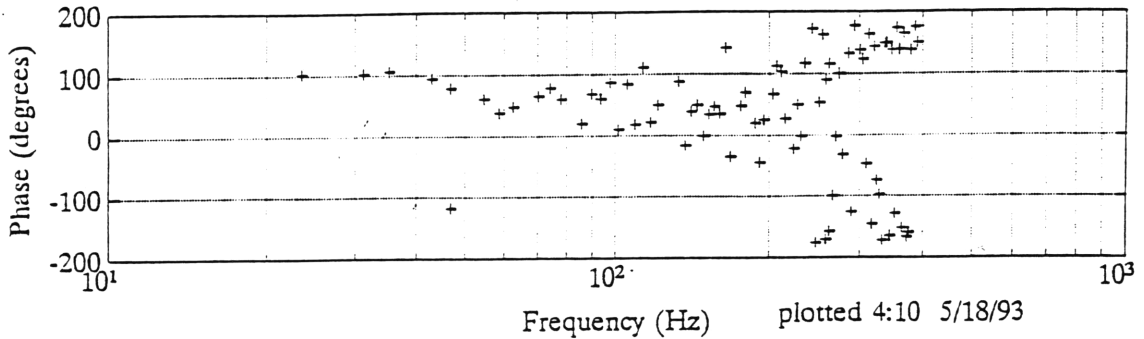
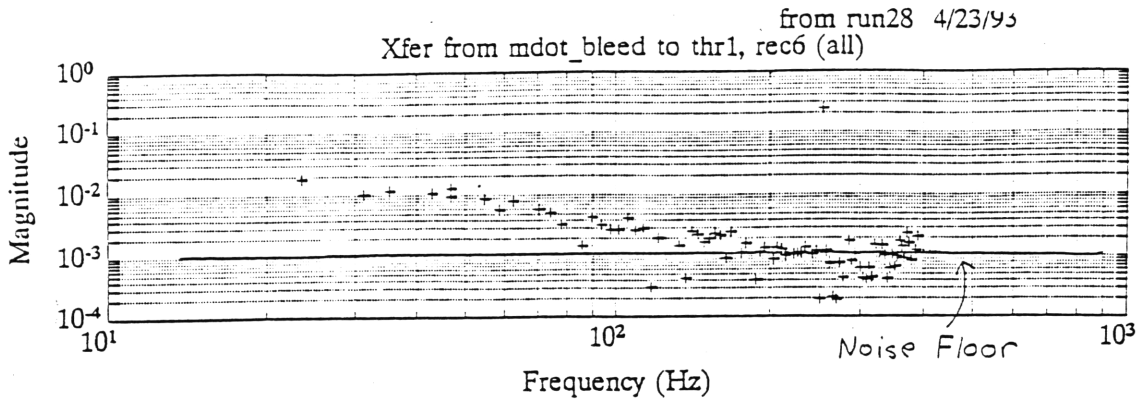


Figure 3.59 : Transfer Function from Customer Bleed Massflow to Zeroth Mode at the Throat

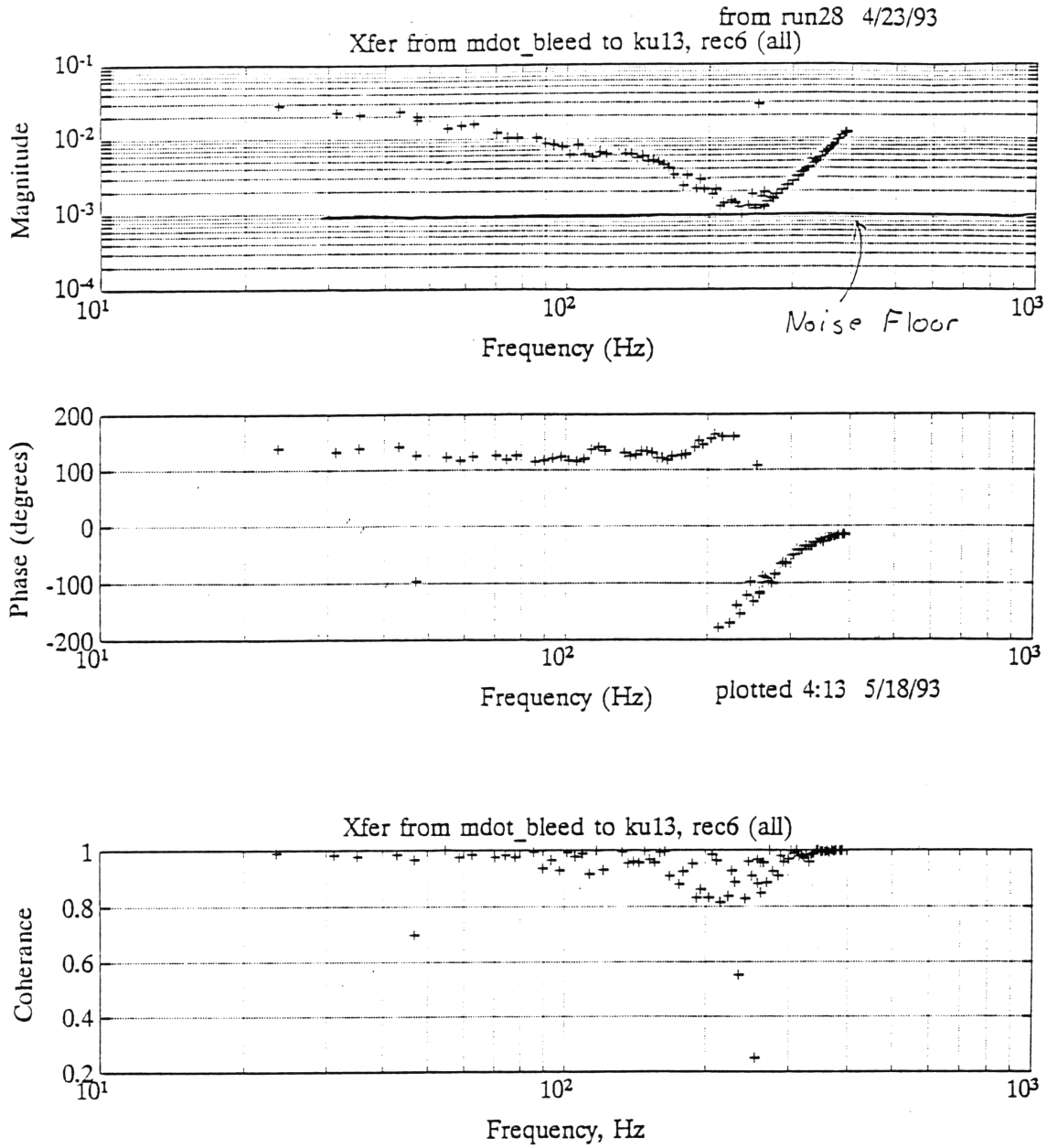


Figure 3.60 : Transfer Function from Customer Bleed Massflow to Combustor Pressure

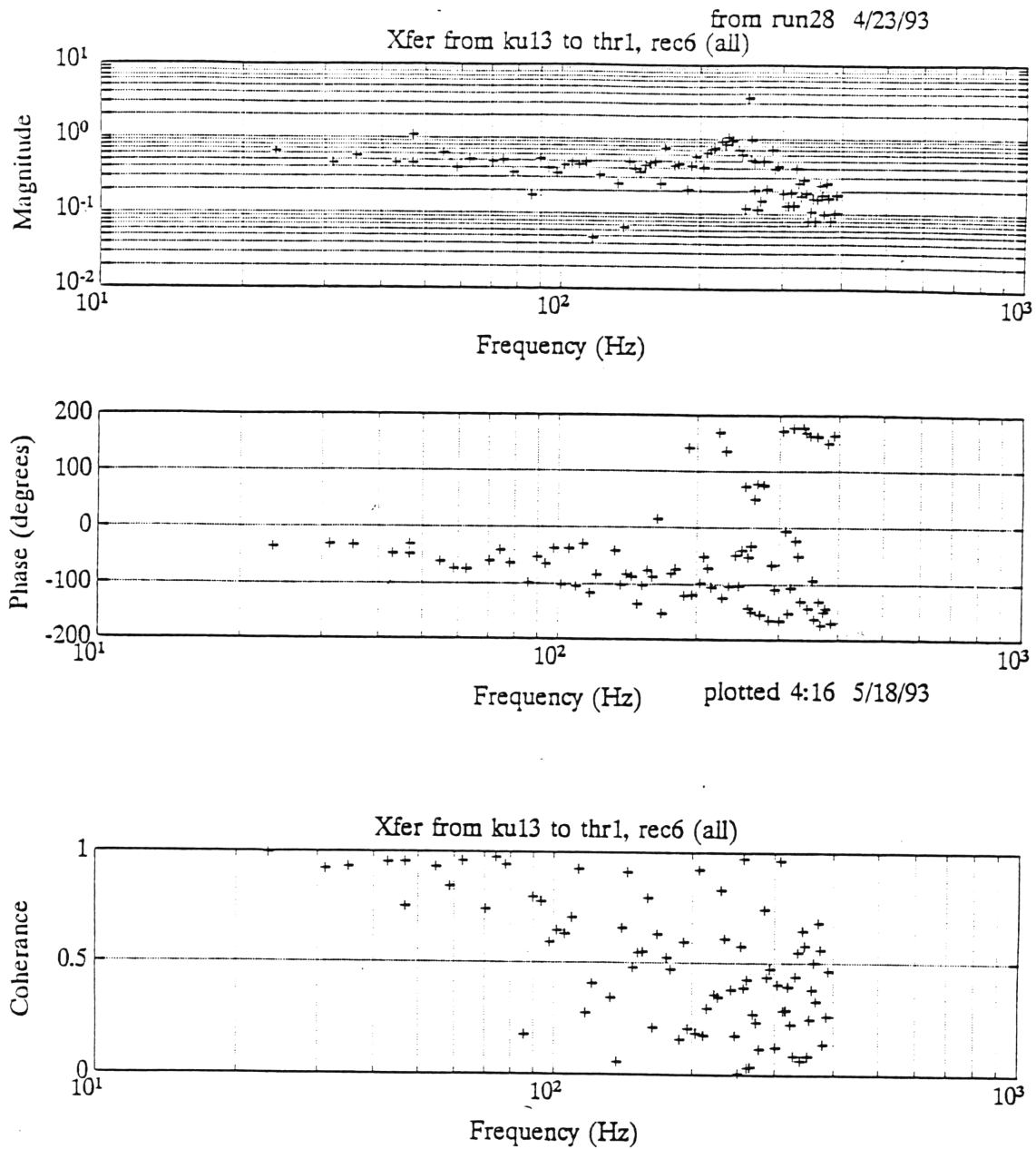


Figure 3.61 : Transfer Function from Combustor Pressure to Zeroth Mode at the Throat

## **4. Summary and Conclusions**

A small turbojet engine has been set up on a test stand at the MIT/GTL. Steady state and high speed data have been collected and used to characterize the engine. A transfer function of the engine with limited frequency range was produced. This chapter contains a summary of the work carried out, and brief statement of the conclusions reached and recommendations for future research.

### **4.1. Summary**

A Lycoming LTS-101 engine, with the power turbine removed, was set up on a test stand at MIT/GTL. The engine is controlled using a computer, which monitors and records steady state data. The computer also sets the throttle position and controls the area of the exit nozzle. With these two controls the engine can be moved to any point on the operating map, including unstable ones. The control computer also monitors and reacts to engine overspeed or over temperature conditions.

Inlet temperature fluctuations of  $\pm 1.5^\circ \text{C}$  on a time scale of minutes were found to produce  $\pm 0.30\%$  variations in the corrected engine speed, while the nozzle and throttle settings were constant. The fuel controller on the engine under compensated for these variations producing  $\pm 0.15\%$  fluctuations in the absolute engine speed. The fluctuations in engine speed caused  $\pm 0.60\%$  variations in the pressure ratio measured across the compressor and  $\pm 0.35\%$  variations in the massflow measured by a calibrated inlet bellmouth. A drop in corrected engine speed of 1 to 2% was also found to occur as the nozzle was closed, at constant throttle setting.

Steady state data was adjusted to compensate for the variations in engine speed. Speed lines were then produced by fitting a curve to the adjusted data. For runs 27 and 28 the resulting speed lines matched each other well within the expected error of the measurements. These calculations indicated that the engine surged within one standard deviation ( $\pm 0.24\%$  of the massflow) of the

calculated zero slope point for runs 25, 27, and 28. It was also qualitatively determined that the engine appeared to surge at a slightly positive slope when there was no external forcing. When the massflow through the customer bleed port was being modulated the engine appeared to surge at a slightly negative slope.

Surge inception data was found to show no evidence of a rotating disturbance in the compressor prior to surge. There was also no clear evidence of an increase in the disturbance levels within the engine prior to surge.

Surge was observed to produce reverse flow through the compressor and a pressure drop of 70 % in the combustor. The engine was observed to surge at 8 to 9 Hz, until the throttle setting was reduced.

The massflow through the customer bleed port was modulated as a method of introducing external forcing to the engine. The resulting disturbances within the engine were used to find several transfer functions. The behavior of the pressure at the customer bleed port appeared to be strongly influenced by the internal acoustic dynamics of the engine.

#### 4.2.Conclusions

The engine and rig behave as designed and intended. The nozzle allows the massflow through the engine to be controlled. Reducing the massflow causes the engine to surge.

The effect, on the disturbances in the engine, of applying external forcing by modulating the customer bleed massflow appears to be small, but it is detectable. Transfer functions between the forcing and the pressures in the engine can be measured, although the frequency range is limited. The bleed massflow modulation also appears to have a destabilizing affect on the engine, causing it to surge at negative, instead of positive, slopes on the pressure ratio vs. massflow curve.

### 4.3. Suggestions for Future Research

There are several issues that appear to be worth pursuing, but are beyond the scope of this thesis. These issues can be conveniently grouped into two classifications, further examinations of the collected data and future experiments or investigations with the engine.

#### 4.3.1. Additional Examination of Collected Data

A very large amount of run data has been collected. While most of it appears to be very similar in nature there was not time to analyze and compare all of it. Some interesting phenomena may have been missed. Therefore, further study of the collected data may reveal new details of the engine's behavior and performance.

The data that has been collected, particularly the transfer functions, may be used to compare the behavior of the engine with the behavior of the models discussed in chapter 1. It may also be used to determine the effectiveness of controlling the disturbances in the engine by modulating the bleed massflow. Both of these applications of the data would be very useful for further work on the engine, especially for applying feedback to delay surge.

#### 4.3.2. Investigations With the Engine

It appears that acoustics may play a greater role in the internal disturbances of this engine than was thought. An investigation of acoustic dynamics of the engine should be carried out to determine what affect they have on stability and on the implementation of feedback control, either active or passive.

As shown in this thesis the magnitude of the response to the modulating the customer bleed massflow is very low. Other methods of applying forcing to the engine should be investigated, possibilities include in-bleed modulation at the inlet, the customer bleed or the diffuser throat. It is hoped that there will be a larger response in the engine to a different method of forcing, allowing the transfer functions to be found over a larger frequency range.

Lowering the minimum excitation frequency might provide additional useful information. The magnitude of the transfer function from the bleed massflow to the locations within the engine grows as the frequency is decreased. At a low enough frequency the bleed massflow oscillation might cause a response at the stator taps or the hotwire.

The addition of more transducers at the stator taps and additional hotwires in the throat is also recommended. This would allow the zeroth rotational mode at the stator taps and the zeroth planar mode at the hotwires to be used to filter the signals there reducing the ambient noise levels and perhaps allowing the measurement of the disturbances caused by the bleedflow oscillations. If more sensitive pressure transducers become available it is recommended that they be installed as well.



## Appendix A

### Calculation of Nozzle position vs. Nozzle Area

A diagram of the nozzle is shown in Figure A.1. The throat of the nozzle is located at the closed approach between the inner and outer sections of the nozzle. The throat will always be perpendicular to the sides of the nozzle. Since the nozzle pieces are conic sections the throat is a third conic section.

Points 1,2, 3 and 4 as labeled in Figure A.1 are used to define the position of the nozzle and the geometry of the throat conic section. Point 1 is always located at the tip of the nozzle centerbody and is used as the zero of the x-axis. Point 2 is the point at which the throat intersects the centerbody. Point 3 is the intersection of the throat and the outer part of the nozzle. Point 4 is located at the beginning of the curve on the outer part of the nozzle, the x position of point 4 is used to establish the nozzle position.  $\alpha$  is the angle between the tangent to the outer nozzle surface at the throat intersection and the x-axis.  $\beta$  is the angle of the centerbody wedge,  $30^\circ$ . The curved section of the outer nozzle has a radius of curvature of 1 inch. The curve between the angled and straight portion of the centerbody has a 0.5 inch radius of curvature and begins 1.4 inches from the tip of the centerbody. The geometry leads to the following equations, (x and r are the axial and radial positions of the point with the corresponding number)

for  $x_2 < 1.4$

$$r_2 = x_2 \times \tan(\beta) + r_1 \quad (\text{A.1})$$

and

$$\alpha = \beta \quad (\text{A.2})$$

for  $x_2 > 1.4$

$$\alpha = \sin^{-1} \left( \frac{0.5 \times \sin(\beta) - x_2 + 1.4}{0.5} \right) \quad (\text{A.3})$$

and

$$r_2 = r_1 + 1.4 \tan(\beta) + 0.5 \left[ \cos(\alpha) - \cos(\beta) \right] \quad (\text{A.4})$$

The following equation apply for any value of  $x_2$ ,

$$r_3 = r_4 + 1 - \cos(\alpha) \quad (\text{A.5})$$

$$x_3 = x_2 - (r_3 - r_2) \tan(\alpha) \quad (\text{A.6})$$

$$x_4 = x_3 - \sin(\alpha) \quad (\text{A.7})$$

The formula for the area of a conic section is now used to find the throat area. For this formula,

$$h = x_3 - x_2 \quad (\text{A.8})$$

$$A = \pi(r_2 + r_3) \sqrt{h^2 + (r_2 - r_3)^2} \quad (\text{A.9})$$

The area vs. position curve is produced by setting  $x_2$  to several values between 0 and 1.65.

The area (A) and the position ( $x_4$ ) are calculated and plotted against one another.

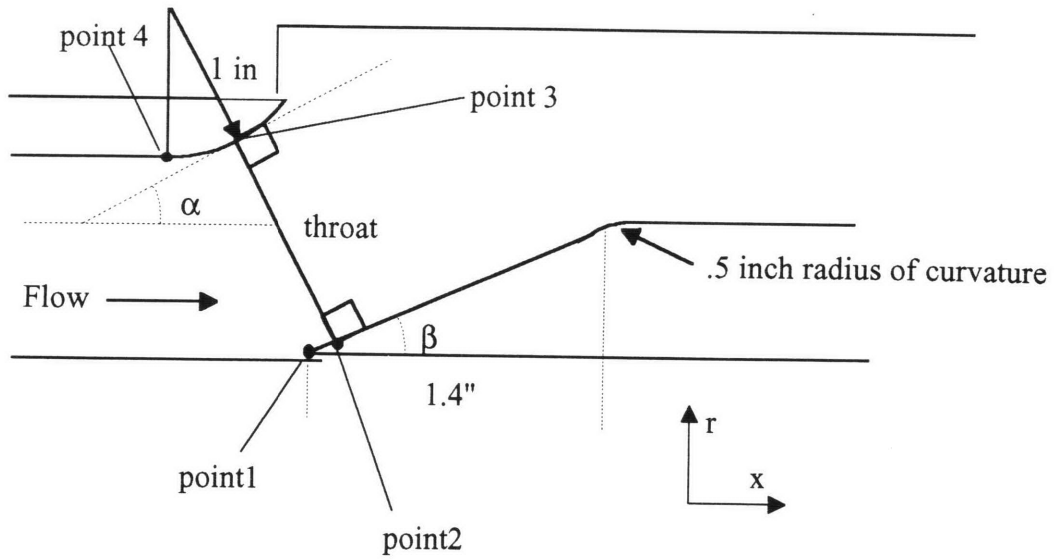


Figure A.1: Diagram of the Nozzle Throat

## Appendix B

### Frequency Response of the Pressure Taps

The pressure transducers that read the static pressures at the stator and throat are not located at the tap, because of the engine geometry. They are mounted on a static pressure probe, consisting of a pressure line and sensing plenum. The probes have an inherent delay time in their response to pressure perturbations at the tap. It is important to determine the frequency response of the probe, because it impacts the detection of rotating stall and the calculation of transfer functions. The static pressure probe is shown in Figure B.1 and the dimensions of the tubes and sensing plenums are listed in Table B.1. The frequency response is calculated using two equations from Grant [7]. He provides equations for the response time probe (time for it to reach 99.3 % of the pressure at the tap) and the helmholz resonance frequency of the probe.

The following definitions are used;

$l$  is the length of the pressure line, in inches.

$d$  is the diameter of the pressure line, in inches.

$v$  is the volume of the sensing plenum, in cubic inches.

$\theta$  is the temperature ratio (temp in probe in °R / 518.7° R)

$\delta$  is the pressure ratio (pressure at tap in psi/ 14.69 psi)

The equation for the response time (in seconds) is,

$$S = \frac{l \times v}{\left(\frac{d}{0.014}\right)^4} \times \frac{\theta^{0.76}}{\delta} \quad (\text{B.1})$$

The response time limits the frequency to,

$$f_r = 1/S. \quad (\text{B.2})$$

The equation for the helmholz frequency is,

$$f_h = \frac{27 \left( \frac{d}{0.014} \right)}{\sqrt{l \times v}} \times \sqrt{\theta} \quad (\text{B.3})$$

The response of the probe drops off sharply above the helmholz frequency. So the frequency response of the probe is limited to the lower frequency. The equations are applied to the conditions at each probe to produce the results shown in Table B.1. Note that the helmholz frequency is the limiting frequency on the response of the probes.

Location	stator	throat
v (in <sup>3</sup> )	4.91*10 <sup>-4</sup>	4.91*10 <sup>-4</sup>
l (in)	14	5.5
d (in)	0.030	0.040
S (sec)	3.002*10 <sup>-4</sup>	1.51*10 <sup>-5</sup>
f <sub>r</sub> (Hz)	3331	66327
f <sub>h</sub> (Hz)	713.3	1733.6

Table B.1: Limiting Frequencies of the Static Pressure Probes

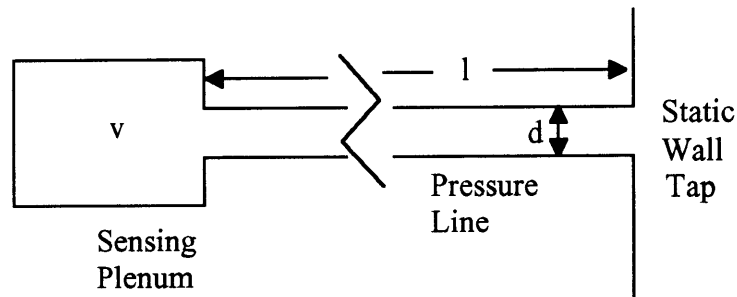


Figure B.1: Diagram of Static Pressure Probe

## Appendix C

### Wiring Schematics for the Control Computer

The next four pages contain schematics of the connections between the control computer, the test stand and the control center in the hall. The first schematic (Figure C.1) is an overview of the connections. The second schematic (Figure C.2) is the connections to the T400 terminal panel attached to the ACPC-I/O board. The third schematic (Figure C.3) is of the connections to the T41 terminal panel which is channel one thru eight of the analog inputs and the digital I/O of the ACPC-16-16 board. The fourth schematic (Figure C.4) is the connections made in the junction box on the test stand.

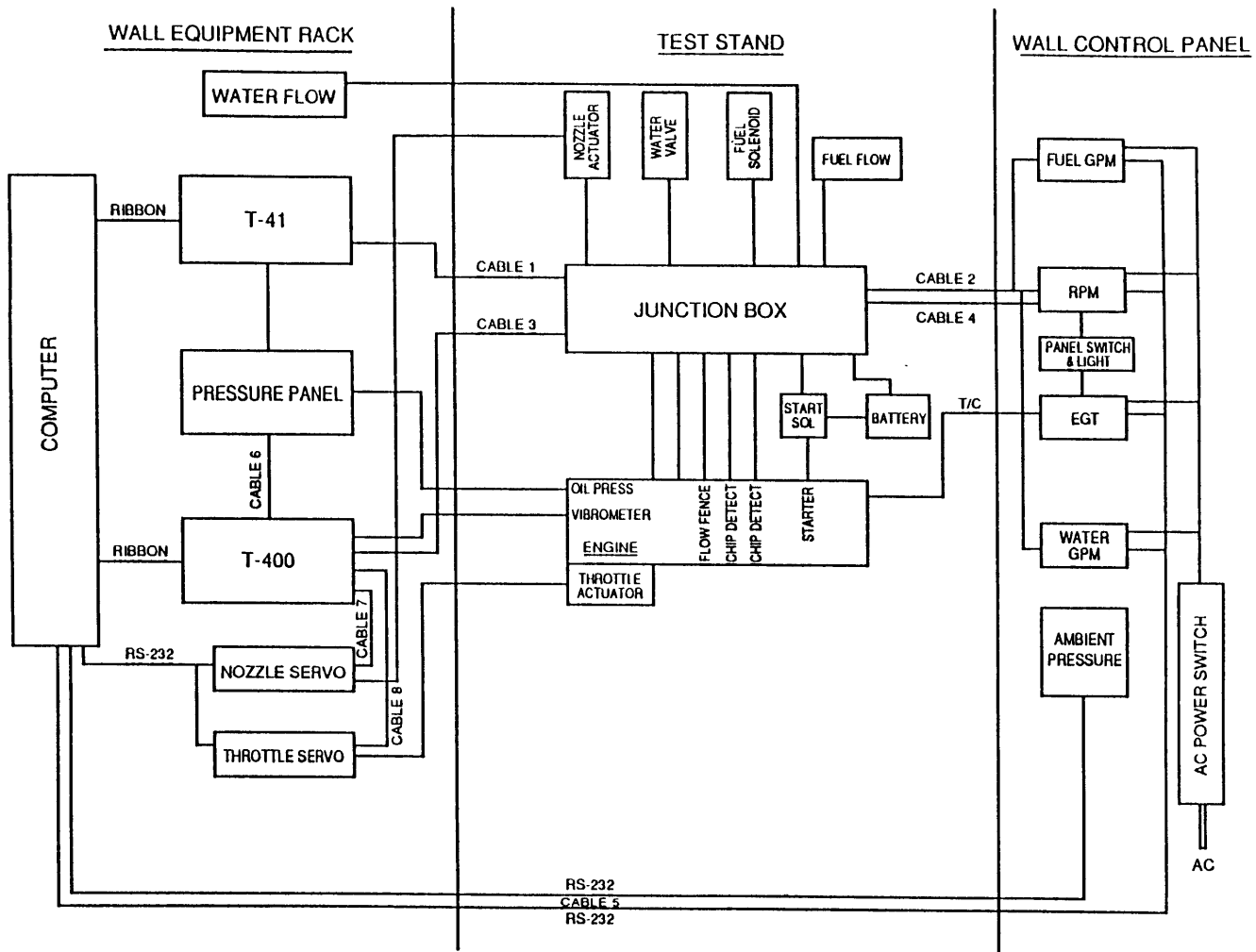


Figure C.1 : Rig Wiring Schematic

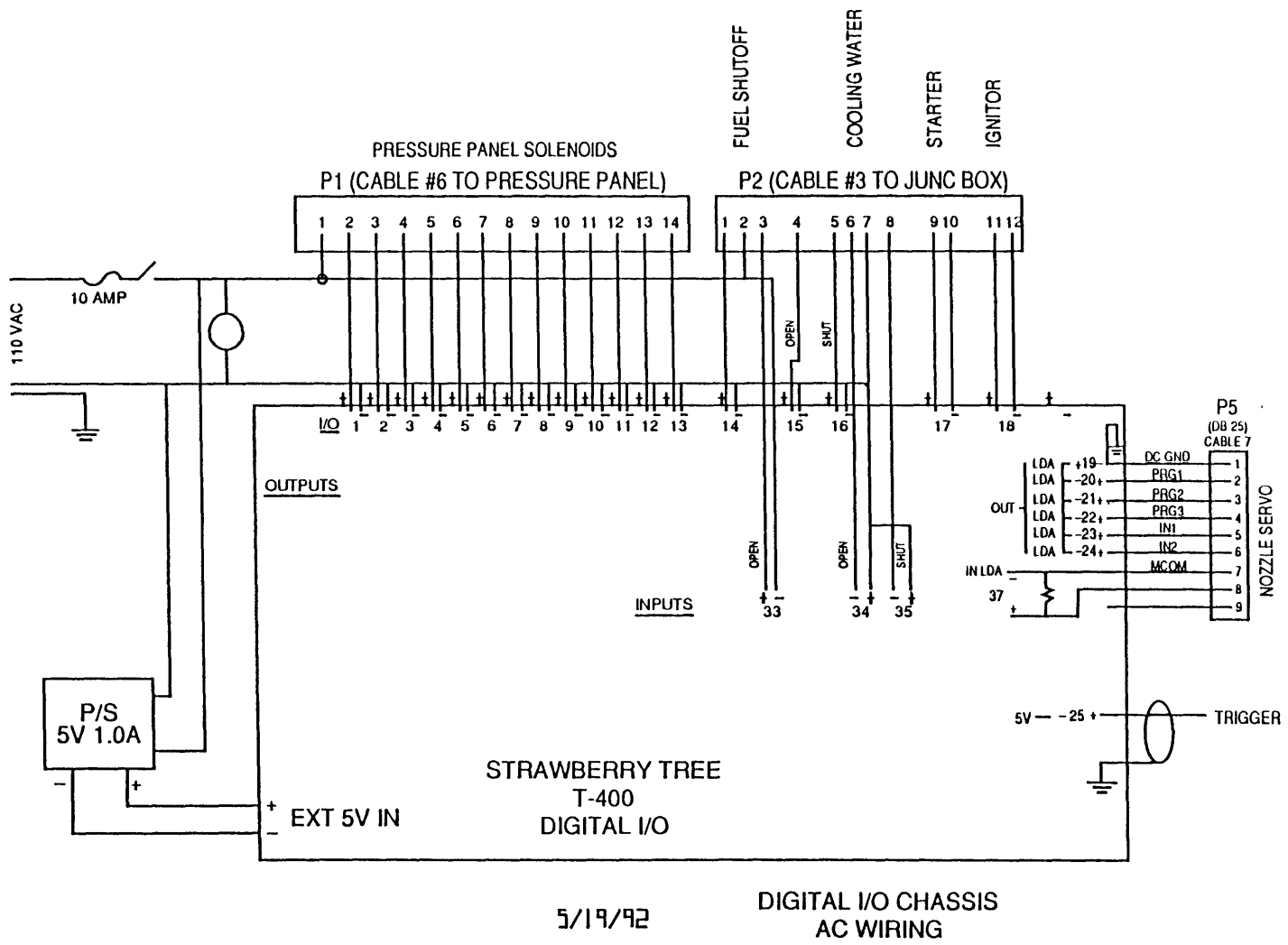


Figure C.2 : Wiring Schematic for T400 Terminal Panel



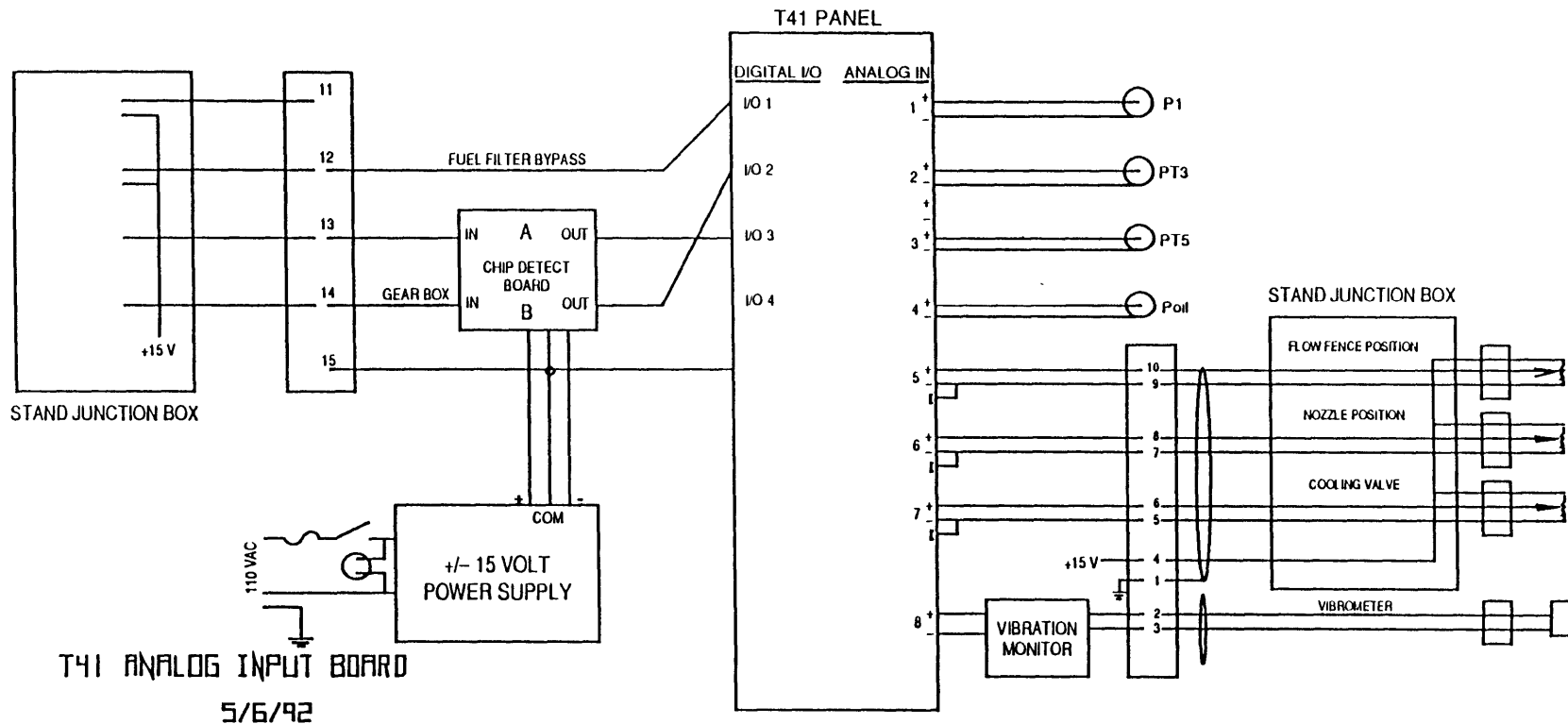


Figure C.3 : Wiring Schematic for T41 Terminal Panel

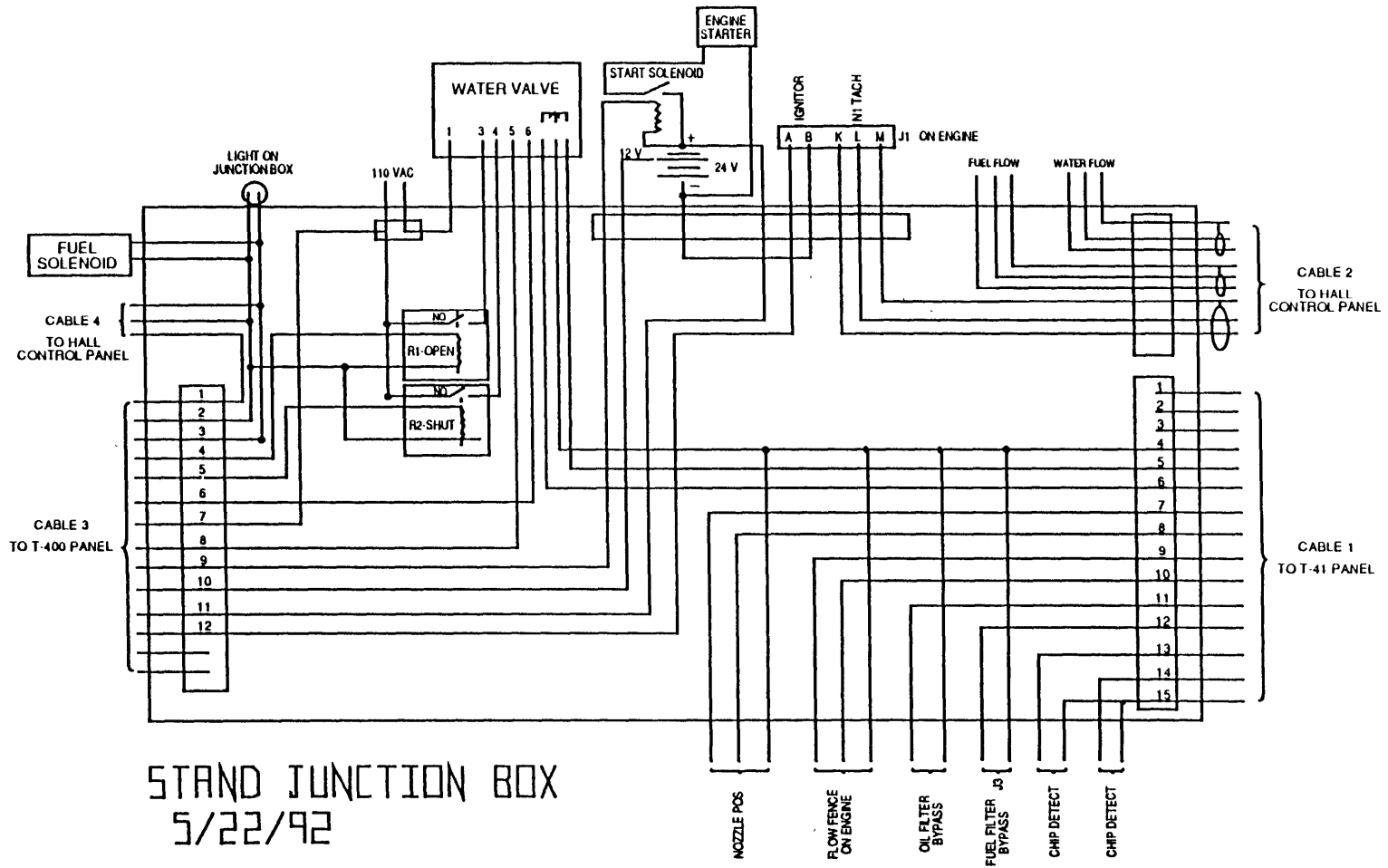


Figure C.4 : Wiring Schematic for the Junction Box

## Appendix D

### Listing of the Original Code Used to Run the Engine

The listing of the original code used to run the engine follows. It is written in Microsoft C 6.0 and uses the device drivers provided by Strawberry Tree Inc. with their A/D and digital I/O boards.

```
/* This one works now I think. 7/3/92 */

#include<stdlib.h>
#include<stdio.h>
#include<conio.h>
#include<ctype.h>
#include<string.h>
#include<math.h>
#include<time.h>
#include<graph.h>

#define ANACNT 32      /* # of analog channels */
#define DIGCNT 192    /* # of digital channels */

unsigned digital[DIGCNT];
float analog[ANACNT];

main()
{
    /*double getthrot(void);*/
    double getPo(void);
    double getN1(void);
    double getfuelflow(void);
    void open(unsigned[]);
    void close(unsigned[]);
    void longopen(unsigned[]);
    void longclose(unsigned[]);
    void initial(void);
    void send_serial(char *,int);
    /*float getthrot(void);*/
    float noz(void);
    float thrott(int,float,float);
    float ana[32];
    float oilp,inp2,inp,comp,turbp,vibr,pnot,N1,To,N1cor,cormas,presrat;
    float nozzpos,gotthrot,pnota,throttle3,throt4,loadcell;
    float AF, TT41, Po, WF;
```

```

int char1=0, fuel1=1, starter1=1, ignitor1=1, nozzact=1, i,j=0;
int trig=1, backp=1;
char char2, *nozzle2, *throttle2, a[50], b[50];
float nozzle1, throttle1;
double fuelflow;

nozzle2=a;
throttle2=b;

/* initialize the board */

initial();

/* initialize the actuators */

strcpy(nozzle2," PU02 1DL02 GH-10 EN SI12 CE99 JA.1 JV10 XP1 ZZ ");
strcpy(throttle2," E FSB1 FSC1 MPA LD3 OSE1 FSD0 GHAS GHAD5 GHV-.5 GH ");

send_serial(nozzle2,3);
send_serial(throttle2,4);

strcpy(throttle2," PZ CPE100 LD3 V.05 A5 AD5 D0 G ");
send_serial(throttle2,4);

nozzle1=0;
throttle1=0;

while (1) /* while the escape key hasn't been hit */
{
/* Calibrate and read analog inputs */
SH_CALL("cm",analog,digital);      /* call A-D driver */

/* Read digital inputs */
SH_CALL("I",analog,digital);      /* call A-D driver */

/* calculate the engineering values */
N1=getN1();
To=analog[12]*9/5+32;
pnota=getPo();
if (!(pnota>15.50 || pnota<=14.00)) pnot=pnota;
Po=pnot*2.036;
N1cor=N1/sqrt((To+459.7)/518.7);
oilp=(analog[3]-1.0273)*39.9;
inp2=analog[0]*.1102+.0013;
if (inp2>0) inp=-.0000001;
    else inp=inp2;
comp=(analog[1])*49.95+.5530;
turbp=analog[2]*10.059+.3100;
vibr=analog[7]*30;
presrat=(comp+pnot)*1.01/pnot;

```

```

cormas=43.32*(.192335*pow((-inp*27.68/(pnot*2.036)),.5)
-.007874*pow((-inp*27.68/(pnot*2.036)),1.5)+.000046);
nozzpos=(analog[5]-5.3681)*.63682+1.331;
loadcell=analog[8]*200;
fuelflow=getfuelflow();
WF=fuelflow*60*6.74;
AF=cormas*(Po/29.92)/sqrt((To+459.7)/518.7)*.9688*3600/(WF*18550/18500);
TT41=72675/AF-302264/(AF*AF)+.9576*analog[14]-6.679*analog[14]/AF+43.6;
TT41=TT41+459.7;

```

```

/* Output to the screen */

```

```

system("cls");
printf("<F1> = shutdown. To activate press Alt-(key). Throttle Controls\n");
printf(" Name      Value      Units      q- down 5, r- up 5\n");
printf("-----  -----  -----  w- down 1, e- up 1\n");
printf("EGT      %15.4f    Degrees C    (T)hrottle position\n",
      analog[15]);
printf("Oil Temp %15.4f    Degrees C    %5.2f degrees\n",
      analog[31],throttle1);
cprintf("Fuel Bypass %13s          (F)uel %6s\nr",
      digital[1] ? "okay" : "bypassed", fuel1 ? "closed" : "open");
cprintf("Chip det 1 %13s          (S)tarter %5s\nr",
      digital[2] ? "chip" : "okay", starter1 ? "off" : "on");
cprintf("Chip det 2 %13s          (I)gnitor %5s\nr",
      digital[3] ? "chip" : "okay", ignitor1 ? "off" : "on");
printf("Oil press %15.4f    psig        (N)ozzle position\n",
      oilp);
printf("Seal metal %14.4f    Degrees C    %2.3f in.\n",
      analog[9],nozzle1);
cprintf("Exhaust %15.4f    Degrees C    %10s\nr",
      analog[17],nozzact ? "in(A)ctive":"(A)ctive");
printf("vibrometer %14.4f    in/sec      actual %4.3f in.\n",
      vibr,nozzpos);
printf("Nozzle metal %12.4f    Inlet T #2 %12.4f Degrees C\n",
      analog[11],analog[16]);
printf("Inlet T #3 %12.4f    Inlet T #4 %12.4f Degrees C\n",
      analog[22],analog[25]);
printf("ambient press %11.4f    psia      Motor Casing %4.3f C\n",
      pnot,analog[10]);
printf("inlet press %13.4f          psig      Cooling water flow\n",
      inp2);
printf("comp press %14.4f          psig      o- increase\n",
      comp);
printf("turb press %14.4f    psig      p- decrease\n",
      turbp);
printf("Pressure ratio %10.3f    ambient/comp    pot %2.3f volts\n",
      presrat,analog[6]);
printf("inlet T #1 %14.4f    Degrees C    Load Cell\n",
      analog[12]);

```

```

printf("TT3    %14.4f    Degrees C    %4.2f lbs\n",
      analog[14],loadcell);
printf("N1    %14.2f    (corr) %8.2f    percent speed\n",
      N1,N1cor);
printf("Massflow (corr) %9.3f    lbs/sec    f/f pot %2.3f V\n",
      cormas,analog[4]);
printf("Fuelflow %8.3f gal/min    TT41 %8.3f degrees R",
      fuelflow,TT41);
if (analog[15]>732.2) printf("EGT overtemp");
/* if (vibr>.8) printf("Vibration warning"); */
if (analog[31]>99) printf("Oil overtemp");
if (N1>102) printf("Engine overspeed");
if (analog[16]>500) printf("Exhaust overtemp");

/* log data I hope */

ana[0]=throt4;          /* actual throttle pos */
ana[1]=throttle1; /* throttle position */
ana[2]=digital[1]*1+digital[2]*2+digital[3]*4+digital[45]*8;
/* fuelbypass * 1, chipdet1 * 2, chipdet2 * 4, fuelvalve * 8 */
ana[2]=ana[2]+digital[48]*16+digital[49]*32+nozzact*64;
/* starter * 16, ignitor * 32, nozzleact * 64 */
ana[2]=ana[2]+j*1000;
/* the thousandths place indicates which inlet pressure
   valve is open */
ana[3]=analog[4]; /* flow fence pot */
ana[4]=0; /* ignitor */
ana[5]=nozzle1; /* nozzle position cmd */
ana[6]=analog[15]; /* EGT */
ana[7]=analog[31]; /* oil temp */
ana[8]=fuelflow; /* fuelflow rate */
ana[9]=TT41; /* TT41 */
ana[10]=trig; /* trigger condition */
ana[11]=oilp; /* oil pressure */
ana[12]=analog[9]; /* seal metal temp */
ana[13]=analog[10]; /* P3 tap temp */
ana[14]=vibr; /* vibrometer */
ana[15]=analog[11]; /* nozzle metal */
ana[16]=analog[16]; /* exhaust #1 */
ana[17]=analog[22]; /* temp by blast gate */
ana[18]=analog[25]; /* temp on roof */
ana[19]=pnot; /* ambient press */
ana[20]=inp2; /* inlet press */
ana[21]=comp; /* compressor press */
ana[22]=turbp; /* turbine press */
ana[23]=presrat; /* pressure ratio */
ana[24]=analog[12]; /* inlet temp */
ana[25]=analog[14]; /* TT3 */
ana[26]=N1cor; /* corrected speed */
ana[27]=cormas; /* corrected massflow */

```

```

ana[28]=analog[6]; /* water          pot          */
ana[29]=N1;        /* engine speed */
ana[30]=nozzpos;  /* actual nozzle pos */
ana[31]=loadcell; /* loadcell */
SH_CALL("\0",ana,ana,digital,ana,ana,ana,ana);

```

```

/* set discrete outs */

```

```

for (i=31;i<64;i++)
    digital[i]=1;
digital[32+j]=0; /* open the valves for the pressure transducers */
if (j>=3)
    j=0;
else
    j=j+1;
digital[38]=0;
digital[40]=0;
digital[50]=nozzact; /* allow separate control of the */
digital[51]=nozzact; /* nozzle actuation switches */
digital[52]=1;
digital[53]=1;
digital[45]=fuel1;
digital[48]=starter1;
digital[49]=ignitor1;
digital[44]=backp;
digital[56]=trig;
trig=1;

```

```

SH_CALL("O",analog,digital); /* call A-D driver */

```

```

/* check for keyboard inputs */

```

```

if (kbhit()!=0)
{
    char1=getch();
    if (char1==23)
    {
        if (ignitor1==1) ignitor1=0;
        else ignitor1=1;
    }
    if (char1==31)
    {
        if (starter1==1) starter1=0;
        else starter1=1;
    }
    if (char1==30)
    {
        if (nozzact==1) nozzact=0;
    }
}

```

```

else nozzact=1;
}
if (char1==33)
{
if (fuel1==1) fuel1=0;
else fuel1=1;
}
if (char1==20 || char1==16 || char1==17
|| char1==18 || char1==19)
throttle1=thrott(char1,throttle1,N1cor);
if (char1==49)
nozzle1=noz();
if (char1==27)
break;
if (char1==24)
open(digital);
if (char1==25)
close(digital);
if (char1==79)
longopen(digital);
if (char1==80)
longclose(digital);
if (char1==48)
{
if (backp==0)
backp=1;
else
backp=0;
}
if (char1==45)
trig=0;
if (char1==60 && N1cor>50)
{
strcpy(nozzle2," ZZ \n");
strcpy(throttle2," D500 G ");
send_serial(nozzle2,3);
send_serial(throttle2,4);
nozzact=0;
throttle1=45;
}
if (char1==59)
{
strcpy(nozzle2," ZZ \n");
strcpy(throttle2," D0 G ");
send_serial(nozzle2,3);
send_serial(throttle2,4);
nozzact=0;
throttle1=0;
}
}
}

```



```

    }

    for (i=31;i<64;i++) digital[i]=1;
    SH_CALL("O",analog,digital);
    strcpy(nozzle2," ZZ \n");
    strcpy(throttle2," D0 G ");
    send_serial(nozzle2,3);
    send_serial(throttle2,4);

    /* close data file */
    ana[0]=0;
    SH_CALL("L\0engine.dat\0",ana,digital);

    printf("\n");
    while (1)
    {
        printf("Now type ctrl-c to exit.\r");
    }
}

```

```

float thrott(int cmd, float othrottle, float N1corr)
{
    void send_serial(char *,int);
    float throttle, position;
    char *ran, *buffer;

    /* get new value for throttle (position) */

    if(cmd == 20)
    {
        printf("\nValue to set throttle in degrees: ");
        scanf("%f",&throttle);
    }
    if(cmd == 16)
    {
        throttle=othrottle-5;
    }
    if(cmd==17)
    {
        throttle=othrottle-1;
    }
    if(cmd==18)
    {
        throttle=othrottle+1;
    }
    if(cmd==19)
    if (N1corr<90)
    {
        throttle=othrottle+5;
    }
}

```

```

    }
else
{
    throttle=othrottle+1;
}

/* make sure it's safe, convert to string, add to buffer and send */

if (throttle <= 0) throttle=0;
if (throttle>=98) throttle=98;

strcpy(buffer," D");
position=floor(throttle*4000/360+.5);/* convert degrees to encoder counts */
gcvt(position,7,ran); /* convert float to string */
strrev(ran);
strnset(ran,32,1);      /* remove decimal point */
strrev(ran);
strcat(ran,"G ");      /* assembling command buffer */
strcat(buffer,ran);
send_serial(buffer,4); /* send command out comm4 */
return throttle;      /* return value */

}

float noz()
{
    void send_serial(char *,int);
    float nozz;
    char *sat, *ran, *buffer;

    printf("\nValue to set nozzle in inches: ");
    scanf("%f", &nozz);      /* get nozzle position from user */

    strcpy(buffer," DL1 AC.1 DC.1 VE05 DA"); /*first part of cmd string*/

    if (nozz>=1.015) nozz=1.015;      /* prevent commanding to hit limit */
    gcvt(nozz,4,ran);
    strcat(ran," GO EN \n"); /*add last part of cmd string to position*/
    strcat(buffer,ran);      /*add position and last part to first part*/
    send_serial(buffer,3); /* send cmd string to port 3 */
    return nozz;
}

void send_serial(char *string,int port)
{
    /* sends the input string out through the specified port */

```

```

int outp(unsigned port, int databyte);
int let,len,i,wait,add;

if (port==1) add=0x3f8;
if (port==2) add=0x2f8;
if (port==3) add=0x100;
if (port==4) add=0x108;

len=strlen(string);

for(i=0;i<len;i++)
{
for(wait=0;wait<15000;wait++);      /* make computer wait for port */
let=*string++;
outp(add,let);
}
for(wait=0;wait<15000;wait++);
/*outp(add,13);      /*carriage return
for(wait=0;wait<5000;wait++);
outp(add,10);      /*line feed*/
}

void initial()
{
/** Read CALIB.DAT file and calibrate the analog inputs **/
float ana[ANACNT];
int i;

SH_CALL( "Fn" , analog, digital );      /* Call A-D driver */

if (digital[0] == 0 && digital[2] == 0) {
printf("\nDriver, ADRIVE.COM, not installed; ");
printf(" or analog card not installed.\n");
exit(1);
}
if (digital[0] == 0 && digital[2] != 0) {
printf("\nNo analog card selected. BRD SEL switch set to 0.\n");
exit(1);
}
if (digital[0] != 0 && digital[6] == 0) {
printf("\nCALIB.DAT file not correct or FIND.EXE was not run.\n");
exit(1);
}
if (digital[0] > digital[6]) {
printf("\nCalibration numbers are not correct.\n");
exit(1);
}
if (digital[0] > ANACNT || digital[2] > DIGCNT) {
printf("\nToo many channels installed.\n");
}
}

```

```

printf("Change size of ANACNT and/or DIGCNT in heading\n");
exit(1);
}

/** Set analog channel resolution */
digital[0] = 18;
SH_CALL( "a" , analog, digital );

/** Set up analog channel range and calibrate */
for (i = 0; i < ANACNT; ++i)
{
digital[i] = 2; /* 10 V */
if (i<4) digital[i]=5; /* +-5 V */
if (i==7) digital[i]=1; /* 500mV */
if (i==8) digital[i]=5; /* +-5 V */
if (i>8) digital[i]=22; /* k type thermocouple */
}
SH_CALL( "rc" , analog, digital );

/** Set up digital channel direction */
for (i = 0; i < DIGCNT; ++i)
{
digital[i] = 0; /* input channels */
if(i>31 && i<63) digital[i]=1; /* output channels */
}
SH_CALL( "S" , analog, digital );

/* set discrete outs */

for (i=31;i<64;i++)
digital[i]=1;
digital[33]=0; /* open the valves for the pressure transducers */
digital[38]=0;
digital[40]=0;
digital[50]=1; /* allow separate control of the */
digital[51]=1; /* nozzle actuation switches */
digital[45]=1;
digital[48]=1;
digital[49]=1;

SH_CALL("O",analog,digital); /* call A-D driver */

/* set up data logging (I hope) */

ana[0]=2; /* log to disk */
ana[1]=0; /* log when called */
ana[3]=1; /* log present data only */
ana[4]=32; /* number of channels to log */
ana[5]=0;
SH_CALL("L\0engine.dat\0",ana,digital); /* call driver */

```

```

}

double getPo()
{
    /* get pressure reading from Setra */

    double ans;
    unsigned add=0x3F8;
    int wait1=0, wait4=0,wait3, wait8=0;
    long wait6;
    char *wait2, *wait5;

    wait2=wait5;                /* output request for data */
    outp(add,80);
    for(wait6=0;wait6<15000;wait6++); /* delay computer for 1200 baud */
    outp(add,32);

    wait3=wait1;
    wait6=0;
    wait4=0;

    while(wait1!=10 || wait4==0) /* receive data */
    {
        wait1=inp(add);
        wait6=wait6+1;
        if (wait1!=10) wait4=1; /* check for beginning of data */
        if (wait1!=wait3 || wait6>2500) /* record new character if changed */
        {
            /* or timed out */
            *wait2++=wait1;          /* store in string */
            wait3=wait1;
            wait6=0;
            wait8=wait8+1;
        }
        if (wait8>35) break; /* stop if it goes crazy */
    }

    wait2=wait5;
    strnset(wait2,32,1); /* clear out first character (sign) */
    ans=atof(wait2); /* convert data to float */
    /* if (wait8>35 && ans<=14.5) ans=-1; error */
    return ans; /* return float */
}

double getN1()
{
    /* get N1 reading from Newport */

    double n;
    unsigned add=0x2F8;

```

```

int wait1=0, wait4=0, wait7, wait8=0;
long wait6;
char *wait2, *wait5;
char wait3[7]="*01X01\r";

wait2=wait5;
for(wait4=0;wait4<6;wait4++) /*send request for data*/
{
    outp(add,wait3[wait4]);
    for(wait6=0;wait6<15000;wait6++); /*delay computer for 1200 baud*/
}
outp(add,wait3[6]);

wait7=wait1;
wait6=0;
wait4=0;

while(wait1!=10 || wait4==0) /* recieve data */
{
    wait1=inp(add);
    wait6=wait6+1;
    if (wait1!=10) wait4=1; /* check for beginning of data */
    if (wait1!=wait7 || wait6>2500)/* record new character when it */
    {
        /* changes or times out */
        *wait2++=wait1; /* store in string */
        wait6=0;
        wait7=wait1;
        wait8=wait8+1;
    }
    if (wait8>20) break;
}
wait2=wait5;
strnset(wait2,32,2); /* remove first two characters (garbage) */
n=atof(wait2); /* convert data to float */
/*if (wait8>20) n=-1; error */
return n; /* return data as float */
}

void open(unsigned digital[])
{
    long wait;

    digital[46]=0;
    SH_CALL("O",digital,digital); /* call A-D driver */
    for(wait=0;wait<100000;wait++);
    digital[46]=1;
    SH_CALL("O",digital,digital); /* call A-D driver */
}

```

```

void close(unsigned digital[])
{
    long wait;

    digital[47]=0;
    SH_CALL("O",digital,digital);      /* call A-D driver */
    for(wait=0;wait<100000;wait++);
    digital[47]=1;
    SH_CALL("O",digital,digital);      /* call A-D driver */

}

void longopen(unsigned digital[])
{
    long wait;

    digital[46]=0;
    SH_CALL("O",digital,digital);      /* call A-D driver */
    for(wait=0;wait<500000;wait++);
    digital[46]=1;
    SH_CALL("O",digital,digital);      /* call A-D driver */

}

void longclose(unsigned digital[])
{
    long wait;

    digital[47]=0;
    SH_CALL("O",digital,digital);      /* call A-D driver */
    for(wait=0;wait<500000;wait++);
    digital[47]=1;
    SH_CALL("O",digital,digital);      /* call A-D driver */

}

float getthrot()
{
    /* get throttle reading from Compumotor */

    double n;
    unsigned add=0x108;
    int wait1=0, wait4=0, wait7, wait8=0, wait9=0;
    long wait6;
    char *wait2, *wait5;
    char wait3[7]="1PX\n";

    wait2=wait5;
    for(wait4=0;wait4<4;wait4++) /*send request for data*/
    {

```

```

    outp(add,wait3[wait4]);
    for(wait6=0;wait6<2000;wait6++); /*delay computer for 9600 baud*/
    }
    outp(add,wait3[4]);

    wait7=wait1;
    wait6=0;
    wait4=0;

    while(wait1!=10 || (wait4==0 || wait9<4)) /* recieve data */
    {
        wait1=inp(add);
        wait6=wait6+1;
        if (wait1!=10) wait4=1; /* check for beginning of data */
        if (wait1!=wait7 || wait6>350)/* record new character when it */
        {
            /* changes or times out */
            *wait2++=wait1; /* store in string */
            wait6=0;
            wait7=wait1;
            wait8=wait8+1;
            if (wait1==10 && wait4!=0) wait9++;
        }
        if (wait8>50) break;
    }
    wait2=wait5;
    strnset(wait2,32,9); /* remove first 8 characters (garbage) */
    n=atof(wait2); /* convert data to float */
    return n;
}

double getfuelflow()
{
    /* get N1 reading from Newport */

    double n;
    unsigned add=0x2F8;
    int wait1=0, wait4=0, wait7, wait8=0;
    long wait6;
    char *wait2, *wait5;
    char wait3[7]="*03X01\r";

    wait2=wait5;
    for(wait4=0;wait4<6;wait4++) /*send request for data*/
    {
        outp(add,wait3[wait4]);
        for(wait6=0;wait6<15000;wait6++); /*delay computer for 1200 baud*/
    }
    outp(add,wait3[6]);

    wait7=wait1;

```



```

wait6=0;
wait4=0;

while(wait1!=10 || wait4==0)          /* recieve data */
{
    wait1=inp(add);
    wait6=wait6+1;
    if (wait1!=10) wait4=1; /* check for beginning of data */
    if (wait1!=wait7 || wait6>2500)/* record new character when it */
    {
        /* changes or times out */
        *wait2++=wait1; /* store in string */
        wait6=0;
        wait7=wait1;
        wait8=wait8+1;
    }
    if (wait8>20) break;
}
wait2=wait5;
strnset(wait2,32,2); /* remove first two characters (garbage) */
n=atof(wait2); /* convert data to float */
/*if (wait8>20) n=-1; error */
return n; /* return data as float */
}

```

## Appendix E

### Initial Pressure Calibrations and Resulting Formulas

The initial pressure calibrations for the inlet, compressor discharge, turbine discharge, and oil pressure transducers are listed in Tables E.1 thru E.4. Following each table is the volts to pressure equation that results from a straight line least squares fit to that calibration data.

Pressure Applied (psi)	Output Voltage
0.000	0.0174
0.036	0.3359
0.072	0.6521
0.110	1.0182
0.144	1.2228
0.182	1.572
0.218	2.0436
0.254	2.3689
0.290	2.6175
0.326	3.0493
0.362	3.3856
0.398	3.7205
0.434	4.0483
0.470	4.3989
0.506	4.7206
0.542	5.0557

Table E.1: Calibration of Inlet Pressure Transducer

Original formula for the inlet pressure

$$pressure(psi) = volts \times 0.1102 + 0.0013 \quad (E.1)$$

Test # 1		Test # 2	
Pressure Applied (psi)	Output Voltage	Pressure Applied (psi)	Output Voltage
0.000	-0.021	0.000	-0.023
10.272	0.1869	10.270	0.1852
20.178	0.3860	20.210	0.3850
30.150	0.5855	30.130	0.5838
40.080	0.7836	40.020	0.7806
50.166	0.9843	50.140	0.9821
60.078	1.8130	60.050	1.7910
70.044	1.3790	70.020	1.3768
80.208	1.5805	80.178	1.5783
90.090	1.7760	90.054	1.7733

Table E.2: Calibration of Compressor Discharge Pressure Transducer

Original formula for compressor discharge pressure

$$pressure(psi) = volts \times 49.95 + 0.5530 \quad (E.2)$$

Test # 1		Test # 2	
Pressure Applied (psi)	Output Voltage	Pressure Applied (psi)	Output Voltage
0.000	-0.0311	0.000	-0.0299
5.040	0.4741	5.020	0.4730
10.010	0.9706	10.050	0.9759
15.050	1.4727	15.080	1.4771
20.000	19.6550	20.020	196.8700
25.070	2.4695	25.070	2.4709
30.024	2.9615	30.010	2.9614
35.050	3.4608	35.020	3.4589
40.100	3.9615	40.080	3.9609
45.070	44.5400	45.050	4.4538
50.050	4.948	50.020	4.946

Table E.3: Calibration of Turbine Discharge Pressure Transducer

Original formula for the turbine discharge pressure

$$pressure(psi) = volts \times 10.059 + 0.3100 \quad (E.3)$$

Pressure Applied (psi)	Voltage Output
0.000	1.0273
10.428	1.2867
20.148	1.5347
30.194	1.7869
40.450	2.0367
50.100	2.2853
60.050	2.5292
70.115	2.7875
80.460	3.0457
90.102	3.2859
100.188	3.5355

Table E.4: Calibration of Oil Pressure Transducer

Original formula for the oil pressure

$$pressure(psi) = (volts - 1.0273) \times 39.9 \quad (E.4)$$

## Appendix F

### Pre-Run Checklist

Checklist for starting the LTS-101 engine.

(4/22/93)

START THE PROGRAM BY TYPING "LTS-101 RUN"

- 1) Blast gate open
  - a) Heater on the roof is off.
- 2) Power to the junction on the stand box is on.
- 3) Both racks in the test cell are plugged in, but not turned on.
- 4) Visual inspection of the engine to verify that all wires are attached, and all fittings tightened.
  - a) Flow fence stuff.
  - b) Fittings under the shroud.
    - i) left side
    - ii) right side
  - c) Fittings on the fuel controller.
- 5) Oil cooler is on.
- 6) Cooling water is turned on.
  - a) To kulites.
  - b) To shroud.
- 7) Vacuum pump is on and valves are closed.
- 8) Oil free air is on (to cool the bleed valve motor) and at the correct pressure.
- 9) Cameras and monitors are on.
- 10) Control panel in the hall is on.

- 11) Bleed valve works and is closed (switch in hall).
- 12) Any additional instrumentation is functional.
  - a) Kulites have been calibrated.
  - b) Vibrometer panel is turned on, vibrometer is attached (pressing 'cont' causes the meter to read '5').
  - c) Hot wire is on and inserted in the flow.
  - d) The frequency to voltage converter (for N1) is on.
  - e) The high speed filter board had been initialized.
- 13) Inlets on roof are open.
- 14) Any personnel in the shop have been warned that the engine is being run, especially if the bleed valve will be in use.
- 15) The oil vent fan is on.
- 16) There is enough fuel for the run.
- 17) The three rack panels in the test cell are turned OFF!  
(end of batch file, Genesis starts)
- 18) Follow instructions on the screen.
- 19) Calibrate the Setras.
- 20) Go to start engine.
- 21) Turn on the fuel supply (through the computer and externally).
- 22) Turn on the starter and ignitor.
- 23) At 10% speed set the throttle to 25 degrees, 'til lightoff, or 1 min.
- 24) At 30% speed turn off the starter and ignitor.
- 25) Go to idle (50 % speed).

## Appendix G

### Filter Board Specifications

The technical specifications of the Techfilter programmable filter board, as provided by the manufacturer, Onsite Instruments, Inc. are,

Roll Off

-75 dB/ octave

Corner Frequency Accuracy

$\pm 0.5 \%$

Phase Difference Between Channels

$\pm 1$  degrees maximum

Channel Crosstalk

Greater than 80 dB

Signal Input Voltage

10 Volts peak to peak

Load Impedance

10,000 ohms

Pass Band Gain

0 dB

Out of Band Rejection

Greater than 80 dB

Total Harmonic Distortion

Less than 0.1 %

Input Impedance

1 Megaohm

## References

- [1] Beers, Y, Introduction to the Theory of Error, Addison-Wesly Publishing Company, Inc., Reading Massachusetts, 1962.
- [2] Bodine, A. G., "Sonic Control of Dynamic Compressor Instability", Symposium on Stall, Surge, and System Response, ASME Gas Turbine Power Division, March 1960.
- [3] Emmons, H. W., Pearson, C. E., and Grant, H.P., "Compressor Surge and Stall Propagation", Transactions of the ASME, 79:455-469, April 1955.
- [4] Epstein, A. H., Ffowcs Williams, F. E., and Grietzer, E. M., "Active Suppression of Compressor Instabilities", Journal of Propulsion, 5(2):204-211, March-April 1989.
- [5] Ffowcs Williams, F. E., and Huang, X., "Active Stabilization of Compressor Surge", Journal of Fluid Mechanics, 204:245-262, 1989.
- [6] Fink, D. A., Surge Dynamics and Unsteady Flow Phenomena in Centrifugal Compressors, Techincal Report 193, Massachusetts Institute of Technology - Gas Turbine Laboratory, Massachusetts Institute of Technology, Cambridge, Massachusetts, June 1988.
- [7] Grant, H. P., "Measuring Time-Averaged Stagnation Pressure in Pulsatile Air Flow", ISA 23<sup>rd</sup> International Instrumentation Symposium, Las Vegas, Nevada, May 1977.
- [8] Greitzer, E. M., "Surge and Rotating Stall in Axial Flow Compressors Part I: Theoretical System Model", Jornel of Engineering for Power, 98:190-198, April 1976.
- [9] Greitzer, E. M., "Surge and Rotating Stall in Axial Flow Compressors Part II: Experimental Results and Comparision With Theory", Jornel of Engineering for Power, 98:199-217, April 1976.



- [10] Gysling, D. L., "Dynamic Control of Centrifugal Compressor Surge Using Tailored Structure", S.M. Thesis, Department of Aeronautics and Astronautics, Massachusetts Institute of Technology, August 1989.
- [11] Hill, P. G., and Peterson, C. R., Mechanics and Therodynamics of Propulsion, Addison-Wesley Publishing Company, Reading, Massachusetts, 1970.
- [12] The Mathworks Inc., MATLAB for 80386-based MS-DOS Personal Computers, The Mathworks Inc., South Natick, MZ, 1990.
- [13] Pinsley, J. E., Guenette, G. R., Epstein, A. H., and Grietzer, E. M., "Active Stabilization of Centrifugal Compressor Surge", Journal of Turbomachinery, 113:723-732, 1991.
- [14] Simon, J. S., Feedback Stabilization of Compression Systems, Technical Report 216, Massachusetts Institute of Technology - Gas Turbine Laboratory, Massachusetts Institute of Technology, Cambridge, Massachusetts, March 1993.